Université Denis Diderot- Paris VII

École doctorale B2T

Thèse

Pour l'obtention du diplôme de

DOCTEUR DE L'UNIVERSITÉ PARIS VII

Spécialité : Biologie et Pharmacologie de l'Hémostase et des Vaisseaux

Soutenue publiquement le 19 Septembre 2013 par

Clarisse EVENO

Processus métastatique : rôle de l'angiogenèse et du microenvironnement tumoral, impact des thérapeutiques établies et à venir

Directeur de Thèse :

Pr Marc POCARD

Devant le Jury composé de :

Pr Valérie PARADIS	Président
Pr Daniel CHERQUI	Rapporteur
Pr Jean-Charles SORIA	Rapporteur
Dr Fabrice SONCIN	Examinateur

TABLE DES MATIERES

Liste des abréviations

ACE	Antigen CarcinoEmbrionic
Ang	Angiopoïétine
CAF	Cancer-Associated Fibroblasts
CCR	Cancer ColoRectal
CDMO	Cellule Dérivée de Moelle Osseuse
CE	Cellule Endothéliale
CSH	Cellule Stellaire Hépatique
DMV	Densité MicroVasculaire
EGF	Epidermal Growth Factor
EPCs	Endothelial Progenitor Cell
FAC	Facteur Angiogénique Circulant
bFGF	basic Fibroblast Growth Factor
HGF	Hepatocyte Growth Factor
HIF	Hypoxia-Inducible Factor
HUVEC	Human Umbilical Vein Endothelial Cells
IGF	Insulin-Like Growth Factor
MB	Membrane Basale
IL	Interleukine
MEC	Matrice ExtraCellulaire
MHCCR	Métastase Hépatique d'origine ColoRectales
MIP	Macrophage inflammatory protein
MMP	Métalloprotéases matricielles

PDGF	Platelet Derived Growth Factor
PlGF	Placental Growth Factor
SMA	Smooth Muscle Actin
TGF-β	Transforming Growth Factor-β
TIMP	Tissue Inhibitor of Metalloproteinase
TNF-α	Tumor Necrosis Factor-α
VEGF	Vascular Endothelial Growth Factor
VEGFR-1	Vascular Endothelial Growth Factor Receptor 1
VEGFR-2	Vascular Endothelial Growth Factor Receptor 2

INTRODUCTION

La progression tumorale sous forme de métastases est décrite comme un processus comprenant plusieurs étapes au cours desquelles les cellules tumorales diffusent a partir de la tumeur primitive pour coloniser les organes a distance.[1] Durant ce processus, les cellules tumorales doivent se détacher de la tumeur primitive, envahir la paroi puis pénétrer la lumière des vaisseaux. Après un « trapping » dans les capillaires, elles envahissent l'organe cible, survivent et prolifèrent pour créer une métastase.[2]

Avec sa combinaison de caractéristiques hémodynamiques et morphologiques particulières, sa localisation spécifique, son flot sanguin lent et tortueux dans les capillaires sinusoïdes et son microenvironnement unique, le foie est le site privilégié des métastases d'origine colorectale. Malgré l'arrêt effectif des cellules tumorales circulantes dans le parenchyme hépatique, le processus métastatique hépatique est un phénomène hautement inefficace, avec, dans un modèle murin de métastases hépatiques de mélanome, moins de 0.02% des cellules tumorales injectées en intra-portal qui deviendront des tumeurs macroscopiques.[3] Cela suggère que la formation de métastases hépatiques macroscopiques est hautement dépendante de l'interaction entre les cellules tumorales et le microenvironnement hépatique.

1) MICROENVIRONNEMENT METASTATIQUE

Le microenvironnement hépatique est composé de cellules stromales de soutien natives, du réseau vasculaire, de facteurs solubles et de nutriments; la matrice extra cellulaire (MEC) assurant son architecture.[4, 5] Le microenvironnement doit en outre être permissif en terme d'inflammation pour permettre à la métastase de se former.[6]

Plusieurs théories se sont succédé sur la relation cellule tumorale – microenvironnement, dont la plus novatrice était celle de Steven Paget en 1889 appelée « seed & soil » ou « de la graine et du sol », qui introduit le concept que le microenvironnement doit être réceptif et permissif envers la cellule tumorale pour sa greffe dans l'organe cible et pour sa prolifération sous forme de métastase.[7, 8] Cette théorie est étayée en clinique humaine par plusieurs types de tumeurs dont le carcinome mammaire, théorie décrite par Paget dans son article princeps, avec possibilités de

formation de métastases dans des territoires spécifiques, non gouvernés par le territoire de drainage de la tumeur primitive.[7, 8] C'est aussi le cas pour le mélanome de la choroïde dont les métastases ont un tropisme hépatique particulier avec un taux de localisation hépatique de 93% dans une large série de 1003 patients.[9]

Cette théorie de nécessité d'un microenvironnement favorisant la greffe tumorale avait été étudiée par James Ewing en 1928 pour qui les métastases étaient déterminées par l'anatomie de drainage vasculaire et lymphatique de la tumeur primitive.[10] Cette théorie a prévalu jusqu'aux travaux de Isaiah Fidler qui ont successivement démontré que les cellules tumorales atteignaient le lit vasculaire de tous les organes, mais les métastases ne se développeraient que dans certains organes.[11, 12]

1-A) Le concept de niche dans les métastases

Le concept de niche métastatique décrit le microenvironnement spécialisé de soutien des cellules tumorales interagissant avec elles et régulant activement leur fonction et prolifération. Ce modèle suggère que le microenvironnement doit être propice à accueillir les cellules tumorales (formant une niche pré-métastatique) et doit évoluer pour que ces cellules tumorales puissent se greffer (formation de la niche métastatique) et proliférer dans des sites secondaires sous forme de micro- puis macro-métastases.

1-B) La niche pré-métastatique:

La diffusion initiale des cellules tumorales aux organes à distance est gouvernée par l'anatomie du réseau vasculaire de drainage de la tumeur primitive, le diamètre de la lumière des vaisseaux, les caractéristiques hémorrhéologiques du flux sanguin et les caractéristiques physiques, chimiques et biologiques des cellules tumorales. Après leur adhésion et leur extravasation, les cellules tumorales doivent survivre puis proliférer pour permettre la formation de métastase.[13, 14] Ce processus requiert un microenvironnement favorable sur le site métastatique à venir.[2]

1-B-1) Initiation de la niche pré-métastatique:

Plusieurs études récentes ont montré que des facteurs de croissance secrétés par la tumeur primitive initiaient la modification de certaines zones du tissu cible pour permettre la greffe tumorale, en attirant des progéniteurs hématopoïétiques qui forment un microenvironnement propice à l'adhésion et à l'invasion cellulaire.[13, 15] Dans des modèles murins de tumeurs sous cutanées de cancer du poumon et de mélanome, Kaplan et al. ont décrit le recrutement de cellules hématopoïétiques dérivées de moelle osseuse et exprimant le récepteur 1 du vascular endothelial growth factor (VEGF), le VEGFR1. Ce recrutement s'effectue sur les sites pré-métastatiques pulmonaires, avant l'arrivée des cellules tumorales dans ces sites.[13] Ce recrutement de cellules progénitrices était stimulé par la tumeur primitive secrétant des facteurs angiogéniques tels que le VEGF et le placental growth factor (PlGF). Ces cellules progénitrices stimulées étaient alors dirigés vers les sites, les organes électifs pour la constitution de niches pré-métastatiques, riches en fibronectine, grâce à leur récepteur à la fibronectine (VLA4 ou intégrine α4β1). Dans une autre étude, Hiratsuka et al. rapportent le rôle des cytokines inflammatoires dans le recrutement des cellules myéloïdes et tumorales dans la niche pré-métastatique. Dans un modèle d'injection intra-dermique de cellules tumorales de mélanome et de cancer du poumon, la sécrétion de VEGFA, TGFβ (transforming growth factor β) et TNFα (tumour necrosis factor α) par la tumeur primitive induit une expression de protéines inflammatoires (S100A8 et A9) spécifiquement localisée dans la niche pré-métastatique pulmonaire. Ces protéines inflammatoires étaient fortement chemoattractives pour les cellules myéloïdes exprimant MAC1 et les cellules tumorales. Leur inhibition par anticorps spécifiques permettait une réduction de 80 à 90% de la colonisation pulmonaire par les cellules tumorales.[15]

1-B-2) La niche pré-métastatique est initiée pour permettre la greffe tumorale:

Les différents composants du microenvironnement jouent un rôle dans la greffe tumorale. Dans la niche pré-métastatique, les cellules myéloïdes nouvellement recrutées collaborent avec les autres types cellulaires dont les cellules stromales et endothéliales résidant dans le parenchyme

cible. Ensemble, ces cellules secrètent des cytokines et facteurs de croissance (TNFα, MIP2 (Macrophage inflammatory protein 2) et TGFβ), permettant d'accélérer le processus de migration des cellules tumorales dans les sites pré-métastatiques et ainsi la formation métastatique.[15]

Le remodelage tissulaire local est essentiel à l'invasion des cellules tumorales et à la croissance métastatique. Les Matrix Metalloproteinases (MMP) permettent de dégrader les composants de la MEC durant les processus de réponse inflammatoire, cicatrisation et croissance tumorale. Il a été montré que MMP9 était surexprimée au niveau des cellules endothéliales et myéloïdes (MAC1 et VEGFR1 positives) des niches pré-métastatiques. Cette surexpression est dépendante du VEGFA et facilite l'invasion des sites par les cellules tumorales ainsi que le relargage de facteurs de croissance et de cytokines comme le ligand soluble KIT qui permettra le recrutement des progéniteurs dérivés de MO et les cellules tumorales exprimant le récepteur de KIT.[13, 16]

La transformation des fibroblastes locaux est importante pour la progression tumorale. Ces fibroblastes « activés » ou CAFs (Cancer-Associated Fibroblasts) se caractérisent par un taux de prolifération plus élevé que les fibroblastes des tissus sains ainsi qu'un plus fort dépôt de composant de la MEC.[17] Les CAFs ont un rôle important dans l'initiation de la tumorigenèse et la progression tumorale en facilitant la prolifération, l'invasion et la motilité des cellules tumorales.[13, 17] Les cellules stellaires hépatiques (CSH), péricytes spécifiques du foie, initialement connues pour leur rôle dans la fibrose hépatique,[18] sont importantes dans la formation de la niche pré-métastatique car elles peuvent se trans-différencier en fibroblastes activés, hautement prolifératifs et motiles. Leur activation peut être induite par les cellules tumorales.[19, 20] Les CSH activées sont responsables d'un remodelage de la MEC et sont impliquées dans la migration tumorale et la croissance métastatiques de plusieurs types de cancers.[19, 21, 22] Dans un modèle murin de mélanome, Olaso et al. décrivent la présence de CSH activées entourant les sinusoïdes hépatiques et associées aux micro-métastases. Ces cellules sont hyperactivées (αSMA positives) et secrètent des MMP et des facteurs chimiotactiques nécessaires à la réalisation d'un microenvironnement propice à la greffe tumorale.[19] Elles peuvent aussi favoriser l'angiogenèse tumorale en produisant plusieurs facteurs angiogéniques dont le VEGF et angiopoietine 1 et 2 (Ang 1 et 2) qui activent les cellules endothéliales.[23-27]

1-B-3) Place de la Matrice Extracellulaire dans la niche pré-métastatique:

La Matrice extra-cellulaire est donc modulée par la sécrétion de MMP, par les précurseurs myéloïdes et les fibroblastes activés.[16, 19] D'autres facteurs comme l'hypoxie tumorale sont impliqués dans la progression tumorale et la formation de métastases.[28] Il a été montré récemment que la lysyl oxidase (LOX), enzyme qui permet l'ancrage du collagène et de l'élastine dans la MEC, est surexprimée et secrétée par les cellules tumorales hypoxiques, permettant d'augmenter leur capacité de migration. Dans un modèle orthotopique de cancer du sein, la LOX est secrétée par les cellules tumorales hypoxiques et s'accumule dans les niches pré-métastatiques pulmonaires ou elle modifie la MEC en adhérant au collagène fibrillaire. Elle permet ainsi la constitution d'un microenvironnement plus réceptif à l'infiltration par les progéniteurs myéloïdes.[29] En outre, l'inhibition de la synthèse de LOX par les cellules tumorales réduit l'accumulation de cellules myéloïdes CD11b+ dans les organes pré-métastatiques et prévient la formation de métastase.

La fibronectine, autre composant de la MEC, joue un rôle important dans la formation de la niche pré-métastatique. Sa sur-production locale est observée autour des bronchioles pulmonaires terminales et de leurs veines satellites, en lieu et place de la future niche pré-métastatique.[13, 29] Bien que sa synthèse apparaisse avant l'arrivée des cellules tumorales,[13] l'utilisation d'un anticorps spécifique de la fibronectine humaine dans un modèle de cancer du sein avec injection de cellules humaines a montré qu'une partie de celle-ci était secrétée par les cellules tumorales.[29] L'expression de LOX et les ilots de cellules myéloïdes sont co-localisés avec la fibronectine, ce qui suggère qu'elle joue un rôle crucial dans l'assemblage des composants de la niche pré-métastatique.

2) ANGIOGENESE DES METASTASES HEPATIQUES

2-A) Passage micro -macro métastase hépatique: place du switch angiogénique:

Les micro-métastases formées de cellules tumorales proliférantes sont initialement avasculaires et tributaires du lit vasculaire natif de l'organe d'accueil qui leur apporte oxygène et nutriments. Il a été décrit un état de « dormance » des micro-métastases, dans lequel la prolifération cellulaire est équilibrée par un phénomène d'apoptose jusqu'à ce que la métastase

puisse avoir une croissance soutenue grâce au recrutement de néo-vaisseaux sanguins.[30, 31] La progression vers une macro-métastase cliniquement détectable nécessite la mise en place d'un lit vasculaire néoformé fonctionnel, processus qui requiert l'activation du « switch angiogénique ». Un changement dans l'équilibre local entre les régulateurs positifs et négatifs de l'angiogenèse se traduit par l'activation de l'endothélium normalement quiescent, débutant le processus de néo-vascularisation. Les cellules tumorales peuvent provoquer ce « phénotype angiogénique » de plusieurs manières, comprenant la surexpression de facteurs pro-angiogéniques, le recrutement de cellules hôtes capables d'altérer le milieu par sécrétion de facteur angiogénique, la mobilisation des protéines angiogéniques de la matrice extracellulaire ou une combinaison de ces procédés. La création de nouveaux vaisseaux sanguins se produit par une série d'étapes. Finalement, les cordons de nouvelles cellules endothéliales développent des lumières vasculaires permettant de créer de nouveaux vaisseaux qui alimenteront la masse de cellules tumorales. Les tumeurs qui ont subi une néo-vascularisation peuvent non seulement entrer dans une phase de croissance rapide, mais également augmenter leur potentiel métastatique.

Des études récentes ont montré le rôle majeur de régulation que jouent les progéniteurs de cellules endothéliales (EPCs) dérivés de moelle osseuse dans le switch angiogénique intra-métastatique.[13, 32] Dans un modèle de cancer du poumon après injection sous-cutanée de cellules cancéreuses et dans un modèle de cancer du sein spontané chez des souris transgéniques, Gao et al. ont montré que le passage de micro (<1mm) a macro-métastase pulmonaire s'accompagnait de la formation d'un réseau vasculaire.[32] Les EPC (CD31 positives et marquées a la GFP) infiltraient la périphérie des micro-métastases avasculaires puis s'incorporaient à la lumière vasculaire des macro-métastases. Le facteur de transcription Id1 est connu pour son rôle dans la néoangiogenèse de tumeurs primitives, les souris Id1 KO présentant une croissance tumorale ralentie par atteinte de l'angiogenèse liée aux progéniteurs de moelle osseuse.[33, 34] Id1 semble être crucial pour la mobilisation des EPC et leur recrutement dans les micro-métastases. Gao et al. ont montré que l'expression d'Id1 était restreinte aux EPC parmi les cellules dérivées de MO (CDMOs) et que lors de son inhibition par shRNA, l'initiale colonisation métastatique pulmonaire n'était pas affectée mais que la néoangiogenèse et la progression vers le stade de macro-métastase étaient inhibées par absence de recrutement des EPC.[32] Cette étude met en exergue l'importance fonctionnelle des EPC

dans le switch angiogénique métastatique puisque ce type cellulaire ne représente que 12% des cellules endothéliales des vaisseaux tumoraux.

Kaplan et al. confirment l'arrivée des EPC VEGFR2+ avec les cellules tumorales dans la niche pré-métastatique formée par les HPC VEGFR1. Le traitement par un anticorps anti-VEGFR2 ne prévenait pas la formation des clusters de HPC mais limitait la progression métastatique.[13]

2-B) Architecture de l'angiogenèse et des métastases hépatiques

Les vaisseaux tumoraux sont tortueux, dilatés, perméables et instables.[35] Ils sont bordés de cellules endothéliales présentant des jonctions de type fenêtré, avec de larges espaces intercellulaires, une lame basale discontinue et peu de péricytes, ce qui contribue à leur instabilité. Ce type de réseau vasculaire, très perméable, favorise le phénomène d'extravasation plasmatique. Les dépôts de fibrine et de fibronectine dans le stroma tumoral, ainsi que l'apport de facteurs de croissance servent alors de matrice à la prolifération cellulaire. La perméabilité accrue des vaisseaux tumoraux favorise le passage de cellules tumorales dans le flux sanguin et l'apparition de foyers métastatiques secondaires.[36] Les vaisseaux tumoraux ne possèdent pas de péricytes fonctionnels (importants dans la stabilité des vaisseaux), les rendant ainsi plus sensibles aux modifications hypoxiques.[37] Le réseau vasculaire désorganisé engendre un flux sanguin anormal. Il comporte des zones où le flux est ralenti et des zones où le flux est accéléré. Ces perturbations entraînent une hypoxie des tissus tumoraux stimulant HIF-1α et la synthèse de facteurs pro-angiogéniques dont le VEGF et le PlGF.

De plus, la paroi vasculaire des vaisseaux tumoraux n'est pas toujours composée d'une couche homogène de cellules endothéliales. En effet, les vaisseaux tumoraux peuvent être bordés d'une couche homogène de cellules tumorales ou d'une mosaïque de cellules endothéliales et de cellules tumorales. L'équipe de Chang a observé que 15 % des vaisseaux d'une xénogreffe de cancer du côlon ainsi que d'un cancer du côlon spontané chez l'homme, étaient composés d'une mosaïque de cellules endothéliales et tumorales.[38]

Tous ces défauts induisent une vascularisation anormale et perméable qui maintient une hypertension interstitielle et induit un défaut de perfusion de la tumeur et limite ainsi la délivrance de molécules thérapeutiques.[39]

Plusieurs types d'angiogenèse existent dans les tumeurs primitives et métastases hépatiques :[40]

1) sprouting capillaire

→ Caractérisé par une dégradation locale de la MB, prolifération et migration des CEs avec formation d'une lumière puis prolifération et migration des péricytes stabilisant le néo-vaisseau. Ce phénomène est régulé par une balance de facteurs pro et anti-angiogéniques.[41]

2) cooption

→ Caractérisé par une incorporation dans la vasculature tumorale de capillaires du parenchyme hôte.[42]

3) mimétisme vasculaire (Vascular Mimicry)

→ En l'absence de CEs, les cellules tumorales hautement invasives et pouvant acquérir des caractéristiques de CEs, s'organisent en canaux permettant la circulation sanguine intra-tumorale.[43, 44]

2-B-1) Aspect de la périphérie tumorale : infiltrant *versus* encapsulé:

L'analyse de l'interface entre la métastase et le parenchyme hépatique non tumoral a montré que les métastases hépatiques d'origine colorectales (MHCCR) ont différents modèles controversés de croissance. Vermeulen et al. décrivent trois types de croissance métastatique : «remplacement», «pushing» et «desmoplastic».[45] Dans le modèle par remplacement, la croissance se fait par remplacement du parenchyme hépatique sain, les cellules tumorales remplacent les hépatocytes en conservant l'aspect trabéculaire du parenchyme et son architecture. Dans ce modèle, l'initiation de l'angiogenèse se fait par cooption des sinusoïdes à l'interface tumeur-

parenchyme hépatique. Les sinusoïdes sont CD34 négatifs et l'endothélium des vaisseaux cooptés commence à exprimer ce marqueur de CEs lorsqu'ils sont entourés de cellules tumorales. Dans le modèle par poussée («pushing type»), les travées hépatocytaires sont poussées de coté et comprimées parallèlement à la circonférence des métastases. Dans le dernier type («desmoplastic»), la croissance métastatique se fait par compression du parenchyme non tumoral avec formation d'une réaction desmoplastique autour de la tumeur. Dans les deux derniers types, l'architecture hépatique est détruite.

Cette même équipe a confirmé ces 3 patterns sur une plus large série de 196 patients opérés pour MHCCR (Fig. 1 et 2).[46] Le type de croissance par poussée, représentant 16% de l'ensemble des métastases, était associé à un pattern angiogénique avec un taux de prolifération des cellules tumorales et endothéliales à l'interface métastases / parenchyme non tumoral plus élevé que dans les autres types. Par ailleurs, cette angiogenèse était, au moins partiellement, induite par l'hypoxie tumorale, avec un taux de prolifération des cellules tumorales et endothéliales plus élevé en cas d'expression accrue de Carbonic Anhydrase 9 (CA9), marqueur d'hypoxie, à la périphérie tumorale. Malgré une absence de différence de survie en fonction du type de croissance métastatique à la fin du suivi, le type de croissance par poussée avait une médiane de survie à 20.5 mois, très inferieure aux autres groupes (43 et 38.4 mois pour les types par remplacement et desmoplastique, respectivement). En outre, le taux de récidives précoces après chirurgie de résection des métastases hépatiques (<12 mois) était plus élevé dans ce groupe de mauvais pronostic.

Une autre série de 55 patients analysait les patterns de croissance et sa relation avec la densité micro-vasculaire de métastases hépatiques d'origine colorectale et de la tumeur primitive associée.[47] Les tumeurs primaires encapsulées étaient associées à des métastases hépatiques (MH) encapsulées et les tumeurs primitives infiltrantes à des MH non-encapsulées, partageant les mêmes caractéristiques de croissance. Il n'y avait pas de différence en termes de survie globale et sans récidive selon que les MH étaient encapsulées ou non. En revanche, lorsque les MH étaient classées en fonction de la densité microvasculaire (DMV), un compte élevé était associé à une survie sans récidive péjorée. Cette différence de survie n'était pas retrouvée lors de l'analyse de la

DMV de la tumeur primitive. Contrairement à l'étude précédente, il n'y avait pas de différence en termes de DMV entre MH encapsulée ou non.

Yamagushi et al. rapportent une série de 42 résections hépatiques à but curatif chez 37 patients ayant des MHCCR isolées. Les MH étaient classées selon leur mode de croissance, infiltrant ou bien limité. L'analyse multivariée a montré que le nombre, la taille des métastases hépatiques et le type de croissance, étaient des facteurs indépendants de pronostic à distance. Parmi ceux-ci, 28 résections hépatiques (inférieures à 6 cm de diamètre ou contenant moins de 4 nodules) ont été classées en fonction de l'histologie. La survie sans récidive à 5 ans était de 64% pour les patients avec des MH bien limitées et 14% pour ceux ayant des MH de type infiltrant (n=14). Le taux de récidive hépatique après résection était de 14% dans le premier groupe et 79% dans le second.[48]

Chez les patients ayant des métastases hépatiques multiples, un seul type de croissance est généralement prédominant. Eefsen et al. ont analysé les types de croissance de 64 MH chez 24 patients ayant eu une résection hépatique sans chimiothérapie préopératoire.[49] Le type de croissance métastatique était desmoplastique dans 25.8% des cas, 33.9% de type pushing, et 21% par remplacement. Chez 20 (83%) patients, le type de croissance était homogène dans toutes les MH. Comme dans leur étude préliminaire, l'angiogenèse, analysée par marquage CD31 et Ki67, était plus prononcée dans les MH de type pushing.

Table 1. Caractéristiques des métastases hépatiques et fonction de leur mode de croissance.

		Par Remplacement	**Par poussée**	**Desmoplastique**
Caractéristiques		Les cellules tumorales remplacent les hépatocytes Conservation de l'architecture du parenchyme hépatique	Compression des hépatocytes en périphérie Isolée	Avec réaction desmoplastique
Proportion[45, 46, 49]		12-36%	20-46%	26-42%
Angiogenèse	**Qualitatif**	Par co-option des sinusoïdes (Type sinusoïdal)	NA	Par « sprouting » (Type Portal)
	Quantitatif	NA	↗↗↗ (marquage CD31)[46, 49]	NA
Médiane de Survie (mois)[46]		43	↘↘ 20.5	38.5

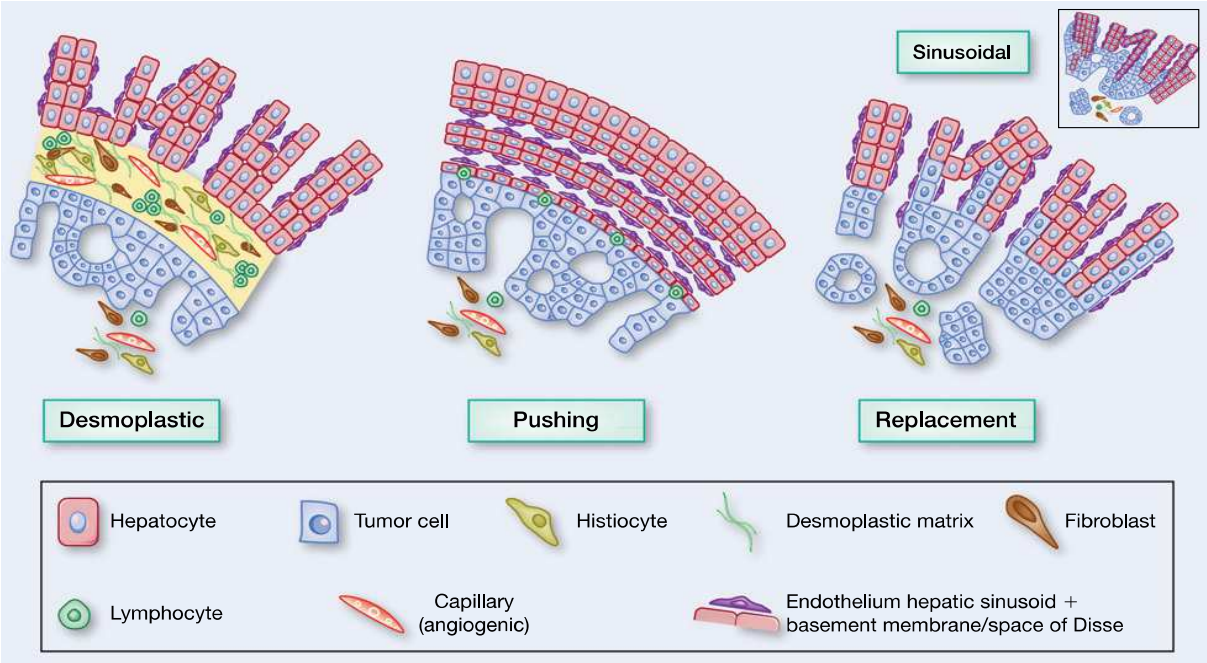

Fig 1 : Exemples de type de croissance des MHCCR, schématisation. Tiré de Van den Eynden et al.[50]

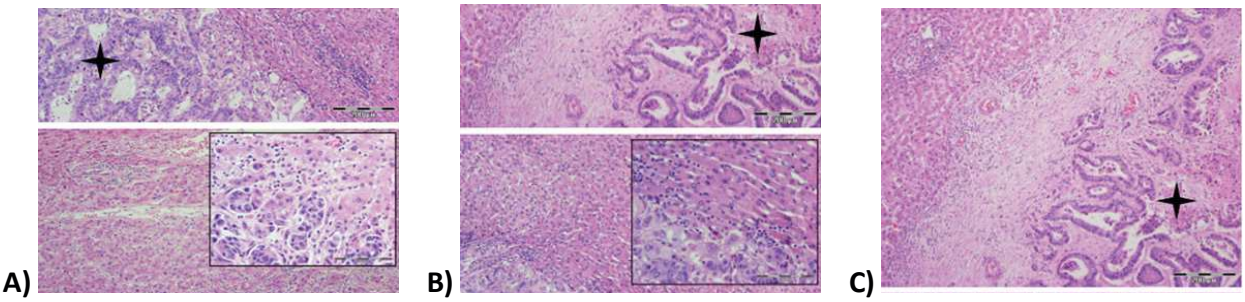

Fig 2: Exemples de type de croissance des MHCCR (coloration HES). A) Desmoplastique, B) Par poussée, C) Par remplacement. Tiré de Van den Eynden et al.[46]

2-B-2) Rôle de la capsule:

La signification pronostique du caractère encapsulé des MHCCR a été analysé dans plusieurs études. Okano et al. rapportent une série de 152 patients classés en 3 groupes, en fonction de l'absence de capsule (groupe 1, 39%) et la présence d'une capsule fine (groupe 2, 30%) ou épaisse (groupe 3, 31%).[51] Les facteurs classiques (MH métachrone, nombre inferieur à 3, taille inférieure à 5cm, absence d'invasion vasculaire ou lymphatique et résection macroscopique complète) ainsi que l'existence d'une capsule ont été associés à un meilleur pronostic. Parmi les patients R0, la survie sans récidive était augmentée en présence d'une capsule et d'autant plus si la capsule était épaisse avec, à 5 ans, un taux de 14%, 33% et 47% dans les groupes 1, 2 et 3, respectivement ($p< 0.001$).

Dans une série de 69 patients ayant eu une résection de MHCCR avec une marge chirurgicale d'au moins 1cm, Lunevicius et al. confirment la tendance à un meilleur pronostic des MHCCR encapsulées avec une survie à 5 ans de 57% contre 34% pour les non encapsulées ($p=0.163$).[52] La présence d'une capsule était associée à un taux de récidive locale plus faible (7% contre 31%, $p<0.05$). L'analyse histologique de la capsule fibreuse objective la présence accrue de cellules stellaires activées αSMA positives et de dépôt diffus de collagène I. Ces observations orientent vers un rôle de barrière mécanique et chimique de cette capsule, luttant contre l'invasion métastatique locale des cellules tumorales.

Cette réaction stromale est en grande partie absente dans le schéma de croissance par remplacement, tout du moins à l'interface MH / foie non tumoral.[45, 53]

2-B-3) Sinusoïdal *versus* Portal :

Paku et al. ont analysé la morphologie de la vascularisation des MH ainsi que son rapport à l'architecture tissulaire et vasculaire du parenchyme hépatique non tumoral.[54] Dans un modèle murin de MH de cancer du poumon après injection intra-splénique, 2 types de vascularisations ont été décrits. Dans le type «sinusoïdal», prépondérant, les cellules tumorales pénètrent entre la membrane basale (MB) et les CEs sinusoïdales entrainant une stimulation la prolifération des CEs ;

elles prolifèrent entre les CEs et la MEC, dans l'espace de Disse. Lors de ce processus, les vaisseaux apparaissent 6 jours après l'injection et sont en continuité avec les sinusoïdes, entrainant le développement dans les nodules tumoraux de vaisseaux larges et tortueux dépourvus de MB (négatifs pour les marquages par Laminine, collagène IV et fibronectine). Le marquage au bromodeoxyuridine (BrdUrd) objective un taux de CEs cooptées dans la MH six fois plus élevé qu'à sa périphérie, suggérant un mécanisme de vascularisation basé sur la cooption des sinusoïdes. Ce type de croissance métastatique n'engendre pas de compression du parenchyme hépatique adjacent et s'accompagne de larges plages centrales de nécrose.

Inversement, le type «portal», minoritaire, développe une angiogenèse par « sprouting ». Ces MH se localisent à proximité des tractus portaux et contiennent de nombreux vaisseaux de petit diamètre, positifs pour les 3 marquages de MB, et sont dépourvues de plage de nécrose.

Le type de croissance par remplacement correspond au type «sinusoïdal», alors que les MH desmoplastiques ont les caractéristiques du type «portal» (Table 1).

Terayama et al. confirment ces résultats en analysant 100 pièces opératoires de résection de MH ayant un type de croissance par remplacement et d'origine variée (24 pulmonaire; 21 pancréatique; 18 gastrique; 14 cholangiolaire; 13 coliques). Ils ont montré que les CEs sinusoïdes cooptées en périphérie métastatique apparaissaient dans les métastases de 200 microns et exprimaient fréquemment le facteur von Willebrand (vWF)21 et l'Ulex europaeus agglutinin (UEA)-121 contrairement aux sinusoïdes à distance (à plus de 1mm), réalisant une capillarisation de l'endothélium.[55] Ces vaisseaux sanguins étaient reliés avec les sinusoïdes du foie environnant.

Dans une seconde étude, Puku et al. ont analysé plus précisément les MH à croissance par poussée, dans un modèle murin de MH colorectale par injection intra-splénique. Ils décrivent un nouveau mécanisme d'apport sanguin.[56] Durant ce processus, les cellules stellaires activées SMA positives prolifèrent à la surface des MH et un phénomène de capillarisation des sinusoïdes se produit dans cette même région. Sous la pression intérieure de la tumeur et extérieure des CSHs proliférantes, les hépatocytes disparaissent de la périphérie tumorale, conduisant à la fusion des sinusoïdes et à l'apparition de lacs vasculaires à la surface tumorale. Avec les CSHs produisant une matrice de collagène, ces lacs vasculaires sont incorporés à la tumeur, formant des colonnes de

tissu conjonctif contenant des vaisseaux traversant la tumeur. Ces colonnes représentent la principale unité structurale et fonctionnelle, permettant un apport sanguin nécessaire à la croissance métastatique.

2-B-4) Vascular Mimicry:

Une seule étude analyse le phénomène de « Vascular Mimicry » (VM) dans le cancer colorectal. Cette analyse porte sur 117 pièces de résection de tumeurs primitives de tous stades.[57] La VM, retrouvée dans 20% des cas, était corrélée à un stade Dukes plus avancé et à une densité microvasculaire élevée. La survie globale des patients avec VM était nulle à 5 ans contre 40% chez les patients sans VM. Dans cette étude, la densité microvasculaire n'était pas retrouvée comme facteur pronostic.

2-C) Cellules stellaires hépatiques activées: Rôle dans le cancer colorectal

Les cellules stellaires hépatiques (CSH), péricytes spécifiques du foie, peuvent se trans-différencier en fibroblastes activés, hautement prolifératifs et motiles. Lors de ce changement phénotypique, elles expriment la α-smooth muscle actin (α-SMA) et produisent des facteurs de croissance et des composants de la matrice extracellulaire. Initialement connues pour leur rôle dans la fibrose hépatique et l'hypertension portale,[58] elles émergent comme un acteur important dans le développement tumoral et métastatique.[23]

2-C-1) Promotion de la croissance tumorale, *in vitro*:

Plusieurs études supportent le fait que les CSHs activées favorisent la migration, la croissance et la survie de cellules tumorales de divers type. *In vitro*, la co-culture de CSHs activées avec des cellules tumorales augmente leur tumorigénicité: dans le carcinome hépatocellulaire (HCC), l'addition de CSHs favorise leur croissance[27, 59] et leur migration par sécrétion de facteur de croissance (Hepatocyte Growth Factor, HGF).[21, 60] Un effet similaire est retrouvé sur des cellules de mélanome en culture, avec sécrétion de MMP et de facteurs chemoattractants par les CSHs entrainant une augmentation de la migration des cellules tumorales.[19] La co-culture augmente aussi la capacité d'invasion des cellules tumorales dans le cancer colorectal[61] et le cholangiocarcinome.[62]

2-C-2) Remodelage de la matrice extracellulaire:

Un remodelage de la MEC peut favoriser l'invasion et la progression tumorale hépatique.[22] Les enzymes protéolytiques comme les métaloprotéinases (MMP) et tissu inhibitor of metalloproteinases (TIMP) peuvent dégrader la MB et permettre aux cellules cancéreuses d'envahir le tissu cible. *In vitro*, en co-culture avec des cellules tumorales de mélanome[19] ou de CHC, [22] les CSHs activées secrètent des MMP. Analysant treize tumeurs hépatiques primaires et secondaires, Musso et al. ont montré que l'ARN messager de MMP2 et TIMP2 étaient exprimés

dans les CSHs activées au niveau du front d'invasion des MH et qu'un plus fort niveau d'ARN messager et d'activité enzymatique de MMP2 était détectés dans les MH par rapport au parenchyme hépatique non tumoral.[63, 64] De plus, les CSHs activées du front d'invasion des MH colorectales secrètent une MMP (ADAM9), protéine capable in vitro de cliver la laminine et de se lier aux cellules tumorales, permettant ainsi l'invasion tumorale.[61] Ces données suggèrent que les CSHs produisent des enzymes protéolytiques impliquées dans la dégradation de la MEC, facilitant ainsi l'invasion tumorale. Les CSHs activées sont le principal type cellulaire responsable de la production de MEC lors de la fibrose hépatique[58] et ce processus peut aussi contribuer à l'effet pro-métastatique de ces cellules en constituant un support physique aux cellules tumorales.

2-C-3) Augmentation du potentiel tumoral, *in vivo*:

→ Effets sur les tumeurs sous-cutanées.

Plusieurs études analysent l'effet de la co-injection de CHSc par voie sous-cutanée et confirment l'augmentation du potentiel tumoral avec une augmentation du volume tumoral lorsqu'elles sont co-injectées avec des cellules de cholangiocarcinome,[65] d'hépatocarcinome[27] et de cancer du colon.[66]

→ Effets sur les métastases hépatiques:

Le rôle des CSHs dans un modèle orthotopique de métastases hépatiques a été analysé par une équipe utilisant 2 types cellulaires. Dans un modèle murin de MH de mélanome par injection intra-splénique, Olaso et al. confirment l'existence de deux types de croissance métastatiques (sinusoïde et portal) et étudient la place des CHSc activées et de l'angiogenèse dans leur développement.[24] Les MH « sinusoïdes », représentant 68% des MH analysées, étaient infiltrées de myofibroblastes suivant un arrangement réticulaire et non-encapsulées avec des limites mal définies. L'architecture hépatique était conservée, les cellules tumorales cooptant le réseau fibrillaire de soutien des sinusoïdes. A l'opposé, les MH « portales », représentant les 32% restants,

étaient incomplètement encapsulées, mais non infiltrées, par les myofibroblastes arrangés en un tractus fibreux. L'architecture hépatique n'était pas conservée, la masse tumorale compressant le parenchyme l'entourant, délimitée par un stroma desmoplastique. Cela conforte les résultats de Lunevicius et al, qui objectivaient des CHSc activées α-SMA positives dans la capsule péri-métastatique.[52]

Dans un modèle de MH colorectales, l'augmentation de la trans-différentiation en myofibroblastes des CSHs (par l'absence d'expression de DDR2, récepteur de tyrosine kinase régulant le relargage de MMP par les CSHs), génère un microenvironnement pro-métastatique et pro-angiogénique.[67]

2-C-4) Promotion de l'angiogenèse:

Plusieurs études supportent l'hypothèse d'un rôle pro-angiogénique des CSHs. *In vitro*, dans un système de co-culture fonctionnelle sphéroïde en trois-dimensions de CEs et de CSHs, les CSHs CEs s'organisent en noyau recouvert d'une couche de CEs, mimant une organisation vasculaire. De plus, dans une matrice de Matrigel, les CSHs forment des réseaux vasculaires avec les CEs sinusoïdales[68] ou avec des HUVECs.[65] *In vivo*, les CSHs produisent plusieurs facteurs angiogéniques dont le VEGF et Ang 1 et 2 qui activent les cellules endothéliales.[26, 27]

Les deux types de MH décrits par Olaso et al. se différencient aussi par leur connexion microvasculaire avec le parenchyme hépatique non tumoral et leur modèle d'angiogenèse.[24] L'expression des marqueurs CD31 et CD34 est restreinte aux larges vaisseaux dans le foie non tumoral et fortement exprimés dans les CEs sinusoïdes tumorales. Les métastases « sinusoïdes » présentent un réseau vasculaire (CD31/CD34 positif) associé à des myofibroblastes, assurant la vascularisation de ce type de MH. A l'opposé, les métastases « portales », entourées par une couche discontinue de myofibroblastes qui pénètre dans la métastase avec les CEs dérivées des vaisseaux du tractus portal formant des tractus angiogéniques exprimant CD31 et CD34.

2-D) Moyens d'évaluation de l'AG des MH et corrélation au pronostic:

L'angiogenèse est un phénomène crucial dans la progression tumorale et métastatique.[36, 69] Différents marqueurs, histologiques ou sanguins, ont été proposés pour quantifier l'AG tumorale et analyser son lien avec le pronostic tumoral et l'efficacité des traitements anti-angiogéniques.

2-D-1) Facteurs histologiques

2-D-1-a) Densité microvasculaire

La densité microvasculaire (DMV), déterminée par le marquage des cellules endothéliales (CD31, FVIII ou CD34) en immunohistochimie, est reconnue comme facteur pronostic dans plusieurs types de cancers comme le cancer de la prostate, du sein et non à petites cellules du poumon.[70-73] Dans le cancer colorectal, la DMV du cancer primitif ou des MH a été étudiée comme facteur pronostic, avec des résultats discordants.

→ Tumeur primitive

Dix-huit études majeures, analysant la DMV sur les pièces opératoires de CCR primitif, présentent des résultats variés, avec 8 études liant une DMV élevée à un mauvais pronostic; [74-81] 3 études avec un résultat inverse[82-84] et 7 études ne mettant pas en évidence de corrélation statistique entre la DMV et le pronostic a long terme.[85-91] Douze de ces études analysent des tumeurs de tous stades (Dukes A à D) et 8 d'entre elles trouvent une corrélation de la DMV avec le stade histologique, sans corrélation avec son caractère pronostique.[74, 80, 84, 86, 87, 89-91] Malgré la méta-analyse de Des Guetz et al. concluant à une corrélation inversement proportionnelle de la DMV et de la la survie, les résultats hétérogènes des principales études ne font pas de la DMV un marqueur couramment utilisé en clinique.[92]

→Métastases hépatiques

Sur une période plus récente, la DMV des MH a été étudiée comme facteur pronostic avec des résultats plus concordants. Quatre études établissent un lien entre une forte DMV et une faible

survie.[47, 93-95] Nanashima et al. ont analysé une large série de 139 patients ayant eu une résection hépatique pour MHCCR. Une forte DMV, par marquage CD34, était corrélée à une survie à 5 ans globale et sans récidive plus faible avec 42 vs. 13% et 19 vs. 0%, respectivement. En outre, la DMV n'était pas corrélée au statut N+ de la tumeur primitive ni au nombre ou au caractère synchrone des MH.[95] Seule une étude de moindre effectif n'objectivait pas de différence en termes de survie globale en fonction de la DMV.[96]

2-D-1-b) Facteurs de croissance : VEGF tissulaire

→Tumeur primitive

Neufs études majeures ont montré un rôle pronostique de l'expression tissulaire du VEGF dans la tumeur primitive, confirmé par une méta-analyse.[92] Six études objectivent le rôle pronostique du VEGF tissulaire avec une survie globale péjorée chez les patients avec un fort niveau d'expression.[86, 87, 97-100] Une autre étude confirme ces résultats en analyse univariée uniquement[101] et deux études ne mettent pas en évidence de lien entre l'expression de VEGF et la survie.[88, 102]

→Métastases hépatiques

Peu d'études analysent le caractère pronostique de l'expression du VEGF dans les MH. Dans une étude de faible effectif, Nanashima et al. n'objectivent pas de différence de survie globale;[103] en revanche, dans une étude plus récente chez 89 patients, Noike et al. trouvent une survie globale à 5 ans de 15% en cas de MH exprimant le VEGF contre 55% en cas de tumeur négative.[104] Ces deux études ne précisaient pas clairement si les patients avaient reçu une chimiothérapie néoadjuvante, ce qui amènerait un biais important.

2-D-2) Facteurs angiogéniques circulants

→ Tumeur primitive

Plusieurs études ont examiné la pertinence biologique de facteurs angiogéniques circulants (FAC) dans diverses tumeurs solides, dont le cancer colorectal.[105] Dix études majeures, analysaient le taux sanguin de VEGF en préopératoire de chirurgie d'exérèse de tumeur primitive colorectale (Table 2)[106-115] . Un taux préopératoire élevé était corrélé à un stade avancé avec des résultats hétérogènes quant à sa relation avec les caractéristiques clinico-pathologiques. Huit études retrouvaient une corrélation péjorative entre un taux élevé et la survie globale ou sans récidive selon les études.[106-112, 115] Seules deux études d'effectif de moyenne importance ne mettaient pas en évidence d'influence diagnostique ou pronostique du VEGF préopératoire.[113, 114]

→ Métastases hépatiques

Yoon et al. ont analysé l'expression et la corrélation pronostique du VEGF, HGF, bFGF et EGF circulants chez 24 patients avant et après la résection de MHCCR. En analyse univariée, il existait une corrélation entre une survie sans récidive péjorative et un taux élevé préopératoire de VEGF et de HGF.[116] Dans une série de 107 patients et 32 témoins sains, Rahbahi et al. ont analysé un panel de 8 FAC (VEGF, PlGF, EGF, PDGF-A et -B, Ang-1 IL-8 et bFGF) avant résection de métastases hépatiques colorectales. En analyse multivariée, seuls un score du MSKCC > à 2 et un faible taux de PlGF étaient des facteurs de mauvaise survie sans récidive.[117] Ces résultats sont en accord avec une série de 40 patients traités par FOLFIRI/ Bevacizumab avant leur résection hépatique n'ayant pas retrouvé de valeur pronostic au VEGF circulant.[118]

Table 2. Caractéristiques des principales études étudiant la corrélation DMV-survie.

1er auteur	**CRC / CT**		**Corrélation**	**Analyse de survie**		**Corrélation**	**Résultat**
	N	**Taux moyen de VEGF (pg/ml)**	**Diagnostique**	**DFS**	**OS**	**Pronostique**	
Min et al.[112]	70 / 0	NA	MH	tendance	NA	NS	Positif
Kwon et al.[111]	132 / 50	620 / 334	Stade T ACE	-	tendance	Survie globale	Positif
Wei et al.[114]	86 / 30	80 / 61	NA	-	NA	-	Négatif
Alabi et al.[106]	93 / 0	168	NA	+	NA	Récidive Locale	Positif
Roumen et al.[113]	33 / 25	NA	-	NA	NA	-	Négatif
De Vita et al.[108]	81 / 50	504 / 78	Age Dukes ACE Chirurgie curative	+	NA	Toutes Récidives	Positif
Karayiannakis et al.[109]	67 / 61	492 / 186	Stade T N+ M+	NA	+	NA	Positif
Chin et al.[107]	81 / 0	NA	Stade T N+ M+	+	NA	Métastases	Positif
Werther et al.[115]	614 / 91	270 / 120	Dukes	NA	+	NA	Positif
Kumar et al.[110]	108 / 136	NA / 217	T3-4, Dukes N+ M+	NA	NA	NA	Positif

3) IMPLICATIONS THERAPEUTIQUES

Le cancer colorectal est la seconde cause de mortalité par cancer dans le monde occidental.[119] Près de 50% des patients développeront des MH, dont 25% au moment du diagnostic. La résection complète de MH est associée à une survie globale à 5 ans de 30 à 50%.[120-122] La chimiothérapie peut permettre de rendre des MH résécables[123] ou, en cas de MH déjà accessibles à la chirurgie, faciliter la chirurgie en diminuant leur taille ainsi sélectionner les malades répondeurs présentant un meilleur pronostic[124] et traiter d'éventuelles micro-MH. En outre, la chimiothérapie péri-opératoire par FOLFOX améliore la survie sans récidive des malades résécables, surtout en cas de taux ACE élevé et de performance statuts non altéré,[125] sans améliorer leur survie globale.[126] La survie des patients a été améliorée lors de la dernière décade,[118] notamment grâce à l'introduction de chimiothérapies plus efficaces et de biothérapies.[127]

Le VEGF est un des régulateurs clé du développement vasculaire,[128] nécessaire tant au plan physiologique lors du processus de cicatrisation ou de régénération hépatique,[129-131] qu'au plan pathologique lors du processus tumoral et métastatique.[36, 39] Il existe un rationnel fondamental à l'utilisation de traitements anti-angiogéniques avec plusieurs études sus-citées mettant en avant une corrélation diagnostique et pronostique de l'angiogenèse (avec le VEFG tissulaire ou circulant et la DMV). Il y a deux hypothèses fondamentales principales expliquant l'effet thérapeutique des traitements anti-angiogéniques, en association à un agent cytotoxique traditionnel. La première étant de couper l'apport sanguin à la tumeur et donc en nutriments, augmentant ainsi l'effet cytotoxique de la chimiothérapie ; la seconde celle de normaliser les vaisseaux, diminuer la pression interstitielle et augmenter temporairement l'oxygénation et la délivrance de la chimiothérapie.[132]

Plusieurs essais cliniques ont montré une amélioration du taux de réponse chez les patients ayant un CCR métastatique traités par du bevacizumab (BEVA, Genentech - Roche, San Francisco, CA, USA), anticorps monoclonal anti-VEGF en association avec une chimiothérapie conventionnelle.[133-136]

Certaines situations cliniques à prise en charge complexe peuvent bénéficier de la recherche fondamentale pour trouver de nouvelles voies thérapeutiques :

1) **Traitement adjuvant après résection de la tumeur colique primitive: traiter la niche pré-métastatique ?**

Deux études cliniques randomisées de phase III ont étudié l'apport d'un traitement par bevacizumab (BEVA) en adjuvant après chirurgie de résection d'un cancer du colon de stade II ou III.[137-139] Le rationnel scientifique de combiner un traitement anti-angiogénique à la chimiothérapie de référence à base d'oxaliplatine[140, 141] reposait sur la volonté d'inhiber l'angiogenèse précoce des MH, du switch angiogénique et ainsi inhiber la croissance des micro-MH.[30, 31] Allegra et al. analysaient 2672 patients recevant du FOLFOX pendant six mois post opératoires, seul ou en association avec du BEVA pendant un an. Il n'y avait pas de différence en terme de survie sans récidive à 3 ans, avec un taux de 77.4% dans le bras BEVA contre 75.5% dans le bras chimiothérapie seule,[137] ni en terme de survie globale.[138] Au cours des 15 premiers mois de suivi, un effet transitoire sur les récidives postopératoires était à la faveur du bras BEVA, non retrouvé à la fin du suivi. De Gramont et al. retrouvaient les mêmes résultats, avec un caractère délétère du BEVA sur la survie globale à 5ans avec plus de récidives et de morts par récidives dans les groupes de patients traités par BEVA.[139]

Plusieurs hypothèses fondamentales peuvent expliquer l'échec du BEVA en adjuvant :

→ *Effet rebond*

Plusieurs mécanismes de résistance aux thérapies anti-angiogéniques sont rapportés,[142] notamment la surexpression d'autres facteurs pro-angiogéniques, pouvant induire un rebond du taux de VEGF après l'arrêt du traitement anti-VEGF. Un effet de rebond a été démontré dans plusieurs études précliniques après l'arrêt d'un agent anti-VEGF[143] ou VEGFR.[144, 145] Cependant, l'arrêt du BEVA chez des patients métastatiques, y compris ceux atteints de cancer colorectal, n'affecte pas le mode de progression de la maladie.[146]

→ *Dormance tumorale*

L'état de « dormance » des micro-métastases, dans lequel la prolifération cellulaire est équilibrée par l'apoptose jusqu'à la progression vers une macro-métastase après activation du « switch angiogénique »,[30, 31] peut être entretenue par un traitement anti-angiogénique.[147]

→ *Période d'administration*

Deux études ont analysé le taux de VEGF sanguin avant et après (aux 7ème et 30ème jours) chirurgie d'exérèse de la tumeur primitive colorectale.[108, 109] Une résection curative a été réalisée chez 55[109] et 68 patients[108] retrouvant un taux de VEGF augmenté au 7ème jour puis une diminution significative au 30ème jour avec des niveaux inférieurs au taux moyen préopératoire.

Dans les deux études cliniques de Allegra et de Gramont et al. l'administration du bevacizumab était réalisée entre le 30ème et le 60ème jour suivant la résection de la tumeur primitive. De Gramont et al. ne trouvaient pas de corrélation entre le taux de VEGF sanguin et la réponse au bevacizumab; cependant nous pourrions nous interroger sur l'opportunité de mettre en place un traitement par bevacizumab lorsque le VEGF sanguin est élevé et que la tumeur primitive exerce un effet pro-angiogénique sur la niche pré-métastatique ; soit en néoadjuvant, et non pas lorsque le taux de VEGF est revenu à la normale. Mais ce traitement serait difficile à mettre en œuvre au vu des risques de complications de la tumeur primitive sous traitement anti-angiogénique.[135, 148-150]

2) Métastases hépatiques synchrones : traiter la tumeur primitive ?

Les options thérapeutiques à proposer aux patients ayant des métastases hépatiques synchrones non résécables avec leur tumeur primitive en place restent débattues. Presque toutes les études réalisées à ce jour sont des études monocentriques et rétrospectives. Une récente méta-analyse de 8 études a montré une amélioration de la survie des patients traités avec résection palliative de leur tumeur primitive, avec une différence moyenne de 6 mois.[151] Venderbosh et al. ont récemment rapporté les résultats de deux études de phase III (CAIRO et CAIRO2) analysant 258 et 289 patients ayant eu la résection de la tumeur primitive et 141 et 159 patients avec leur tumeur primitive laissée en place. Dans l'étude CAIRO, les médianes de survie globale et sans récidive étaient significativement meilleures dans le groupe avec résection avec 16,7 contre 11,4 mois et

6,7 contre 5,9 mois (p <0,0001, HR 0,61 et p = 0,004, HR 0,74) respectivement.[152] Dans une série de même design étudiant 208 patients, Karoui et al. observaient un gain de survie médiane de 9 mois (soit 31 mois) après résection de la tumeur primitive; la chimiothérapie combinée avec anti-VEGF étant un facteur important associé positivement à la survie globale en analyse multivariée.[153]

Les raisons de l'amélioration de la survie chez les patients ayant une résection de leur tumeur primitive sont mal connues. Une hypothèse impliquant l'existence d'une niche pré-métastatique a été initialement décrite par Kaplan et al. montrant que des cellules hématopoïétiques dérivées de moelle osseuse exprimant VEGFR-1 colonisent les sites pré-métastatiques dans un modèle murin de cancer du poumon, préparant ainsi la voie à l'arrivée des cellules tumorales métastatiques.[13] Ce nouveau concept de niche pré-métastatique a été salué comme une avancée majeure, cependant, le modèle animal utilisé n'était pas un modèle orthotopique mais de tumeur sous cutanée, loin de reproduire le processus métastatique chez l'homme. Sept ans après, une analyse de pièces opératoires de résections hépatiques pour MHCCR confirme cette découverte en clinique humaine.[154] L'étude visait à déterminer si la présence de tumeur primitive laissée en place était associée à des modifications du parenchyme hépatique non tumoral, adjacent aux métastases, reflet de la niche métastatique. Les auteurs ont comparé trois groupes de patients selon le traitement réalisé: (1) résection simultanée de métastases hépatiques synchrones et de la tumeur primitive (groupe SS), (2) résection de métastases hépatiques synchrones, 3 à 12 mois après la résection de la tumeur primitive (groupe LS) et (3) la résection des métastases métachrones, plus de 14 mois après la résection de la tumeur primitive (groupe M). L'expression génique et la localisation des marqueurs vasculaires (CD31), d'hypoxie (HIF-1α) ainsi que les composants des voies du VEGF et des angiopoïétines ont été étudiées par RT-PCR quantitative et immunohistochimie, dans les métastases hépatiques et le parenchyme hépatique non tumoral adjacent. Dans les trois groupes, les facteurs angiogéniques étaient plus fortement exprimés dans le parenchyme hépatique adjacent que dans les MH. Le gène du VEGFR-2 était surexprimé dans le parenchyme hépatique adjacent par rapport aux MH, des trois groupes mais particulièrement dans le groupe SS. L'expression du VEGF-A et du VEGFR-1 dans le parenchyme adjacent du groupe SS était 2,5 et 10 fois supérieure à celles du groupe M, respectivement. Le ratio Ang-2/Ang-1, en faveur d'un effet angiogénique, était plus élevé dans le groupe SS, tant dans les

MH que le foie adjacent. Ce phénomène s'accompagnait d'un fort taux de renouvellement des cellules tumorales.

Les auteurs concluaient qu'en présence de la tumeur primitive, le parenchyme hépatique adjacent aux métastases hépatiques synchrones fournissait un environnement pro-angiogénique favorisant la croissance des métastases. Cela confirmerait la nécessité de réséquer la tumeur primitive lors de MH associées ou de proposer des combinaisons de chimio- et bio-thérapies spécifiques, pour contrôler la formation de niches pré-métastatiques.

3) Impact d'un traitement anti-angiogénique sur la chirurgie des MHCCR

→ *Préparation à la chirurgie*

L'amélioration récente de la survie après résection des MHCCR[118] est due aux progrès des techniques et des stratégies opératoires (ie embolisation portale et hépatectomies en 2 temps)[155-157] ainsi qu'au développement de chimiothérapies et de biothérapies plus efficaces, permettant d'amener un nombre croissant de patients à la chirurgie.[126, 135, 158-160] L'administration préopératoire de bevacizumab en association avec une chimiothérapie à base d'oxaliplatine ou d'irinotecan conduit à des taux accrus de réponse tumorale et de résécabilité ; l'étude de Phase II BOXER rapportant 33% des patients ayant des MHCCR initialement irrésécables rendu résécables après chimiothérapie combinée au bevacizumab.[160] La réponse pathologique à la chimiothérapie préopératoire, gradée selon plusieurs systèmes, de absente à majeure ou complète, est fortement corrélée à la survie globale.[161-163] Cinq études démontrent l'intérêt du bevacizumab avec une réponse pathologique augmentée de 33 à 50% chez les patients traités par oxaliplatine + BEVA par rapport à ceux traités par oxaliplatine seule.[161, 162, 164-166] Cet effet était constant quelque soit le nombre de cycle de chimiothérapie, suggérant que l'amélioration de la régression tumorale avec le bevacizumab survient tôt au cours du traitement et se maintient pendant toute la durée du traitement. En outre, l'ajout de bevacizumab a un effet bénéfique en diminuant l'incidence et la gravité du syndrome d'obstruction sinusoïdale, fréquent lors du traitement prolongé par l'oxaliplatine et ayant un effet propre délétère sur la survie.[167]

→ *Chirurgie en elle-même*

Le VEGF joue un rôle crucial dans la régénération hépatique après une hépatectomie partielle (ou une embolisation portale), soulevant la question de l'effet potentiellement nocif du bevacizumab en préopératoire. La régénération est contingente à l'angiogenèse et survient très rapidement au cours des 7 à 10 premiers jours après hépatectomie.[168, 169] Le pic de VEGF est atteint à la 48ème heure et est directement impliqué dans le recrutement et la prolifération des précurseurs de cellules endothéliales et donc de l'initiation de la néoangiogenèse.[170] Dans des modèles murins d'hépatectomie partielle, l'inhibition du VEGF[171] ou de son récepteur[172, 173] compromettent la régénération hépatique. Malgré certains arguments biologiques faisant craindre un effet délétère du bevacizumab sur la régénération hépatique, comme l'inactivation persistante en postopératoire du VEGF par l'anticorps,[174] et certains résultats cliniques discordants[175, 176]; une étude récente de plus grand effectif, étudiait 82 patients appariés ayant reçu une chimiothérapie avec ou sans bevacizumab n'objectivant pas de différence en terme de régénération hépatique avec une volumétrie et un taux de complication postopératoires de grade 3-4 comparable entre les 2 groupes.[177]

→ *Après la chirurgie*

Plusieurs études fondamentales analysent la morphologie et la fonction de la couronne hyper-vasculaire qui entoure les métastases hépatiques.

Van der Wal et al. rapportent un environnement permissif proangiogénique du parenchyme hépatique péri-tumoral, avec une surexpression de facteurs angiogéniques par rapport aux métastases de manière plus prononcée chez les patients dont la tumeur primitive est en place.[154]

Terayama et al. analysaient 100 pièces opératoires de résection de MH ayant un type de croissance par remplacement et d'origine variée et ont montré que les CEs sinusoïdes co-optées en périphérie métastatique subissaient une capillarisation de l'endothélium.[55] Ces vaisseaux sanguins étaient reliés avec les sinusoïdes du foie environnant. Ce phénomène a été confirmé dans un modèle murin de MH colorectale à croissance par poussée par injection intra-splénique.[56] Durant ce processus, les CSHs αSMA positives prolifèrent à la surface des MH et un phénomène de

capillarisation des sinusoïdes se produit dans cette même région. Sous la pression intérieur de la tumeur et extérieure des CSHs proliférantes, les hépatocytes disparaissent de la périphérie tumorale, conduisant à la fusion des sinusoïdes et à l'apparition de lacs vasculaires à la surface tumorale.

Van den Eynden et al. décrivaient 3 types de croissance des MH,[46] celui par poussée étant associé à un pattern angiogénique avec un taux de prolifération des cellules tumorale et endothéliales à la jonction métastases / parenchyme non tumoral plus élevé que dans les autres types. Le taux de récidives précoces après chirurgie de résection des métastases hépatiques (<12 mois) était plus élevé dans ce groupe de mauvais pronostic, interrogeant le lien entre une angiogenèse accrue et la récidive tumorale hépatique.

Seules quelques études évaluent l'apport du bevacizumab en adjuvant de chirurgie hépatique pour MHCCR. Kemeny et al. analysent 73 patients traités en postopératoire par une chimiothérapie intra artérielle associée à une chimiothérapie systémique avec ou sans bevacizumab, sans avantage de survie dans le groupe bevacizumab mais avec une toxicité biliaire accrue dans ce groupe, représentée par l'élévation de la bilirubine (0 vs14%) ou la nécessité de mise en place de stent biliaires (0 vs 11%).[178] Wong et al. rapportent une série de 45 patients ayant des MHCCR de mauvais pronostic, définies comme initialement non résécables (n=30) ou résécables mais avec une tumeur primitive en place (n=15), traités par une chimiothérapie à base d'oxaliplatine associée à du bevacizumab en péri-opératoire. Cette équipe confirmait l'intérêt de ce schéma thérapeutique, sans analyser le rôle du bevacizumab administré en période post-opératoire.[160] Turan et al. analysent 204 patients ayant eu une résection de MHCCR, traités en post-opératoire par une chimiothérapie à base d'oxaliplatine ou d'irinotecan avec (n=87) ou sans bevacizumab (n=117).[179] Il n'y avait pas de différence en terme de survie globale et sans récidive entre les deux groupes malgré le taux de résections R1 de 26% dans le groupe bevacizumab contre 16% dans le groupe contrôle, ce qui peut faire évoquer un rôle bénéfique au bevacizumab chez les patients R1 avec comme hypothèse de traiter des cellules tumorales résiduelles localisées dans un environnement proangiogénique.

CONCLUSION

Nous commençons seulement à comprendre la complexité liée à la niche métastatique et à l'angiogenèse dans l'évolution des métastases hépatiques et particulièrement lorsque l'origine est colorectale. Des progrès substantiels sur le plan de la connaissance fondamentale sont nécessaires pour améliorer la compréhension du processus métastatique et mettre en œuvre de nouvelles thérapeutiques spécifiques comme de nouvelles stratégies.

Les objectifs de ce travail on été :

1) de créer un model murin de MHCCR, permettant

- Une analyse cinétique de l'architecture des MHCCR et des déterminants de l'angiogenèse et du microenvironnement

- Une étude de la phase précoce d'établissement des MHCCR et du rôle des cellules stellaires dans ce processus

- L'analyse de la place des progéniteurs de moelle osseuse dans le développement des MHCCR

2) d'étudier l'angiogenèse comme cible thérapeutique, avec l'analyse

- de la pertinence de l'utilisation du bevacizumab chez la souris

- l'effet de la Netrine 4, protéine anti-angiogénique, dans plusieurs modèles murins de tumeurs primitive et de métastases d'origine colorectale

- des complications cliniques du bevacizumab

- de l'implication dans la stratégie chirurgicale des métastases hépatiques colorectales du taux de VEGF et du potentiel angiogénique du microenvironnement

3) Mettre au point une technique non invasive d'évaluation par Echographie-Doppler de l'angiogenèse tumorale et physiologique

RESULTATS

1ère Partie

Création d'un model murin de MHCCR, permettant

- Une analyse cinétique de l'architecture des MHCCR et de déterminants de l'angiogenèse et du microenvironnement

- Avec étude de la phase précoce d'établissement des MHCCR et du rôle des cellules stellaires dans ce processus

- Et l'analyse de la place des progéniteurs de MO dans le développement des MHCCR

Article 1 :

Kinetic analysis of colorectal liver metastasis process: proof of the concept of prometastatic niche induction by hepatic stellate cells.

Eveno C, Hainaud P, Rampanou A, Bonnin P, Bakhouche S, Dupuy E, Contreres JO, Pocard M.

Clin Can Res, (soumis)

Dans notre étude, nous avons d'abord établi un modèle murin reproductible de métastases hépatiques d'origine colorectale et défini 4 grands stades évolutifs de ces métastases, concordant avec les résultats décrits chez l'homme en termes de taille et d'apparence. Ce modèle nous a permis d'analyser les déterminants tumoraux, de l'angiogenèse et du microenvironnement de manière cinétique.

Dans notre modèle, nous avons montré que l'infiltration des cellules stellaires hépatiques (CSHs), activées en myofibroblastes, a lieu avant le recrutement et l'organisation des cellules endothéliales (CEs) en un réseau de néovaisseaux dans les métastases.

En effet, au stade le plus précoce (J9), les cellules tumorales prolifèrent; les micrométastases étant non vascularisées, mais infiltrées par des CSHs activées et possèdent un réseau riche en laminine.

La phase d'angiogenèse active débute à J14 avec le recrutement des CEs formant un réseau vasculaire. En parallèle, nous avons observé une accentuation de la prolifération des cellules tumorales. Lors des dernières étapes (J28 et J39), une nécrose centrale apparaît progressivement au sein des métastases, avec disparition de la vascularisation centrale. Le réseau de laminine persiste, réalisant une impression du réseau vasculaire disparu, comme précédemment décrit par Mancuso et al.[143]

En outre, les CSHs synthétisent des facteurs angiogéniques tels que le VEGF et le PIGF, qui facilitent le recrutement des CEs dans la niche métastatique. La coopération entre les cellules tumorales et les CSHs a été étudiée dans de nombreux types de cancers, à la fois in vitro avec une augmentation de la prolifération, de la migration et l'invasion de plusieurs types de cellules cancéreuses et in vivo dans des modèles de tumeurs sous-cutanées avec une augmentation de la taille tumorale lorsque les souris sont co-injectées avec CSHs.[27, 59, 65, 66] Les CSHs peuvent être activées par les cellules tumorales et synthétiser des facteurs angiogéniques et des protéines de la matrice extracellulaire.[23-27] L'utilisation de modèles orthotopiques est moins fréquente dans la littérature, et le rôle pro-angiogénique des CSHs activées lors de métastases hépatiques a été démontré dans deux modèles de métastases hépatiques de mélanome et de cancer colique.[19, 24, 67]

Dans notre étude, nous avons utilisé des CSHs activées purifiées issues d'hépatocarcinome murin. In vitro, ces cellules ont un effet pro-angiogénique par l'augmentation du réseau vasculaire d'HUVEC sur matrigel en émettant des filopodes vers les cellules endothéliales. Cela confirme l'hypothèse que les CSHs activées sont capables de s'adapter à un phénotype de péricyte fonctionnel et induire la formation de néovaisseaux par sprouting à partir des CEs pour promouvoir la néoangiogenèse.[68]

Nous avons également montré que les CSHs activées exprimaient fortement la laminine, les individualisant comme la source potentielle in vivo de la laminine déposée dans la matrice extracellulaire pour préparer la niche métastatique et le switch angiogénique.

Nous avons montré que les CSHs présentes au début du processus ont été activés en myofibroblastes pour préparer la phase angiogénique en sécrétant de la laminine et des facteurs pro-angiogéniques. Le réseau vasculaire apparait au 14ème jour, et le double marquage

CD31/desmine en immunohistochimie a montré que les CSHs activées sont co-localisées avec CEs dans le réseau vasculaire. Les CSHs activées sont observées à proximité ou à la jonction du maillage de ce réseau principalement composé de CEs. Cette même localisation de CSHs a été reproduite *in vitro* sur Matrigel avec des HUVECs.

Ces résultats nous ont poussé à étudier si les CSHs activées par la tumeur pouvaient accroître le potentiel pro-angiogenique et métastatique dans notre modèle de métastases hépatiques. Les métastases hépatiques chez les souris co-injectées avec des CSH activées et des cellules tumorales étaient plus fréquentes, plus vascularisées et avec un taux de prolifération plus élevé avec un marquage Ki67 et CD31 plus prononcé. Dans ce groupe, l'infiltration des CSHs activées était présente au sein de la tumeur et fortement à la périphérie, ce qui sous-tend un rôle précoce dans la création des métastases hépatiques. Ces résultats sont concordants avec nos marquages préliminaires de métastases hépatiques d'origine humaine, orientant vers un rôle précoce des CSHs activées dans le processus métastatique hépatique. Toutefois, l'obtention de métastases aux stades précoces par prélèvement chirurgical chez l'homme est souvent difficile, ce d'autant qu'il est souvent effectué une chimiothérapie, d'autant plus avec des anti-angiogéniques associés en préopératoire, pouvant perturber l'analyse des différents marqueurs. En outre, la relevance clinique de tous nos modèles expérimentaux est discutable, l'injection directe de cellules dans le foie de souris immunodéprimées n'étant pas la réplique exacte de ce qui se passe chez l'homme. De ce fait, une validation complète de notre hypothèse pourrait être difficile à obtenir.

En conclusion, nous avons établi un modèle en 4 étapes reproductible de métastases hépatiques d'origine colorectale, permettant une analyse cinétique du processus métastatique et de ses déterminants. Le modèle actuel permet de tester de nouvelles cibles thérapeutiques à différentes étapes du processus métastatique. Nos données fournissent la preuve que les cellules stellaires hépatiques, activées par les cellules tumorales, précèdent l'infiltration de cellules endothéliales et permettent de construire un microenvironnement permissif pour le switch angiogénique et la croissance métastatique. Elles jouent donc un rôle dans la formation de la niche métastatique. Ainsi, les cellules hépatiques stellaires pourraient être une nouvelle cible thérapeutique pour l'inhibition de l'interaction tumeur-stroma dans le cancer colorectal métastatique.

Kinetic analysis of colorectal liver metastasis process: proof of the concept of prometastatic niche induction by hepatic stellate cells.

EVENO Clarisse[1,2], HAINAUD Patricia[1], RAMPANOU Aurore[1], BONNIN Philippe[1,3], BAKHOUCHE Sana [1], DUPUY Evelyne[1], CONTRERES Jean-Olivier[1†], POCARD Marc[1,2]

1 Univ Paris Diderot, Sorbonne Paris Cité, INSERM U965, Angiogenèse et recherche translationnelle, Hôpital Lariboisière, Paris, France

2 Univ Paris Diderot, Sorbonne Paris Cité, AP-HP, Hôpital Lariboisière, Chirurgie Digestive, Paris, France

3 Univ Paris Diderot, Sorbonne Paris Cité, AP-HP, Hôpital Lariboisière, Physiologie Clinique Explorations Fonctionnelles, Paris, France

† Deceased

Address correspondence to:
Pr. Marc Pocard, INSERM U965, Angiogenèse et recherche translationnelle, Hôpital Lariboisière, 2 rue Ambroise Paré, 75475 Paris CEDEX 10, France.
E-mail: marc.pocard@inserm.fr
Phone: +33149958258; Fax: +3314999102

Conflict of interest:

Employment or Leadership Position: None; Consultant or Advisory Role: Pocard M. Roche;[(C)] Stock Ownership: None; Honoraria: None; Research Funding: Roche award in clinical research; Expert Testimony: None; Other Remuneration: None.

Author Contributions:

EVENO Clarisse: study concept and design; acquisition of data; analysis and interpretation of data; drafting of the manuscript; critical revision of the manuscript for important intellectual content; statistical analysis; obtained funding, study supervision

HAINAUD Patricia: acquisition of data; analysis and interpretation of data; technical, or material support

RAMPANOU Aurore: acquisition of data; technical, or material support

BONNIN Philippe: analysis and interpretation of data; drafting of the manuscript; critical revision of the manuscript for important intellectual content

BAKHOUCHE Sana: acquisition of data; technical, or material support

DUPUY Evelyne: analysis and interpretation of data; drafting of the manuscript; critical revision of the manuscript for important intellectual content

CONTRERES Jean-Olivier: acquisition of data; analysis and interpretation of data; technical, or material support

POCARD Marc: Study concept and design; analysis and interpretation of data; drafting of the manuscript; critical revision of the manuscript for important intellectual content; obtained funding; study supervision

Abstract (252 words)

Background & Aims: An interaction between tumor cells and the microenvironment, as well as the development of angiogenesis, are required to form liver metastases (LM). Methods: Immunofluorescence detection of α-smooth muscle actin (αSMA), desmin, Ki67, laminin and CD31 was used to analyze the kinetics of tumor angiogenesis determinants, especially the contribution of hepatic stellate cells (HSC) to angiogenesis in hepatic metastasis produced by intrasplenically

injected LS174 colorectal cancer cells. Immunostaining was performed at various times (Days 9, 14, 28, 39). Results: At the earliest stage, micro-metastases consisted of proliferating cancer cells, a well-organized network of activated HSCs and laminin deposits. No vascular network was observed. As the LMs grew in size, an organized vascular network appeared; the laminin network colocalized with CD31 immunostaining. At the later stages, all of the immunostained markers became peripheral as a central necrosis developed. Purified activated HSCs isolated from the livers of transgenic mice developing hepatocellular carcinoma secreted laminin and showed enhanced HUVEC network formation in a Matrigel assay. In a coinjection LM experiment, activated-HSCs enhanced the metastatic process. Moreover, colorectal LMs from six patients were analyzed, and a pattern of marker distribution similar to the coinjection experiment was found in human LMs. Conclusions: for the first time, our results show that HSCs play a crucial role in organizing and accelerating the progression of metastasis in modulating the prometastatic niche, interacting with colorectal cancer cell recruitment and the organization of angiogenesis during colorectal LM development. Therefore, HSCs may be an early therapeutic target in colorectal cancer therapies.

Keywords:

Activated Hepatic Stellate Cells; Angiogenesis; Colorectal Liver Metastases; Metastatic Niche; Microenvironment.

Financial Support:

This study was partly supported by a grant for training in translational research in oncology from the French National Cancer Institute (INCa).

List of Abbreviations:

LM: Liver Metastases

α-SMA; α-Smooth Muscle Actin

CD31: Cluster of Differentiation 31

HSC: Hepatic Stellate Cells

HUVECs: Human Umbilical Vein Endothelial Cells

VEGF: Vascular Endothelial Growth Factor

FOLFOX: Fluorouracil Leucovorin Oxaliplatin

ECs: Endothelial Cells

HES: Hematin Eosin Safran

HCC: Hepatocellular Carcinoma

EBM: Minimum Essential Medium

TBS: Tris-Buffered Saline

BSA: Bovine Serum Albumin

Introduction

Tumor progression towards metastasis is a multistage process in which malignant cells spread from the primary tumor to colonize distant organs.[1] Paget's 'seed and soil' theory for metastasis introduced the concept that a receptive microenvironment is required for malignant cells to engraft into distant tissues and form metastases.[2] The term metastatic niche describes the specialized microenvironment that supports malignant cell maintenance and actively regulates cell function and proliferation, suggesting that a suitably conducive microenvironment [3] must evolve for tumor cells to be able to engraft (metastatic niche) and proliferate to form clinically detectable metastases. The progression from micro- to macro-metastases requires the assembly of a functional vasculature to enable cellular expansion, a process for which the activation of an "angiogenic switch" is mandatory.[4,5]

Colorectal cancer is the second leading cause of cancer death in North America and Western Europe.[6,7] Approximately 20% of patients have detectable liver metastases at diagnosis, and nearly 50% of the patients will develop metachronous liver metastasis, which is the predominant cause of death.[8-10] Bevacizumab, a humanized monoclonal antibody targeting vascular endothelial growth factor (VEGF), is a pioneering antiangiogenic drug that demonstrates clinical benefits in combination with chemotherapy in patients with advanced metastatic colorectal cancer.[11,12] In several clinical trials, Bevacizumab reduced the growth of liver metastasis; however, in conjunction with FOLFOX therapy, Bevacizumab failed to significantly prolong disease-free survival in stage II and III colon cancer patients,[13] failing to target the early angiogenesis of colorectal LM and the "angiogenesis switch". The failure of Bevacizumab to prevent the initiation of the metastatic process in clinical trials underlines the fact that angiogenic factors could be different at early or late stages in the development of liver metastasis. Therefore, the development of new therapeutic strategies involving angiogenic factors and other components in the microenvironment of the metastatic niche is critical to improve the prognosis for patients with colorectal liver metastasis. We need to analyze the kinetic of the determinant of angiogenesis and microenvironment to suitably target them at the proper step of the liver metastasis process. This prometastatic microenvironment in the liver consists of both noncellular and cellular components,[14,15] including hepatocytes, Kupffer cells, hepatic stellate cells (HSCs), endothelial cells (ECs) and lymphocytes.

Hepatic stellate cells (HSCs), which are liver-specific pericytes, are important in forming pre-metastatic niches because they can transdifferentiate from a state of quiescence into highly proliferative and mobile myofibroblasts upon induction by tumor cells[16,17] and tumor-activated sinusoidal cells.[18] Activated-HSCs are responsible for remodeling and depositing a tumor-associated extracellular matrix and have been involved in the migration and growth of several types of metastatic cells.[14,16,17,19,20] These cells also promote tumor angiogenesis by producing multiple angiogenic factors, including VEGF and angiopoietin 1 and 2, that promote endothelial cell (EC) function.[21-25]

Here, we established a murine model of colorectal liver metastasis mimicking the human metastatic process to analyze the kinetics of the different markers of angiogenesis, as well as the role of HSCs in this process.

Material and methods

Animal Models of Liver Metastasis:

Every experimental protocol satisfied all of the standard requirements of the European community guidelines for the care and use of laboratory animals. Five-week-old female Nod Scid mice (Charles River Laboratories International Inc., Wilmington, MA) were acclimated for 1–2 weeks before tumor transplantation. Animals were anesthetized with xylazine (20 µg/g body weight, Bayer, Division Santé Animale, Puteaux, France) and ketamine (50 µg/g body weight, Virbac, Carros, France).

Under sterile conditions, LS174 cells (*$2x10^6$ cells*) with or without the co-injection of activated-HSCs (*$1x10^6$ cells*) were surgically injected into the spleen. First, a 10-mm left subcostal incision was made to expose the spleen over the peritoneum. The cell suspension was then injected into the spleen using a 27 G needle. Following light splenic compression, the spleen was repositioned into the abdominal cavity, peritoneum and muscles were sutured closed with some stitches and the wound was closed with a clip. To analyze the multistep angiogenic processes during metastasis progression, mice were sacrificed at 9, 14, 28 and 39 days after inoculation with

tumor cells (10 animals sacrificed on each date). Microspecimens of the liver were harvested at different times for pathological confirmation of liver metastasis by hematin eosin safran (HES) coloration: at days 9 (micrometastasis stage), 14 (beginning of metastasis visibility), 28 and 39.

Animal models of hepatocellular carcinoma

Transgenic C57Bl6/ASV-B male mice developing hepatocellular carcinoma (HCC) in a multistep angiogenic and tumor progression from the hyperplastic to the diffuse stage of HCC have been previously described.[26] Briefly, precise targeting of the SV40 T early region expression in the liver of transgenic mice was achieved using 700 base pairs of the antithrombin regulatory sequences to control oncogene expression.[27]

Cell Lines

Hepatic stellate cells were isolated from HCC livers of ASV-B mice (16 weeks of age). HCC mice were anesthetized with xylazine (20 µg/g body weight, Bayer, Division Santé Animale, Puteaux, France) plus ketamine (50 µg/g body weight, Virbac, Carros, France) to expose the portal vein via a laparotomy. The liver was perfused through the portal vein with a canula (22 G, Vygon, Ecouen, France) connected to a peristaltic pump. The hepatic vein was split. The liver was perfused with 250 ml of perfusion buffer (0.2 M NaCl, 2.7 mM KCl, 0.7 mM Na_2HPO_4, 10 mM Hepes pH 7.65) at 37 °C at a flow rate of 10 ml/min, followed by 100 ml of perfusion buffer supplemented with 6.5 mM $CaCl_2$ and 20 µg/ml Liberase (Roche Diagnostics GmbH, Penberg, Germany) at 37 °C at a flow rate of 5 ml/min. After perfusion, the liver was carefully excised and rinsed two times with 20 ml of perfusion buffer. The liver capsule was peeled off, and the liver was dissociated in 100 ml of M199-10% FCS at 37 °C to dissociate the cells. To eliminate the hepatocyte fraction, the crude cell suspension was filtered through a 60-pm mesh nylon screen **(**SCRYNEL NY60HC, VWR, Fontenay-sous-Bois, France**)** with 100 ml of M199 medium (20% FCS, 15 mM HEPES, 2 mM glutamine plus antibiotics, Gibco) followed by sedimentation of the cell suspension for 30 min. The supernatant fraction was washed four times in M199 10% SVF with centrifugation at 800 rpm for 5 min. The

cells were cultivated in EBM (20% FCS, 2 mM glutamine, 15 mM HEPES pH 7.5 plus antibiotics (Promocell)) on collagen type I-coated dishes (Roche). The primary cell cultures showed two major populations that were identified as endothelial cells and HSCs using CD31 and desmin labeling, respectively. Activated-HSCs were selected using their typical morphological appearance and presence of lipid inclusions, and expanded in EBM2-20% FCS. Immunostaining for desmin was used to assess the purity of the cultures.

Human umbilical vein endothelial cells (HUVECs) isolated from the human umbilical vein by collagenase digestion were cultured in EBM2 supplemented with 20% FCS and 2 ng/ml FGF-2. For cell experiments, subconfluent HUVEC cultures were serum-deprived in M199-3% BSA for 18 hours.

Migration Assay

Activated-HSCs ($5x10^4$ cells/well) were plated on collagen coated 6-well plates in EBM-20% FCS for 5 days. Mechanical wounding of 50% of the culture was performed and HUVECs ($3x10^4$ cells/well) were seeded in the wounded area and cultured for 3 days in EBM-20% FCS before immunostaining.

Matrigel™ Assay

To characterize the HUVEC interaction with activated-HSCs, cells ($1x10^6$) were first labeled for 5 min at 37°C then for 15 min at 4°C with either 4 µg/ml Dio SP-Dioc (HUVECs) or 1 µg/ml CM-Dil (activated-HSCs), then washed twice in phosphate-buffered saline (PBS) before seeding. Activated-HSCs, HUVECs or both cell types ($1x10^6$cells/well) were seeded onto Matrigel (BD Biosciences, Le Pont-de Claix, France) in 12-well culture plates in EBM2 with or without 20% FCS. Capillary-like structure formation was observed after 24 hours (Zeiss, Axio Observer Z.1). Images were acquired using a digital camera (Baumer TXD14. Radeberg, Germany). The number of sprouts

was quantified with Histolab software (Microvision, Evry, France). The results were the mean ± S.D. of three experiments performed in duplicate.

Immunofluorescence staining

Serial liver sections were prepared as previously described. [28] For the assays, 5-µm-thick cryostat sections were fixed in cold acetone for 10 minutes, washed with Tris-buffered saline (TBS)/0.05% Tween-20 three times, and then incubated for 20 minutes in a TBS/Tween-20/0.75% normal serum blocking solution. The primary antibody was either omitted or incubated with an excess of blocking peptide for negative controls. Liver sections were incubated with the specific primary antibody, followed by the appropriate Alexa Fluor® antibodies. For desmin/CD31, α-SMA/CD31, laminin/CD31 double immunostaining, the sections were incubated with rat anti-CD31 antibody (1/50) and then with rabbit anti-desmin, anti-α-SMA or anti-laminin antibodies. This was followed by incubation with an Alexa Fluor® 488 goat anti-rat antibody for CD31 and an Alexa Fluor® 555 goat anti-rabbit antibody for the other primary antibodies.

Cells were fixed in cold acetone for 10 minutes, washed twice in phosphate–buffered saline (PBS), blocked in PBS containing 10 mg/ml bovine serum albumin (BSA) and incubated with the specific primary antibody in PBS-BSA followed by the appropriate Alexa Fluor® antibodies. Immunostained cells were analyzed using a standard fluorescence microscope (Zeiss, Microvision, Evry, France).

Reagents

The following antibodies were used for immunofluorescence staining experiments: rat anti-mouse CD31 (1/50) (Pharmingen Becton Dickinson, Le Pont de Claix, France), rabbit anti-smooth muscle actin (α-SMA) (1/50), rabbit antiKi67 (1/100) (Abcam, Cambridge, UK), rabbit anti-laminin (1/100) (L-9393) (Sigma, Saint Louis, MO, USA), rabbit anti-desmin (1/50) (RB-9014) (Neomarker Inc. Fremont, CA, U.S.A.) and mouse anti-pancytokeratin (1/100) (Abcam, Cambridge, UK). Secondary antibodies for immunostaining were goat anti-rabbit Alexa Fluor® 488 (1/200) and

donkey anti-rat Alexa Fluor® 555 (1/200) (Interchim, Asnières, France). All cell culture reagents were obtained from Invitrogen (Cergy, France).

Patients

Human and experimentally induced animal colorectal LMs were compared. For the comparison, we analyzed the angiogenic characteristics of liver metastases in humans. Six patients who underwent surgical resection for colorectal liver metastasis were selected from our institutional database. Fresh tissue samples of tumors were taken during hepatectomy. The histologic diagnosis was confirmed for each specimen. Immunostaining was performed as described for animal models. Written informed consent for molecular analysis of surgical samples was obtained from each patient, and our ethical committee approved the protocol.

Results

Activated-HSC Infiltration Precedes the formation of a Neovessel Network and Colocalizes with Endothelial Cell Recruitment Sites in Hepatic Metastasis. At the earliest stages, three days after LS174 cell injection, the cancer cells, depicted in the lumen of the sinusoid vessel, adhere to the endothelium (Fig. Supl 1A), invade the basal membrane matrix (Fig. Supl 1B) and start to duplicate in the liver parenchyma (Fig. Supl 1C).

Concurrent assessment of hepatic stellate cells (HSCs) and endothelial cells (ECs) by specific immunostaining revealed that the infiltration of the HSCs activated into myofibroblasts occurred before the recruitment and organization of ECs into a neovessel network within the metastasis.

By day 9, pan-cytokeratin-positive LS174 cells proliferated in the metastasis as revealed by Ki67 immunostaining (Fig. 1B). The major event at this stage was the infiltration of the metastases by desmin-positive HSCs (Fig. 1D, E) and the presence of an extracellular matrix rich in laminin within the metastases (Fig. 1F). These intra-metastatic HSCs were activated into myofibroblasts and expressed α-SMA (Fig. Supl 2). A few CD31-positive endothelial cells were mainly observed at the

periphery of the metastasis without any formation of a neovessel network (Fig. 1C, D). At day 14, LS174 cells were highly proliferative (Fig. 2B). Desmin-positive HSCs and CD31-positive ECs formed a well-organized neovessel network within the metastases (Fig. 2C, D). Desmin/CD31 double immunostaining showed that HSCs and ECs colocalized in this network, in which the extracellular matrix was composed of laminin. Interestingly, HSCs were mainly observed at the sprout junctions of this network. Later at day 28, necrosis began to occur within metastases with many LS174 cells that did not express Ki67 (Fig. 3B). We observed a disruption of the neovessel network with a marked decrease of CD31-positive ECs and many desmin-positive HSCs, while a laminin-positive network was still observed, as shown by the immunostaining of serial liver sections (Fig. 3C, D). When CD31-positive ECs were still observed within the metastases, they did not form a network but were associated with laminin. At day 39, a central necrosis was present in the metastasis with decreased detection of Ki67-positive LS174 cells (Fig. 4B). Interestingly, the vascular network was localized at the periphery of the metastasis where the extracellular matrix was composed of laminin (Fig. 4C, D). Semi-quantitative kinetics of the different angiogenesis markers could thus be established. The SMA marker was maximal at day 9 then decreased. Laminin, CD31, desmin and Ki67 markers were maximal at day 14 then slightly decreased (Fig. Supl 3).

HSCs isolated from HCC livers are activated and interact with ECs

The non-parenchymal crude primary cell cultures isolated from HCC livers showed two major cell populations, identified as endothelial cells labeled by CD31 and smaller HSCs labeled by desmin (Fig. 5A). HSCs harboring a typical stellate morphology (arrow, Fig. 5A) were selected and amplified. Positive desmin and negative CD31 or MAC3 (data not shown) immunostaining confirmed the purity of the culture (Fig. 5B). Some of the HSCs isolated from the HCC livers had already acquired a myofibroblast phenotype with a fusiform shape and expression of α-SMA (Fig. 5C). These activated-HSCs showed cytoplasmic expression of laminin (Fig. 5D) and were used for coculture experiments. We thus investigated whether crosstalk between HSCs and endothelial cells (ECs) occurred. Close interactions were observed when HUVECs were cocultured with HSCs. HSCs

covered the monolayer of HUVECs and interacted through the extension of long filopodia towards the ECs (Fig. 5E, F).

We thus studied the interactions of HUVECs and HSCs in Matrigel. HUVECs formed a few sprouts without any network organization and HSCs showed a stellate morphology (Fig. 6A). The network formed by both HUVECs and HSCs was markedly enhanced when plated together on Matrigel (mean ± SEM: 21 ± 1.73; 3.3 ± 0.33 and 47 ± 7.01 for HUVECs alone; HSCs alone and HUVECs+HSCs, respectively, $p<0.05$, Fig. 2B). To analyze the cellular interactions, HUVECs were labeled with DiI [180] and HSCs with DIOC [181]. Interestingly, the network was mainly composed of ECs, and the HSCs were located at the junction of the network and extended filopodia towards the ECs (Fig. 6C). This aspect has been also observed *in vivo* at day 39 (Fig Supl 4).

Activated HSCs Promote Liver Metastasis

Nine days after tumor transplantation, the incidence of liver metastasis development in mice was significantly greater in the group where HSCs were co-injected with LS174 cells compared to the group in which LS174 cells alone were injected (n=10 and 12 per group, 80% *vs.* 33%, respectively for LS174+HSCs and LS174 groups, $p < 0.01$, Fig. 7A). The number of liver metastases per mouse was significantly increased in the LS174+HSCs group (6.5 ± 0.80) compared to the LS174 group (1.67 ± 0.33) ($P < 0.001$, Fig. 7B), indicating that the injection of activated-HSCs increases the tumor growth of orthotopically implanted colorectal liver metastasis.

The morphology of liver metastases resulting from the co-injection of colorectal tumor cells and HSCs appeared to have the same pattern as regular liver metastases at the same stage. Pan-cytokeratin-positive LS174 cells proliferated at a high rate in the metastases (Fig. 7C), which were poorly vascularized as shown by CD31 staining (Fig. 7E); however, the presence of an extracellular matrix rich in laminin within the metastases (Fig. 7D) and the infiltration by desmin-positive HSCs (Fig. 7F), which were also more pronounced at the periphery, affirmed the implication of HSCs in the enhancement of the liver metastatic process.

Human Liver Metastasis shows the same pattern as liver metastasis in mice

We confirmed the colorectal origin of the human LM with hematoxylin-eosin (Figure Supl 5A) and pancytokeratin immunostaining (Fig. Supl 5B). Laminin (Fig. Supl 5F) and CD31 (Fig. Supl 5C) immunostaining revealed an irregular network in the same pattern as that of the intermediate stage murine LM. Immunostaining for desmin (Fig. Supl 5D) and α-SMA (Fig. Supl 5E) was present in only a small part of the LM, indicating that if activated-HSC participation is occurring, it might occur in the anterior portion during early LM.

Discussion

The development of colorectal liver metastasis depends on the interactions between tumor cells and the liver microenvironment.[29] The most important of the metastatic steps,[30] i.e., the "angiogenic switch", allowing the progression from non-vascularized micro-metastases to macro-metastases,[4,5,31] is essential and considered to be rate-limiting.[32] To date, no treatment is able to target the liver metastasis "angiogenic switch". The combination of Bevacizumab and FOLFOX failed to significantly prolong disease-free survival in stage II and III colon cancer patients.[13] The need to find new treatments targeting the metastatic process and early angiogenesis requires the use of preclinical models to understand the process and to test new strategies.[33] In our study, we first established a reliable mouse model of colorectal LM and defined 4 main stages of liver metastasis evolution consistent with previous findings in human regarding size and appearance. This model allows us to analyze tumor, angiogenic and microenvironment determinants in a kinetic manner.

Here, we show that infiltration of HSCs activated into myofibroblasts occurred before the recruitment and organization of ECs into a neovessel network within metastases. Indeed, at the earliest stage (day 9), the micro-LM was slowly proliferating and poorly vascularized, but was infiltrated by activated hepatic stellate cells (HSCs) and rich in extra cellular matrix (ECM) laminin. The angiogenic phase began at day 14 with the recruitment of ECs and the formation of a vascular network. In parallel, a high cancer cell proliferation rate was observed. At the latest stages, as

central necrosis began to appear in the LM, and the central vascularization disappeared; interestingly, the laminin network was still present and making a print of the past vascular network, as previously shown by Mancuso et al.[34] When necrosis filled the LM, activated HSCs were again found at the periphery of the metastasis with a rich laminin network in the adjacent liver parenchyma that accompanies tumor cell proliferation ready to reinitiate the 4-stage cycle of LM progression. We also showed that activated-HSCs strongly expressed laminin that was deposited in the extracellular matrix to prepare the metastatic niche and the angiogenic switch. Moreover, HSCs synthesized the angiogenic growth factors VEGF and PlGF, which facilitate the recruitment of ECs to the metastatic niche. Crosstalk between tumor cells and HSCs has been investigated in numerous types of cancer, both *in vitro* with an increase of proliferation, migration and invasion of several types of examined cancer cells and in subcutaneous tumor models with an increase of tumor size observed when mice are co-injected with HCSs.[25,35-37] HSCs may be activated by tumor cells to synthesize angiogenic factors and extracellular matrix proteins.[21-25]

The utilization of orthotopic models is less common, and the proangiogenic role of activated HSCs during liver metastasis has been shown in two models of melanoma and colon LM.[16,22,38] In our study, we first purified HCC-activated HSCs and confirmed that these cells promote angiogenesis *in vitro* by improving the HUVEC vascular network and extending filopodia towards ECs. These activated HSCs may also participate in ECM remodeling through laminin secretion. This confirms the hypothesis that activated-HSCs are capable of adapting to a functional pericyte phenotype and inducing the formation of tubular sprouts by ECs to promote neoangiogenesis.[39]

In our current model, we show that HSCs present at the beginning of the process were activated into myofibroblasts to prepare for the angiogenic phase by secreting laminin and proangiogenic factors. The vascular network appeared at day 14, and CD31/desmin double immunostaining showed that HSCs co-localized with ECs in the vascular network. HSCs were observed near or at the sprout junctions of this network mainly composed of ECs (Fig 3, Supporting Fig. 3). The similar localization of HSCs was observed in the *in vitro* Matrigel assay performed with HUVECs.

These results prompted us to investigate whether tumor-activated HSCs can increase angiogenesis and metastatic potential in our model of liver metastasis. Liver metastases in the co-injected mice

were more frequent, more proliferative and more vascularized with Ki67 and CD31 immunostaining strongest within the LM. In this group, HSC infiltration was present within the tumor and strongly at the periphery, underlying its role in the establishment of early liver metastasis. We also report some preliminary results in human LMs, attesting to the early role of HSCs in the metastatic process in the liver. However, obtaining very early metastasis in human liver surgical specimens is very difficult. Because the actuality of all of our experimental models is debatable, as direct injection of cells into the livers of immunocompromised mice is not exactly what happens in humans, a complete validation of our hypothesis could be difficult to obtain.

In conclusion, we established a reproducible 4-step model of colorectal liver metastasis, allowing for a kinetic analysis of the metastatic process and its determinants. The current model allows testing some new targets and sequential stages. Thus, our data provide evidence that tumor-activated hepatic stellate cells precede endothelial cell infiltration and build a permissive microenvironment for the angiogenic switch and metastatic growth. Thus, HSCs could be a new therapeutic target for the inhibition of the tumor–stromal interaction in metastatic colorectal cancer.

Figure Legends:

Figure 1: Microscopic appearance of colorectal LM growth, tumor angiogenesis and tumor cell proliferation in nude mice 9 days after an intra-splenic LS174 cell xenograft.

(A) Confirmation with HES coloration of the presence of a micro LM (star). (B) Proliferation of colon cancer cells in the LM (Ki67 immunostaining). (C) Low density of ECs within the LM (CD31 immunostaining) (D). High density of activated HSCs in the LM (desmin immunostaining) with secretion of laminin (F) making an early network in the extracellular network. (E) Confirmation of the arrival of activated-HSCs prior to vessel network realization (CD31/desmin double immunostaining). Original magnification, X 20.

Figure 2: Microscopic appearance of colorectal LM growth, tumor angiogenesis and tumor cell proliferation in nude mice 14 days after an intra-splenic LS174 cell xenograft.

(A) Macro LM (star) in HES coloration. (B) A high rate of cancer cell proliferation is observed within the LM (Ki67 immunostaining). (C-E) The organization of a vascular network is observed within the LM with co-localization of ECs (CD31 immunostaining) and pericytes (desmin immunostaining). (F) The persistence of the laminin network is observed. Original magnification, X 20.

Figure 3: Microscopic appearance of colorectal LM growth, tumor angiogenesis and tumor cell proliferation in nude mice 28 days after an intra-splenic LS174 cell xenograft.

(A) LM (star) in HES coloration. (B) A decrease in the proliferation rate of cancer cells is observed (Ki67 immunostaining). (C-E) A decrease in vascular density within the LM with the appearance of necrosis is observed. (F) The persistence of the laminin network is observed. Original magnification, X 20.

Figure 4: Microscopic appearance of colorectal LM growth, tumor angiogenesis and tumor cell proliferation in nude mice 39 days after an intra-splenic LS174 cell xenograft.

(A) LM in HES coloration. (B) A decrease in the proliferation rate of cancer cells is observed (Ki67 staining). (C-E) A decrease in the vascular density persistent at the LM periphery with a large

central area of necrosis (star) is observed. (F) The persistence of the laminin network is observed. Original magnification, X 20.

Figure 5: HSCs isolated from HCC livers are activated and interact with ECs

(A) Non-parenchymal crude primary cell cultures with two identified major cell populations, endothelial cells (green, CD31 stained) and HSCs (red, desmin stained) with a characteristic stellate form (arrows). (B) Ascertainment of HSC culture purity (desmin positive) with a proportion of activated cells expressing the myofibroblast phenotype (α-SMA positive, C) and an extracellular matrix protein (laminin, D). (E and F) When cocultured with HUVECs, HSCs interact through the extension of long filopods. Original magnification, X 20; *inset*, X 100.

Figure 6: The network formed by both HUVECs and HSCs was markedly enhanced when plated together on Matrigel (A and B) Alone, HUVECs formed few sprouts, and HSCs shared their stellate morphology; the network formed by both cells in the co-culture was markedly enhanced on Matrigel. Original magnification, X 20. (C) The network was mostly composed of ECs (Dill staining in red), and the HSCs (DIOC immunostaining in green) were located at the junction of the network and extended filopodia towards the ECs. Original magnification, X 40. *, $P<0.05$.

Figure 7: Activated HSCs Promote Liver Metastasis (A and B) Ten days after tumor transplantation, the incidence of mice developing visible LMs and the number of LMs were significantly greater in the LS174 and HSCs co-injection group compared with the LS174 alone group. **, $P<0.01$; ***, $P<0.001$. The morphological appearance of liver metastasis resulting from co-injection of colorectal tumor cells and HSCs: tumor cells are highly proliferative (pan-cytokeratin immunostaining, C) and poorly vascularized (CD31 immunostaining, E), with an extracellular matrix rich in laminin (D) and infiltration by desmin-positive HSCs more pronounced (F). Original magnification, X 10.

Figure Suppl 1: Three days after an intra-splenic LS174 cell xenograft.

The cancer cells in the lumen of the sinusoids adhere to the endothelium (A), invade it (B) and start to multiply in the liver parenchyma (C). Original magnification, X 100 (A and B), X 10 (C).

Figure Suppl 2: Nine days after an intra-splenic LS174 cell xenograft.

(A) Alpha-SMA immunostaining highlights the LM infiltration by activated-HSCs. Original magnification, X 20.

Figure Suppl 3: Semi-quantitative analysis of the kinetics of the different angiogenic markers.

Figure Suppl 4: Thirty-nine days after an intra-splenic LS174 cell xenograft.

(A) Vascular network at the LM periphery with co-localization of ECs (green, CD31 immunostaining) and pericytes (red, desmin immunostaining). Original magnification, X 100.

Figure Suppl 5: Human Liver Metastasis shows the same pattern as liver metastasis in mice (A and B) The colorectal origin of the human LM (star) was confirmed using HES and pan-cytokeratin immunostaining. Laminin (F) and CD31 (C) immunostaining exhibit an irregular network. Desmin (D) and α-SMA (E) immunostaining was present in only a small part of the LM (arrows). Original magnification, X 10.

References:

1. Gupta GP, Massague J. Cancer metastasis: building a framework. Cell 2006;127:679-695.

2. Paget S. The distribution of secondary growths in cancer of the breast. 1889. Cancer Metastasis Rev 1989;8:98-101.

3. Kaplan RN, Riba RD, Zacharoulis S, Bramley AH, Vincent L, Costa C, MacDonald DD, et al. VEGFR1-positive haematopoietic bone marrow progenitors initiate the pre-metastatic niche. Nature 2005;438:820-827.

4. Holmgren L, O'Reilly MS, Folkman J. Dormancy of micrometastases: balanced proliferation and apoptosis in the presence of angiogenesis suppression. Nat Med 1995;1:149-153.

5. Naumov GN, Akslen LA, Folkman J. Role of angiogenesis in human tumor dormancy: animal models of the angiogenic switch. Cell Cycle 2006;5:1779-1787.

6. Jemal A, Siegel R, Ward E, Hao Y, Xu J, Murray T, Thun MJ. Cancer statistics, 2008. CA Cancer J Clin 2008;58:71-96.

7. Lieberman D. Progress and challenges in colorectal cancer screening and surveillance. Gastroenterology 2010;138:2115-2126.

8. Leonard GD, Brenner B, Kemeny NE. Neoadjuvant chemotherapy before liver resection for patients with unresectable liver metastases from colorectal carcinoma. J Clin Oncol 2005;23:2038-2048.

9. Mahmoud N, Bullard Dunn K. Metastasectomy for stage IV colorectal cancer. Dis Colon Rectum 2010;53:1080-1092.

10. Stangl R, Altendorf-Hofmann A, Charnley RM, Scheele J. Factors influencing the natural history of colorectal liver metastases. Lancet 1994;343:1405-1410.

11. Kabbinavar F, Hurwitz HI, Fehrenbacher L, Meropol NJ, Novotny WF, Lieberman G, Griffing S, et al. Phase II, randomized trial comparing bevacizumab plus fluorouracil (FU)/leucovorin (LV) with FU/LV alone in patients with metastatic colorectal cancer. J Clin Oncol 2003;21:60-65.

12. Kabbinavar FF, Hambleton J, Mass RD, Hurwitz HI, Bergsland E, Sarkar S. Combined analysis of efficacy: the addition of bevacizumab to fluorouracil/leucovorin improves survival for patients with metastatic colorectal cancer. J Clin Oncol 2005;23:3706-3712.

13. Allegra CJ, Yothers G, O'Connell MJ, Sharif S, Petrelli NJ, Colangelo LH, Atkins JN, et al. Phase III trial assessing bevacizumab in stages II and III carcinoma of the colon: results of NSABP protocol C-08. J Clin Oncol 2011;29:11-16.

14. Ahmad SA, Berman RS, Ellis LM. Biology of colorectal liver metastases. Surg Oncol Clin N Am 2003;12:135-150.

15. Vidal-Vanaclocha F. The prometastatic microenvironment of the liver. Cancer Microenviron 2008;1:113-129.

16. Olaso E, Santisteban A, Bidaurrazaga J, Gressner AM, Rosenbaum J, Vidal-Vanaclocha F. Tumor-dependent activation of rodent hepatic stellate cells during experimental melanoma metastasis. Hepatology 1997;26:634-642.

17. Shimizu S, Yamada N, Sawada T, Ikeda K, Kawada N, Seki S, Kaneda K, et al. In vivo and in vitro interactions between human colon carcinoma cells and hepatic stellate cells. Jpn J Cancer Res 2000;91:1285-1295.

18. Mendoza L, Carrascal T, De Luca M, Fuentes AM, Salado C, Blanco J, Vidal-Vanaclocha F. Hydrogen peroxide mediates vascular cell adhesion molecule-1 expression from interleukin-18-activated hepatic sinusoidal endothelium: implications for circulating cancer cell arrest in the murine liver. Hepatology 2001;34:298-310.

19. Monvoisin A, Bisson C, Si-Tayeb K, Balabaud C, Desmouliere A, Rosenbaum J. Involvement of matrix metalloproteinase type-3 in hepatocyte growth factor-induced invasion of human hepatocellular carcinoma cells. Int J Cancer 2002;97:157-162.

20. Theret N, Musso O, Turlin B, Lotrian D, Bioulac-Sage P, Campion JP, Boudjema K, et al. Increased extracellular matrix remodeling is associated with tumor progression in human hepatocellular carcinomas. Hepatology 2001;34:82-88.

21. Kang N, Gores GJ, Shah VH. Hepatic stellate cells: partners in crime for liver metastases? Hepatology 2011;54:707-713.

22. Olaso E, Salado C, Egilegor E, Gutierrez V, Santisteban A, Sancho-Bru P, Friedman SL, et al. Proangiogenic role of tumor-activated hepatic stellate cells in experimental melanoma metastasis. Hepatology 2003;37:674-685.

23. Taura K, De Minicis S, Seki E, Hatano E, Iwaisako K, Osterreicher CH, Kodama Y, et al. Hepatic stellate cells secrete angiopoietin 1 that induces angiogenesis in liver fibrosis. Gastroenterology 2008;135:1729-1738.

24. Torimura T, Ueno T, Kin M, Harada R, Taniguchi E, Nakamura T, Sakata R, et al. Overexpression of angiopoietin-1 and angiopoietin-2 in hepatocellular carcinoma. J Hepatol 2004;40:799-807.

25. Zhao W, Zhang L, Yin Z, Su W, Ren G, Zhou C, You J, et al. Activated hepatic stellate cells promote hepatocellular carcinoma development in immunocompetent mice. Int J Cancer 2011;129:2651-2661.

26. Dupuy E, Hainaud P, Villemain A, Bodevin-Phedre E, Brouland JP, Briand P, Tobelem G. Tumoral angiogenesis and tissue factor expression during hepatocellular carcinoma progression in a transgenic mouse model. J Hepatol 2003;38:793-802.

27. Dubois N, Bennoun M, Allemand I, Molina T, Grimber G, Daudet-Monsac M, Abelanet R, et al. Time-course development of differentiated hepatocarcinoma and lung metastasis in transgenic mice. J Hepatol 1991;13:227-239.

28. Hainaud P, Contreres JO, Villemain A, Liu LX, Plouet J, Tobelem G, Dupuy E. The role of the vascular endothelial growth factor-Delta-like 4 ligand/Notch4-ephrin B2 cascade in tumor vessel remodeling and endothelial cell functions. Cancer Res 2006;66:8501-8510.

29. van der Wal GE, Gouw AS, Kamps JA, Moorlag HE, Bulthuis ML, Molema G, de Jong KP. Angiogenesis in synchronous and metachronous colorectal liver metastases: the liver as a permissive soil. Ann Surg 2012;255:86-94.

30. Hanahan D, Weinberg RA. The hallmarks of cancer. Cell 2000;100:57-70.

31. Hanahan D, Folkman J. Patterns and emerging mechanisms of the angiogenic switch during tumorigenesis. Cell 1996;86:353-364.

32. Luzzi KJ, MacDonald IC, Schmidt EE, Kerkvliet N, Morris VL, Chambers AF, Groom AC. Multistep nature of metastatic inefficiency: dormancy of solitary cells after successful extravasation and limited survival of early micrometastases. Am J Pathol 1998;153:865-873.

33. Van Cutsem E, Lambrechts D, Prenen H, Jain RK, Carmeliet P. Lessons from the adjuvant bevacizumab trial on colon cancer: what next? J Clin Oncol 2011;29:1-4.

34. Mancuso MR, Davis R, Norberg SM, O'Brien S, Sennino B, Nakahara T, Yao VJ, et al. Rapid vascular regrowth in tumors after reversal of VEGF inhibition. J Clin Invest 2006;116:2610-2621.

35. Amann T, Bataille F, Spruss T, Muhlbauer M, Gabele E, Scholmerich J, Kiefer P, et al. Activated hepatic stellate cells promote tumorigenicity of hepatocellular carcinoma. Cancer Sci 2009;100:646-653.

36. Matsusue R, Kubo H, Hisamori S, Okoshi K, Takagi H, Hida K, Nakano K, et al. Hepatic stellate cells promote liver metastasis of colon cancer cells by the action of SDF-1/CXCR4 axis. Ann Surg Oncol 2009;16:2645-2653.

37. Okabe H, Beppu T, Hayashi H, Ishiko T, Masuda T, Otao R, Horlad H, et al. Hepatic stellate cells accelerate the malignant behavior of cholangiocarcinoma cells. Ann Surg Oncol 2011;18:1175-1184.

38. Badiola I, Olaso E, Crende O, Friedman SL, Vidal-Vanaclocha F. Discoidin domain receptor 2 deficiency predisposes hepatic tissue to colon carcinoma metastasis. Gut 2011.

39. Wirz W, Antoine M, Tag CG, Gressner AM, Korff T, Hellerbrand C, Kiefer P. Hepatic stellate cells display a functional vascular smooth muscle cell phenotype in a three-dimensional co-culture model with endothelial cells. Differentiation 2008;76:784-794.

Eveno et al. Fig. 1

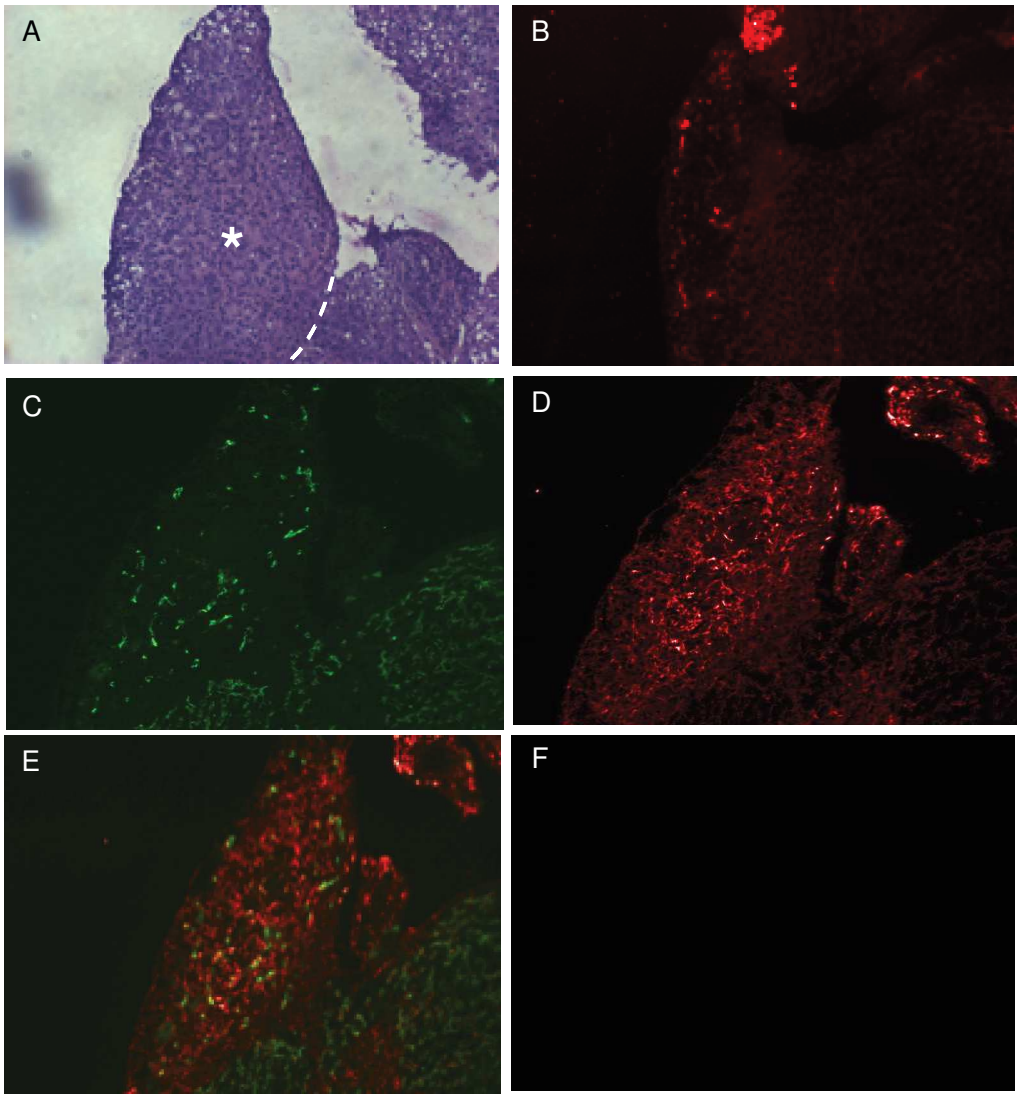

Eveno et al. Fig. 2

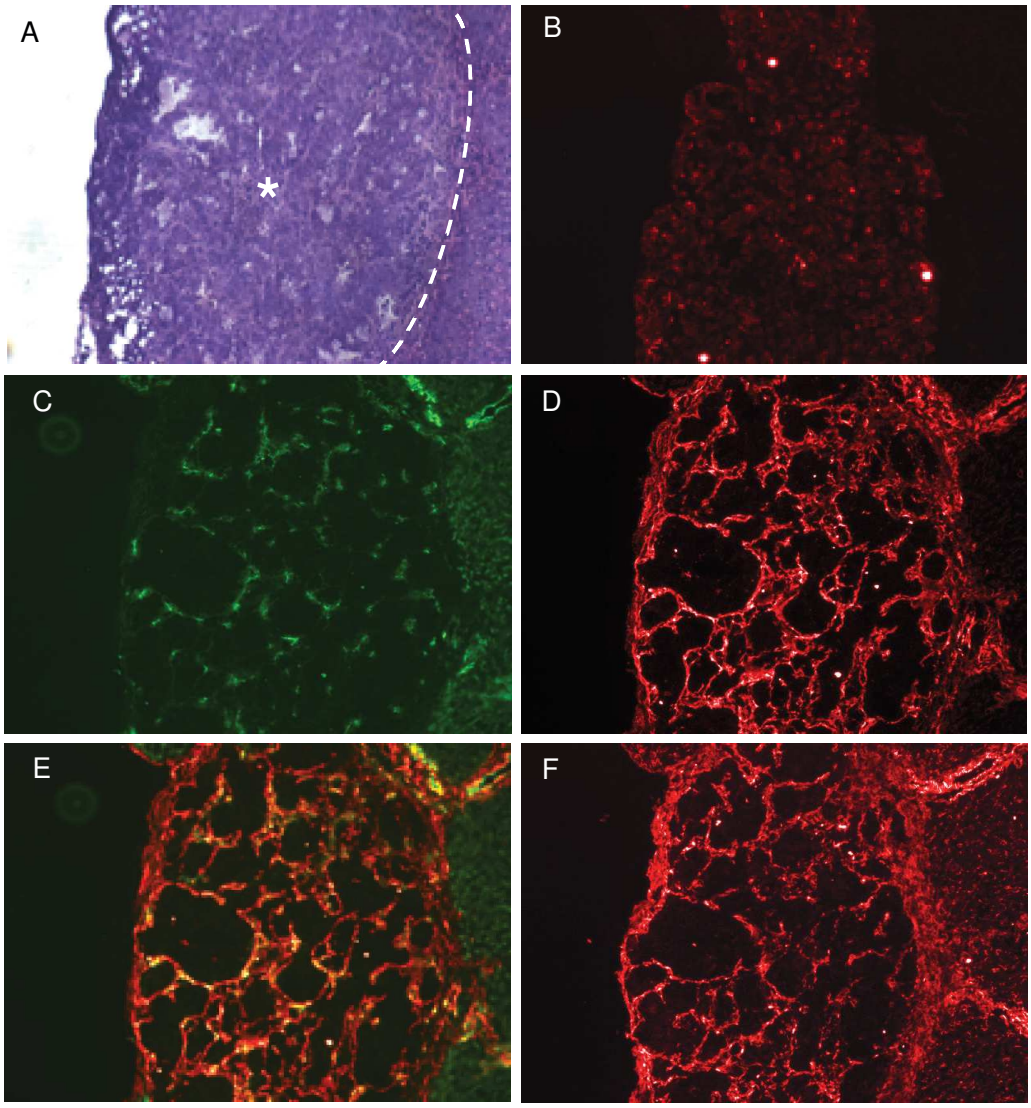

Eveno et al. Fig. 3

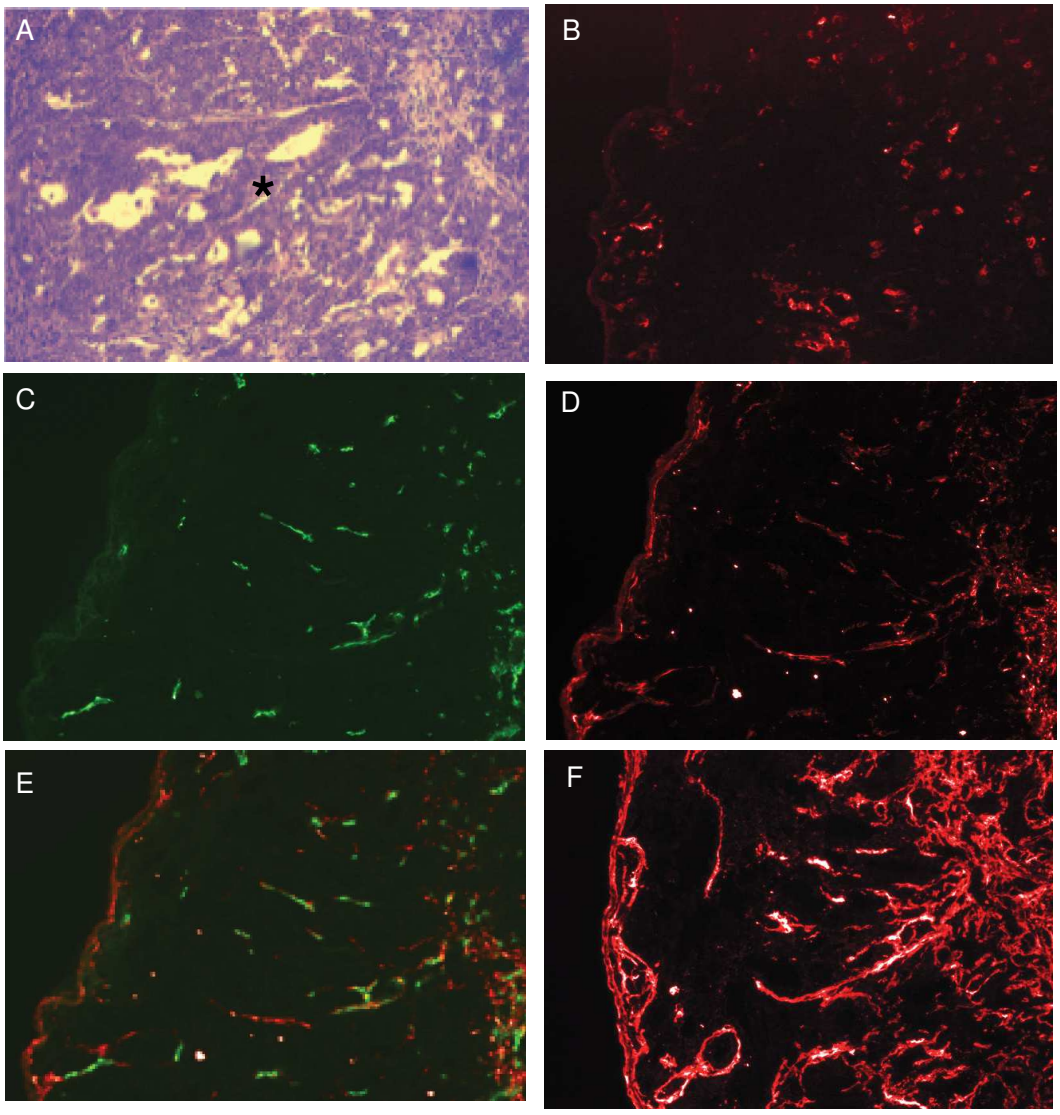

Eveno et al. Fig. 4

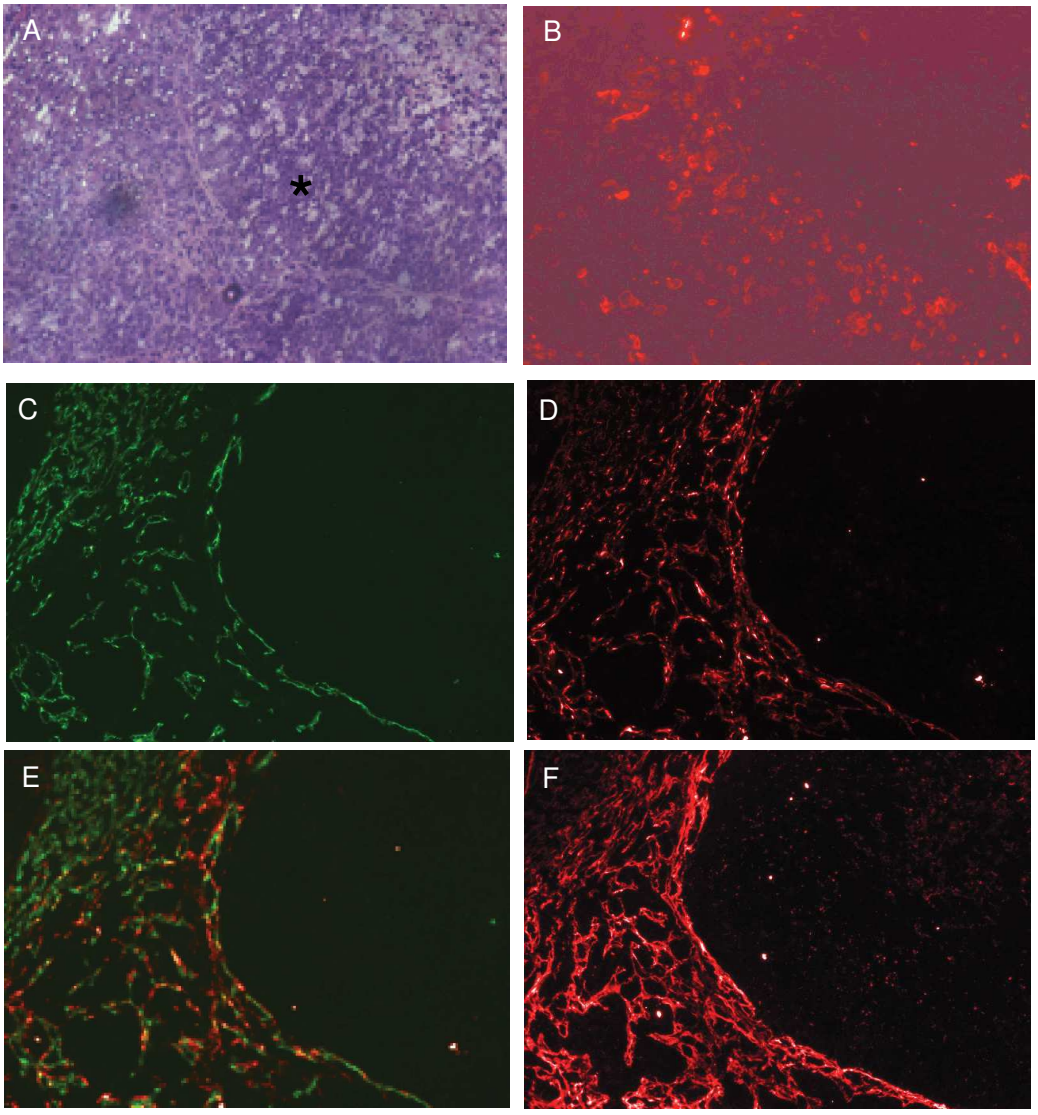

Eveno et al. Fig. 5

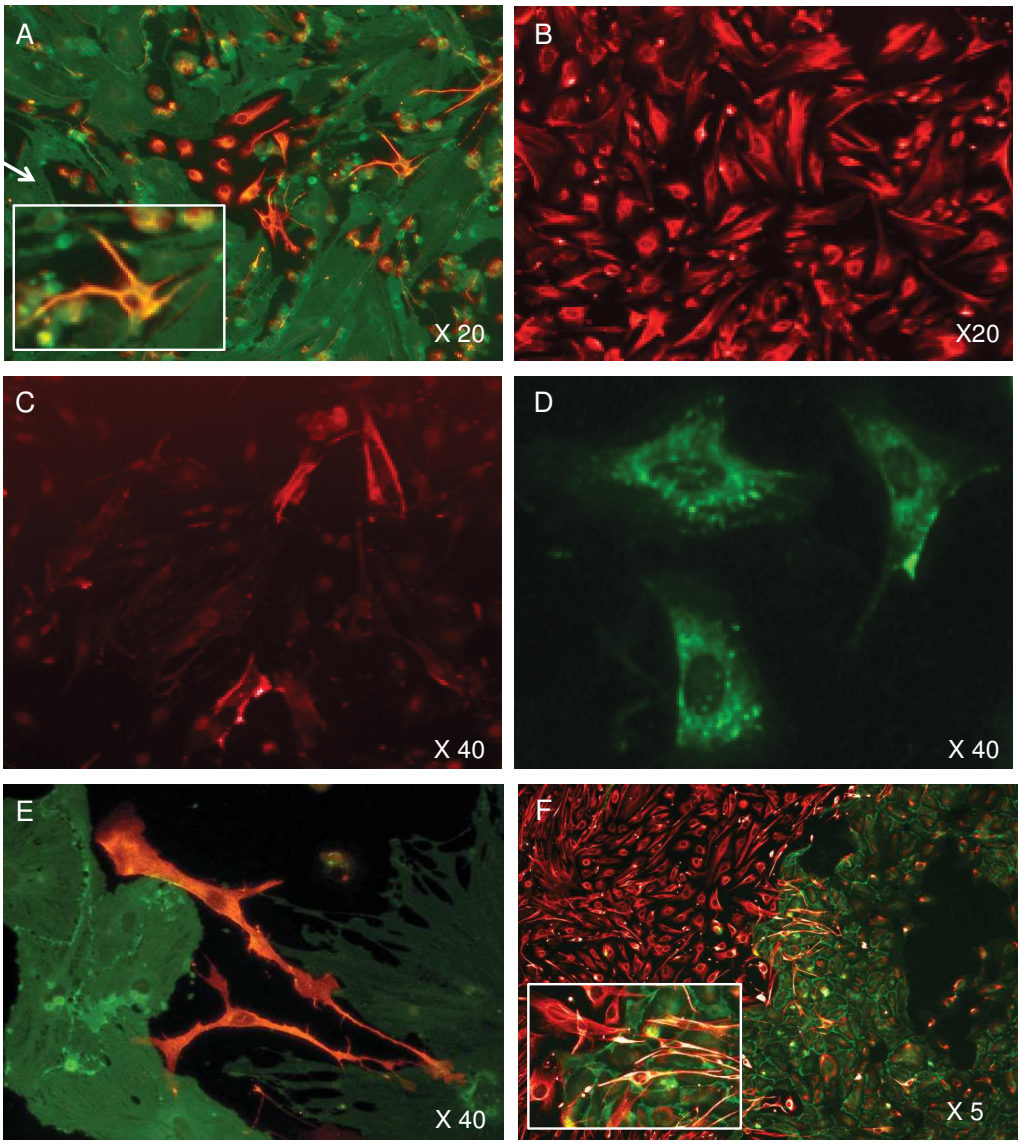

Eveno et al. Fig. 6

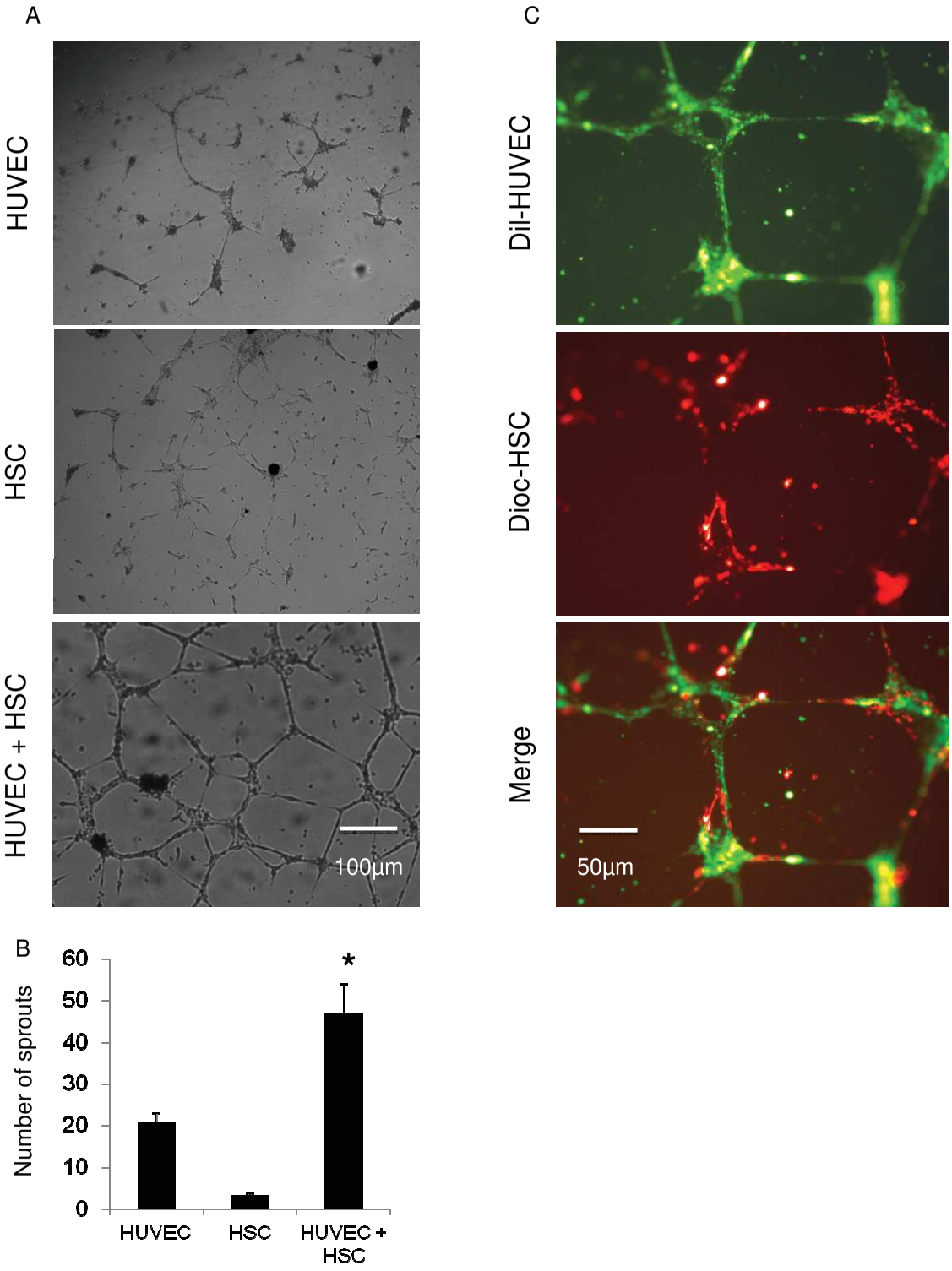

Eveno et al. Fig. 7

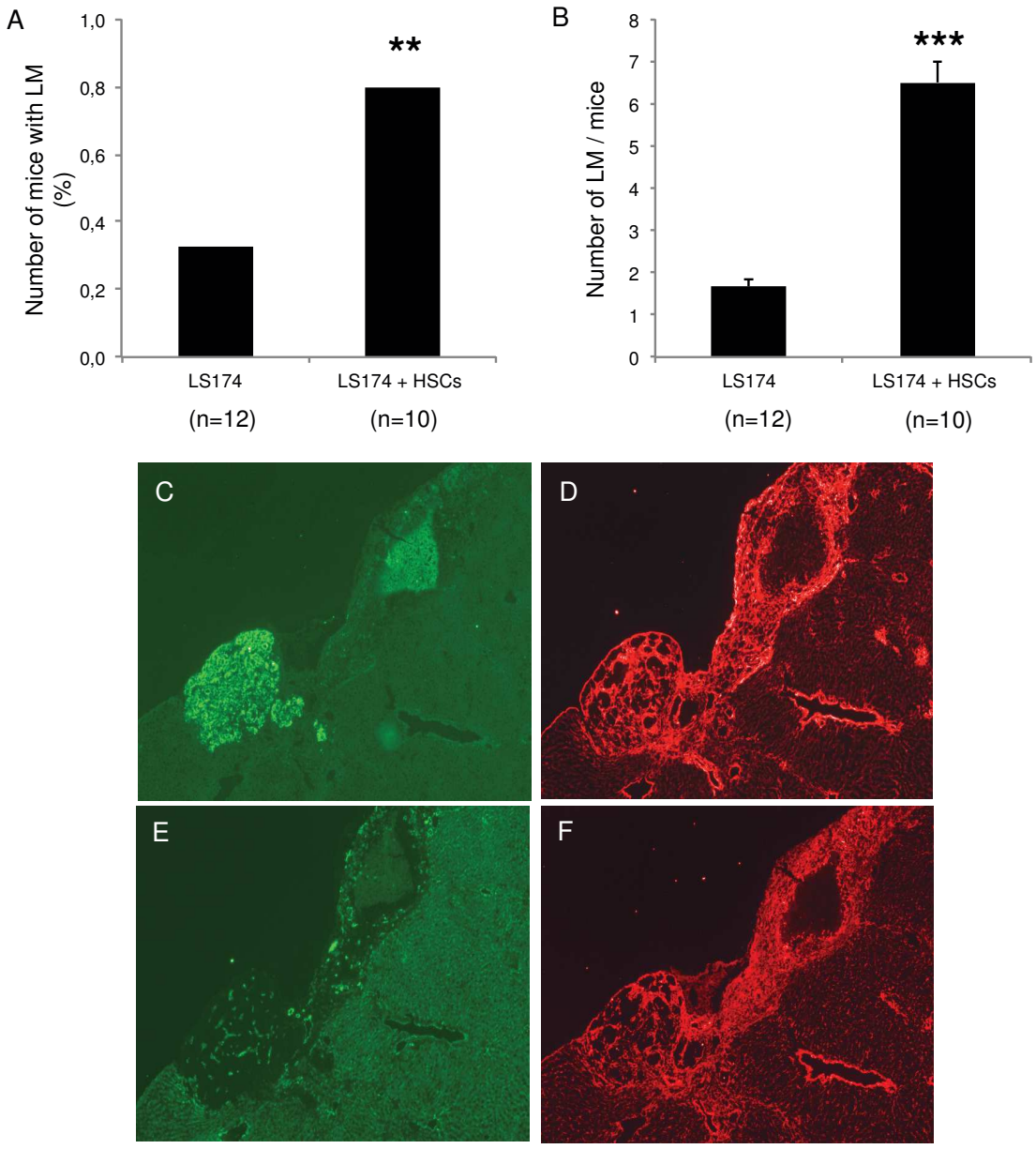

Eveno et al. Fig. SUPL 1

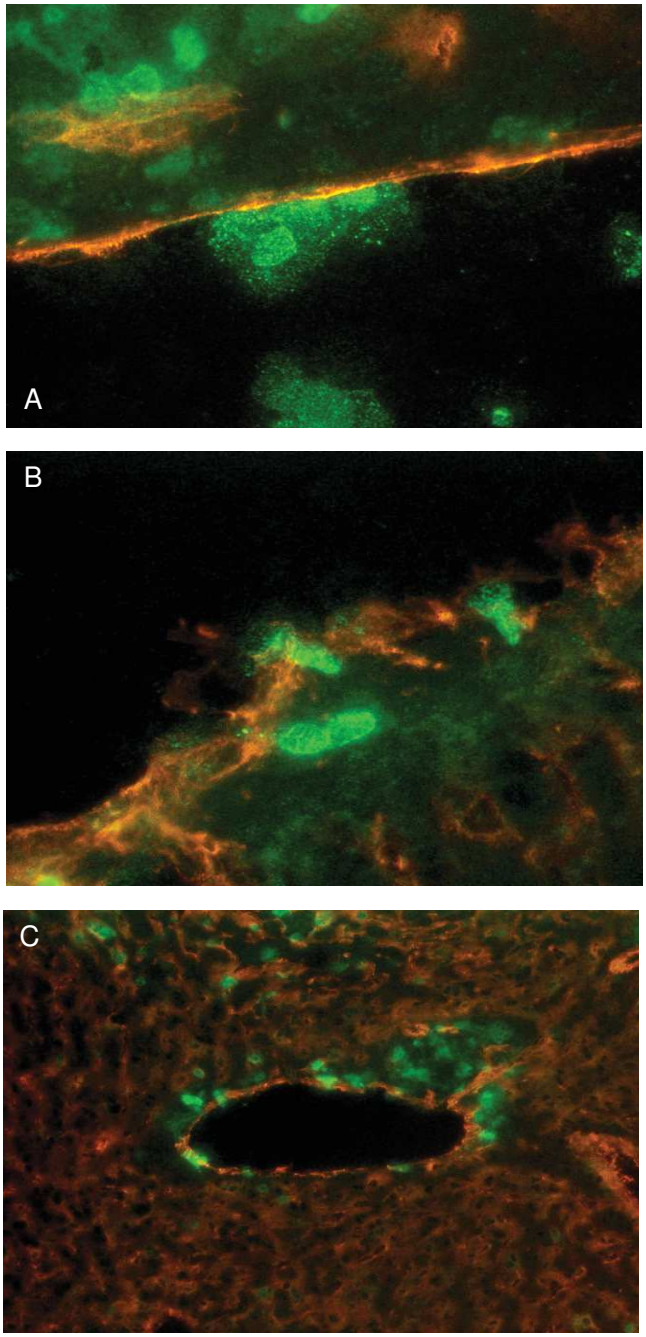

Eveno et al. Fig. SUPL 2

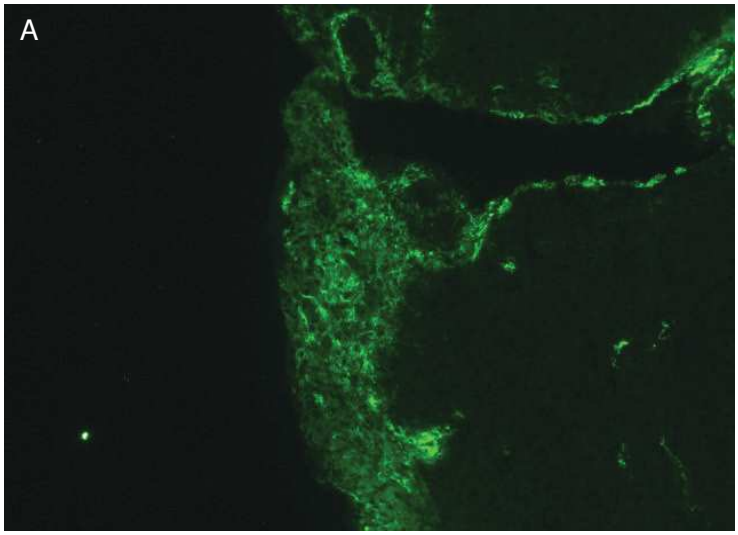

Eveno et al. Fig. SUPL 3

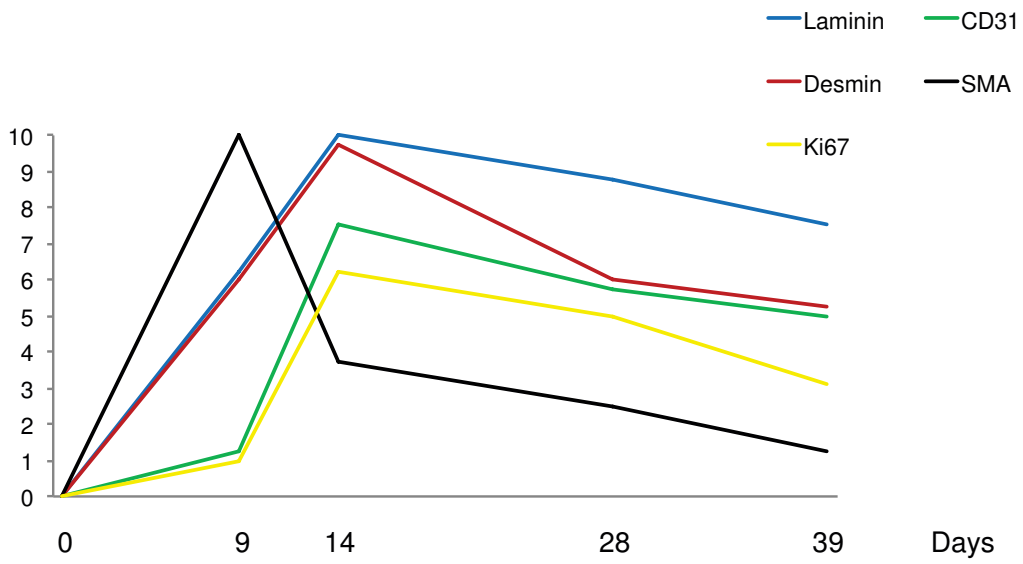

Eveno et al. Fig. SUPL 4

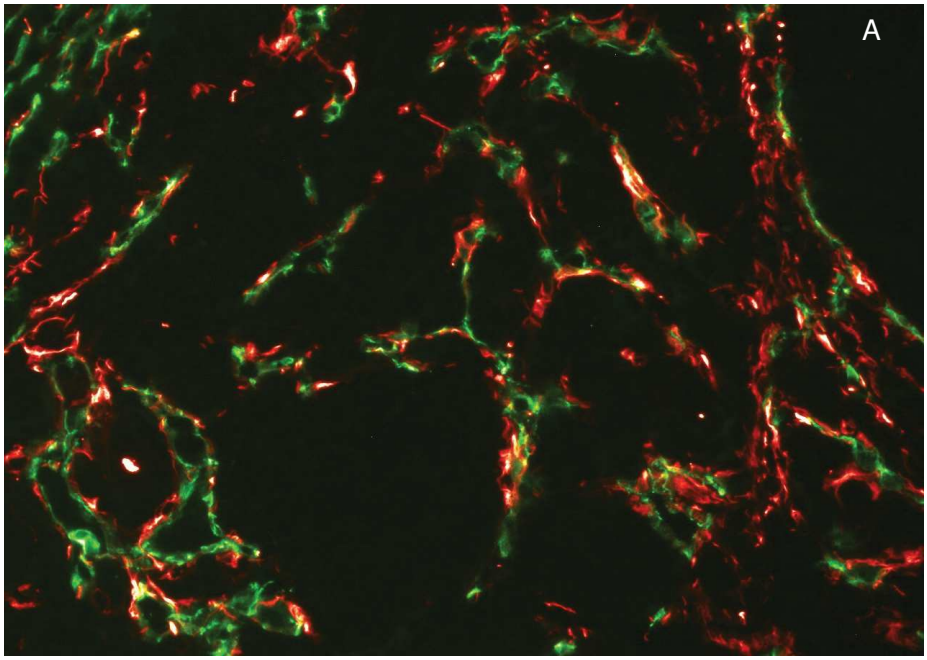

Eveno et al. Fig. SUPL 5

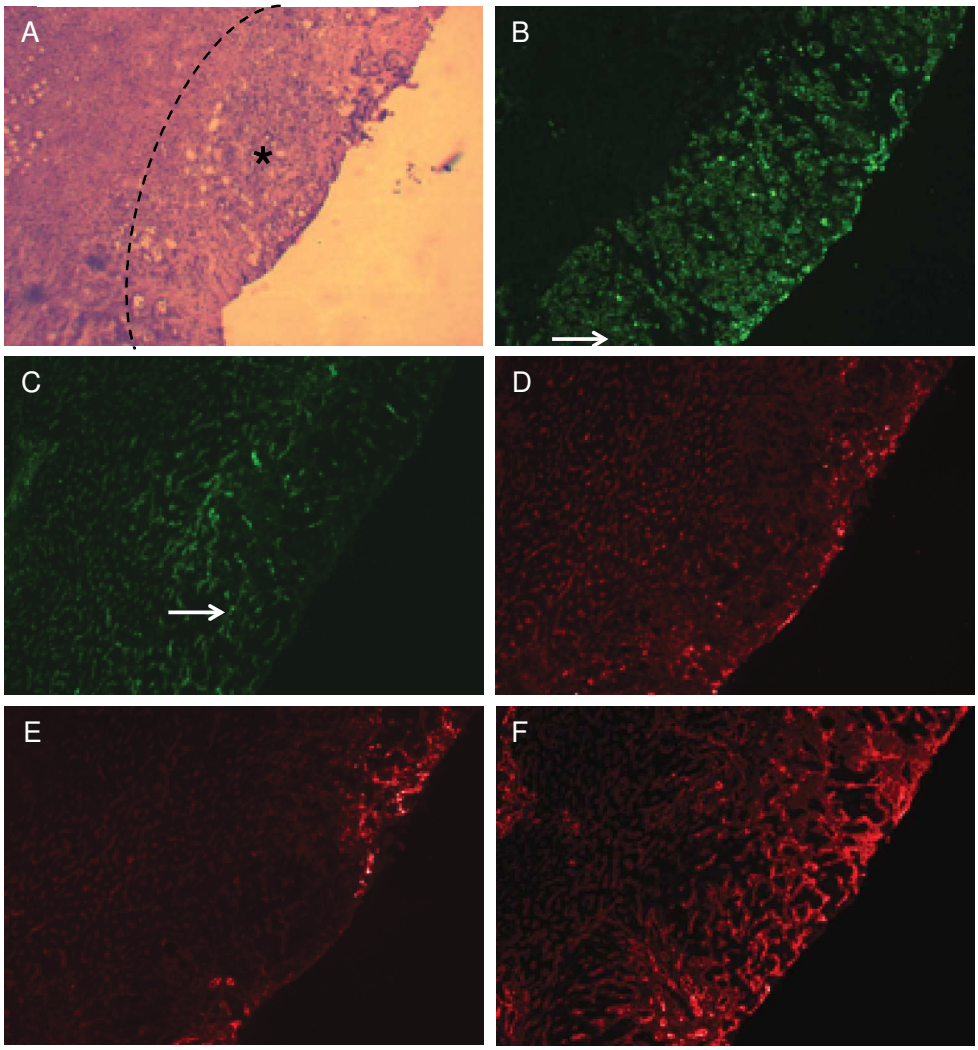

Lettre à l'éditeur 1 :

Bone marrow-derived endothelial and hematopoietic precursors cells enhance the metastasis of colon cancer in an orthotopic murine model.

Audollent R, Eveno C, Contreres JO, Hainaud P, Rampanou A, Dupuy E, Brouland JP, Pocard M.

Int J Cancer. 2011 Nov 1;129(9):2304-5.

Les cellules dérivées de moelle osseuse (CDMOs) participent au microenvironnement tumoral et à la progression métastatique,[13, 15, 16, 182] par la modification du site prémétastatique avant l'arrivée des cellules tumorales, préparant la niche prémétastatique. Shinagawa et al. évaluent la coinjection intrasplénique de cellules de cancer colique humaines KM12SM avec des cellules souches mesenchymateuses (CSMs).[183] Ils rapportent une augmentation du potentiel métastatique dans le groupe avec CSMs avec un nombre plus élevé de métastases hépatiques après 4 semaines. De plus, les CSMs entouraient la tumeur et étaient fonctionnellement incorporé dans le stroma tumoral et exprimaient les marqueurs de fibroblastes associés au cancer.

Ce manuscrit nous a incité à analyser la pertinence du modèle murin et rapporter notre expérience dans notre modèle orthotopique de métastases hépatiques par injection intra-splénique de cellules de cancer colique LS174.

Nous avons trié les CDMOs par fluorescence, obtenues à partir de moelle osseuse de souris GFP C57 BL/6-Tg, par gradient de densité. La population cellulaire contenait 30% de précurseur endothéliaux et hématopoïétiques dérivés de moelle osseuse exprimant CD 133. A J0 (jour de l'injection intra-splénique de LS174), nous avons injecté des CDMOs ou du PBS dans la veine caudale de la queue des souris porteuses de tumeurs.

Au 38ème jour, l'injection de CDMOs augmentait le processus métastatique avec un taux de 56% de micro ou macrométastases dans le groupe CDMOs contre 20% dans le groupe PBS. Le marquage en immunofluorescence par GFP des CDMOs montre que ces cellules sont localisés au front d'invasion tumorale et colocalisés avec les cellules endothéliales.

Nous avons donc montré que les BMDCs injectées par voie systémique se localisent préférentiellement autour de la tumeur. Améliorer la compréhension des mécanismes moléculaires de l'interaction entre les cellules tumorales et CDMOs pourrait permettre de mettre au point de nouvelles thérapies ciblées pour traiter les métastases hépatiques d'origne colorectale. Il semble aussi important d'identifier des situations cliniques ou les CDMOs pourraient être activées et voir leur concentration augmenter ce qui favoriserait un processus métastatique et imaginer des stratégies pour contrôler les CDMOs dans ces situations cliniques. L'ischémie, en particulier post hépatectomie pourait être une de ces situations.

UICC
global cancer control

IJC
International Journal of Cancer

Bone marrow-derived endothelial and hematopoietic precursors cells enhance the metastasis of colon cancer in an orthotopic murine model

Raphaelle Audollent[1], Clarisse Eveno[1,2,3], Jean-Olivier Contreres[1], Patricia Hainaud[1], Aurore Rampanou[1], Evelyne Dupuy[1,3], Jean-Philippe Brouland[1,3,4] and Marc Pocard[1,2,3]

[1] Unité Inserm U965, équipe "Angiogenèse et Recherche Translationnelle," hôpital Lariboisière, Institut des Vaisseaux et du Sang, 8, rue Guy-Patin, 75475 Paris cedex 10, France
[2] Département médico-chirurgical de pathologie digestive, Hôpital Lariboisière, 2, rue Ambroise-Paré, 75475 Paris cedex 10, France
[3] Université Paris-Diderot, Paris-7, France
[4] Département d'Anatomopathologie, Hôpital Lariboisière, 2, rue Ambroise-Paré, 75475 Paris cedex 10, France

Dear Sir,

We have read with great interest the article by Shinagawa *et al.*[1] In their study, they evaluated transplantation of the KM12SM human colon cancer cell line mixed with mesenchymal stem cells (MSCs) into the spleen. They reported a significantly greater number of liver metastases at 4 weeks with the cell mixture than with the transplantation of KM12SM cells alone. Additionally, MSCs surrounding the tumour were functionally incorporated into the stroma of the orthotopic colon tumour and expressed carcinoma-associated fibroblast markers.

This manuscript prompted us to analyze the relevance of the murine model.

To induce liver metastasis, a human colon cancer line (LS174) was injected into the spleen of nude mice. First, we characterized the bone marrow-derived cell (BMDC) population by fluorescence-activated cell sorting isolated on green mice C57 BL/6-Tg obtained after a density gradient. The population contained 30% of BM-derived endothelial precursor cells and derived haematopoietic precursor cells that expressed CD 133. At day 0, we injected BMDCs or PBS into the tail veins of tumor-bearing mice.

At day 38, the injection of BMDCs enhanced the metastatic process in our model of liver metastasis with a number of micro or macrometastases in 56% of the BMDC group ($n = 16$) versus 20% in the PBS group ($n = 20$), $p < 0.05$. Immunofluorescent staining of cut liver specimens has demonstrated that BMDCs labelled with Green fluorescent protein (GFP) always localized to the tumour invasion front and colocalized with endothelial cells (Fig. 1).

There is increasing evidence that BMDCs participate in the tumour microenvironment and metastatic progression,[2–5] possibly by previous modification of the metastatic site by the BM-derived precursor cell before tumour cell arrival,[4] which has led to the emergence of the concept of the premetastatic niche.

We have corroborated the findings of Shinagawa *et al.* with a second type of human colon cancer cell line (LS174) in another original murine model of orthotopic liver metastasis. This method of BMDC supply was even systemic, which is more interesting than coinjection because the BMDCs localize preferentially and not around the tumour by necessity. Our choice of BMDCs was innovative due to the absence of sorting of the different cells that constitute the injected solution; this solution was at least a third bone marrow-derived endothelial and haematopoietic precursors cells.

For the first time, we have proposed a functional role for bone marrow-derived endothelial and haematopoietic precursors cells in tumour angiogenesis and metastasis enhancement in an orthotopic nude mice model.

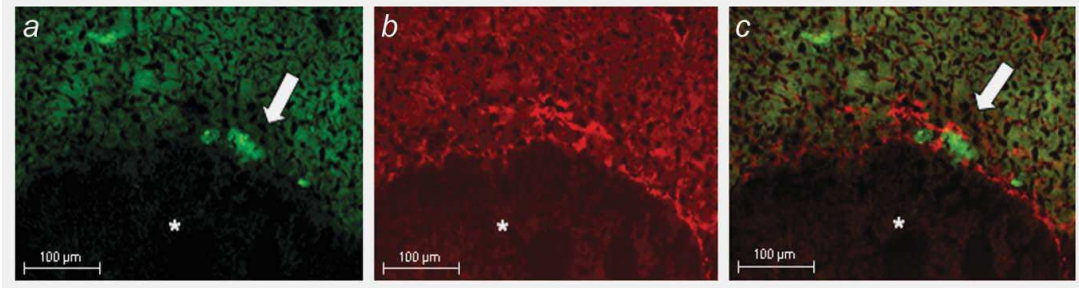

Figure 1. Migration of BMDCs to the stroma of a metastatic liver tumor (*): GFP-labeled BMDCs are localized to the tumor invasion front (*a*) and colocalized with endothelial cells (CD31 labeling in red) (*b*). (*c*) Merge (green and red).

Controlling the effects of BMDCs and understanding the molecular pathways of interaction between tumour cells and BMDCs or MSCs could be a new targeted therapy for liver colon metastasis.

Yours sincerely,
Raphaelle Audollent
Clarisse Eveno
Jean-Olivier Contreres
Patricia Hainaud
Aurore Rampanou
Evelyne Dupuy
Jean-Philippe Brouland
Marc Pocard

References

1. Shinagawa K, Kitadai Y, Tanaka M, Sumida T, Kodama M, Higashi Y, Tanaka S, Yasui W, Chayama K. Mesenchymal stem cells enhance growth and metastasis of colon cancer. *Int J Cancer* 2010;127: 2323–33.
2. Hiratsuka S, Nakamura K, Iwai S, Murakami M, Itoh T, Kijima H, Shipley JM, Senior RM, Shibuya M. MMP9 induction by vascular endothelial growth factor receptor-1 is involved in lung-specific metastasis. *Cancer Cell* 2002;2:289–300.
3. Hiratsuka S, Watanabe A, Aburatani H, Maru Y. Tumour-mediated upregulation of chemoattractants and recruitment of myeloid cells predetermines lung metastasis. *Nat Cell Biol* 2006;8:1369–75.
4. Kaplan RN, Riba RD, Zacharoulis S, Bramley AH, Vincent L, Costa C, MacDonald DD, Jin DK, Shido K, Kerns SA, Zhu Z, Hicklin D, et al. VEGFR1-positive haematopoietic bone marrow progenitors initiate the pre-metastatic niche. *Nature* 2005;438:820–7.
5. Psaila B, Lyden D. The metastatic niche: adapting the foreign soil. *Nat Rev Cancer* 2009;9:285–93.

DOI: 10.1002/ijc.25882
History: Received 17 Nov 2010; Accepted 2 Dec 2010; Online 28 Dec 2010

Correspondence to: Marc Pocard, Département Médico-Chirurgical de Pathologie Digestive, Hôpital Lariboisière, 2, rue Ambroise Paré, 75475 Paris Cedex 10, France, Tel.: 00331-49-95-82-58, Fax: 00331-49-95-91-02, E-mail: marc.pocard@lrb.aphp.fr

2nde Partie

Etudier l'angiogenèse comme cible thérapeutique, avec l'analyse

- de la pertinence de l'utilisation du bevacizumab chez la souris

- l'effet de la Netrine 4, protéine anti-angiogénique, dans plusieurs modèles murins de tumeurs primitive et de métastases d'origine colorectale

Le bevacizumab diminue la croissance des métastases hépatiques dans plusieurs essais cliniques, mais ne prolonge pas significativement la survie sans récidive des patients ayant un cancer du colon de stade III.[137-139] L'échec du bevacizumab à inhiber l'angiogenèse présente au début du processus métastatique et le "switch angiogénique" souligne le fait que les facteurs angiogéniques pourraient être différents à des stades précoces ou tardifs durant le développement des métastases hépatiques. Il semble donc nécessaire de développer de nouvelles thérapeutiques pour les stades précoces, ainsi que pour les stades tardifs car la résistance est fréquente aux anti-angiogéniques.

Dans la seconde partie de notre travail, nous nous sommes tout d'abord interrogés sur la pertinence de l'utilisation du bevacizumab dans les modèles murins puis nous avons étudié l'effet d'une nouvelle molécule anti-angiogénique, la Nétrine-4, sur le processus métastatique dans plusieurs modèles de cancer coliques.

Lettre à l'éditeur 2 :

Did animal offer relevant model for Bevacizumab testing?

Eveno C, Gaujoux S, Tobelem G, Pocard M.

Br J Cancer. 2008 Nov 4;99(9):1555

Pour tester la pertinence de l'utilisation du bevacizumab dans les modèles précliniques murins, nous avons comparé le taux de prolifération des cellules endothéliales humaines (HUVEC) en présence de VEGF murin ou humain. Nous avons remarqué une courbe dose-réponse en cloche caractéristique pour le VEGF humain et murin en l'absence de bevacizumab. En présence de la concentration la plus efficace du VEGF (12,5 g /ml), nous avons observé une différence d'inhibition de prolifération des HUVECs par le bevacizumab en présence de VEGF murin et humain. La prolifération des HUVEC avec le VEGF humain inhibée de 35% contre 17% avec le VEGF murin.

Plusieurs raisons peuvent expliquer l'inefficacité du bevacizumab lorsqu'il est testé seul pour inhiber la progression de tumeurs d'origine humaine dans un modèle de xénogreffe murin: (i) certaines études montrent que le bevacizumab ne parvient pas à neutraliser efficacement le VEGF murin du fait d'une interaction faible,[184, 185] (ii) le VEGF en quantité suffisante pour promouvoir l'angiogenèse tumorale proviendrait de diverses cellules hôtes tels que les plaquettes, les cellules musculaires et les cellules stromales associées à la tumeur et ne serait donc que faiblement diminué,[186] (iii) le VEGF murin serait suffisamment efficace pour promouvoir la croissance des cellules humaines.

Notre étude interroge la validité de l'évaluation, à l'aide de modèles précliniques murins, de la pertinence clinique du bevacizumab.

British Journal of Cancer (2008) 99, 1555–1556

www.bjcancer.com

Letters to the Editor

Did animal offer relevant model for Bevacizumab testing?

C Eveno[1,2], S Gaujoux[2], G Tobelem[1,2,3] and M Pocard[*,1,2,3]

[1]Unité Inserm U689, équipe 'angiogenèse et cibles thérapeutiques', hôpital Lariboisière, Institut des Vaisseaux et du Sang, 8, rue Guy-Patin, Paris, cedex 10 75475, France; [2]Département médico-chirurgical de pathologie digestive, hôpital Lariboisière, 2, rue Ambroise-Paré, Paris, cedex 10 75475, France; [3]Université Paris-Diderot, Paris 7, France

British Journal of Cancer (2008) 99, 1555–1556. doi:10.1038/sj.bjc.6604693 www.bjcancer.com
Published online 7 October 2008

Sir,

We have read with great interest the article by Bozec et al (2008). In their study, they evaluated on an orthotopic xenograft model, the antitumour efficacy of bevacizumab, erlotinib and irradiation, alone and in combination, on a vascular endothelial growth factor (VEGF) -secreting human head and neck tumour cell line (CAL33). They reported a significant primary tumour mass decrease with drug association but not with bevacizumab alone. And the authors concluded that the efficacy of the combination of bevacizumab, erlotinib and RT might be of clinical importance in the management of head and neck cancer patients.

This work prompted us to analyse the murine model pertinence. We tested human endothelial cell proliferation in the presence of murine or human VEGF. We noticed a characteristic bell-shaped dose–response curve for both human and murine VEGF in the absence of bevacizumab (Figure 1). In the presence of the most efficient concentration of VEGF (12.5 mg ml^{-1}), we observed a difference of bevacizumab inhibition between murine and human VEGF-induced proliferation (Figure 2). The endothelial cell proliferation with human VEGF was more inhibited when compared with murine VEGF (with 35 vs 17% of decrease).

Several reasons can explain the inefficacy of bevacizumab when tested alone to inhibit human tumour progression in a xenograft mice model: (i) increasing evidences (Liang et al, 2006; Yu et al, 2008) show that bevacizumab fails to neutralise efficiently murine VEGF because of a weak interaction; (ii) VEGF in sufficient amounts to promote tumour angiogenesis originates from various host cells in the body such as platelets, muscle cells, tumour-associated stromal cells, and in scar (Kerbel, 2008); (iii) murine VEGF is efficient enough to promote human cell growth.

In our opinion, animal models should not be used to conclude on the clinical pertinence of bevacizumab, unless animals express a humanised form of VEGF (Gerber et al, 2007).

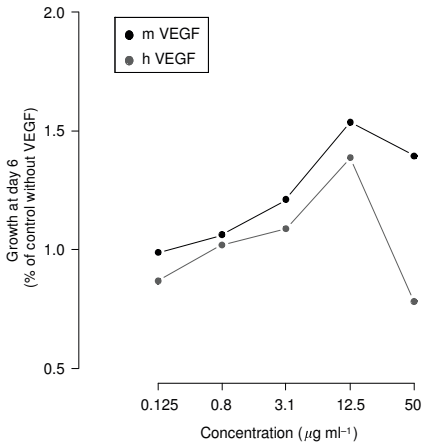

Figure 1 Endothelial cell proliferation assay: HUVECs (human umbilical vein endothelial cells) were incubated with increasing concentrations of h-VEGF (human) or m-VEGF (murine).

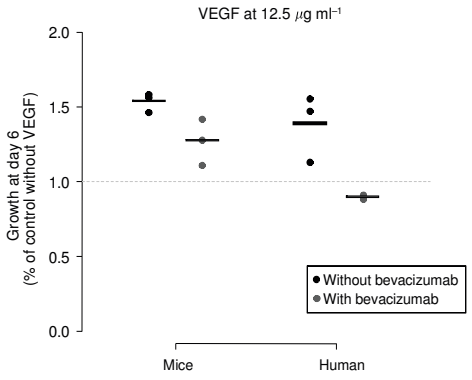

Figure 2 Endothelial cell proliferation assay: HUVECs (human umbilical veinous endothelial cells) were incubated with h-VEGF or m-VEGF (12.5 mg ml^{-1}), without and with Bevacizumab.

*Correspondence: Professor M Pocard, Unité Inserm U689, équipe 'angiogenèse et cibles thérapeutiques', Institut des Vaisseaux et du Sang, hôpital Lariboisière, 8, rue Guy-Patin, Paris, cedex 10 75475, France; E-mail: marc.pocard@lrb.aphp.fr
Published online 7 October 2008

REFERENCES

Bozec A, Sudaka A, Fischel JL, Brunstein MC, Etienne-Grimaldi MC, Milano G (2008) Combined effects of bevacizumab with erlotinib and irradiation: a preclinical study on a head and neck cancer orthotopic model. Br J Cancer 99: 93–99

Gerber HP, Wu X, Yu L, Wiesmann C, Liang XH, Lee CV, Fuh G, Olsson C, Damico L, Xie D, Meng YG, Gutierrez J, Corpuz R, Li B, Hall L, Rangell L, Ferrando R, Lowman H, Peale F, Ferrara N (2007) Mice expressing a humanized form of VEGF-A may provide insights into the safety and efficacy of anti-VEGF antibodies. Proc Natl Acad Sci USA 104: 3478–3483

Kerbel RS (2008) Tumor angiogenesis. N Engl J Med 358: 2039–2049

Liang WC, Wu X, Peale FV, Lee CV, Meng YG, Gutierrez J, Fu L, Malik AK, Gerber HP, Ferrara N, Fuh G (2006) Cross-species vascular endothelial growth factor (VEGF)-blocking antibodies completely inhibit the growth of human tumor xenografts and measure the contribution of stromal VEGF. J Biol Chem 281: 951–961

Yu L, Wu X, Cheng Z, Lee CV, LeCouter J, Campa C, Fuh G, Lowman H, Ferrara N (2008) Interaction between bevacizumab and murine VEGF-A: a reassessment. Invest Ophthalmol Vis Sci 49: 522–527

Article 2 :

Netrin-4 delays colorectal cancer carcinomatosis by inhibiting tumor angiogenesis.

Eveno C, Broqueres-You D, Feron JG, Rampanou A, Tijeras-Raballand A, Ropert S, Leconte L, Levy BI, Pocard M.

Am J Pathol. 2011 Apr;178(4):1861-9.

Article 3 :

Netrin-4 overexpression suppresses primary and metastatic colorectal tumor progression.

Eveno C, Contreres JO, Hainaud P, Nemeth J, Dupuy E, Pocard M.

Oncol Rep. 2013 Jan;29(1):73-8.

Initialement identifiées comme des molécules de guidage axonale, les Nétrines sont des protéines sécrétées qui ont été récemment impliquées dans l'angiogenèse et la formation du réseau vasculaire.[187] Comme observé dans le système nerveux, les Nétrines agissent également en tant que modulateurs bi-fonctionnels dans l'angiogenèse. En effet, les deux effets pro-angiogéniques et anti-angiogénique de la Nétrine ont été reportés.[188-190] Une étude récente a montré que la surexpression de la Nétrine-4 (NT-4) inhibait l'angiogenèse tumorale en se liant à son récepteur néogénine dans un modèle de xénogreffe sous-cutanée.[191]

Dans notre étude, nous avons analysé l'effet de la Nétrine 4 (NT4), dans plusieurs modèles murins de tumeurs primitives et de métastases d'origine colorectale.

In vitro, à l'aide d'un essai sur Matrigel, nous avons montré que la NT-4 inhibe l'angiogenèse non tumorale induite par le VEGF et le bFGF. Puis nous avons utilisé une lignée de cancer du colon, LS174 (exprimant de manière basale la NT-4), que nous avons transfectée de manière stable avec

l'ADN de la NT-4, de manière à créer une lignée de LS174-NT4 sur-exprimant la NT-4. Nous avons alors comparé les deux lignées tumorales, LS174 et LS174-NT4, dans plusieurs modèles de xénogreffes.

Dans un modèle de tumeur sous-cutanée, la surexpression de la NT4 diminue la croissance tumorale, conformément aux résultats obtenus par d'autres équipes.[191, 192] Bien que la croissance tumorale fût inhibée dans ce modèle, avec une diminution de la prolifération et de l'apoptose des cellules tumorales dans les tumeurs du groupe NT4, il semble que le NT4 n'exerce pas un effet direct sur la prolifération et l'apoptose des cellules LS174 en culture. Il existe une diminution de la densité microvasculaire tumorale, évaluée par marquage CD31, dans le groupe NT4, ce qui suggère que la NT4 peut diminuer la prolifération tumorale, accroître l'apoptose tumorale, et inhiber la croissance tumorale en inhibant l'angiogenèse tumorale *in vivo*. La Nétrine-4 pourrait exercer cet effet anti-angiogénique en inhibant la différenciation et la migration des CEs et en stimulant la différenciation et la migration des cellules musculaires lisses.[191, 192] Dans un modèle de xénogreffe orthotopique par greffe caecale, nous avons démontré que la surexpression de la NT4 diminue le volume de la tumeur au 8ème jour après la greffe tumorale, ainsi que le taux de récidive locale et de métastases au 70ème jour après résection de la tumeur primitive. Ces résultats suggèrent que le NT-4 pourrait présenter un potentiel thérapeutique pour le traitement du cancer colorectal primitif.

L'effet inhibiteur sur le processus tumoral de la NT4 a été vérifié dans trois modèles orthotopiques de métastases de cancer colique: hépatique, pulmonaire et péritonéale.

Trente jours après l'injection splénique de LS174 sauvages ou surexprimant la NT4, le nombre de métastases hépatiques était significativement plus faible dans le groupe NT4 par rapport au groupe contrôle (n = 10 par groupe, 25 vs 90%, respectivement, P <0,001). Le volume du foie était nettement réduit dans le groupe NT4 par rapport au groupe contrôle (n = 10 par groupe, 4 ± 1 mm^3 et 709 ± 190 mm^3, respectivement, P <0,05)

Dans un modèle orthotopique de métastases pulmonaires après injection dans la veine caudale de la queue, les souris du groupe NT4 étaient indemnes de toute prolifération tumorale ; celles du

groupe contrôle présentant des métastases pulmonaires, hépatique ou des adénopathies cervicales et axillaires tumorales, pour 90% des animaux.

Lorsque l'on compare l'effet de la NT4 et du bevacizumab dans un modèle de carcinose péritonéale d'origine colorectale par greffe orthotopique, la NT4 et le bevacizumab diminuaient le volume de l'ascite tumorale ; mais seule la NT4 inhibait le processus métastatique en diminuant le score PCI. Nous avons montré, grâce à un test au bleu Evans, que mécanisme de diminution de la formation d'ascite par le bevacizumab était probablement lié à l'inhibition de la perméabilité vasculaire aigüe induite par le VEGF. La NT4 n'a pas le même mécanisme d'action mais pourrait agir en diminuant la superficie totale de la surface de la membrane capillaire disponible, objectivé par un compte de vaisseaux péritonéaux plus faible dans le groupe NT4.

Dans la dernière partie de ce travail, nous avons montré, *in vitro* avec un test d'angiogenèse sur Matrigel, que l'effet anti-angiogénique de la NT4 était médié par son récepteur Néogenine.

En conclusion, la NT4 ralentit la croissance tumorale et le processus métastatique dans plusieurs modèles murins de xénogreffes orthotopiques ainsi que la formation d'ascite tumorale par inhibition de l'angiogenèse tumorale, Ces résultats mettent en évidence un intérêt thérapeutique majeur de la NT4 comme une alternative prometteuse aux traitements anti-VEGF dans le traitement du cancer colorectal.

The American Journal of Pathology, Vol. 178, No. 4, April 2011

DOI: 10.1016/j.ajpath.2010.12.019

Tumorigenesis and Neoplastic Progression

Netrin-4 Delays Colorectal Cancer Carcinomatosis by Inhibiting Tumor Angiogenesis

Clarisse Eveno,* Dong Broqueres-You,*† Jean-Guillaume Feron,*† Aurore Rampanou,* Annemilaï Tijeras-Raballand,*† Stanislas Ropert,*† Laurence Leconte,*† Bernard I. Levy,*† and Marc Pocard*

From INSERM U965 (Paris 7 University) and the Vessels and Blood Institute (IVS),† Hôpital Lariboisière, Paris, France*

A close relationship between tumor angiogenesis, growth, and carcinomatosis has been observed. Netrin-4 (NT-4) has been shown to regulate angiogenic responses. We aimed to examine the effects of NT-4 on colon tumor angiogenesis, growth, and carcinomatosis. We showed that NT-4 was expressed in human colon cancer cells (LS174). A 20-fold increase in NT-4 expression was stably induced by NT-4 pcDNA in LS174 cells. *In vivo*, a Matrigel angiogenesis assay showed that NT-4 overexpression altered vascular endothelial growth factor (VEGF)/basic fibroblast growth factor–induced angiogenesis. In nude mice with LS174 xenografts, NT-4 overexpression inhibited tumor angiogenesis and growth. In addition, these NT-4-involved inhibitory effects were associated with decreased tumor cell proliferation and increased tumor cell apoptosis. Using an orthotopic peritoneal carcinomatosis model, we demonstrated that NT-4 overexpression decreased colorectal cancer carcinomatosis. Moreover, carcinomatosis-related ascites formation was significantly decreased in mice transplanted with NT-4 LS174 cells versus control LS174 cells. The antiangiogenic activity of NT-4 was probably mediated by binding to its receptor neogenin. Netrin-4 had a direct effect on neither *in vitro* apoptosis and proliferation of cultured LS174 cells nor the VEGF-induced acute increase in vascular permeability *in vivo*. We propose that NT-4 overexpression decreases tumor growth and carcinomatosis, probably via an antiangiogenic effect, underlying the potential therapeutic interest in NT-4 in the treatment of colorectal cancer growth and carcinomatosis. ***(Am J Pathol 2011, 178:1861–1869; DOI: 10.1016/j.ajpath.2010.12.019)***

Colorectal cancer (CRC) is the second leading cause of cancer death in North America and Western Europe, constituting approximately 10% of new colon cancer cases every year.[1,2] Despite recent progress in the treatment of CRC, for 19% of patients diagnosed as having metastatic CRC, survival times are poor, with 5-year survival being just 10%.[3] Indeed, the survival rate is negatively related to the presence of carcinomatosis, a specific metastatic condition leading to significant morbidity and mortality. The development of new therapeutic strategies for CRC carcinomatosis is very much required, with the aim of delaying metastatic cancer progression and increasing survival rates.

Aberrant angiogenesis, the formation of new blood vessels from preexisting blood vessels and vascular endothelial cells (EC), is important in cancer progression.[4] In neoplasms, tumor-derived factors promote angiogenesis.[5] The neovascularization expands the vascular bed, causing tumor growth and a continuity with the systemic circulation; these changes provide a critical growth advantage for tumor progression and metastasis,[6,7] suggesting that targeting the tumor's dependence on angiogenesis could, effectively, slow metastatic progression. Recently, several new drugs targeting specific molecules involved in angiogenesis have clinically validated this conjecture.[8] Because elevated vascular endothelial growth factor (VEGF) levels have been documented in many cancers, and VEGF overexpression correlates with an increased risk of metastatic disease and overall poor prognosis in different cancers, researchers have focused on the inhibition of VEGF/VEGF receptor pathways.[9–13] Indeed, VEGF inhibitors are in broad use for the treatment of metastatic renal cell carcinoma, gastrointestinal stromal tumors, and hepatocellular carcinoma, and are being developed for the treatment of many other cancers, including CRC, non-small cell lung cancer, and pancreatic cancer.[8] However, experience with biological antiangiogenic agents, such as bevacizumab, indicates that disruption of VEGF

This study was supported in part by Association pour la Recherche sur le Cancer of France.

Accepted for publication December 17, 2010.

Address reprint requests to Dong Broqueres-You, M.D., Ph.D., Vessels and Blood Institute, INSERM U965 (Paris 7 University), Hôpital Lariboisière, 8 rue Guy Patin, 75010 Paris, France. E-mail: youdong777@hotmail.com.

function often leads to severe secondary effects, such as delayed wound healing, renal damage, and subsequent hypertension.[14] In addition, recent studies showed a resistance of tumor vessels to anti-VEGF therapy,[15–17] highlighting the importance of developing other potential antiangiogenic strategies for cancer treatment.

Neuronal and vascular development requires guidance to establish a precise branching pattern of these systems in the vertebrate body. Several molecules implicated in axon navigation have also been shown to regulate vessel sprouting.[18,19] Among these guidance cues, netrins constitute a family of diffusible molecules with a regulatory role in axon pathfinding and in other developmental processes, including vascular development.[18] The netrin system comprises at least five ligands (netrins 1, 2, 4, G1a, and G1b) and seven receptors (neogenin, DCC, Unc5A, Unc5B, Unc5C, Unc5D, and A2b).[20,21] Although the significance of the netrin-dependent pathway in tumor angiogenesis is not totally understood, emerging evidence indicates that it plays an important role in the development of different cancers in animal models.[20] It might, therefore, be a potential therapeutic target for cancer treatment. A previous study showed that netrin-4 (NT-4) overexpression delayed tumor angiogenesis through binding to neogenin and recruitment of Unc5B in an s.c. xenograft model.[22] In addition, a recent study showed that NT-4 regulated angiogenic responses and inhibited the growth of CRC cells.[23]

The aim of this study was to examine the effects of NT-4 overexpression on tumor angiogenesis and growth *in vitro* in human colon cancer cells (LS174) and *in vivo* in a mouse model of orthotopic peritoneal CRC carcinomatosis. We identified NT-4 as a protein expressed *in vitro* in LS174 human colon cancer cells. We demonstrated an inhibitory role of NT-4 in tumor progression by an effect on tumor angiogenesis but not by directly altering tumor cell proliferation and apoptosis. Finally, we obtained evidence that NT-4 exerts antiangiogenic activity, probably by binding to neogenin, and decreases CRC carcinomatosis and ascites formation.

Materials and Methods

Cell Culture and Cell Transfection

LS174 human colon cancer cells obtained from the American Type Culture Collection were maintained in Dulbecco's modified Eagle's medium supplemented with 10% heat-inactivated fetal bovine serum/penicillin (50 U/mL)/streptomycin (50 μg/mL) (Gibco BRL Life Technologies Inc, Grand Island, NY) in a humidified atmosphere of 95% air and 5% CO_2 at 37°C.

Acquisition of cDNA for NT-4

Total RNA was extracted from cultures of human umbilical artery endothelial cells, and reverse transcription was performed using the AMV Kit (Roche Applied Science, Indianapolis, IN). Two sets of primers (1-1039 and 914-1884) were used to amplify the sequence with Taq DNA polymerase (Roche Applied Science). Products from the two PCR reactions were mixed 1:1 and were used as the template to obtain NT-4 cDNA. The construct was subcloned into a pcDNA3.1(−)/His-myc C vector (Invitrogen, Carlsbad, CA). The vector containing NT-4 was transfected into LS174 cells using Lipofectin (Invitrogen) according to the manufacturer's protocol. Cells were cultured in a selective medium (10% fetal bovine serum–Dulbecco's modified Eagle's medium) containing 200, 300, 400, or 500 μg/mL of G418 (Geneticin; Gibco BRL Life Technologies Inc). Cell clones were subsequently screened by means of enzyme-linked immunosorbent assay to detect an increase in NT-4 expression relative to that in the pcDNA-transfected cells collected after 3 days in conditioned medium (data not shown). For *in vivo* experiments, LS174 cells transfected with NT-4 were harvested. Cells were washed in 10% fetal bovine serum–Dulbecco's modified Eagle's medium, counted, and suspended in Dulbecco's modified Eagle's medium for injection.

Matrigel Angiogenesis Assay

A modified *in vivo* assay of neovessel growth, as described by Passaniti et al,[24] was performed. Under anesthesia, 300 μL of Matrigel (BD Biosciences, Franklin Lakes, NJ), 12.5 mg/mL mixed with PBS, or 6 μg/mL of NT-4 was s.c. injected into female athymic nude mice (5 weeks old) along the dorsal midline in the presence or absence of 300 ng/mL of VEGF-A and 300 ng/mL of basic fibroblast growth factor (bFGF) (R&D Systems, Minneapolis, MN). After 7 days, the Matrigel plugs were harvested from underneath the skin. The plugs were homogenized in 1 mL of HEPES (20 mmol/L, pH 7.4) on ice and were cleared by means of centrifugation at 10,000 rpm for 6 minutes at 4°C. The supernatant was collected and used to measure hemoglobin content using Drabkin's reagent along with a hemoglobin standard according to the manufacturer's protocol (Sigma-Aldrich, St. Louis, MO).

Animal Models of Tumor Xenograft and Peritoneal Carcinomatosis

All the experimental protocols met all the standards required by the European community guidelines for the care and use of laboratory animals. Five-week-old female athymic nude mice (Charles River Laboratories International Inc., Wilmington, MA) were acclimatized for 1 to 2 weeks before tumor transplantation (8 to 10 animals per experimental group).

For LS174 s.c. transplantation, animals were anesthetized with 2 mg/mL of xylazine and 20 mg/mL of ketamine (Virbac, Carros, France). Under sterile conditions, either NT-4-transfected LS174 cells (NT-4 LS174 cells) or control LS174 cells (CT LS174 cells; 1×10^6 cells) were injected s.c. The tumor volume was recorded using a caliper twice a week and was calculated using the following formula: [length (mm) × [width (mm)]^2 × p]/6. Animals were sacrificed 30 days after LS174 transplantation.

For the peritoneal carcinomatosis orthotopic model, the animals were anesthetized. Under sterile conditions, either NT-4 or CT LS174 cells (1×10^6 cells)

were injected into the peritoneal cavity. Beginning 7 days after tumor transplantation, the mice received intravenous treatments consisting of bevacizumab (5 mg/kg) or saline twice per week for 3 weeks. The animals were monitored daily and were sacrificed at 30 days. Ascitic fluid was collected by performing a lower midline incision, and ascites volume was measured. The incision was then extended to allow photography of the peritoneal cavity and determination of the extent of peritoneal carcinomatosis using a modified Peritoneal Cancer Index (PCI).[25] The PCI (range, 1 to 39) allows assessment of the distribution of cancer in the abdomen and pelvis and is calculated by summing lesion size scores (0 to 3) in the abdominopelvic regions (0 to 13). The PCI was adapted to tumor sizes in mice with the following lesion size scores: tumor smaller than 2.0 mm (lesion size 1), 2.1 to 5.0 mm (lesion size 2), and greater than 5.0 mm or confluence (lesion size 3), as previously described.[26] Tumor tissue was then harvested and frozen for subsequent immunohistochemical analysis.

Immunohistologic Analysis

For the evaluation of CD31 and Ki-67 staining, each frozen tumor sample was sectioned at 5-μm thickness using a cryostat (Leica Microsystems GmbH, Wetzlar, Germany). The sections were incubated with anti-CD31 antibody, anti-desmin antibody, anti–Ki-67 antibody, and DAPI (BD Biosciences) for 1 hour at room temperature and then with the second antibody. Images were acquired using a fluorescence microscope equipped with appropriate filters (Observer.Z1; Carl Zeiss Inc). Histo-Lab software (version 7.0; Microvision Instruments, Evry, France) was used to quantify the results. The results are expressed as the ratio of CD31 staining surface to desmin staining surface and the ratio of Ki-67 staining surface to DAPI staining surface.

Cell Proliferation and Apoptosis Assays

To evaluate *in vitro* tumor cell proliferation and apoptosis, CT and NT-4 LS174 cells were maintained under normal growth conditions, described previously herein. One hundred thousand cells were seeded in triplicate into each well of a 6-well flat-bottom plate. The cells were allowed to attach and grow overnight. Tumor cell proliferation was assessed at days 0, 3, 4, 5, and 7 by counting the cells using a Neubauer counting chamber. Using a terminal deoxynucleotidyl transferase-mediated dUTP nick-end labeling (TUNEL) kit (Roche Diagnostics), the apoptosis of LS174 cells was determined in frozen sections of each tumor xenograft sample and in cultured CT LS174 and NT-4 LS174 cells at day 7. The ratio of surface occupied by TUNEL staining to total surface examined for the cross-sections and the percentage of TUNEL–stained cells to DAPI-stained cells for the cultured LS174 *in vitro* were determined using a customized application (Histolab).

Western Blot Analysis

At day 7 of cell culture, NT-4 LS174, CT LS174, and human umbilical vein endothelial cells (HUVEC) were homogenized in radioimmunoprecipitation assay lysis buffer [50 mmol/L Tris-HCl, 150 mmol/L NaCl, 1 mmol/L EDTA, 1% Triton X-100 (Roche Diagnostics GmbH, Mannheim, Germany), 0.1% SDS, 1% deoxycholate, pH 7.4] containing protease inhibitors (Boehringer Mannheim Corp., New York, NY). Proteins were separated in 4% to 12% gradient SDS–polyacrylamide gel electrophoresis precast gels and were blotted onto a nitrocellulose sheet (Amersham Biosciences, Piscataway, NJ). Antibodies directed against NT-4, actin, and neogenin (R&D Systems) were used at a dilution of 1:500, 1:400, and 1:500, respectively. Specific protein was detected by chemiluminescent reaction (Amersham Biosciences).

Acute Vascular Permeability Assay

Vascular endothelial growth factor has been reported to exert angiogenic effects by augmenting vascular permeability.[9] To investigate the acute effect of NT-4 on vascular permeability, an intradermal Miles assay was performed.[27] Briefly, the guinea pigs (n = 6; Charles River Laboratories International Inc.) were anesthetized. A total of 500 μL of 0.5% Evans blue (Sigma-Aldrich) was injected into animals via the jugular vein. After 30 minutes, the guinea pigs were given multiple 100-μL intradermal injections on the back. PBS, VEGF-A (5, 10, and 100 ng/mL), VEGF-A (5, 10, and 100 ng/mL) + NT-4 (10 μg/mL), or VEGF-A (5, 10, and 100 ng/mL) + bevacizumab (5 μg/mL) was then injected intradermally. Twenty minutes after VEGF treatment, the animal was sacrificed and the skin was excised. Evans blue dye in the excised site of intradermal injection was photographed. For quantification of extravasated dye, skin samples were incubated for 48 hours in formamide at 4°C, and the dye quantity was measured spectrophotometrically at 620 nm.

EC Tube Formation Assay

HUVEC were cultured in endothelial basal medium (Clonetics, Lonza Walkersville Inc, Walkersville, MD) supplemented with 10% fetal bovine serum. The HUVEC cells (6×10^4) were then seeded in duplicate in a 24-well plate precoated with 10 mg/mL of Matrigel. Capillary-like tube formation was induced by the addition of 50 ng/mL of VEGF for 2 hours. Then, CT and NT-4 LS174 cells were added into wells in either the presence or absence of 10 μg/mL of neutralizing antibody against neogenin. Eighteen hours later, the media was removed and the cells were washed and stained with 4 μg/mL of calcein (Invitrogen) in a PBS solution at 37°C. Endothelial cell tube formation was quantified by determining the number of new EC tubes.

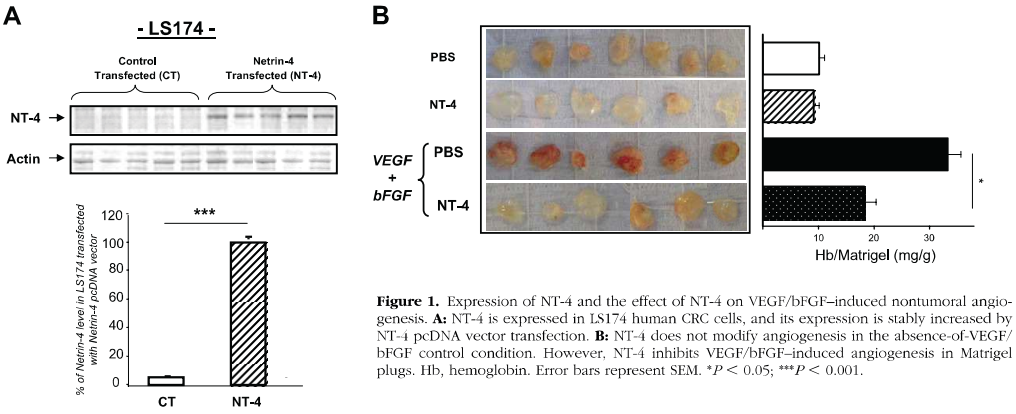

Figure 1. Expression of NT-4 and the effect of NT-4 on VEGF/bFGF–induced nontumoral angiogenesis. **A:** NT-4 is expressed in LS174 human CRC cells, and its expression is stably increased by NT-4 pcDNA vector transfection. **B:** NT-4 does not modify angiogenesis in the absence-of-VEGF/bFGF control condition. However, NT-4 inhibits VEGF/bFGF–induced angiogenesis in Matrigel plugs. Hb, hemoglobin. Error bars represent SEM. $^{*}P < 0.05$; $^{***}P < 0.001$.

Statistical Analysis

The results are expressed as mean ± SEM. The unpaired *t*-test was used to compare two different experimental groups. The comparisons between more than two different experimental groups were performed using 1-way analysis of variance followed by a Bonferroni posttest. A $P < 0.05$ was considered significant.

Results

NT-4 Is Expressed in Human Colon Cancer Cells

The protein expression of NT-4 was determined by means of Western blot analysis (Figure 1A). After transfection with the NT-4 pcDNA vector, LS174 human colon cancer cells exhibited a 20-fold increase in NT-4 level compared with CT LS174 cells, with this increase being reproducible and stable ($P < 0.001$; Figure 1A).

NT-4 Alters VEGF/Basic FGF-Induced Nontumoral Angiogenesis In Vivo

We first investigated the role of NT-4 in angiogenesis induced by VEGF/bFGF, the key factors involved in physiologic and pathologic angiogenesis. Recombinant NT-4 protein did not modify the hemoglobin content in the absence-of-VEGF/bFGF control condition (mean ± SEM: 10.1 ± 1.0 mg/g and 9.2 ± 0.9 mg/g for the PBS and NT-4 groups, respectively; Figure 1B). Seven days after VEGF-A and FGF-2 treatment, increased hemoglobin content was observed using an angiogenesis assay in Matrigel, confirming that VEGF-A and FGF-2 promote angiogenesis. Recombinant NT-4 protein significantly inhibited this angiogenesis induced by VEGF and FGF (mean ± SEM: 33.4 ± 2.3 mg/g and 10.1 ± 1.0 mg/g for the VEGF/bFGF + PBS and VEGF/bFGF + NT-4 groups, respectively; $P < 0.5$; Figure 1B).

NT-4 Inhibits Colorectal Tumor Growth, Impairs Tumor Angiogenesis, and Affects Tumor Cell Proliferation and Apoptosis in Human Colon Cancer Cell Xenograft

To examine whether NT-4 could decrease colon tumor growth and angiogenesis, CT and NT-4 LS174 human colon cancer cells were s.c. injected into nude mice. In animals with an NT-4 LS174 xenograft, the tumor volume was significantly smaller than that of animals receiving CT LS174 cells (Figure 2A). The VEGF inhibitor bevacizumab had no significant effect on tumor growth. In addition, bevacizumab did not further decrease the tumor volume in animals transplanted with NT-4 LS174 cells (Figure 2A).

Decreased tumor progression was related to a reduction in the ratio of CD31 to desmin staining surface in animals in the NT-4 group, suggesting that NT-4 exerts an inhibitory effect on tumor angiogenesis (mean ± SEM: 0.73 ± 0.05 and 0.47 ± 0.06 for the CT and NT-4 groups, respectively; $P < 0.05$; Figure 2B).

Moreover, NT-4 overexpression dramatically decreased the ratio of Ki-67 to DAPI staining surface in the tumor, indicating that NT-4 impairs tumor proliferation *in vivo* (mean ± SEM: 1 ± 0.14 and 0.48 ± 0.07 for the CT and NT-4 groups, respectively; $P < 0.01$; Figure 2C). Tumor cell apoptosis detected by means of TUNEL staining was greatly increased in the NT-4 group compared with the CT group (mean ± SEM: 0.12 ± 0.02 and 0.32 ± 0.10 for the CT and NT-4 groups, respectively; $P = 0.05$; Figure 2D).

NT-4 Has No Direct Effect on Tumor Cell Proliferation and Apoptosis in Vitro

To ascertain whether NT-4 directly affects the proliferation and apoptosis of colon cancer cells, we investigated the effect of NT-4 overexpression on proliferation and apoptosis of LS174 cells *in vitro*. There was no difference in cell numbers between the CT and NT-4 LS174 dishes during the 7-day cell culture period, indicating that NT-4 did not directly alter the proliferation of human colon cancer cells

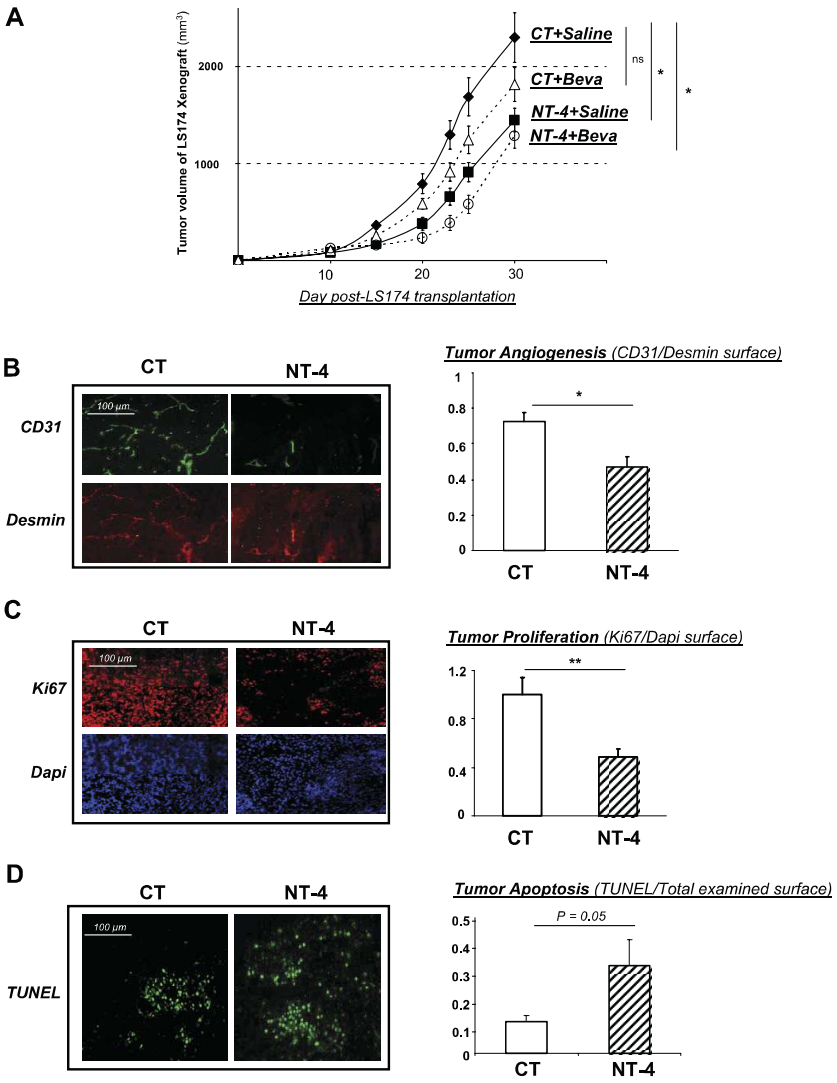

Figure 2. Effects of NT-4 and bevacizumab (Beva) on colorectal tumor growth, tumor angiogenesis, tumor cell proliferation, and apoptosis in nude mice with an s.c. LS174 cell xenograft. **A:** NT-4 overexpression in LS174 cells delays tumor growth, whereas bevacizumab has no significant inhibitory effect. **B:** Vascular density (CD31/desmin staining surface) is significantly less pronounced in tumors transplanted with NT-4-overexpressing LS174 cells compared with CT LS174 cells. **C:** NT-4 overexpression in LS174 cells is related to a significant decrease in tumor cell proliferation (Ki-67/DAPI staining surface) *in vivo*. **D:** NT-4 overexpression in LS174 cells significantly increases tumor apoptosis *in vivo*. ns, not significant. Error bars represent SEM. $^{*}P < 0.05$; $^{**}P < 0.01$.

(Figure 3A). Moreover, NT-4 overexpression did not significantly modify the tumor cell apoptotic process *in vitro* (Figure 3B).

NT-4 Decreases CRC Carcinomatosis and Its Related Ascites Formation

We next examined the effects of NT-4 overexpression, compared with bevacizumab, on CRC carcinomatosis using a modified PCI assessment. Day 30 after cancer cell transplantation, the PCI was significantly decreased in animals receiving NT-4 LS174 cells compared with CT LS174 cells, suggesting that NT-4 affects the distribution of transplanted cancer in the abdomen and pelvis (mean ± SEM: 18.6 ± 3.7 and 7.8 ± 1.6 for the CT and NT-4 groups, respectively; $P < 0.05$; Figure 4, A and C). The VEGF inhibitor bevacizumab had no effect on the PCI. Moreover, bevacizumab could not further enhance the

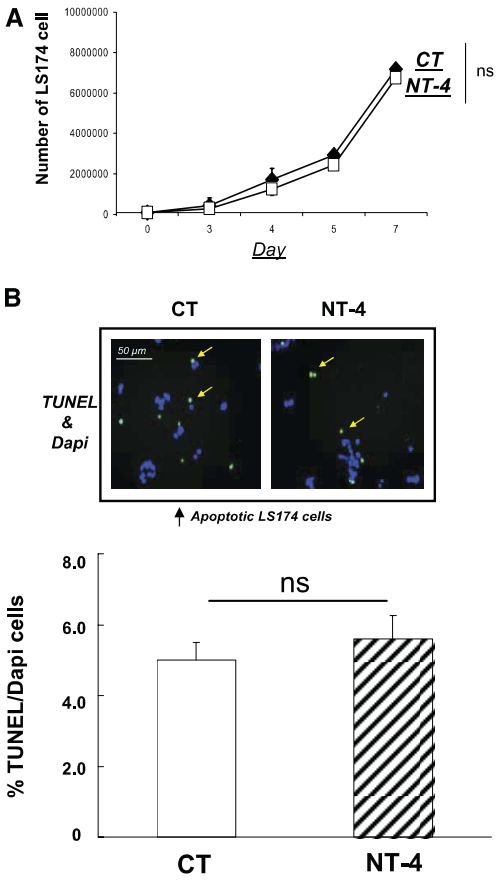

Figure 3. *In vitro* effects of NT-4 overexpression on colorectal tumor cell proliferation and apoptosis. **A:** NT-4-overexpressing LS174 cells exhibit a similar proliferation capability as CT LS174 cells. **B:** NT-4-overexpression has no significant effect on tumor apoptosis. ns, not significant; TUNEL, terminal deoxynucleotidyl transferase-mediated dUTP nick-end labeling. Error bars represent SEM.

inhibitory effect of NT-4 on CRC carcinomatosis (Figure 4A).

Colorectal cancer carcinomatosis is often related to ascites formation. Both NT-4 and bevacizumab were capable of significantly decreasing the ascites volume in nude mice with LS174 transplantation (mean ± SEM: 0.94 ± 0.23, 0.16 ± 0.06, 0.13 ± 0.06, and 0.13 ± 0.07 mL for the CT, NT-4, bevacizumab, and NT-4 + bevacizumab groups, respectively; $P < 0.05$; Figure 4B). However, bevacizumab did not further decrease ascites formation in animals injected with NT-4 LS174 cells.

Qualitative photography showed fewer blood vessels in the parietal peritoneum (Figure 4C) and abdominal cavity (Figure 4D) in the NT-4 group compared with the CT group, suggesting that NT-4 has an inhibitory effect on tumor angiogenesis of CRC carcinomatosis.

NT-4 Has No Direct Effect on a VEGF-Induced Acute Increase in Vascular Permeability

Then, we investigated the acute effect of NT-4 on vascular permeability using an intradermal Miles *in vivo* permeability assay in the guinea pig, with or without the presence of VEGF. As originally described by Miles and Miles,[27] rapid leakage of Evans blue dye was observed in the skin of animals in the presence of VEGF in a dose-dependent manner (Figure 5). Recombinant NT-4 protein did not modify the leakage of Evans Blue in the presence of VEGF, suggesting that NT-4 has no direct effect on a VEGF-induced acute increase in vascular permeability. However, bevacizumab totally blocked the VEGF-induced acute increase in vascular permeability (Figure 5).

The Receptor Neogenin Mediates the Antiangiogenic Activity of NT-4

To investigate the involvement of the receptor neogenin in NT-4's antiangiogenic activity, we used a Matrigel EC tube formation assay. First, the protein expression of neogenin was evidenced by means of Western blot analysis in HUVEC (Figure 6A). In the presence of VEGF, HUVEC were capable of forming new vascular tubes. Co-culture of HUVEC with LS174 cells significantly increased the number of new EC tubes (mean ± SEM: 22 ± 4, 127 ± 7, and 328 ± 30/mm^2 for the PBS, VEGF, and VEGF + CT groups, respectively; $P < 0.001$; Figure 6, B and C), indicating that tumor cells facilitate EC angiogenesis. However, after a short-term (18-hour) cell culture, there was no difference in EC tube formation between the VEGF + CT and VEGF + NT-4 groups (mean ± SEM: 293 ± 19/mm^2 for the VEGF + NT-4 group).

In the presence of neutralizing antibody directed against neogenin, the mean ± SEM number of new vascular tubes was dramatically enhanced compared with the VEGF + CT and VEGF + NT-4 groups (749 ± 41/mm^2 for the VEGF + NT-4 + antineogenin group, $P < 0.001$; Figure 6, B and C), suggesting that neogenin mediates the antiangiogenic activity of LS174 cell-secreted NT-4.

Discussion

Interference with the activation of growth factor receptors and/or with intracellular growth factor-activated signal transduction pathways represents a promising strategy for the development of novel and selective anticancer therapies. With the clinical validation of several new drugs specifically targeting molecules involved in angiogenesis, antiangiogenic therapy is in broad use for the treatment of cancers. Indeed, more than 40 VEGF inhibitors are currently in development.[8] The present study showed that bevacizumab (a humanized monoclonal antibody targeting the VEGF/VEGF receptor pathway) significantly decreases carcinomatosis-related ascites formation but alone is unable to cause a reduction in tumor growth and tumor carcinomatosis.

Recent studies have indicated that human cancers can acquire resistance after anti-VEGF treatments, ag-

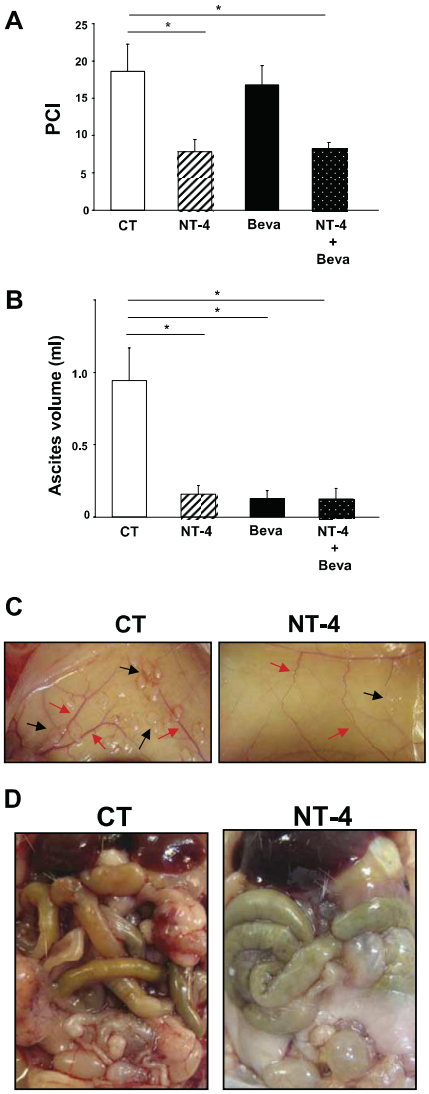

Figure 4. Effects of NT-4 on tumor carcinomatosis, ascites formation, and tumor angiogenesis in an orthotopic peritoneal carcinomatosis model in athymic mice. **A:** Overexpression of NT-4, but not bevacizumab (Beva), decreases the distribution of transplanted cancer in the abdomen and pelvis using modified PCI assessment. **B:** Both NT-4 overexpression in LS174 cells and Beva inhibit carcinomatosis-related ascites formation. **C:** Photography demonstrates that NT-4 overexpression in LS174 decreases tumor carcinomatosis and blood vessels in the parietal peritoneum. **Black arrows** indicate LS174 metastasis, **red arrows** indicate blood vessels. **D:** Photography shows fewer blood vessels in the abdominal cavity in the NT-4 group compared with the CT group, suggesting that NT-4 has an inhibitory effect on tumor angiogenesis. Error bars represent SEM. $^{*}P < 0.05$.

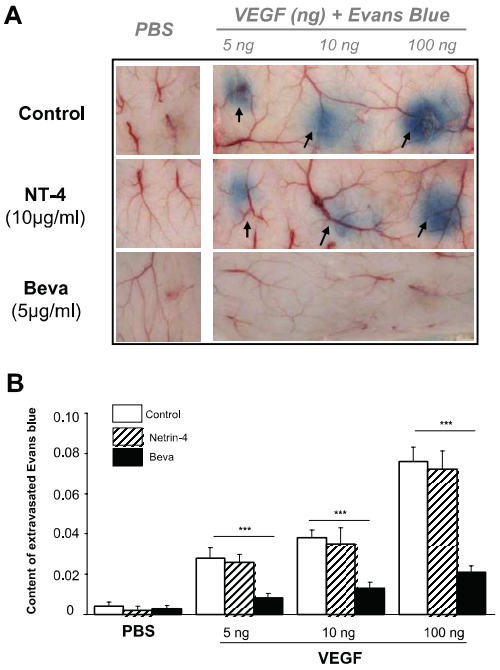

Figure 5. Acute effect of NT-4 on VEGF-induced augmentation of vascular permeability in guinea pig using Evans blue. **A:** Representative photos. **Arrows** indicate leakage of Evans blue in the skin. **B:** NT-4 has no effect on VEGF-induced acute augmentation of vascular permeability. In contrast, bevacizumab (Beva) efficiently inhibits the VEGF-induced acute increase in vascular permeability. Error bars represent SEM. $^{***}P < 0.001$.

gravating the pathologic situation.[15–17] In addition, the disruption in VEGF function often leads to severe secondary effects, such as delayed wound healing, renal damage, and subsequent hypertension.[14] As potential targets in cancer treatment, the netrin family is receiving more attention. Originally identified as axonal guidance molecules, netrins are laminin-like secreted proteins that have recently been shown to be involved in angiogenesis and blood vessel network formation.[28] As observed in the nervous system, netrins also act as bifunctional modulators in angiogenesis. Indeed, both proangiogenic and antiangiogenic effects of netrin have been reported.[29–31]

Using Matrigel angiogenesis assay, we showed that NT-4 inhibits VEGF/bFGF-induced, nontumoral angiogenesis. In many cancers, elevated VEGF levels have been documented.[9–13] It has also been suggested that VEGF may induce the expression of antiangiogenic factors, such as thrombospondin and NT-4. We showed that NT-4 is expressed in LS174 human colon cancer cells and that NT-4 overexpression can be stably induced in these cells. Therefore, NT-4 could be a negative feedback regulator of pathologic angiogenesis, such as CRC-related tumor angiogenesis. In fact, the present study demonstrated that NT-4 overexpression significantly decreases tumor growth in an s.c. CRC xenograft model, in accordance with results obtained by other research groups.[22,23] Although this inhibited tumor growth is associated with decreased tumor cell proliferation and enhanced tumor cell apoptosis *in vivo*, it seems that NT-4 does not exert a direct effect on tumor proliferation and

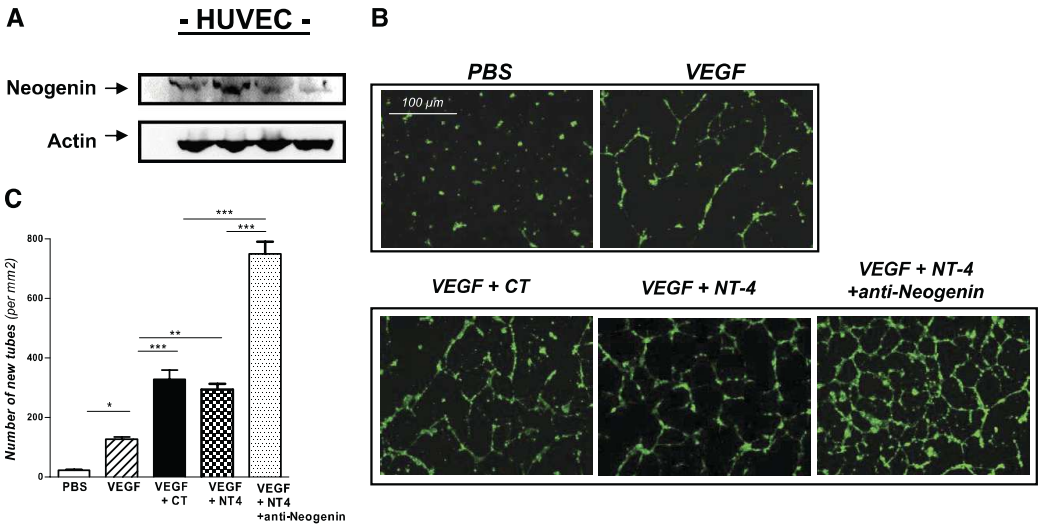

Figure 6. Involvement of neogenin in NT-4-related antiangiogenic activity in a Matrigel EC tube formation model. **A:** Neogenin is expressed in HUVEC. **B:** Representative images of Matrigel HUVEC tube formation from different experimental groups. **C:** In the presence of VEGF, the number of new EC tubes is enhanced by CT and NT-4 LS174 cells. Antibody directed against neogenin further increases EC tube formation. Error bars represent SEM. $^{*}P < 0.05$; $^{**}P < 0.01$; $^{***}P < 0.001$.

tumor apoptosis. Indeed, the present study showed that NT-4 overexpression has no direct *in vitro* effect on the proliferation of cultured LS174 cells. It has been reported that NT-4 inhibits *in vitro* proliferation of several tumor cell lines, such as pancreatic (Panc-1), liver (Hep3B), lung (SKLU1), and colon (HT29) tumor cell lines.[23] The *in vitro* effect of NT-4 on tumor cell proliferation seems to be cell line-dependent. Our *in vitro* study showed that NT-4 overexpression has no direct effect on the apoptosis of cultured tumor cells, in accordance with a previous study.[23] These results indicate that NT-4 does not exert an inhibitory effect on apoptosis of some tumor cell lines. A decrease in vascular EC is observed in tumor tissues after s.c. CRC xenograft, suggesting that NT-4 can decrease tumor proliferation, increase tumor apoptosis, and impair tumor growth by inhibiting tumor angiogenesis. Netrin-4 could exert this antiangiogenic effect by inhibiting the differentiation and migration of EC and stimulating the differentiation and migration of smooth muscle cells.[22,23]

In patients with CRC, the survival rate is negatively related to the extent of carcinomatosis, an advanced tumor stage leading to significant morbidity and mortality. This study demonstrated that NT-4 overexpression decreases the distribution of transplanted CRC in the abdomen and pelvis, indicating that NT-4 could delay carcinomatosis processes and suggesting a potential therapeutic interest of NT-4 in the treatment of cancer and/or carcinomatosis. In contrast, bevacizumab alone does not modify colorectal tumor carcinomatosis.

Bevacizumab significantly decreases colon cancer carcinomatosis-related ascites. Indeed, capillary permeability, the overall capillary membrane surface area available for filtration, hydraulic pressure, and oncotic pressure are all involved in the pathogenesis of malignant ascites. Previous studies showed that VEGF can rapidly induce the augmentation of vascular permeability[32,33]; thus, bevacizumab could decrease ascites formation, probably by rapidly reducing vascular permeability. Using the acute vascular permeability assay in guinea pigs, the present results showed that bevacizumab significantly decreases VEGF-induced acute augmentation of vascular permeability.

We showed that NT-4 overexpression is also capable of reducing carcinomatosis-related ascites in a similar manner as bevacizumab. However, NT-4 protein cannot directly block VEGF-induced acute augmentation of vascular permeability, suggesting that NT-4 inhibits carcinomatosis-related ascites by different mechanisms than the action of bevacizumab. Interestingly, we demonstrated by means of photography that fewer blood vessels are observed in the parietal peritoneum and abdominal cavity in animals with intraperitoneal transplantation of NT-4 LS174 cells. Netrin-4 could exert this antiangiogenic effect by inhibiting the differentiation and migration of EC.[22] These data suggest that NT-4 could inhibit ascites formation, at least in part, by decreasing the overall capillary membrane surface area available for filtration. In addition, it has been reported that NT-4 could stimulate the differentiation and migration of smooth muscle cells,[22,23] suggesting that NT-4 could decrease the permeability of the tumor vascular network by chronically promoting vessel maturation. However, this hypothesis should be verified by further experiments.

The present study showed that co-culture with LS174 cells augments EC tube formation, indicating that tumor cells promote angiogenesis, in accordance with a previous study.[34] It has been reported that NT-4 recombinant protein and NT-4 small interfering RNA could inhibit HUVEC tube

formation.[22,23] We did not detect a significant difference in EC tube formation between CT and NT-4 LS174 cells, probably owing to insufficient NT-4 protein secretion induced by NT-4 pcDNA vector transfection during a short-term (18-hour) cell culture. The neutralizing antibody directed against neogenin, a receptor of NT-4, dramatically increases EC tube formation, strongly suggesting that neogenin mediates the antiangiogenic activity of NT-4.[22,23] The activity of NT-4 is due to a baseline secretion of LS174 rather than to an overexpression of NT-4 induced by NT-4 pcDNA vector transfection.

In conclusion, NT-4 decreases tumor growth, delays carcinomatosis, and reduces ascites formation by inhibiting tumor angiogenesis. These findings highlight a therapeutic interest in NT-4 as a promising alternative to anti-VEGF treatments in the implementation of therapies against cancer.

References

1. Jemal A, Siegel R, Ward E, Hao Y, Xu J, Murray T, Thun MJ: Cancer statistics, 2008. CA Cancer J Clin 2008, 58:71–96
2. Lieberman D: Progress and challenges in colorectal cancer screening and surveillance. Gastroenterology 2010, 138:2115–2126
3. Ries LA, Wingo PA, Miller DS, Howe HL, Weir HK, Rosenberg HM, Vernon SW, Cronin K, Edwards BK: The annual report to the nation on the status of cancer, 1973–1997, with a special section on colorectal cancer. Cancer 2000, 88:2398–2424
4. Dvorak HF: Angiogenesis: update 2005. J Thromb Haemost 2005, 3:1835–1842
5. Ferrara N, Kerbel RS: Angiogenesis as a therapeutic target. Nature 2005, 438:967–974
6. Folkman J: Tumor angiogenesis: therapeutic implications. N Engl J Med 1971, 285:1182–1186
7. Zhong H, Bowen JP: Antiangiogenesis drug design: multiple pathways targeting tumor vasculature. Curr Med Chem 2006, 13:849–862
8. Ivy SP, Wick JY, Kaufman BM: An overview of small-molecule inhibitors of VEGFR signaling. Nat Rev Clin Oncol 2009, 6:569–579
9. Dvorak HF: Vascular permeability factor/vascular endothelial growth factor: a critical cytokine in tumor angiogenesis and a potential target for diagnosis and therapy. J Clin Oncol 2002, 20:4368–4380
10. Karkkainen MJ, Petrova TV: Vascular endothelial growth factor receptors in the regulation of angiogenesis and lymphangiogenesis. Oncogene 2000, 19:5598–5605
11. Nagy JA, Vasile E, Feng D, Sundberg C, Brown LF, Detmar MJ, Lawitts JA, Benjamin L, Tan X, Manseau EJ, Dvorak AM, Dvorak HF: Vascular permeability factor/vascular endothelial growth factor induces lymphangiogenesis as well as angiogenesis. J Exp Med 2002, 196:1497–1506
12. Schlessinger J, Ullrich A: Growth factor signaling by receptor tyrosine kinases. Neuron 1992, 9:383–391
13. Ullrich A, Schlessinger J: Signal transduction by receptors with tyrosine kinase activity. Cell 1990, 61:203–212
14. Eremina V, Jefferson JA, Kowalewska J, Hochster H, Haas M, Weisstuch J, Richardson C, Kopp JB, Kabir MG, Backx PH, Gerber HP, Ferrara N, Barisoni L, Alpers CE, Quaggin SE: VEGF inhibition and renal thrombotic microangiopathy. N Engl J Med 2008, 358:1129–1136
15. Helfrich I, Scheffrahn I, Bartling S, Weis J, von Felbert V, Middleton M, Kato M, Ergun S, Schadendorf D: Resistance to antiangiogenic therapy is directed by vascular phenotype, vessel stabilization, and maturation in malignant melanoma. J Exp Med 2010, 207:491–503
16. Huang D, Ding Y, Zhou M, Rini BI, Petillo D, Qian CN, Kahnoski R, Futreal PA, Furge KA, Teh BT: Interleukin-8 mediates resistance to antiangiogenic agent sunitinib in renal cell carcinoma. Cancer Res 2010, 70:1063–1071
17. Priceman SJ, Sung JL, Shaposhnik Z, Burton JB, Torres-Collado AX, Moughon DL, Johnson M, Lusis AJ, Cohen DA, Iruela-Arispe ML, Wu L: Targeting distinct tumor-infiltrating myeloid cells by inhibiting CSF-1 receptor: combating tumor evasion of antiangiogenic therapy. Blood 2010, 115:1461–1471
18. Freitas C, Larrivee B, Eichmann A: Netrins and UNC5 receptors in angiogenesis. Angiogenesis 2008, 11:23–29
19. Pasquale EB: Eph receptors and ephrins in cancer: bidirectional signalling and beyond. Nat Rev Cancer 2010, 10:165–180
20. Cirulli V, Yebra M: Netrins: beyond the brain. Nat Rev Mol Cell Biol 2007, 8:296–306
21. Dumartin L, Quemener C, Laklai H, Herbert J, Bicknell R, Bousquet C, Pyronnet S, Castronovo V, Schilling MK, Bikfalvi A, Hagedorn M: Netrin-1 mediates early events in pancreatic adenocarcinoma progression, acting on tumor and endothelial cells. Gastroenterology 2010, 138:1595–1606.
22. Lejmi E, Leconte L, Pedron-Mazoyer S, Ropert S, Raoul W, Lavalette S, Bouras I, Feron JG, Maitre-Boube M, Assayag F, Feumi C, Alemany M, Jie TX, Merkulova T, Poupon MF, Ruchoux MM, Tobelem G, Sennlaub F, Plouet J: Netrin-4 inhibits angiogenesis via binding to neogenin and recruitment of Unc5B. Proc Natl Acad Sci U S A 2008, 105:12491–12496
23. Nacht M, St Martin TB, Byrne A, Klinger KW, Teicher BA, Madden SL, Jiang Y: Netrin-4 regulates angiogenic responses and tumor cell growth. Exp Cell Res 2009, 315:784–794
24. Passaniti A, Taylor RM, Pili R, Guo Y, Long PV, Haney JA, Pauly RR, Grant DS, Martin GR: A simple, quantitative method for assessing angiogenesis and antiangiogenic agents using reconstituted basement membrane, heparin, and fibroblast growth factor. Lab Invest 1992, 67:519–528
25. Harmon RL, Sugarbaker PH: Prognostic indicators in peritoneal carcinomatosis from gastrointestinal cancer. Int Semin Surg Oncol 2005, 2:3
26. Otto J, Jansen PL, Lucas S, Schumpelick V, Jansen M: Reduction of peritoneal carcinomatosis by intraperitoneal administration of phospholipids in rats. BMC Cancer 2007, 7:104
27. Miles AA, Miles EM: Vascular reactions to histamine, histamine-liberator and leukotaxine in the skin of guinea-pigs. J Physiol 1952, 118:228–257
28. Eichmann A, Makinen T, Alitalo K: Neural guidance molecules regulate vascular remodeling and vessel navigation. Genes Dev 2005, 19:1013–1021
29. Larrivee B, Freitas C, Trombe M, Lv X, Delafarge B, Yuan L, Bouvree K, Breant C, Del TR, Brechot N, Germain S, Bono F, Dol F, Claes F, Fischer C, Autiero M, Thomas JL, Carmeliet P, Tessier-Lavigne M, Eichmann A: Activation of the UNC5B receptor by Netrin-1 inhibits sprouting angiogenesis. Genes Dev 2007, 21:2433–2447
30. Lu X, Le NF, Yuan L, Jiang Q, De Lafarge B, Sugiyama D, Breant C, Claes F, De SF, Thomas JL, Autiero M, Carmeliet P, Tessier-Lavigne M, Eichmann A: The netrin receptor UNC5B mediates guidance events controlling morphogenesis of the vascular system. Nature 2004, 432:179–186
31. Wilson BD, Ii M, Park KW, Suli A, Sorensen LK, Larrieu-Lahargue F, Urness LD, Suh W, Asai J, Kock GA, Thorne T, Silver M, Thomas KR, Chien CB, Losordo DW, Li DY: Netrins promote developmental and therapeutic angiogenesis. Science 2006, 313:640–644
32. Numnum TM, Rocconi RP, Whitworth J, Barnes MN: The use of bevacizumab to palliate symptomatic ascites in patients with refractory ovarian carcinoma. Gynecol Oncol 2006, 102:425–428
33. Wright JD, Hagemann A, Rader JS, Viviano D, Gibb RK, Norris L, Mutch DG, Powell MA: Bevacizumab combination therapy in recurrent, platinum-refractory, epithelial ovarian carcinoma: a retrospective analysis. Cancer 2006, 107:83–89
34. Agarwal A, Das K, Lerner N, Sathe S, Cicek M, Casey G, Sizemore N: The AKT/I κ B kinase pathway promotes angiogenic/metastatic gene expression in colorectal cancer by activating nuclear factor-κ B and β-catenin. Oncogene 2005, 24:1021–1031

Netrin-4 overexpression suppresses primary and metastatic colorectal tumor progression

CLARISSE EVENO[1,2], JEAN-OLIVIER CONTRERES[1], PATRICIA HAINAUD[1], JUDITH NEMETH[3], EVELYNE DUPUY[1] and MARC POCARD[1,2]

[1]INSERM U965 Angiogenesis and Translational Research, Departments of [2]Digestive Diseases and [3]Pathology, Paris Diderot, Paris 7 University, Lariboisière Hospital, AP-HP, 75010 Paris, France

DOI: 10.3892/or_xxxxxxxx

Abstract. Tumor angiogenesis is closely associated with clinical staging and has been proposed to correlate with clinical response in terms of subsequent metastases following primary resection. Netrin-4 (NT-4) regulates angiogenic responses. Therefore, we sought to examine the effects of NT-4 on the primary tumor growth of colon cancer cells, liver and lung metastases of colon cancer cells, and responses following primary tumor resection. We used 3 different mouse models of orthotopic primary tumor and liver and lung metastases, comparing 2 human colon cancer cells lines: wild-type (low expression of NT-4) and NT-4 (overexpression of NT-4) LS174 cells. NT-4 overexpression inhibited the primary tumor growth of colorectal LS174 xenografts in nude mice (144.3±12.9 vs. 62.4±4.5 mm^3; P<0.0001) as well as its related local and systemic recurrence (38 vs. 0%; P<0.01). NT-4 overexpression also markedly decreased colorectal cancer progression in terms of tumor number and volume of liver metastases in the NT-4 group of the orthotopic liver metastasis model (25 vs. 90% and 4±1 vs. 709±190 mm^3, P<0.001 and P<0.05). Collectively, our findings indicate that NT-4 overexpression decreases colorectal lung metastasis and its associated lymph node involvement. NT-4 overexpression decreases tumor recurrence and metastasis after surgical resection, likely via an anti-angiogenic effect. These observations suggest that NT-4 may hold therapeutic potential in the treatment of colorectal cancer growth and major metastatic sites.

Introduction

Colorectal cancer (CRC) is the second leading cause of cancer deaths in North America and Western Europe, comprising about 10% of new cancer cases every year (1,2). Approximately 20% of patients have detectable liver metastases at diagnosis, which is the predominant cause of death in patients with CRC (3-5). Only patients with a limited number of isolated, organ-confined metastases exhibit prolonged survival or the possibility of complete response following surgical resection (6-8). The development of new therapeutic strategies is critical for improving pre-existing therapeutic approaches to increase survival rates, particularly in patients with colorectal liver metastasis. Adhesion, invasion, angiogenesis, inflammation, tumor microenvironment and tumor cell growth are all mechanistic factors that facilitate liver metastasis in CRC. The growth and metastasis of solid tumors depends critically on tumor angiogenesis (9). This concept has promoted the development of angiogenesis inhibitors targeting the vascular endothelial growth factor (VEGF) pathway, which has been validated by clinical trials. Bevacizumab, a humanized monoclonal antibody targeting VEGF, is the first anti-angiogenic drug that, when administered in combination with conventional chemotherapy, has demonstrated improvements in tumor response rates and progression-free survival among patients with liver metastatic in CRC (10,11). However, the adverse side effects and the limited efficacy of the anti-VEGF inhibitors due to intrinsic and/or acquired resistance have hampered their clinical benefits and precluded their further inclusion as an adjuvant treatment (12). For these reasons, the evaluation of new anti-angiogenic targets is crucial, and other targets, such as placenta growth factor (PlGF), have been proposed (13).

Netrins comprise a family of diffusible molecules including at least five ligands (netrins 1, 2, 4, G1a and G1b) and seven receptors (neogenin, DCC, Unc5A, Unc5B, Unc5C, Unc5D and A2b) that have regulatory roles in vascular development (14,15). Although the significance of the netrin-dependent pathway in tumor angiogenesis remains unclear, emerging evidence indicates that this pathway has an important role in the development of different cancers in animal models (14). NT-4 may therefore represent a potential therapeutic target for cancer treatment. A previous study showed that netrin-4 (NT-4) overexpression delayed tumor angiogenesis through binding to neogenin and recruitment of Unc5B in a subcutaneous (s.c.) xenograft model (16). In addition, a recent study demonstrated that NT-4 regulated angiogenic responses and inhibited the growth of CRC cells (17).

Correspondence to: Professor Marc Pocard, INSERM U965 Angiogenesis and Translational Research (Paris 7 University), Hôpital Lariboisière, 8 rue Guy Patin, 75010 Paris, France
E-mail: marc.pocard@inserm.fr

Key words: angiogenesis, colon cancer, liver metastasis, mice, Netrin-4,

We previously identified NT-4 as a protein expressed in LS174 human colon cancer cells grown *in vitro* and further demonstrated that NT-4 inhibits tumor progression by exerting inhibitory effects on tumor angiogenesis, without altering tumor cell proliferation or apoptosis. Furthermore, we found that NT-4 exerts antiangiogenic activity, likely by binding to neogenin and decreasing CRC carcinomatosis and ascites formation, in animal models (18).

The aim of this study was to examine the effects of NT-4 overexpression on tumor angiogenesis and growth *in vivo* using 3 mouse models that mimic clinical situations: orthotopic primary tumor resection as a treatment of a local tumor stage, liver and lung metastasis as a treatment of an advanced tumor stage. For these purposes, we designed a model of CRC primary tumor and liver and lung metastases in which control or NT-4-transfected LS174 tumor cells were subsequently transplanted. Our study showed that NT-4 overexpression delayed primary tumor growth, lymph node involvement and liver and lung metastases.

Materials and methods

In the present study, we successively studied the link between NT-4 and primary and metastatic tumor development in three orthotopic murine models: i) primitive tumor (n=20 per group), ii) liver metastasis (n=10 per group), and iii) and lung metastasis (n=8 per group).

Cell culture. LS174 human colon cancer cells obtained from the American Type Culture Collection were maintained in Dulbecco's modified Eagle's medium (DMEM) supplemented with 10% heat-inactivated fetal bovine serum (FBS)/penicillin (50 U/ml)/streptomycin (50 μg/ml) (Gibco-BRL Life Technologies Inc., Grand Island, NY, USA) in a humidified atmosphere of 95% air and 5% CO_2 at 37°C.

Synthesis of NT-4 cDNA. Total RNA was extracted from cultures of human umbilical artery endothelial cells (HUAEC), and reverse transcription was performed using the AMV kit (Roche Applied Science, Indianapolis, IN, USA). Two sets of primers (1-1039 and 914-1884) were used to amplify the NT-4 sequence with Taq DNA polymerase (Roche Applied Science). Products from the two PCR reactions were mixed 1:1 and used as the template to obtain a NT-4 cDNA. The construct was subcloned into a pcDNA3.1(-)/His-myc C vector (Invitrogen, Carlsbad, CA, USA).

LS174 cell transfection. The NT-4-containing vector was transfected into LS174 cells with Lipofectin (Invitrogen), according to the manufacturer's protocol. Cells were cultured in a selective media (10% FBS-DMEM) containing 200, 300, 400 and 500 μg/ml of G418 (Geneticin; Gibco-BRL Life Technologies Inc.). Cell clones were subsequently screened by enzyme-linked immunosorbent assay (ELISA) to detect increases in NT-4 expression relative to that in the pcDNA-transfected cells that were collected after 3 days in conditioned medium (data no shown).

For the *in vivo* experiments, wild-type (WT) or NT-4-transfected LS174 cells were harvested, washed with 10% FBS-DMEM, counted and resuspended in DMEM prior to injection. Cell viability was assessed by trypan blue exclusion, which verified that the cell viability was >95% in both cell lines.

Animal tumor xenograft models. Each experimental protocol satisfied all of the standard requirements of the European community guidelines for the care and use of the laboratory animals. Five-week-old female nude or nod scid mice (Charles River Laboratories International Inc., Wilmington, MA, USA) were acclimated for 1-2 weeks before tumor transplantation (10 animals per experimental group). For all *in vivo* models, the animals were anesthetized with xylazine (2 mg/ml) and ketamine (20 mg/ml) (Vibrac, Carros, France).

Animal models of primary tumor resection. We first analyzed the effect of NT-4 overexpression in a primary tumor model 19 by orthotopic xenograft on the colon of nude mice. For this purpose, either NT-4-transfected (NT-4 LS174) or wild-type (WT-LS174) LS174 cells ($1x10^6$ cells) were subcutaneously injected into 5-week-old female nude mice. The tumor volume was recorded using a caliper twice weekly. Animals were sacrificed 30 days after engraftment. After resection of the subcutaneous tumor (Fig. 1A), 1 mm^3 tumor fragments were prepared (Fig. 1B) and a surgical orthotopic implantation was performed on the colon of nude mice. The colon was exposed by a small midline incision (Fig. 1C) to allow for the implantation of the tumor fragment on the colon by 5-0 surgical sutures under the serosa of the ascending colon (Fig. 1D). The application of biological glue followed by peritoneal and skin closures completed the procedure (Fig. 1E and F).

On Day 8, to reproduce human clinical care, a midline laparotomy was performed to expose the colon (Fig. 1G), and a clip was applied to provide hemostasis and digestive integrity. The colonic tumor was resected (Fig. 1I) and the tumor volume (cm^3) was calculated by using the following equation: V= length x $width^2$ x p/6 (Fig. 1J). Mice were monitored to analyze recurrence patterns and were sacrificed on Day 70.

Animal models of liver metastasis. Under sterile conditions, either NT-4 or WT-LS174 cells ($2x10^6$ cells) were intrasplenically injected into 5-week-old female nod scid mice. First, a 10-mm left subcostal incision was made to expose the spleen over the peritoneum. Then, the cell suspension was injected into the spleen using a 27 G needle. Following light splenic compression, the spleen was repositioned back in the abdominal cavity, peritoneum and muscles were sutured closed with one stitch and the wound was closed with a clip. Thirty days after inoculation with tumor cells, the mice were sacrificed, and the liver weight was recorded to evaluate the tumor metastases. Microspecimens of the spleen and liver were harvested for pathological confirmation of liver metastasis by HES stain.

Animal models of lung metastasis. In the LS174 lung metastasis model, either NT-4 or WT LS174 cells ($2x10^6$) were injected via the tail vein of 5-week-old female nude mice. Thirty days after inoculation, the mice were sacrificed, and the lung weight was recorded for evaluation of tumor metastasis.

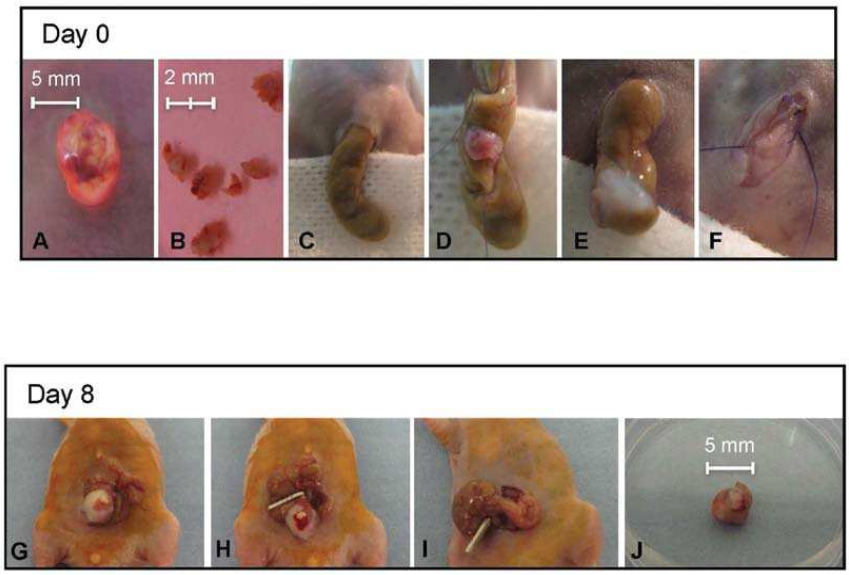

Figure 1. Intraoperative view of the primary tumor xenograft. (A) Subcutaneous tumor ablation; (B) procurement of 1 mm^3 fragment; (C) exposure of the colon by a small midline incision; (D) implantation of the tumor fragment by suture; (E) application of biological glue; (F) peritoneal and skin closure. Intraoperative view of the primary tumor xenograft resection on Day 8. (G) Midline laparotomy, colon exposure; (H) clip application providing hemostasis and digestive integrity; (I) resection of colonic tumor; (J) specimen.

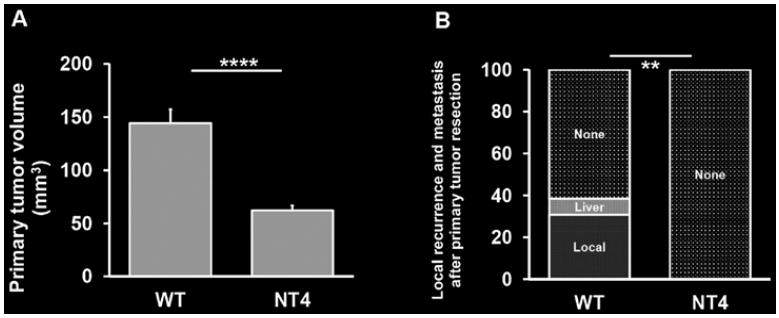

Figure 2. WT LS174 mice exhibited voluminous primary tumors (A) and local recurrence and metastases (B) whereas NT-4 LS174 mice exhibited small primary tumors and no recurrence.

Microspecimens of the lung, mediastinal and cervical lymph nodes were harvested for pathological confirmation of metastasis by HES stain. The sera of sacrificed mice were assessed for carcinoembryonic antigen (CEA).

Statistical analysis. All results are expressed as the mean ± SEM. We used StatView® and R programs (R is available at http://www.R-project.org) for the statistical analysis. We tested associations between epidemiological and prognostic variables using the Mann-Whitney test or Fisher's exact test. A Kruskall-Wallis test was applied for the analysis of variance. P-values of 0.05 (*) or less ($^{**}P<0.01$, $^{***}P<0.001$) were considered to indicate statistical significance.

Results

NT-4 overexpression decreases colorectal primary tumor growth and increases response to surgical resection. The primary tumor volume was significantly reduced in animals injected with NT-4 LS174 tumor cells compared with WT LS174 cells (n=20 per group, mean ± SEM; 62.4±4.5 and 144.3±12.9 mm^3 for NT-4 and WT LS174 tumors, respectively; P<0.0001; Fig. 2A), suggesting that NT-4 expression affects the primary tumor growth of orthotopically transplanted colorectal cancer.

Seventy days after tumor transplantation and 62 days after surgical resection, the number of local and systemic

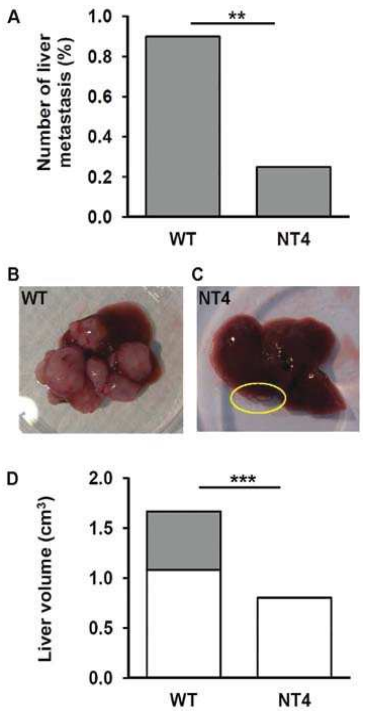

Figure 3. Macroscopic aspects of liver metastases after removal of the liver at animal sacrifice, 30 days after splenic injections. WT LS174 mice (A, B and D) exhibited numerous voluminous metastases whereas NT-4 LS174 mice (C) exhibited small metastases localized at the periphery of the liver (yellow circle).

recurrences was significantly decreased in the NT-4 LS174 tumor group compared with WT LS174 group. The WT group exhibited four local and one disseminated liver tumor recurrences whereas the NT-4 group exhibited no recurrences, suggesting that NT-4 expression affects the metastatic progression of orthotopically transplanted cancer (n=13 per group, 38 and 0% for the WT and NT-4 groups, respectively; P<0.01) (Fig. 2B).

NT-4 overexpression decreases colorectal liver metastasis. Thirty days after splenic injection of WT or NT-4-transfected LS174 tumor cells, the number and tumor volume of liver metastases were assessed. The number of liver metastases was significantly lower in the NT-4 group compared with the WT group (n=10 per group, 25 vs. 90%, respectively for NT-4 and WT LS174 groups, P<0.001) (Fig. 3A-C). The liver volume was markedly reduced in the NT-4 group compared with the WT LS174 groups (n=10 per group, 4±1 mm^3 and 709±190 mm^3, respectively for NT-4 and WT LS174 groups, P<0.05) (Fig. 3D).

NT-4 overexpression decreases colorectal lung metastasis and its related lymph nodes involvement. The effects of NT-4 overexpression were analyzed in the lung metastasis model employing tail vein injection of WT- or NT-4-transfected LS174 tumor cells. In the WT group, tumor microemboli were detected in one mouse, and liver metastases were detected in another mouse. However, in this WT group, all mice had large, cervical, axillary, mediastinal and retroperitoneal pathological lymph nodes (Fig. 4A-F). A histological analysis of lymph nodes revealed diffuse tumor infiltration in 5 of 8 mice (62.5%). In contrast, the mice in the NT-4 group developed neither lung nor liver metastases, nor did they exhibit lymph node enlargement.

Serum levels of ACE were significantly increased in the WT mice, with lymph node involvement averaging 2.78±0.43 ng/ml compared with 0.05 ng/ml (detection limit) in the control mice (P<0.05).

Discussion

Anti-angiogenic therapies are broadly applied in the treatment of several cancers, particularly CRC. Bevacizumab, the humanized monoclonal antibody targeting vascular endothelial growth factor, is a pioneering anti-angiogenic drug that demonstrates clinical benefit in combination with chemotherapy in patients with advanced metastatic CRC. No adjuvant anti-angiogenic therapy has previously exhibited success in prolonging disease-free survival of non-metastatic colon cancer patients. Recently, in adjunction of FOLFOX therapy, bevacizumab failed to significantly prolong disease-free survival in stage II and III colon cancer patients (12). In addition to the possibility of rebound effect (20), adverse and fatal effects such as hemorrhage, wound healing complications, gastrointestinal perforation, hypertension and proteinuria were elicited by anti-VEGF therapies (21-25). Furthermore, most tumors have been found to develop mechanistic resistance to anti-angiogenic agent (26).

Originally identified as axonal guidance molecules, the netrin family has recently been shown to be involved in angiogenesis and blood vessel network formation (27). As observed in the nervous system, netrins also act as bifunctional modulators in angiogenesis. Indeed, both pro- and anti-angiogenic effects of netrin have been reported (28-30). The ability of human umbilical artery endothelial cells (HUAEC) to migrate and organize into tubular structures was inhibited by the NT-4 overexpression. Reciprocally, silencing the N4 gene in HUAEC was shown to increase both cellular branching and their ability to form tubular structures on Matrigel, when compared with non-transfected or control siRNA-transfected cells (16). Netrin 4 inhibits *in vitro* human microvascular ECs and tube formation (17). However, Netrin 4 has been shown to potentially inhibit the proliferation of various tumor cells *in vitro* with modest effects on the proliferation of endothelial cell and non-transformed cells (17). We have previously demonstrated that Netrin-4 overexpression attenuates CRC carcinomatosis by inhibiting tumor angiogenesis, with no direct effects on tumor cell proliferation or apoptosis (18).

This investigation aimed to evaluate the *in vivo* effects of NT-4 on tumor angiogenesis and tumor growth in an orthotopic tumor and a liver and lung metastasis model of CRC. For this purpose, LS174 tumor cells were either transfected or not transfected with NT-4 before injection.

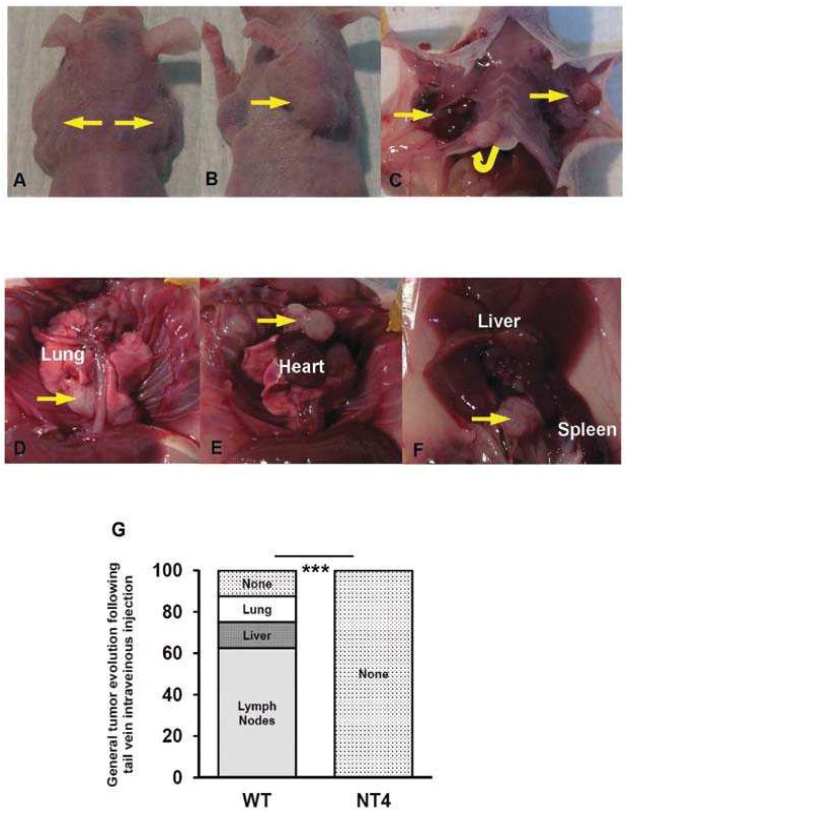

Figure 4. Macroscopic aspects of lymph node metastases, 30 days after tail vein injections. (A) Cervical lymph nodes, external view (arrow). (B) Axillary lymph nodes, external view (arrow). (C) Axillary (arrow) and parasternal (curved arrow) lymph nodes, internal view. (D and E) Mediastinal lymph nodes, internal view (arrow). (F) Retroperitoneal lymph nodes, internal view (arrow). WT LS174 mice exhibited numerous metastases (G), whereas NT-4 LS174 mice exhibited no sign of metastasis.

In the orthotopic CRC xenograft model, we demonstrated that NT-4 overexpression decreases the tumor volume on Day 8 after colonic CRC transplantation, indicating that NT-4 expression may delay tumor process. These findings suggest that NT-4 may exhibit therapeutic potential for the treatment of primary cancer. Furthermore, in this model, NT-4 overexpression significantly reduced the primary tumor volume and abolished local recurrence and metastasis up to 62 days after primary tumor resection.

In investigating the effect of NT-4 on distal metastasis, we found that NT-4 overexpression also reduced liver and lung metastases in the two CRC metastasis models examined.

Our previous results confirm that the differences in primary tumor and metastatic outcomes are specifically conferred by NT-4 overexpression, rather than the effects of clonal selection resulting from our technique or our usage of only one cell line. Despite the limitation of the number of CRC cell lines tested, our findings suggest that NT-4 may be exploited for anti-CRC therapy in humans. Future studies are necessary to evaluate the potential of the NT-4 as an anti-CRC target, identify the target of NT-4 in human tumors and evaluate the effect of NT-4 in a study of patients who require the resection of metastatic disease.

References

1. Jemal A, Siegel R, Ward E, Hao Y, Xu J, Murray T and Thun MJ: Cancer statistics, 2008. CA Cancer J Clin 58: 71-96, 2008.
2. Lieberman D: Progress and challenges in colorectal cancer screening and surveillance. Gastroenterology 138: 2115-2126, 2010.
3. Leonard GD, Brenner B and Kemeny NE: Neoadjuvant chemotherapy before liver resection for patients with unresectable liver metastases from colorectal carcinoma. J Clin Oncol 23: 2038-2048, 2005.
4. Mahmoud N and Bullard Dunn K: Metastasectomy for stage IV colorectal cancer. Dis Colon Rectum 53: 1080-1092, 2010.
5. Stangl R, Altendorf-Hofmann A, Charnley RM and Scheele J: Factors influencing the natural history of colorectal liver metastases. Lancet 343: 1405-1410, 1994.
6. Fortner JG, Silva JS, Golbey RB, Cox EB and Maclean BJ: Multivariate analysis of a personal series of 247 consecutive patients with liver metastases from colorectal cancer. I. Treatment by hepatic resection. Ann Surg 199: 306-316, 1984.
7. Scheele J, Stang R, Altendorf-Hofmann A and Paul M: Resection of colorectal liver metastases. World J Surg 19: 59-71, 1995.

8. Tomlinson JS, Jarnagin WR, DeMatteo RP, *et al*: Actual 10-year survival after resection of colorectal liver metastases defines cure. J Clin Oncol 25: 4575-4580, 2007.
9. Folkman J: Tumor angiogenesis: therapeutic implications. N Engl J Med 285: 1182-1186, 1971.
10. Kabbinavar F, Hurwitz HI, Fehrenbacher L, *et al*: Phase II, randomized trial comparing bevacizumab plus fluorouracil (FU)/leucovorin (LV) with FU/LV alone in patients with metastatic colorectal cancer. J Clin Oncol 21: 60-65, 2003.
11. Kabbinavar FF, Hambleton J, Mass RD, Hurwitz HI, Bergsland E and Sarkar S: Combined analysis of efficacy: the addition of bevacizumab to fluorouracil/leucovorin improves survival for patients with metastatic colorectal cancer. J Clin Oncol 23: 3706-3712, 2005.
12. Allegra CJ, Yothers G, O'Connell MJ, *et al*: Phase III trial assessing bevacizumab in stages II and III carcinoma of the colon: results of NSABP protocol C-08. J Clin Oncol 29: 11-16, 2011.
13. Van de Veire S, Stalmans I, Heindryckx F, *et al*: Further pharmacological and genetic evidence for the efficacy of PlGF inhibition in cancer and eye disease. Cell 141: 178-190, 2010.
14. Cirulli V and Yebra M: Netrins: beyond the brain. Nat Rev Mol Cell Biol 8: 296-306, 2007.
15. Dumartin L, Quemener C, Laklai H, *et al*: Netrin-1 mediates early events in pancreatic adenocarcinoma progression, acting on tumor and endothelial cells. Gastroenterology 138: 1595-1606, 2010.
16. Lejmi E, Leconte L, Pedron-Mazoyer S, *et al*: Netrin-4 inhibits angiogenesis via binding to neogenin and recruitment of Unc5B. Proc Natl Acad Sci USA 105: 12491-12496, 2008.
17. Nacht M, St Martin TB, Byrne A, Klinger KW, Teicher BA, Madden SL and Jiang Y: Netrin-4 regulates angiogenic responses and tumor cell growth. Exp Cell Res 315: 784-794, 2009.
18. Eveno C, Broqueres-You D, Feron JG, *et al*: Netrin-4 delays colorectal cancer carcinomatosis by inhibiting tumor angiogenesis. Am J Pathol 178: 1861-1869, 2011.
19. Hoffman RM: Orthotopic metastatic mouse models for anticancer drug discovery and evaluation: a bridge to the clinic. Invest New Drugs 17: 343-359, 1999.
20. Miles D, Harbeck N, Escudier B, *et al*: Disease course patterns after discontinuation of bevacizumab: pooled analysis of randomized phase III trials. J Clin Oncol 29: 83-88, 2011.
21. Chen HX and Cleck JN: Adverse effects of anticancer agents that target the VEGF pathway. Nat Rev Clin Oncol 6: 465-477, 2009.
22. Gressett SM and Shah SR: Intricacies of bevacizumab-induced toxicities and their management. Ann Pharmacother 43: 490-501, 2009.
23. Higa GM and Abraham J: Biological mechanisms of bevacizumab-associated adverse events. Expert Rev Anticancer Ther 9: 999-1007, 2009.
24. Ranpura V, Hapani S and Wu S: Treatment-related mortality with bevacizumab in cancer patients: a meta-analysis. JAMA 305: 487-494, 2011.
25. Zangari M, Fink LM, Elice F, Zhan F, Adcock DM and Tricot GJ: Thrombotic events in patients with cancer receiving antiangiogenesis agents. J Clin Oncol 27: 4865-4873, 2009.
26. Eikesdal HP and Kalluri R: Drug resistance associated with antiangiogenesis therapy. Semin Cancer Biol 19: 310-317, 2009.
27. Eichmann A, Makinen T and Alitalo K: Neural guidance molecules regulate vascular remodeling and vessel navigation. Genes Dev 19: 1013-1021, 2005.
28. Larrivee B, Freitas C, Trombe M, *et al*: Activation of the UNC5B receptor by Netrin-1 inhibits sprouting angiogenesis. Genes Dev 21: 2433-2447, 2007.
29. Lu X, Le Noble F, Yuan L, *et al*: The netrin receptor UNC5B mediates guidance events controlling morphogenesis of the vascular system. Nature 432: 179-186, 2004.
30. Wilson BD, Ii M, Park KW, *et al*: Netrins promote developmental and therapeutic angiogenesis. Science 313: 640-644, 2006.

3ème Partie :

Mettre au point une technique non invasive d'évaluation par Echographie-Doppler de l'angiogenèse tumorale et physiologique hépatique

Article 4:

Tumor and non-tumor liver angiogenesis is traced and evaluated by hepatic arterial ultrasound in murine models.

Eveno C, Le Henaff C, Audollent R, Soyer P, Rampanou A, Nemeth J, Brouland JP, Dupuy E, Pocard M, Bonnin P.

Ultrasound Med Biol. 2012 Jul;38(7):1195-204.

Dans le traitement des métastases hépatiques, il est essentiel d'avoir des techniques d'imagerie performantes pour permettre un diagnostic précoce ainsi que pour évaluer la réponse au traitement. Plusieurs études précliniques ont analysé l'architecture microvasculaire et la perfusion vasculaire des métastases hépatiques avec des résultats contradictoires.[193-196] Certains auteurs ont décrit un changement de perfusion hépatique lors du développement de métastases hépatiques dans un modèle murin, avec une diminution du flux portal associé à une augmentation de la perfusion artérielle ;[194, 197] tandis que d'autres n'ont observé aucun changement de flux par scanner.[193] Cuenod et al. rapportent, dans un modèle murin de métastases hépatique après injection intra-splénique, une diminution du débit portal associée à une augmentation du temps de transit sanguin hépatique évalués par scanner. Cette modification de flux était observée aussi bien dans les cas présentant des métastases macroscopiques que dans ceux présentant des métastases occultes.[193] Des études cliniques scannographiques de petit effectif ont trouvé une corrélation entre l'augmentation de la perfusion artérielle hépatique et la présence de macro- ou micrométastases.[198, 199] Ces résultats ont donné lieu à une étude en cours (menée sous la direction du Pr Vilgrain à l'Hôpital Beaujon) sur la valeur pronostique sur l'apparition de métastases

hépatiques de l'Index de Perfusion Hépatique (correspondant au rapport entre la perfusion hépatique d'origine artérielle et la perfusion hépatique totale) pré-thérapeutique évalué par scanner de perfusion chez des malades atteints de cancer colique initialement non métastatique.

Leen et al. ont suggéré qu'un index Doppler anormal (Doppler Perfusion Indice [DPI], rapport du débit dans l'artère hépatique sur la somme du flux artériel et porte hépatique) pourrait être un important facteur prédictif de la présence de micrométastases hépatiques d'origine colorectale.[200] Après 5 ans de suivi de 120 patients ayant eu une chirurgie curative pour un cancer colorectal isolé, un DPI augmenté été corrélée avec un stade Dukes C et un taux élevé de récidive.[200]

Nous avons analysé par Echographie Doppler l'angiogenèse tumorale accompagnant les métastases hépatiques d'origine colorectale dans un modèle murin et caractérisé les variations de la VFm dans les artères hépatique et mésentérique avec ou sans traitement anti-angiogénique. Dans le groupe injecté avec des cellules LS174 sauvages, les animaux présentaient une atteinte diffuse hépatique avec un flux dans l'artère hépatique, nourrissant les métastases, élevé par rapport au groupe contrôle sans injection de cellule tumorale. Cela met en avant la possibilité d'évaluer par Echo-Doppler l'angiogenèse d'aval, dont le flux dans l'artère nourricière (ici hépatique) est un reflet. Dans le groupe injecté avec des LS174 surexprimant la NT4, anti-angiogénique délivré par voie locale, l'atteinte tumorale était inhibée, avec des métastases plus petites et moins nombreuses. Dans ce groupe, le flux dans l'artère hépatique était diminué, reflet de l'inhibition de l'angiogenèse tumorale. Dans notre modèle de métastases hépatiques, la VFm de l'artère mésentérique, ne vascularisant pas les métastases, étaient similaires et stables dans les deux groupes ; témoignant de la spécificité de la modification du flux dans le territoire artériel hépatique qui est le reflet de la néo-angiogenèse tumorale.

Pour valider notre technique d'évaluation de l'angiogenèse d'aval par Echographie Doppler, nous avons créé un modèle murin d'hépatectomie de 50% stimulant une angiogenèse physiologique au cours de la régénération hépatique. Après hépatectomie partielle il existe en effet une phase non vasculaire de régénération hépatique pendant les 2 premiers jours après la chirurgie et une phase ultérieure vasculaire caractérisée par une prolifération endothéliale et une

angiogenèse active.[168, 172] Dans notre modèle, après la phase non vasculaire de régénération hépatique, le nombre de vaisseaux augmentait progressivement à partir de 2ème jour. Les cellules endothéliales proliféraient et le nombre de vaisseaux était restauré aux 7ème et 16ème jours. La VFm augmentait progressivement dans l'artère hépatique, avec un débit de pointe semblable au 7ème jour dans les deux artères hépatique et mésentérique, indicatifs d'une augmentation à la fois artérielle et veineuse des flux hépatiques. Les VFm des artères hépatique et mésentérique revenaient aux valeurs initiales au 16ème jour lorsque le foie était régénéré en volume. Par conséquent, la VFm évaluée par Echographie Doppler pourrait fournir une évaluation fonctionnelle de la vascularisation, en particulier lors de la régénération hépatique chez les patients qui ont eu une hépatectomie partielle pour métastase hépatique.

En conclusion, notre méthode d'analyse de l'angiogenèse d'aval par Echographie Doppler dans des modèles murins est une technique simple et non invasive qui peut être utilisé pour évaluer l'angiogenèse tumorale et physiologique et en particulier pour tester l'efficacité des traitements anti-angiogéniques. Nos résultats précliniques suggèrent que cette technique d'imagerie peut être appliquée pendant le suivi des patients pour détecter précocement des métastases hépatiques ou juger de l'efficacité d'un traitement anti-angiogénique. Cette technique a déjà été validée chez l'homme par notre équipe dans la maladie de Crohn, avec une corrélation entre un flux accéléré dans l'artère mésentérique supérieure chez les patients en poussée aigüe par rapports au groupe contrôle et une normalisation du flux sous traitement efficace par anti-TNFα.[201]

Ultrasound in Med. & Biol., Vol. 38, No. 7, pp. 1195–1204, 2012

0301-5629/$ - see front matter

doi:10.1016/j.ultrasmedbio.2012.03.004

d Original Contribution

TUMOR AND NON-TUMOR LIVER ANGIOGENESIS IS TRACED AND EVALUATED BY HEPATIC ARTERIAL ULTRASOUND IN MURINE MODELS

CLARISSE EVENO,[*y] CAROLE LE HENAFF,[z] RAPHAËLLE AUDOLLENT,[*] PHILIPPE SOYER,[x] AURORE RAMPANOU,[*] JUDITH NEMETH,[jj] JEAN-PHILIPPE BROULAND,[jj] EVELYNE DUPUY,[*] MARC POCARD,[*y] and PHILIPPE BONNIN[*{]

[*] Université Paris-Diderot, Sorbonne Paris Cité, INSERM, UMR-S 965, Paris, France; [y]Université Paris-Diderot, Sorbonne Paris Cité, AP-HP, Hôpital Lariboisière, Chirurgie Digestive, Paris, France; [z]Unité INSERM U926, Reims, France; [x]Université Paris-Diderot, Sorbonne Paris Cité, AP-HP, Hôpital Lariboisière, Radiologie Viscérale, Paris, France; [jj]Université Paris-Diderot, Sorbonne Paris Cité, AP-HP, Hôpital Lariboisière, Anatomopathologie, Paris, France; and [{] Université Paris-Diderot, Sorbonne Paris Cité, AP-HP, Hôpital Lariboisière, Physiologie Clinique-Explorations-Fonctionnelles, Paris, France

(Received 15 December 2011; revised 22 February 2012; in final form 4 March 2012)

Abstract—We studied the relationships between hepatic and mesenteric mean blood-flow velocities (mBFVs) measured by ultrasound imaging and (1) downstream tumor angiogenesis during liver metastasis induced by spleen injection of LS174 human colon cells overexpressing the antiangiogenic Netrin4 (LS174-NT4) or not (LS174-WT) and (2) downstream normal angiogenesis during hepatic regeneration after 50% hepatectomy. Liver volume and mBFVs were measured before and after surgery, at day 30 in the first model and at days 2, 7 and 16 in the second model. LS174-NT-4 vs. LS174-WT mice presented fewer metastases (25% vs. 90%, p , 0.001) and decreased hepatic mBFVs (16.5 ± 0.8 vs. 21.8 ± 1.4 cm s^{21}, p , 0.01), without difference in mesenteric mBFVs. After partial hepatectomy, hepatic and mesenteric mBFVs increased at day 7, from 12.4 ± 1.7 and 11.8 ± 2.6 to 19.1 ± 1.8 and 17.5 ± 2.4 cm s^{21}, respectively, (p , 0.01) then returned to baseline as liver volume. Duplex Doppler ultrasonography reliably assesses normal or tumor angiogenesis and may provide follow-up functional evaluation. (E-mail: philippe.bonnin@lrb.aphp.fr) Ó 2012 World Federation for Ultrasound in Medicine & Biology.

Key Words: Ultrasonography, Liver, Metastasis, Angiogenesis, Mice, Liver regeneration.

INTRODUCTION

The liver is the most common site of colorectal metastasis. Approximately 25% of patients with colorectal cancer will present with synchronous hepatic lesions and over half will ultimately develop liver metastasis during the course of their disease (Jemal et al. 2008; Leonard et al. 2005; Stangl et al. 1994). Patients with a small number of isolated, organ-confined metastases can expect prolonged survival or even cure by partial hepatic resection (Fortner et al. 1984; Scheele et al. 1995; Tomlinson et al. 2007).

To our knowledge, no duplex Doppler ultrasonography or microvascular density analysis have been tested to detect or quantify active angiogenesis in specific association with liver metastasis (Cianchi et al. 2002; Nanashima et al. 1998; Rajaganeshan et al. 2007). Moreover, duplex Doppler ultrasonography has been proposed to evaluate drug effects after only one course of anticancer treatment (Lassau et al. 2006). This information is important to determine whether or not a change in treatment regimen is needed. Determining the most appropriate strategy is now one of the most difficult problems to solve regarding liver metastases from colorectal cancer (Van Cutsem et al. 2010) because several alternate options including two-step strategy (Adam et al. 2000; Wicherts et al. 2008) or preoperative portal vein embolization are now available (Covey et al. 2008; Elias et al. 2002). In parallel, the potential effects of antiangiogenic therapy on hepatic parenchyma must also be included as a part of the comparison between the different treatment procedures (Wicherts et al. 2011). However, the effects of antiangiogenic therapy on liver regeneration are still unknown because clinical studies have led to inconclusive results (Aussilhou et al. 2009; Zorzi et al. 2008).

Address correspondence to: Dr. Philippe Bonnin, Université Paris-Diderot, Sorbonne Paris Cité, AP-HP, Hôpital Lariboisière, Physiologie Clinique-Explorations-Fonctionnelles, 75010, Paris, France. E-mail: philippe.bonnin@lrb.aphp.fr

Over 10 years ago, Leen et al. demonstrated that duplex Doppler ultrasonography helped predict a high risk for occurrence of liver metastases after primary tumor resection (on the basis of the ratio of hepatic arterial to total liver blood flow [Leen et al. 2000]). This study suggested a relationship between angiogenesis modification and early-stage intra-liver metastases. Similarly, a group of researchers have demonstrated a relationship between angiogenesis and hepatic blood inflow a transgenic hepatocellular carcinoma mouse model (Bonnin et al. 2007; Vincent et al. 2009). In this model, multistep processes of tumor growth and tumor angiogenesis were characterized by a remodeling of tumor sinusoids and the acquisition of an arterial phenotype by tumor sinusoidal endothelial cells (Hainaud et al. 2006). Using this model, we developed noninvasive measurements of liver volume and quantification of neovascularization by conventional two-dimensional (2-D), color-coded and duplex Doppler ultrasonography. In addition, the increase in hepatic blood flow velocity was found proportional to an increase in microvessel density, as shown by CD31-immunostaining of the sinusoids (Dupuy et al. 2003). The purpose of our study was to evaluate the relationships between changes in blood flow velocity in the hepatic artery and downstream normal and tumoral angiogenesis in a murine model.

MATERIALS AND METHODS

In vivo *studies*

All experimental protocols met all standards required by the European Community guidelines for the care and use of laboratory animals (agreement number B 75-10-03). Five-week-old female athymic NOD/SCID mice (Charles River Laboratories International Inc., Wilmington, MA, USA) were acclimated for 1–2 weeks before tumor transplantation.

Animal models of tumor xenograft and liver metastasis

To analyze hepatic tumor angiogenesis, we created a murine model of human colorectal liver metastasis. Animals were anesthetized with xylazine (2 mg/mL) and ketamine (20 mg/mL) (Vibrac, Carros, France). A 10 mm left subcostal incision was performed to expose the spleen over the peritoneum. Cell suspensions (NT-4 LS174 or WT LS174, 2×10^6 cells) were injected into the spleen using a 27-gauge needle. After soft splenic compression, the spleen was returned to the abdominal cavity, the peritoneum was sutured with one stitch and the wound was closed with a clip. Thirty days after inoculation with tumor cells, the mice were sacrificed after duplex Doppler ultrasonography and the liver weight was recorded for the evaluation of tumor metastasis. A micro specimen of the liver was analyzed and liver metastases were confirmed histopathologically. Duplex Doppler ultrasonography was used to quantify the increase in liver angiogenesis. The antiangiogenic effect was considered in this same model. As bevacizumab could be ineffective to inhibit human tumor progression in a xenograft mice model when tested alone (Eveno et al. 2008) and that rapid vascular regrowth could be observed after reversal of vascular endothelial growth factor (VEGF) inhibition (Ebos et al. 2009; Mancuso et al. 2006), we choose to evaluate the direct effect of an antiangiogenic molecule, locally expressed, without any systemic first passage. We postulated that the antiangiogenic drugs had to be first delivered to the liver. To obtain such a model, tumor cells were transfected to express an antiangiogenic molecule directly at the liver site.

Netrin-4 (NT-4) was previously demonstrated as having substantial antiangiogenic effects (Eveno et al. 2011). Netrins belong to a family of diffusible molecules with a regulatory role in axon pathfinding and in other developmental processes, including vascular development (Freitas et al. 2008). Overexpression of NT-4 correlates with delayed tumor angiogenesis in a subcutaneous xenograft model (Lejmi et al. 2008) and decreased tumor growth and carcinomatosis *via* an antiangiogenic effect, which suggests a therapeutic potential for NT-4 in the treatment of colorectal cancer growth and carcinomatosis (Eveno et al. 2011). This prompted us to quantitatively evaluate the effect of NT-4 overexpression in our murine model of liver metastasis by comparing two human colon cancer cell lines, LS174 wild-type (LS174-WT, with low expression of NT4) in 10 mice and NT4-transfected LS174 cells (NT4-LS174, overexpressing NT4) in 12 mice, by using duplex Doppler ultrasonography.

Cell culture and cell transfection

LS174 human colon cancer cells were obtained from the American Type Culture Collection and maintained in Dulbecco's modified Eagle medium (DMEM) supplemented with 10% heat-inactivated fetal bovine serum, penicillin (50 U/mL) and streptomycin (50 μg/mL) (Gibco BRL Life Technologies Inc., Grand Island, NY, USA) in a humidified atmosphere of 95% air and 5% CO_2 at 37°C. Acquisition of cDNA for NT-4 was performed as previously described (Eveno et al. 2011).

For the *in vivo* experiments, LS174 cells transfected with NT-4 or wild-type LS174 cells were harvested. The cells were washed in 10% fetal bovine serum DMEM, counted and suspended in DMEM for injection. Cell viability was assessed by trypan blue exclusion to make sure that cell viability was greater than 95% in both cell lines.

Animal model of liver regeneration

To validate our technique of angiogenesis evaluation by duplex Doppler ultrasonography, we created a 50% hepatectomy murine model to evaluate physiologic angiogenesis during liver regeneration. Liver regeneration was induced by subjecting mice to 50% partial hepatectomy. After a midline laparotomy, the liver was exposed and both the upper left lobe and the lower left lobe were ligated (Vicryl 3-0) and resected, resulting in the removal of 50% of the liver volume. Before closure of the abdominal wall in two layers (Vicryl 5-0), 250 μL of a 5% glucose solution (37°C) was injected into the abdominal cavity. Histopathologic examinations were performed with hematoxylin-eosin stain to quantify vessel density at days 0, 2, 7 and 16. Slides were examined at low-power magnification (×2.5) to identify the area with the highest density of vessels. The most vascularized areas were selected and vessels measuring more than 5 μm in diameter were counted in 3 fields of 0.31 mm^2 at ×20 magnification (Axioscope A1; AxioCam ICc1, Zeiss, Gottingen Germany). The average count was recorded for analysis.

Partial hepatectomy is associated with an early, no-vascular phase of liver regeneration during the first 2 days after surgery and a later vascular phase characterized by endothelial proliferation and angiogenesis (Ding et al. 2010; Drixler et al. 2002). Duplex Doppler ultrasonography was performed before surgery (day 0) and after partial hepatectomy at different times (at days 2, 7 and 16) in eight mice to analyze the changes in hepatic arterial blood flow velocity that occur during liver regeneration.

Ultrasonographic study

Mice were anesthetized with isoflurane (0.5%) and monitored to prevent any cardiorespiratory depression. The animals were shaved to increase probe contact and placed in the left lateral decubitus position on a heating-blanket (38°C). This position avoided placing pressure on the abdomen with the transducer and subsequent bradycardia or hypotension.

An ultrasonographic unit (Vivid 7; GE Medical Systems Ultrasound, Horten, Norway) equipped with a 12 MHz linear transducer, was used (Bonnin et al. 2007; Vincent et al. 2009). All data were transferred online to an image workstation for differed analysis (PC EchoPAC; GE Medical Systems *ultrasound*®, Horten, Norway). Two-dimensional ultrasound imaging was used to measure liver sizes, including the transverse diameter, anterior-posterior diameter and height of the liver (Fig. 1a–c). The transducer was placed on the anterior abdominal wall; a cross-sectional B-mode image of the upper part of the abdomen allowed measurements of the transversal diameter of the liver (Dt). A turn of 90° of the transducer gave access to an anterior longitudinal B-mode image of the abdomen and measurements of the height (Ht) and anterior-posterior diameter (Dap) of the liver. Imaging depth was set at 2–3 cm when applying zoom, frame-rate was 49.5 frames per second. Color-Doppler mode was activated on an anterior longitudinal view of the abdomen crossing the longitudinal axis of the aorta. Hepatic and mesenteric arteries were localized on the screen by their color-coded blood flow (Fig. 1d). The color Doppler frequency emission was 6.7 MHz, pulsed repetition frequency set at 3.5 kHz and low velocity rejection at 1.65 cm s^{-1}. Frame-rate was 37.8 frames per second. A pulsed Doppler sample was placed on the longitudinal axis of each vessel and the pulsed Doppler spectrum was recorded with simple repositioning of the pulsed Doppler sample from the hepatic artery (Fig. 1e) to the mesenteric artery (Fig. 1f). The Doppler frequency emission was 6.7 MHz, pulsed repetition frequency was set between 4.3 and 10.8 kHz, the sample volume was at 1 mm and the low velocity rejection at 0.6 cm s^{-1}. Ultrasound beam width of pulsed Doppler was small enough (1.1 mm) to ensure that flow from neighboring vessels were not superimposed in the measurement volume centred on hepatic or mesenteric artery as assessed by the spectral Doppler analysis of the obtained Doppler waveforms. Time-average mean blood flow velocity (mBFV) was measured from the pulsed Doppler spectrum of each artery by simple redrawing the blue line drawn on the Doppler spectrum. All mBFV were measured with correction of the angle between the long axis of each vessel and the Doppler beam. Use of the steer mode of the Doppler beam helped to avoid angle correction greater than 10°. Liver sizes and BFVs were measured by the same investigator. Measurements were repeated three times and averaged. Accuracy of length and velocity measurements was previously determined by performing the calculation of the intraobserver repeatability coefficients (British Standards Institution 1979). Repeatability coefficients were 110 μm for the Dt and the Da-p, 120 μm for the Ht of the liver and were 1.7 and 2.5cm s^{-1} for the mean BFV of mesenteric and hepatic arteries, respectively. The echo-derived volume of the liver was calculated assuming that liver volume is a cylinder, using the following formula: liver volume = $[\pi \times (Dt/2) \times (Dap/2)] \times [Ht]$ as previously reported (Bonnin et al. 2007). This algorithm was verified in our two models. A significant correlation was found in the set of experiments with partial hepatectomy with a positive linear regression close to the line of identity ($n = 8$, slope of 1.11 ± 0.26, intercept to –0.10 ± 0.27, R = 0.87, $p = 0.005$). The correlation was also significant in the set of experiments with hepatic metastasis induction with a positive linear regression, slope was slightly

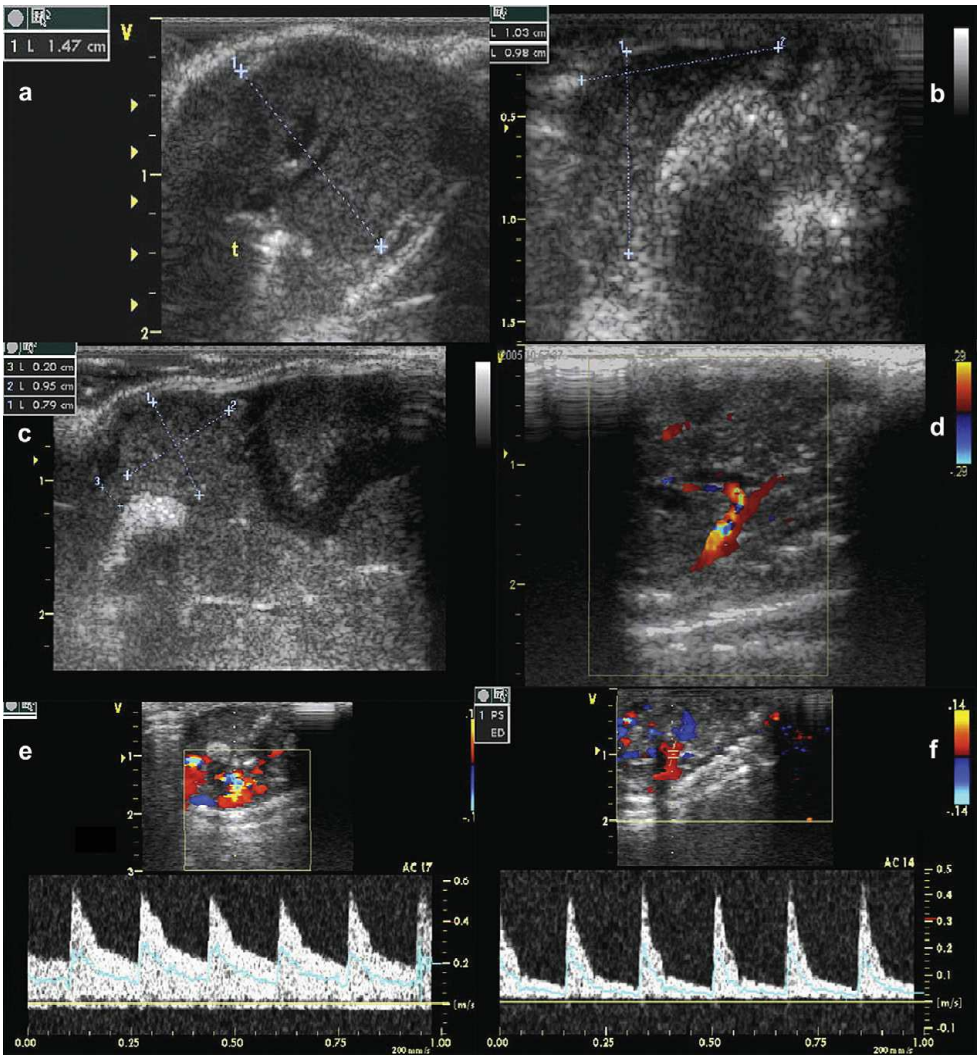

Fig. 1. Two-dimensional US imaging of the liver of splenic LS174 wild-type injected mice. (a) Upper abdominal, transverse, cross-sectional view; a dashed line represents the transverse diameter (Dt = 1) of the liver. (b) Anterior, sagittal, medial cross-sectional view of the abdomen; dashed lines represent the anterior-posterior diameter (Dap = 1) and height (Ht = 2) of the liver. (c) Liver metastasis developed at the periphery of the liver (1 = 0.79 mm, 2 = 0.95 mm). Thickness of the hepatic left lobe: 3 = 0.20 mm. (d) Two-dimensional and color-coded Doppler US imaging of the hepatic (left artery directed toward the hepatic pedicle) and mesenteric arteries (right artery directed toward the gut) in an LS174 wild-type injected mouse. Spectral analysis of the pulsed Doppler signal recorded in the hepatic (e) and in the mesenteric (f) arteries. Doppler recordings provide access to the measurements of systolic, end-diastolic and time-averaged mean BFVs (blue line).

different from the line of identity (n = 20, slope = 1.31 ± 027, intercept to –0.32 ± 0.74 (R = 0.75, $p <$ 0.001). A possible explanation could be the modification of the liver architecture by metastasis at the surface of the liver, particularly at the anterior and inferior bordure of the liver, which increases, particularly Dap and Ht, and what could not be taken into account by the formula. However, correlations were obtained for all measurements offering the possibility to test hypothesis in a controlled system.

Statistical analysis

All results were expressed as means ± standard deviation. One-way analysis of variance (ANOVA) with *post hoc* Bonferroni and paired or unpaired Student's *t*-tests were used to analyze differences between groups using MedCalc Software (Mariakerke, Belgium), after verification of the power of the tests (>80%, http://www.anastats.fr). Linear regression analysis was done to analyze the correlation between mean BFV in the hepatic artery and tumor using MedCalc Software. A p value of ≤.05 was considered significant. Only differences superior to the repeatability coefficient for each measurements were retained.

RESULTS

Liver metastasis model: Morphologic results

Thirty days after xenograft, the percentage of hepatic involvement by tumor was significantly lower in the group of NT-4 LS174 xenograft mice in comparison with the group of mice with LS174-WT cells (25% vs. 90%, respectively, $p < 0.001$). Similarly, tumor volume was significantly lower in the group of mice with NT-4 LS174 cells, by comparison with the group of mice with LS174-WT cells (4 ± 1 mm^3 and 709 ± 190 mm^3, respectively, $p < 0.05$) (Fig. 2). The volume of the liver as calculated with ultrasonography was smaller in the NT-4 LS174 group by comparison with the volume calculated in the LS174-WT group (0.81 ± 0.08 cm^3 vs. 1.67 ± 0.23 cm^3, respectively, $p < 0.001$). In the control group (*i.e.*, non-injected mice), the volume of the liver remained constant at 0.87 ± 0.05 cm^3 during an observation period of 30 days.

Liver metastasis model: Blood flow velocities in hepatic and mesenteric arteries

No significant differences in heart rates were observed between the different groups. In the control group, the mean blood flow velocity (mBFV) in the hepatic artery remained constant to 14 ± 1.39 cm s^{-1} over the 30-day observation period. In the NT-4-LS174 xenograft mice, time-averaged mBFV in the hepatic artery was lower than in the LS174-WT group (16.5 ± 0.85 and 21.8 ± 1.43 cm s^{-1}, respectively, $p < 0.01$) (Fig. 3a). In contrast, no changes in the time-averaged mBFV were observed in the mesenteric artery in the two groups regardless the xenograft type (7.6 ± 0.57 cm s^{-1} and 7.7 ± 1.01, respectively; N.S.) (Fig. 3b). A positive linear regression was found between mBFV in the hepatic artery and tumor volume ($r^2 = 0.5865$, $p < 0.001$) (Fig. 3c).

Partial hepatectomy: Morphologic results

Before hepatectomy, the liver volume was 1.24 ± 0.05 cm^3. After a 50% hepatectomy, the estimated liver volume derived from the surgical specimen was decreased to 0.62 ± 0.05 cm^3 (posthepatectomy liver volume). Compared with posthepatectomy, the liver volume progressively increased to 0.84 ± 0.06 cm^3 at day 2 and to 0.95 ± 0.07 cm^3 at day 7 ($p < 0.05$ and 0.01), respectively). The liver achieved full restoration at day 16 at 1.07 ± 0.05 cm^3 ($p < 0.001$ vs. post-hepatectomy and N.S vs. before hepatectomy) (Fig. 4a).

Partial hepatectomy: Vessel count

Before surgery, the number of hepatic vessels per field was 180 ± 15. At day 2, the hepatic vessels count decreased to 116 ± 4 vessels per field ($p < 0.05$ vs. before surgery). At day 7 and day 16, the hepatic vessel count was restored to 159 ± 13 and 197 ± 26 vessels per field, respectively (Figs. 4b and 5).

Partial hepatectomy: Blood flow velocities in hepatic and mesenteric arteries

After partial hepatectomy, mBFV in the hepatic artery increased progressively from 12.4 ± 1.7 cm s^{-1}

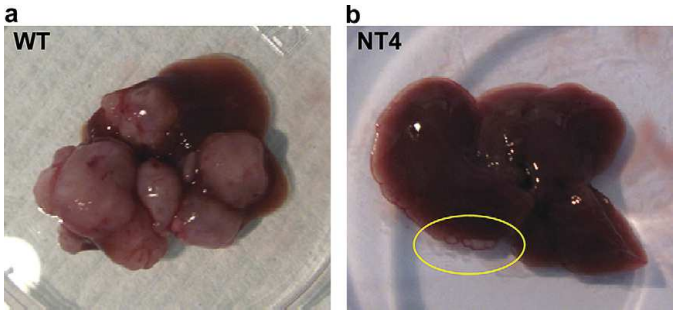

Fig. 2. Samples of the macroscopic aspects of liver metastasis after removal of the liver upon animal sacrifice, 30 days after splenic injections. (a) LS174-WT mice ($n = 10$) displayed numerous and voluminous metastasis whereas (b) NT-4 LS174 mice ($n = 12$) displayed small metastases localized at the liver periphery (yellow circle).

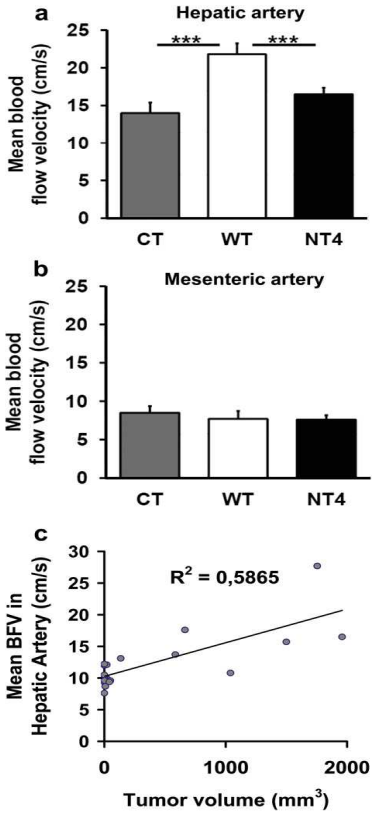

Fig. 3. US Doppler imaging of the hepatic and mesenteric arteries. Mean blood flow velocity (mBFV) measured in the hepatic (a) and the mesenteric (b) arteries at 30 days after splenic cell injections with LS174 wild-type (WT) ($n = 10$) or with NT-4 LS174 (NT4) ($n = 12$) compared with control mice (CT) (*i.e.*, without splenic injection). WT animals displayed a significant increase in mBFV in the hepatic artery compared to CT or NT4 animals, suggesting angiogenesis. Hepatic mBFV was only slightly increased in NT4 animals, suggesting an antiangiogenic effect. Mean BFVs were not different in the mesenteric artery between groups. (c) Linear regression between the mean blood flow velocity in the hepatic artery and tumor volume. There was a good correlation between the mBFV in the hepatic artery and tumor volume ($r^2 = 0.59$), suggesting that tumor angiogenesis was proportional to tumor genesis (***$p < 0.001$).

before surgery to 19.1 ± 1.83 at day 7 ($p < 0.01$ vs. before hepatectomy) and returned to basal values at day 16. At day 2, during the nonvascular phase, the mBFV in the hepatic artery remained constant (14.5 ± 2.1 cm s^{-1}, N.S. vs. before hepatectomy), while the hepatic vessel count was reduced, suggesting an adaptive phenomena consisting of vasodilation (Fig. 4b and c). At day 7, while endothelial cells and vessels proliferated and while the liver was regenerating, mBFV in the hepatic artery was dramatically increased, suggesting hyperemia. At day 16, liver volume and vessel numbers were fully restored and mBFV in the hepatic artery returned to basal values (13.6 ± 1.80 cm s^{-1}, $p < 0.05$). Changes in mBFV in the mesenteric artery followed mBFV changes in the hepatic artery, with a maximum at day 7 of 17.5 ± 2.4 cm s^{-1} vs. 11.8 ± 2.6 cm s^{-1} before surgery ($p < 0.01$; Fig. 4d).

DISCUSSION

In our study, we demonstrated that increase in mean blood flow velocity recorded in the hepatic artery and, thus, in the hepatic arterial inflow were able to reflect the tumor angiogenesis that accompanied the tumor growth in case of liver metastasis. During liver regeneration after partial hepatectomy, increase in mBFV recorded in the hepatic and mesenteric arteries was able to reflect the physiologic angiogenesis of the normal hepatic tissues. In this case, changes in mBFV in the hepatic artery were then representative of the increase in hepatic arterial inflow that accompanied the regeneration of a normal hepatic arterial vascular network, whereas changes in mBFV in the mesenteric artery were indirectly indicative of the concomitant increase in hepatic venous inflow that accompanied the regeneration of a normal portal vascular network.

Almost 50% of patients with colorectal cancer will ultimately develop liver metastasis, which is an important prognostic factor (Baker and Pelley 1995). Surgical resection of liver metastases from colorectal cancer offers the only hope for cure, with 5-year survival rates ranging from 21%–48% (Fong et al. 1997; Scheele and Altendorf-Hofmann 1999). Recently, a new strategy, which is based on inhibition of neoangiogenesis, has been proposed to control malignant proliferation and metastasis growth (Folkman 1971). Bevacizumab is a humanized, monoclonal antibody directed against VEGF that has been examined in combination with fluorouracil and leucovorin (Kabbinavar et al. 2003, 2005), or to FOLFIRI or FOLFOX (Hurwitz et al. 2004), leading to improved tumor response rates and progression-free survival for patients with metastatic colorectal cancer.

Preclinical, animal studies are needed to better understand the development and vascularization of liver metastases. Diagnostic means are essential for an early detection of liver metastasis, which presumably would allow earlier initiation of an appropriate therapeutic

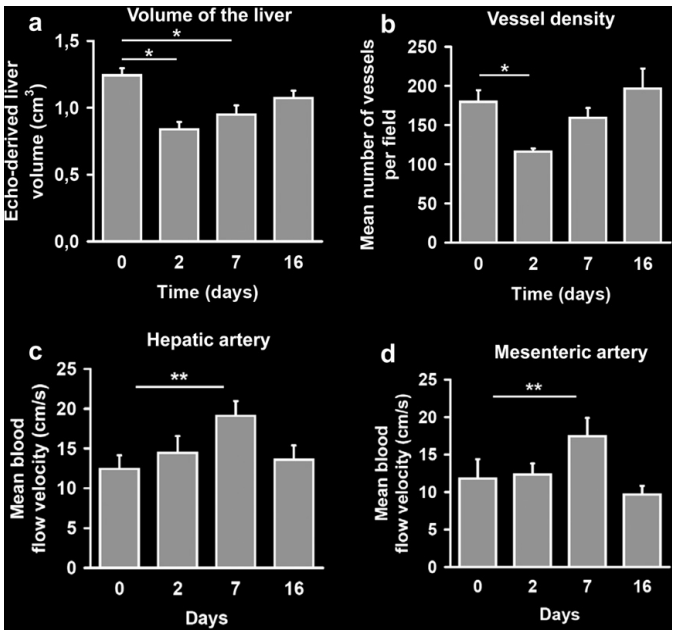

Fig. 4. Model of 50% partial hepatectomy ($n = 8$). (a) Echo-derived liver volume was decreased at days 2 and 7 compared with the values measured before hepatectomy. Volume was restored at day 16. (b) Hepatic vessel density was decreased at day 2 in relation to the classical, nonvascular first phase of hepatic regeneration. From day 7, vessel density was restored. (c) Mean blood flow velocity in the hepatic artery was dramatically increased from day 7, whereas vessel density was normal, suggesting microvessel vasodilation. (d) Mean blood flow velocity in the mesenteric artery was also increased at day 7, suggesting elevated blood flow in the portal vein and a hyperemia of both arterial and venous hepatic inflows ($*p < 0.05$; $**p < 0.01$).

option. Similarly, diagnostic tools are needed to evaluate the response to therapy. During the last decade, several preclinical studies have addressed the better understanding of the microvascular architecture and blood perfusion of hepatic metastases with conflicting results (Cuenod et al. 2001; Kruskal et al. 2000, 2004; Yarmenitis et al. 2000). Some authors described a change in hepatic perfusion in mouse livers developing liver metastases with a decrease in portal perfusion in association with an increased arterial perfusion (Kruskal et al. 2004; Liu and Matsui 2007) whereas others have not observed any change in arterial blood flow (Cuenod et al. 2001). Some clinical studies based on the computed tomography evaluation of small populations of patients found a correlation between increased liver arterial perfusion and the presence of macro- or micrometastasis (Leggett et al. 1997; Platt et al. 1997). Leen et al. have suggested that an abnormal Doppler ratio (Doppler perfusion index [DPI], hepatic artery flow to the sum of hepatic arterial blood flow and portal venous blood flow) might be an important predictor for the presence of small or occult

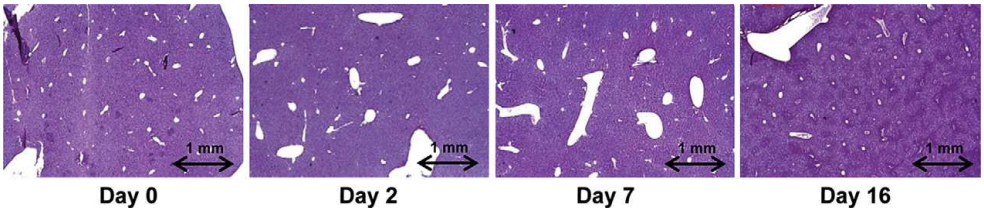

Fig. 5. Histological assessment of liver vascularization after 50% partial hepatectomy. Vessel density was decreased at day 2 and restored at day 7 and day 16 compared with day 0.

hepatic metastases from colorectal cancer in human (Leen et al. 2000). After a 5-year follow-up of 120 patients undergoing curative surgery for isolated colorectal cancer, increased DPI was correlated with Dukes stage C tumors and recurrence. Six percent of patients with normal DPI developed recurrent disease by contrast with 73% in patients who had an abnormal DPI.

The other major interest for using diagnostic tools in colorectal liver metastasis is to evaluate the effectiveness of an antiangiogenic therapy. Traditional size-based radiologic criteria, as well as the response evaluation criteria in solid tumors (RECIST) score, might not reflect the actual tumor response when targeted therapies are used (Klinger et al. 2009; Ratain and Eckhardt 2004). Therefore, for gastrointestinal stromal tumors treated with imatinib mesylate (Gleevec®, Novartis Pharmaceuticals, East Hanover, NJ), new computed tomography-response criteria have been proposed (Choi et al. 2007). The adjunct of bevacizumab to cytotoxic therapy does not appear to increase the radiologic tumor response using RECIST criteria (Klinger et al. 2009). New computed tomography-based morphologic features, as overall attenuation, tumor-liver interface and the peripheral rim of enhancement are used (Chun et al. 2009). This fact can be supported by a recent study that showed that the adjunct of bevacizumab to cytotoxic therapy led to a survival benefit, even in nonresponding patients (Grothey et al. 2008).

In our study, we analyzed the mechanisms of angiogenesis in liver metastases from colorectal cancer by a noninvasive method, to characterize BFV variations in the hepatic and mesenteric arteries in a murine model with or without antiangiogenic treatment. The mouse group that received a basal level of Netrin-4 had a more diffuse involvement of the liver by comparison with the group of mice that overexpressed Netrin-4. The antiangiogenic activity of this protein appears to reduce the growth of metastases. We found that the changes in mBFV in the hepatic artery, which is the tumor-feeding artery correlated with the expression of Netrin-4. At this stage, we showed an increase in time-average BFV only in the hepatic artery in the non-overexpressing, Netrin-4 injected mice. In our model, the BFV of the gut-feeding mesenteric artery upstream from non-tumor microvasculature were similar and stable in both groups. Taken together, these data suggest that the increase in mBFV in the hepatic artery indicates an only arterial low inflow vascular resistance during metastatic liver processes. This could be the result of the development of an only hepatic artery-dependent tumor vascular network. Our data are, therefore, strictly in accordance with the previously demonstrated changes in the DPI in the presence of hepatic metastasis from colorectal cancer in human (Leen et al. 2000).

To validate our technique of downstream angiogenesis evaluation by duplex Doppler ultrasonography, we created a 50% hepatectomy murine model of physiologic angiogenesis during liver regeneration. Partial hepatectomy is associated with an early, nonvascular phase of liver regeneration during the first 2 days after surgery and a later vascular phase characterized by endothelial proliferation and angiogenesis (Ding et al. 2010; Drixler et al. 2002). In our model, liver regeneration began early and the liver volume was restored at day 16. After a nonvascular phase of liver regeneration, the number of hepatic vessels increased progressively from day 2. Endothelial cells began to proliferate and the vessel numbers were restored at days 7 and 16. The mBFV increased progressively in the hepatic artery, with a similar peak flow at day 7 in both hepatic and mesenteric arteries indicative of increase in both arterial and venous hepatic inflows. This could be indicative of a similar contribution of both arterial and venous portal vasculogenesis and angiogenesis to the development of the hepatic vascular networks that accompanies normal liver regeneration. Mean BFV in both hepatic and mesenteric arteries then return to basal values at day 16 when liver regeneration is achieved. Therefore, mBFV as evaluated by duplex Doppler ultrasonography could provide a functional evaluation of non-tumor and/or tumor vascularity especially during liver regeneration in patient who had partial hepatectomy when a surgical resection of liver metastasis is indicated.

In conclusion, our method of downstream angiogenesis analysis by duplex Doppler ultrasonography in murine models is a simple and noninvasive technique that can be used to evaluate tumor and physiologic angiogenesis and particularly to test the efficacy of antiangiogenic drugs. Our preclinical results suggest that this imaging test may be applied during patient follow-up to detect liver metastases with enhanced tumor angiogenesis expression at an early stage, to decide whether an antiangiogenic treatment should be used instead of another targeted therapy for liver metastasis and to follow the effect of antiangiogenic therapy.

REFERENCES

Adam R, Laurent A, Azoulay D, Castaing D, Bismuth H. Two-stage hepatectomy: A planned strategy to treat irresectable liver tumors. Ann Surg 2000;232:777–785.

Aussilhou B, Dokmak S, Faivre S, Paradis V, Vilgrain V, Belghiti J. Preoperative liver hypertrophy induced by portal flow occlusion before major hepatic resection for colorectal metastases can be impaired by bevacizumab. Ann Surg Oncol 2009;16:1553–1559.

Baker ME, Pelley R. Hepatic metastases: Basic principles and implications for radiologists. Radiology 1995;197:329–337.

Bonnin P, Villemain A, Vincent F, Debbabi H, Silvestre JS, Contreres JO, Levy BI, Tobelem G, Dupuy E. Ultrasonic assessment of hepatic blood flow as a marker of mouse hepatocarcinoma. Ultrasound Med Biol 2007;33:561–570.

British Standards Institution. Precision of test method (BS5497, part 1). London: BSI; 1979.

Choi H, Charnsangavej C, Faria SC, Macapinlac HA, Burgess MA, Patel SR, Chen LL, Podoloff DA, Benjamin RS. Correlation of computed tomography and positron emission tomography in patients with metastatic gastrointestinal stromal tumor treated at a single institution with imatinib mesylate: Proposal of new computed tomography response criteria. J Clin Oncol 2007;25: 1753–1759.

Chun YS, Vauthey JN, Boonsirikamchai P, Maru DM, Kopetz S, Palavecino M, Curley SA, Abdalla EK, Kaur H, Charnsangavej C, Loyer EM. Association of computed tomography morphologic criteria with pathologic response and survival in patients treated with bevacizumab for colorectal liver metastases. JAMA 2009; 302:2338–2344.

Cianchi F, Palomba A, Messerini L, Boddi V, Asirelli G, Perigli G, Bechi P, Taddei A, Pucciani F, Cortesini C. Tumor angiogenesis in lymph node-negative rectal cancer: Correlation with clinicopathological parameters and prognosis. Ann Surg Oncol 2002;9:20–26.

Covey AM, Brown KT, Jarnagin WR, Brody LA, Schwartz L, Tuorto S, Sofocleous CT, D'Angelica M, Getrajdman GI, DeMatteo R, Kemeny NE, Fong Y. Combined portal vein embolization and neoadjuvant chemotherapy as a treatment strategy for resectable hepatic colorectal metastases. Ann Surg 2008;247:451–455.

Cuenod C, Leconte I, Siauve N, Resten A, Dromain C, Poulet B, Frouin F, Clement O, Frija G. Early changes in liver perfusion caused by occult metastases in rats: Detection with quantitative CT. Radiology 2001;218:556–561.

Ding BS, Nolan DJ, Butler JM, James D, Babazadeh AO, Rosenwaks Z, Mittal V, Kobayashi H, Shido K, Lyden D, Sato TN, Rabbany SY, Rafii S. Inductive angiocrine signals from sinusoidal endothelium are required for liver regeneration. Nature 2010;468:310–315.

Drixler TA, Vogten MJ, Ritchie ED, van Vroonhoven TJ, Gebbink MF, Voest EE, Borel Rinkes IH. Liver regeneration is an angiogenesis-associated phenomenon. Ann Surg 2002;236:703–711. discussion 11–12.

Dupuy E, Hainaud P, Villemain A, Bodevin-Phèdre E, Brouland JP, Briand P, Tobelem G. Tumoral angiogenesis and tissue factor expression during hepatocellular carcinoma progression in a transgenic mouse model. J Hepatol 2003;38:793–802.

Ebos JM, Lee CR, Cruz-Munoz W, Bjarnason GA, Christensen JG, Kerbel RS. Accelerated metastasis after short-term treatment with a potent inhibitor of tumor angiogenesis. Cancer Cell 2009;15: 232–239.

Elias D, Ouellet JF, De Baere T, Lasser P, Roche A. Preoperative selective portal vein embolization before hepatectomy for liver metastases: Long-term results and impact on survival. Surgery 2002; 131:294–299.

Eveno C, Broqueres-You D, Feron JG, Rampanou A, Tijeras-Raballand A, Ropert S, Leconte L, Levy BI, Pocard M. Netrin-4 delays colorectal cancer carcinomatosis by inhibiting tumor angiogenesis. Am J Pathol 2011;178:1861–1869.

Eveno C, Gaujoux S, Tobelem G, Pocard M. Did animal offer relevant model for Bevacizumab testing? Br J Cancer 2008;99:1555. author reply 56.

Folkman J. Tumor angiogenesis: Therapeutic implications. N Engl J Med 1971;285:1182–1186.

Fong Y, Cohen AM, Fortner JG, Enker WE, Turnbull AD, Coit DG, Marrero AM, Prasad M, Blumgart LH, Brennan MF. Liver resection for colorectal metastases. J Clin Oncol 1997;15:938–946.

Fortner JG, Silva JS, Golbey RB, Cox EB, Maclean BJ. Multivariate analysis of a personal series of 247 consecutive patients with liver metastases from colorectal cancer. I. Treatment by hepatic resection. Ann Surg 1984;199:306–316.

Freitas C, Larrivee B, Eichmann A. Netrins and UNC5 receptors in angiogenesis. Angiogenesis 2008;11:23–29.

Grothey A, Hedrick EE, Mass RD, Sarkar S, Suzuki S, Ramanathan RK, Hurwitz HI, Goldberg RM, Sargent DJ. Response-independent survival benefit in metastatic colorectal cancer: A comparative analysis of N9741 and AVF2107. J Clin Oncol 2008;26:183–189.

Hainaud P, Contreres JO, Villemain A, Liu LX, Plouët J, Tobelem G, Dupuy E. The role of the vascular endothelial growth factor-Delta-like 4 ligand/Notch4-ephrin B2 cascade in tumor vessel remodeling and endothelial cell functions. Cancer Res 2006;66:8501–8510.

Hurwitz H, Fehrenbacher L, Novotny W, Cartwright T, Hainsworth J, Heim W, Berlin J, Baron A, Griffing S, Holmgren E, Ferrara N, Fyfe G, Rogers B, Ross R, Kabbinavar F. Bevacizumab plus irinotecan, fluorouracil, and leucovorin for metastatic colorectal cancer. N Engl J Med 2004;350:2335–2342.

Jemal A, Siegel R, Ward E, Hao Y, Xu J, Murray T, Thun MJ. Cancer statistics, 2008. CA Cancer J Clin 2008;58:71–96.

Kabbinavar F, Hurwitz HI, Fehrenbacher L, Meropol NJ, Novotny WF, Lieberman G, Griffing S, Bergsland E. Phase II, randomized trial comparing bevacizumab plus fluorouracil (FU)/leucovorin (LV) with FU/LV alone in patients with metastatic colorectal cancer. J Clin Oncol 2003;21:60–65.

Kabbinavar FF, Hambleton J, Mass RD, Hurwitz HI, Bergsland E, Sarkar S. Combined analysis of efficacy: The addition of bevacizumab to fluorouracil/leucovorin improves survival for patients with metastatic colorectal cancer. J Clin Oncol 2005;23:3706–3712.

Klinger M, Eipeldauer S, Hacker S, Herberger B, Tamandl D, Dorfmeister M, Koelblinger C, Gruenberger B, Gruenberger T. Bevacizumab protects against sinusoidal obstruction syndrome and does not increase response rate in neoadjuvant XELOX/FOLFOX therapy of colorectal cancer liver metastases. Eur J Surg Oncol 2009;35: 515–520.

Kruskal JB, Thomas P, Kane RA, Goldberg SN. Hepatic perfusion changes in mice livers with developing colorectal cancer metastases. Radiology 2004;231:482–490.

Kruskal JB, Thomas P, Nasser I, Cay O, Kane RA. Hepatic colon cancer metastases in mice: Dynamic *in vivo* correlation with hypoechoic rims visible at US. Radiology 2000;215:852–857.

Lassau N, Lamuraglia M, Chami L, Leclere J, Bonvalot S, Terrier P, Roche A, Le Cesne A. Gastrointestinal stromal tumors treated with imatinib: Monitoring response with contrast-enhanced sonography. AJR. Am J Roentgenol 2006;187:1267–1273.

Leen E, Goldberg JA, Angerson WJ, McArdle CS. Potential role of doppler perfusion index in selection of patients with colorectal cancer for adjuvant chemotherapy. Lancet 2000;355:34–37.

Leggett DA, Kelley BB, Bunce IH, Miles KA. Colorectal cancer: Diagnostic potential of CT measurements of hepatic perfusion and implications for contrast enhancement protocols. Radiology 1997;205: 716–720.

Lejmi E, Leconte L, Pedron-Mazoyer S, Ropert S, Raoul W, Lavalette S, Bouras I, Feron JG, Maitre-Boube M, Assayag F, Feumi C, Alemany M, Jie TX, Merkulova T, Poupon MF, Ruchoux MM, Tobelem G, Sennlaub F, Plouet J. Netrin-4 inhibits angiogenesis *via* binding to neogenin and recruitment of Unc5B. Proc Natl Acad Sci USA 2008;105:12491–12496.

Leonard GD, Brenner B, Kemeny NE. Neoadjuvant chemotherapy before liver resection for patients with unresectable liver metastases from colorectal carcinoma. J Clin Oncol 2005;23:2038–2048.

Liu Y, Matsui O. Changes of intratumoral microvessels and blood perfusion during establishment of hepatic metastases in mice. Radiology 2007;243:386–395.

Mancuso MR, Davis R, Norberg SM, O'Brien S, Sennino B, Nakahara T, Yao VJ, Inai T, Brooks P, Freimark B, Shalinsky DR, Hu-Lowe DD, McDonald DM. Rapid vascular regrowth in tumors after reversal of VEGF inhibition. J Clin Invest 2006;116: 2610–2621.

Nanashima A, Ito M, Sekine I, Naito S, Yamaguchi H, Nakagoe T, Ayabe H. Significance of angiogenic factors in liver metastatic tumors originating from colorectal cancers. Dig Dis Sci 1998;43: 2634–2640.

Platt JF, Francis IR, Ellis JH, Reige KA. Liver metastases: Early detection based on abnormal contrast material enhancement at dual-phase helical CT. Radiology 1997;205:49–53.

Rajaganeshan R, Prasad R, Guillou PJ, Chalmers CR, Scott N, Sarkar R, Poston G, Jayne DG. The influence of invasive growth pattern and microvessel density on prognosis in colorectal cancer and colorectal liver metastases. Br J Can 2007;96:1112–1117.

Ratain MJ, Eckhardt SG. Phase II studies of modern drugs directed against new targets: If you are fazed, too, then resist RECIST. J Clin Oncol 2004;22:4442–4445.

Scheele J, Altendorf-Hofmann A. Resection of colorectal liver metastases. Langenbeck Arch Surg 1999;384:313–327.

Scheele J, Stang R, Altendorf-Hofmann A, Paul M. Resection of colorectal liver metastases. World J Surg 1995;19:59–71.

Stangl R, Altendorf-Hofmann A, Charnley RM, Scheele J. Factors influencing the natural history of colorectal liver metastases. Lancet 1994;343:1405–1410.

Tomlinson JS, Jarnagin WR, DeMatteo RP, Fong Y, Kornprat P, Gonen M, Kemeny N, Brennan MF, Blumgart LH, D'Angelica M. Actual 10-year survival after resection of colorectal liver metastases defines cure. J Clin Oncol 2007;25:4575–4580.

Van Cutsem E, Dicato M, Arber N, Berlin J, Cervantes A, Ciardiello F, De Gramont A, Diaz-Rubio E, Ducreux M, Geva R, Glimelius B, Glynne Jones R, Grothey A, Gruenberger T, Haller D, Haustermans K, Labianca R, Lenz HJ, Minsky B, Nordlinger B, Ohtsu A, Pavlidis N, Rougier P, Schmiegel W, Van de Velde C, Schmoll HJ, Sobrero A, Tabernero J. Molecular markers and biological targeted therapies in metastatic colorectal cancer: Expert opinion and recommendations derived from the 11th ESMO/World Congress on Gastrointestinal Cancer, Barcelona, 2009. Ann Oncol 2010;21(Suppl. 6):vi1–10.

Vincent F, Bonnin P, Clemessy M, Contreres JO, Lamande N, Gasc JM, Vilar J, Hainaud P, Tobelem G, Corvol P, Dupuy E. Angiotensinogen delays angiogenesis and tumor growth of hepatocarcinoma in transgenic mice. Cancer Res 2009;69:2853–2860.

Wicherts DA, de Haas RJ, Sebagh M, Saenz Corrales E, Gorden DL, Levi F, Paule B, Azoulay D, Castaing D, Adam R. Impact of bevacizumab on functional recovery and histology of the liver after resection of colorectal metastases. Br J Surg 2011;98:399–407.

Wicherts DA, Miller R, de Haas RJ, Bitsakou G, Vibert E, Veilhan LA, Azoulay D, Bismuth H, Castaing D, Adam R. Long-term results of two-stage hepatectomy for irresectable colorectal cancer liver metastases. Ann Surg 2008;248:994–1005.

Yarmenitis SD, Kalogeropoulou CP, Hatjikondi O, Ravazoula P, Petsas T, Siamblis D, Kalfarentzos F. An experimental approach of the Doppler perfusion index of the liver in detecting occult hepatic metastases: Histological findings related to the hemodynamic measurements in Wistar rats. Eur Radiol 2000;10:417–424.

Zorzi D, Chun YS, Madoff DC, Abdalla EK, Vauthey JN. Chemotherapy with bevacizumab does not affect liver regeneration after portal vein embolization in the treatment of colorectal liver metastases. Ann Surg Oncol 2008;15:2765–2772.

SYNTHESE & PERSPECTIVES

Dans notre étude, nous avons mis au point des modèles murins reproductibles de cancer primitif colorectal aussi bien que des modèles de métastases hépatiques, péritonéales et pulmonaires. Nous avons adapté ces modèles à l'évaluation de la résection chirurgicale des tumeurs réalisée en clinique humaine; soit de la tumeur primitive dans le modèle de greffe caecale orthotopique soit des métastases hépatiques avec un modèle d'hépatectomie. Nous avons aussi établi dans nos modèles de métastases hépatiques et d'hépatectomie une technique reproductible et non invasive d'évaluation de l'angiogenèse hépatique physiologique et tumorale.

Nous avons pu tester une nouvelle protéine anti-angiogénique, la Nétrine-4, et montrer son efficacité anti-tumorale et anti-angiogénique dans l'ensemble de nos modèles, y compris dans le traitement de l'ascite tumorale. Nous avons, par ailleurs, étudié dans notre modèle de métastases hépatiques le rôle de différents acteurs de la niche prémétastatique que sont les progéniteurs endothéliaux et hématopoïétiques dérivés de moelle osseuse ainsi que les cellules stellaires hépatiques.

Nous avons décrit le rôle fonctionnel des progéniteurs endothéliaux et hématopoïétiques dérivés de moelle osseuse dans le processus métastatique avec une localisation préférentielle au front d'invasion métastatique et un contact étroit avec les cellules endothéliales. Ces cellules étaient responsables d'une facilitation du potentiel métastatique.

Nous avons analysé le rôle cinétique des cellules stellaires hépatiques au cours de la formation et du développement des métastases hépatiques d'origine colorectales ainsi que l'évolution de différents déterminants de l'angiogenèse tumorale au cours de ce processus. Les cellules stellaires hépatiques sont actives dans la préparation de la niche prémétastatique ; elles arrivent avant la formation du réseau vasculaire, sécrètent de la laminine, élément de la matrice extracellulaire favorable à la progression métastatique locale, et accélèrent le potentiel métastatique lorsqu'elles sont co-injectées avec les cellules tumorales. Notre étude préliminaire de métastases hépatiques chez l'homme objective la même architecture des différents déterminants tumoraux et de l'angiogenèse.

La synthèse de nos résultats et ceux de la littérature peut être présentée sous forme de figure :

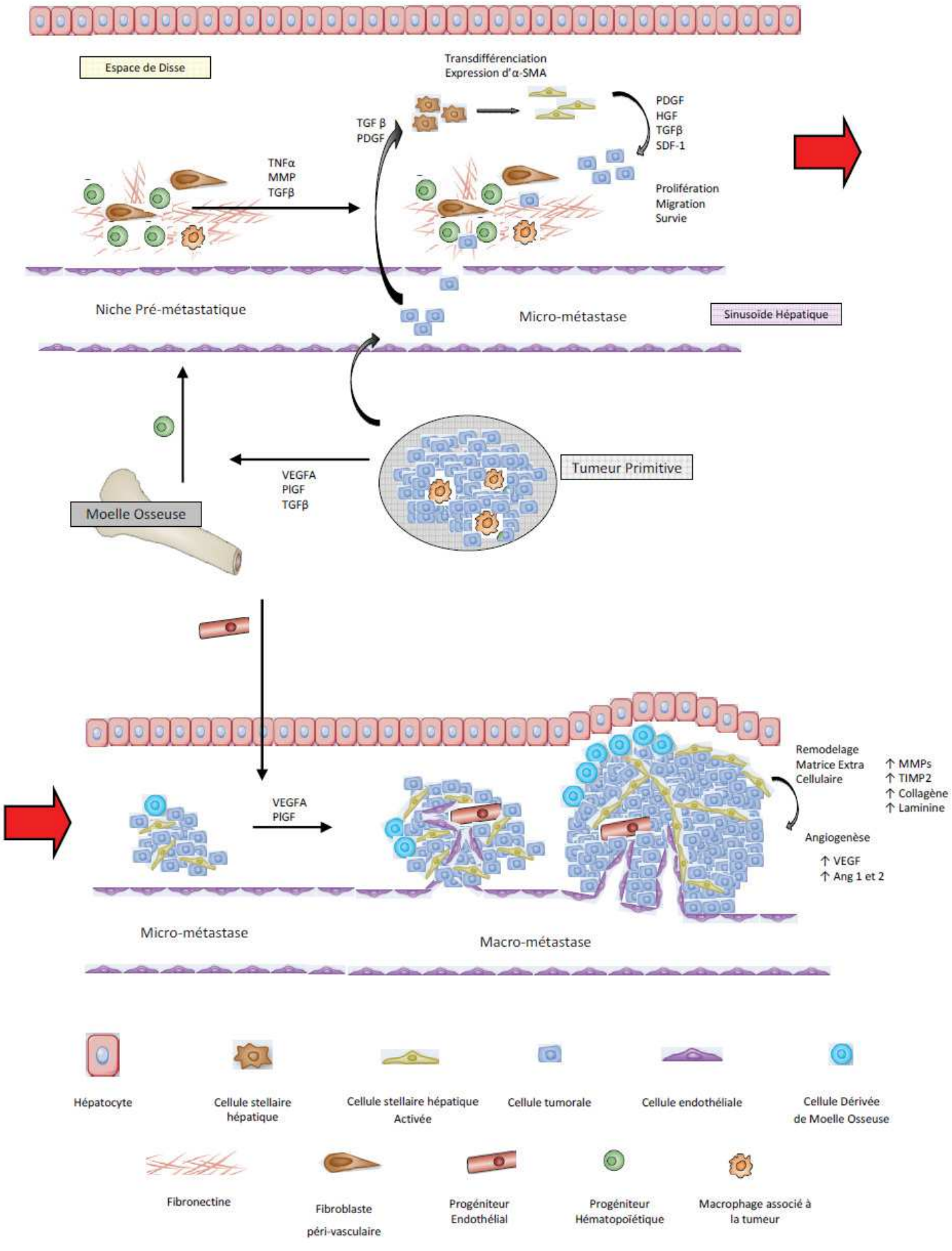
Espace de Disse
Transdifférenciation
Expression d'α-SMA
TGF β
PDGF
PDGF
HGF
TGFβ
SDF-1
TNFα
MMP
TGFβ
Prolifération
Migration
Survie
Niche Pré-métastatique
Micro-métastase
Sinusoïde Hépatique
Tumeur Primitive
VEGFA
PlGF
TGFβ
Moelle Osseuse
VEGFA
PlGF
Remodelage
Matrice Extra
Cellulaire
↑ MMPs
↑ TIMP2
↑ Collagène
↑ Laminine
Angiogenèse
↑ VEGF
↑ Ang 1 et 2
Micro-métastase
Macro-métastase
Hépatocyte
Cellule stellaire hépatique
Cellule stellaire hépatique Activée
Cellule tumorale
Cellule endothéliale
Cellule Dérivée de Moelle Osseuse
Fibronectine
Fibroblaste péri-vasculaire
Progéniteur Endothélial
Progéniteur Hématopoïétique
Macrophage associé à la tumeur

Plusieurs axes de réflexions sont envisageables pour poursuivre ce travail :

1) Poursuivre l'analyse des déterminants tumoraux et de l'angiogenèse dans les métastases hépatiques humaines à différents temps de leur évolution, pour valider notre analyse cinétique chez l'homme. Ceci permettrait de proposer de choisir une cible pour une drogue selon le stade de vascularisation des métastases et de ne pas considérer toutes les métastases de la même façon.

2) Valider comme cibles thérapeutiques les progéniteurs dérivés de moelle osseuse et les cellules stellaires hépatiques

    a. Valider le rôle primordial des progéniteurs médullaires pour la création de la niche prémétastatique par l'utilisation du modèle de tumeur primitive par greffe orthotopique intra-caecale. On analysera les marqueurs spécifiques de ces cellules et du microenvironnement tumoral hépatique après greffe caecale (sans ou avec résection de la tumeur)

    b. Il sera alors possible de tester l'effet de l'inhibition de ces cellules, par inhibition de la migration ou par action inhibitrice cellulaire directe, pouvant mener à la création de nouveaux traitements adjuvants à la résection de la tumeur primitive ; un traitement anti-angiogénique classique par inhibition du VEGF par bevacizumab étant inefficace.

    c. Valider le rôle des cellules stellaires hépatiques dans la création de la niche prémétastatique par injection systémique de ces cellules dans le modèle de métastases hépatiques après injection intra-splénique. Le tropisme des cellules stellaires hépatiques au niveau des futurs sites métastatiques serait une preuve majeure.

3) Tester de nouvelles stratégies thérapeutiques dans nos modèles murins

Nous avons prouvé la validité de nos modèles de tumeur primitive et de métastases hépatiques et péritonéales d'origine colorectale pour tester de nouvelles molécules thérapeutiques et notamment anti-angiogéniques.

D'autres traitements pourront être évalués dans ces modèles avec :

    a. Analyse possible des marqueurs du microenvironnement

    b. Utilisation de notre modèle d'hépatectomie pour moduler le microenvironnement tumoral et tester de nouvelles stratégies thérapeutiques

c. Utiliser notre technique d'Echo-Doppler pour en évaluer l'efficacité. Notre équipe a mis au point un modèle murin de pseudomyxome péritonéal avec évaluation de l'angiogenèse tumorale par Echo-Doppler du flux dans l'artère mésentérique supérieure. L'efficacité du bevacizumab a été testée et corrélée à la baisse du débit dans cette artère. Une étude pilote d'évaluation pré- et post-opératoire du flux dans l'artère mésentérique supérieure et sa corrélation à la masse tumorale et à la récidive vient d'être débutée dans une cohorte de patients.

ANNEXES

Annexe 1:

Réflexions autour des complications cliniques du bevacizumab et de l'implication dans la stratégie chirurgicale des métastases hépatiques colorectale du taux de VEGF et du potentiel angiogénique du microenvironnement.

Clinics and Research in Hepatology and Gastroenterology (2011) xxx, xxx–xxx

Available online at ScienceDirect
www.sciencedirect.com

Elsevier Masson France
EM|consulte
www.em-consulte.com

CASE REPORT

Late anastomotic colonic dehiscence due to antiangiogenic treatment, a specific drug-class complication requiring specific treatment: An example of pazopanib complication

Clarisse Eveno[a,b], Christine le Maignan[c], Philippe Soyer[d], Marine Camus[e], Emmanuel Barranger[f], Marc Pocard[a,*,b]

[a] *Service de chirurgie digestive, hôpital Lariboisière, AP–HP, université Paris-Diderot–Paris-7, 2, rue Amboise-Paré, 75010 Paris, France*
[b] *Unité mixte de recherche U 965, Inserm–Paris-7, 75010 Paris, France*
[c] *Service d'oncologie médicale, hôpital Saint-Louis, AP–HP, université Paris-Diderot–Paris-7, 1, avenue Claude-Vellefaux, 75010 Paris, France*
[d] *Service de radiologie viscérale, hôpital Lariboisière, AP–HP, université Paris-Diderot–Paris-7, 2, rue Amboise-Paré, 75010 Paris, France*
[e] *Service de gastro-entérologie, hôpital Lariboisière, AP–HP, université Paris-Diderot–Paris-7, 2, rue Amboise-Paré, 75010 Paris, France*
[f] *Service de gynécologie-obstétrique, hôpital Lariboisière, AP–HP, université Paris-Diderot–Paris-7, 2, rue Amboise-Paré, 75010 Paris, France*

Summary Bevacizumab, a recombinant humanized monoclonal antibody against vascular endothelial growth factor (VEGF), was the first angiogenesis inhibitor approved for the first-line treatment of metastatic colorectal cancer in combination with intravenous fluorouracil-based chemotherapy. Two major cohort studies – BRiTE and BEAT – reported a 2% incidence of bowel perforation, which remains a rare, but serious, complication of bevacizumab treatment. Late anastomotic complications, arising > 3 months after surgery, are emerging occurrences that may be associated with bowel perforation. We report here on such a case caused by pazopanib, a new antiangiogenic agent, and also include a review of the published cases in the literature ($n = 23$) and an analysis of their management. Proctectomy was the initial surgery in 17 patients (74%) with rectal cancer, and 13 of these patients had undergone adjuvant radiation prior to surgery. The majority (84%) of the complications occurred with antiangiogenic treatment after a mean number of four cycles. Patients' management was invariably associated with withdrawal of the antiangiogenic agent, together with conservative treatment in 14 patients (66%).

* Corresponding author.
E-mail address: marc.pocard@lrb.aphp.fr (M. Pocard).

2210-7401/$ – see front matter © 2011 Elsevier Masson SAS. All rights reserved.
doi:10.1016/j.clinre.2010.10.003

Please cite this article in press as: Eveno C, et al. Late anastomotic colonic dehiscence due to antiangiogenic treatment, a specific drug-class complication requiring specific treatment: An example of pazopanib complication. Clin Res Hepatol Gastroenterol (2011), doi:10.1016/j.clinre.2010.10.003

Introduction

Vascular endothelial growth factor (VEGF) plays a crucial role in tumor growth, progression and metastasis by promoting angiogenesis [1,2]. Antiangiogenic agents have become the standard therapy for a variety of solid tumors, including breast, colorectal, kidney, liver and lung cancers. Bevacizumab, a recombinant humanized monoclonal antibody against VEGF, was the first angiogenesis inhibitor approved for the first-line treatment of metastatic colorectal cancer in combination with intravenous fluorouracil-based chemotherapy [3—7].

In initial trials evaluating bevacizumab in combination with intravenous irinotecan, 5-fluorouracil and leucovorin (IFL), serious complications such as bleeding, thromboembolic events and bowel perforation were seen in < 2% of cases [7]. In a phase-III study of colorectal cancer, Hurwitz et al. [5] reported six cases of gastrointestinal perforation in a series of 393 patients who were receiving bevacizumab (6/393 patients; 1.5%). Two major cohort studies, the BRiTE in the US and the BEAT in Europe, also reported incidences of bowel perforation of 2% [8,9]. Thus, such an event remains a rare, but serious, complication of bevacizumab therapy. In the majority of cases, bowel perforation occurred within 2 to 3 months of starting the drug. Also, bowel perforations have been described in non-pathological tissues (in the case of chest cancer), at the site of the tumor and in bowel anastomosis.

Late anastomotic complications, arising > 3 months after surgery, are emerging occurrences that may be associated with bowel perforation. Such complications have been reported previously with bevacizumab; however, these may also be drug-class complications rather than associated with any specific treatment.

The following case report does not involve bevacizumab. Also included here is a review of published cases in the literature so far and an analysis of their management.

Case report

In May 2009, a 45-year-old woman underwent complete surgical resection, including cytoreductive surgery with total hysterectomy, bilateral salpingo-oophorectomy and omentectomy, for stage IIIc ovarian carcinoma. Proctectomy with a laterotermínal coloanal stapled anastomosis for localized peritoneal carcinomatosis were also performed, but with no diverting stoma. The postoperative course was clinically uneventful and, for this reason, the anastomosis was not controlled following the procedure. Adjuvant chemotherapy was initiated, including paclitaxel and carboplatin for six cycles, followed by pazopanib at a dose of 800 mg/day.

In December 2009, after the sixth complete cycle of therapy and 7 months after the surgical procedure, the patient developed excruciating rectal pain and fever. Computed tomography (CT) demonstrated a presacral collection consistent with an anastomotic leak (Fig. 1). Colonoscopy revealed a large anastomotic ulcer and cul-de-sac perforation (Fig. 2). Pazopanib was withdrawn, and the outcome was favorable with conservative treatment based on antibiotic medication without percutaneous drainage. The pain ceased after 4 days, and bowel function was restored a week later.

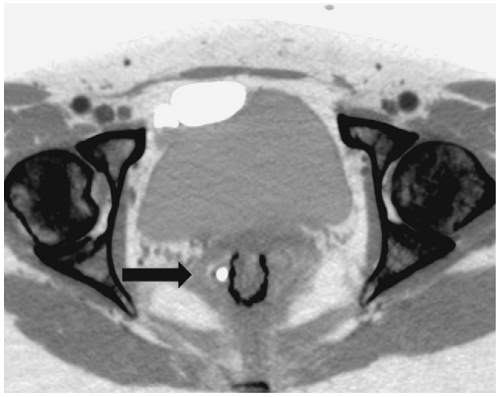

Figure 1 Computed tomography, axial view, shows marked thickening of the presacral space consistent with an anastomotic leak (arrow).

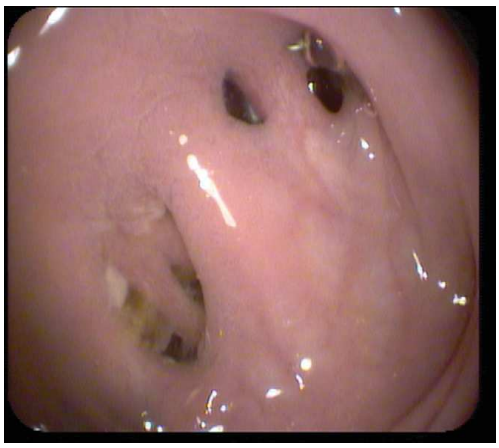

Figure 2 Colonoscopy reveals a large anastomotic ulcer and cul-de-sac perforation.

Discussion

Late anastomotic complications tend to occur after an unusual delay following surgery, after the first three postoperative months and, most often, after a year. For this reason, we reviewed all published cases of late anastomotic complications while receiving an antiangiogenic agent and described their management.

Bevacizumab was approved as a first-line treatment for metastatic colorectal cancer [3—7] in patients with untreated metastatic breast carcinoma in combination with paclitaxel [10], in patients with metastatic renal cell carcinoma when combined with interferon-α [11], and also in

Please cite this article in press as: Eveno C, et al. Late anastomotic colonic dehiscence due to antiangiogenic treatment, a specific drug-class complication requiring specific treatment: An example of pazopanib complication. Clin Res Hepatol Gastroenterol (2011), doi:10.1016/j.clinre.2010.10.003

Table 1 Delayed anastomotic complications with antiangiogenic agents reported in the literature thus far.

Study	Age/ gender	Tumor	Early surgical complications	Agent	Number of cycles	Treatment-complication delay (months)	Symptoms	Anastomotic complications	Interval (months)	Management
Lordick et al. [16]	42 M	Rectum	No	Beva	5	0	Perianal pain	Ischemic ulcer	7	Conservative
	60 F	Rectum	No	Beva	5	0	Perianal pain	Ischemic ulcer	17	Conservative
Adenis et al. [17]	50 F	Rectum	Anastomotic leak	Beva	2	0	Abdominal pain, fever	Leak	23	Conservative
Ley et al. [18]	72 F	Rectum	No	Beva	12	0	Rectovaginal fistula	Rectovaginal fistula	36	NA
Badgwell et al. [19]	NA	Pancreas	NA	Beva	NA	NA	NA	Leak	18	Conservative
	NA	Right colon	NA	Beva	NA	NA	NA	Leak	6	Conservative
	NA	Esophagus	Anastomotic	Beva	NA	NA	NA	Leak	4	Conservative
	NA	Rectum	leak	Beva	NA	NA	NA	Leak	3	Conservative
			NA							
Wolf et al. [20]	70 M	Rectum	No	Beva	3	0	Perianal pain, abscess	Rectocutaneous fistula	2	Protective ileostomy
	53 F	Rectum	NA	Beva	1	0			36	
	66 F	Rectum	NA	Beva	2	0	NA	Rectovaginal fistula	6	Colostomy
							Pelvic pain, fever	Rectocutaneous fistula		NA
August et al. [21]	58 M	Rectum	Anastomotic	Beva	3	0	Abdominal pain	Leak	26	Conservative
	74 F	Rectum	leak	Beva	10	3	Abdominal pain	Leak	33	Stoma
	65 F	Right colon	No	Beva	4	1	Colocutaneous fistula	Colocutaneous fistula	5	Conservative
			No							
Abbrederis et al. [22]	61 F	Right colon	Anastomotic hematoma	Beva	4	2	Abdominal pain, fever	Leak	10	Stoma
Bege et al. [23]	46 M	Rectum	Anastomotic	Beva	1	0	Pelvic abscess	Leak	52	Stoma + pelvic drainage
	54 M	Rectum	leak	Beva	2	0	Pelvic abscess	Leak	57	
	51 M	Rectum	Anastomotic	Beva	2	0	Pelvic abscess	Leak	21	Stoma + pelvic drainage
	55 F	Rectum	leak	Beva	3	0	Leak	Leak	11	Stoma + pelvic drainage
			No							Conservative
			No							
Deshaies et al. [24]	58 M	Duodenum	Anastomotic	Aflibercept	4	0	Abdominal pain, fever	Leak	13	Conservative
	74 M	Rectum	leak	Beva	4	0		Ischemic ulcer	18	Conservative
	68 M	Rectum	No	Beva	8	0	Rectal pain	Ischemic ulcer	78	Conservative
			No				Rectal bleeding			
Present case	46 F	Ovary with rectal resection	No	Pazopanib	6	0	Abdominal pain, fever	Leak	7	Conservative

M: male; F: female; Beva: bevacizumab; NA: not applicable.

Please cite this article in press as: Eveno C, et al. Late anastomotic colonic dehiscence due to antiangiogenic treatment, a specific drug-class complication requiring specific treatment: An example of pazopanib complication. Clin Res Hepatol Gastroenterol (2011), doi:10.1016/j.clinre.2010.10.003

those with advanced non-small-cell lung cancer (NSCLC) in combination with carboplatin and paclitaxel [12].

Hapani et al. [13] analyzed 17 randomized controlled trials in which bevacizumab was compared with controls in combination with standard antineoplastic therapy for the treatment of various types of tumors. The incidence of gastrointestinal perforation ranged from 0% to 1.5%, and was significantly increased with bevacizumab use (relative risk: 2.14). The risk of gastrointestinal perforation was dose-dependent, varied according to tumor type (renal cell > colorectal > breast > NSCLC > pancreatic), and was higher in patients with metastatic disease compared with those in whom bevacizumab was used as an adjuvant therapy.

In randomized phase-II and -III trials for metastatic colorectal cancer, the use of bevacizumab was associated with a 1—2% rate of gastrointestinal perforation [5—7]. In the BRiTE and BEAT observational cohort studies, gastrointestinal perforations were observed in 1.9% and 2% of the 1953 and 1914 patients, respectively, who had metastatic colorectal cancer treated with a first-line chemotherapy regimen and with bevacizumab, respectively [8,9]. In both these studies, 1.7% of previously resected tumors underwent perforation. In the BRiTE study, the gastrointestinal perforation rate was higher with intact primary tumors, a recent history of sigmoidoscopy or colonoscopy and with adjuvant radiotherapy [8]. Such gastrointestinal perforation, defined as the presence of a pneumoperitoneum on imaging, did not always require surgery, as some cases were successfully managed conservatively.

In addition to colorectal cancer, patients with ovarian cancer treated with bevacizumab can also present with bowel perforation. In fact, an investigational new drug (IND) warning letter from the US Food and Drug Administration (FDA) reported an 11% (five of 44 patients) incidence of gastrointestinal perforation in a phase-II trial by Cannistra et al. [14] with bevacizumab in patients with metastatic ovarian cancer. In a recent phase-III trial presented at the 2010 American Society of Clinical Oncology (ASCO) Annual Meeting, Burger et al. [15] reported on 1873 patients with stage III or IV epithelial ovarian cancer, primary peritoneal cancer or fallopian tube cancer, treated with standard chemotherapy and placebo (R1) or with concurrent (R2) ± maintenance bevacizumab (R3). Grade ≥ 3 gastrointestinal perforation, hemorrhage or fistula occurred in 0.8% (R1), 2.6% (R2) and 2.3% (R3) of these patients.

Our present case describes late anastomotic complications with pazopanib, an antiangiogenic treatment targeting vascular endothelial growth-factor receptors (VEGFR), platelet-derived growth-factor receptors (PDGFR) and the cytokine receptor C-kit. To our knowledge, 22 other cases of late anastomotic complications with antiangiogenic treatment have also been reported thus far (Table 1) [16—24].

In cases of bowel perforation, the observed mortality reported in a recent meta-analysis was 21.7% (95% confidence interval [CI]: 11.5—37%) [13]. In observational studies such as the BEAT study, the mortality rate was 87.5%. However, lower mortality rates were reported in cases of late anastomotic complications most likely because, in the majority of cases, it occurs in a pelvic anastomosis and not in a free abdominal cavity, thereby excluding peritonitis.

In our present review, proctectomy was the initial surgery in 17 patients (74%) with a primary tumor ($n = 16$) or localized ovarian peritoneal carcinomatosis ($n = 1$), and 13 of these patients with rectal cancer underwent adjuvant radiation prior to surgery. The majority (84%) of complications occurred during antiangiogenic treatment after a mean number of four cycles. Only three patients (16%) experienced late anastomotic complications at 1—3 months after stopping the drugs.

The management of late anastomotic complications is invariably associated with withdrawal of the antiangiogenic agent. The treatment implemented was conservative in 14 cases (66%), whereas seven patients (33%) underwent abdominal surgery, with the creation of diverting stoma with pelvic drainage in three cases.

Patients' management of such complications needs to be standardized and, in cases of preoperative pelvic radiation associated with difficult postoperative healing, caution is necessary. The diagnosis of late anastomotic fistula must be suspected with the presence of pelvic pain and fever. However, as these symptoms are non-specific, the diagnosis requires careful endoscopy and radiological examination to detect dehiscence. Conservative management, even in cases of bowel perforation, should be preferred together with withdrawal of the antiangiogenic agent. Definitive cancellation of treatment was seen in all cases but, in cases of bowel perforation with bevacizumab, some authors took the risk of reintroducing bevacizumab — with no perforation recurrence. Indeed, the final recommendations for the use of antiangiogenic treatment have yet to be codified.

Conflict of interest statement

None.

References

[1] Folkman J. Tumor angiogenesis: therapeutic implications. N Engl J Med 1971;285(21):1182—6.
[2] Folkman J. Role of angiogenesis in tumor growth and metastasis. Semin Oncol 2002;29(6 Suppl. 16):15—8.
[3] Gerber HP, Ferrara N. Pharmacology and pharmacodynamics of bevacizumab as monotherapy or in combination with cytotoxic therapy in preclinical studies. Cancer Res 2005;65(3):671—80.
[4] Giantonio BJ, Catalano PJ, Meropol NJ, O'Dwyer PJ, Mitchell EP, Alberts SR, et al. Bevacizumab in combination with oxaliplatin, fluorouracil, and leucovorin (FOLFOX4) for previously treated metastatic colorectal cancer: results from the Eastern Cooperative Oncology Group Study E3200. J Clin Oncol 2007;25(12):1539—44.
[5] Hurwitz H, Fehrenbacher L, Novotny W, Cartwright T, Hainsworth J, Heim W, et al. Bevacizumab plus irinotecan, fluorouracil, and leucovorin for metastatic colorectal cancer. N Engl J Med 2004;350(23):2335—42.
[6] Hurwitz HI, Fehrenbacher L, Hainsworth JD, Heim W, Berlin J, Holmgren E, et al. Bevacizumab in combination with fluorouracil and leucovorin: an active regimen for first-line metastatic colorectal cancer. J Clin Oncol 2005;23(15):3502—8.
[7] Kabbinavar F, Hurwitz HI, Fehrenbacher L, Meropol NJ, Novotny WF, Lieberman G, et al. Phase II, randomized trial comparing bevacizumab plus fluorouracil (FU)/leucovorin (LV) with FU/LV alone in patients with metastatic colorectal cancer. J Clin Oncol 2003;21(1):60—5.

Please cite this article in press as: Eveno C, et al. Late anastomotic colonic dehiscence due to antiangiogenic treatment, a specific drug-class complication requiring specific treatment: An example of pazopanib complication. Clin Res Hepatol Gastroenterol (2011), doi:10.1016/j.clinre.2010.10.003

[8] Grothey A, Sugrue MM, Purdie DM, Dong W, Sargent D, Hedrick E, et al. Bevacizumab beyond first progression is associated with prolonged overall survival in metastatic colorectal cancer: results from a large observational cohort study (BRiTE). J Clin Oncol 2008;26(33):5326—34.
[9] Van Cutsem E, Rivera F, Berry S, Kretzschmar A, Michael M, DiBartolomeo M, et al. Safety and efficacy of first-line bevacizumab with FOLFOX, XELOX, FOLFIRI and fluoropyrimidines in metastatic colorectal cancer: the BEAT study. Ann Oncol 2009;20(11):1842—7.
[10] Miller K, Wang M, Gralow J, Dickler M, Cobleigh M, Perez EA, et al. Paclitaxel plus bevacizumab versus paclitaxel alone for metastatic breast cancer. N Engl J Med 2007;357(26):2666—76.
[11] Escudier B, Pluzanska A, Koralewski P, Ravaud A, Bracarda S, Szczylik C, et al. Bevacizumab plus interferon alfa-2a for treatment of metastatic renal cell carcinoma: a randomised, double-blind phase III trial. Lancet 2007;370(9605):2103—11.
[12] Sandler A, Gray R, Perry MC, Brahmer J, Schiller JH, Dowlati A, et al. Paclitaxel-carboplatin alone or with bevacizumab for non-small-cell lung cancer. N Engl J Med 2006;355(24):2542—50.
[13] Hapani S, Chu D, Wu S. Risk of gastrointestinal perforation in patients with cancer treated with bevacizumab: a meta-analysis. Lancet Oncol 2009;10(6):559—68.
[14] Cannistra SA, Matulonis UA, Penson RT, Hambleton J, Dupont J, Mackey H, et al. Phase II study of bevacizumab in patients with platinum-resistant ovarian cancer or peritoneal serous cancer. J Clin Oncol 2007;25(33):5180—6.
[15] Burger RA, Bookman MA, Walker JL, Homesley HD, Fowler J, Monk BJ, et al. Phase III trial of bevacizumab (BEV) in the primary treatment of advanced epithelial ovarian cancer (EOC), primary peritoneal cancer (PPC), or fallopian tube cancer (FTC): a gynecologic oncology group study. J Clin Oncol 2010;28:18s.
[16] Lordick F, Geinitz H, Theisen J, Sendler A, Sarbia M. Increased risk of ischemic bowel complications during treatment with bevacizumab after pelvic irradiation: report of three cases. Int J Radiat Oncol Biol Phys 2006;64(5):1295—8.
[17] Adenis A, Vanseymortier L, Foissey D, Colombel JF. Bevacizumab and postponed suture leakages after surgery for ulcerative colitis and rectal cancer. Gut 2007;56(5):734.
[18] Ley EJ, Vukasin P, Kaiser AM, Ault G, Beart Jr RW. Delayed rectovaginal fistula: a potential complication of bevacizumab (avastin). Dis Colon Rectum 2007;50(6):930.
[19] Badgwell BD, Camp ER, Feig B, Wolff RA, Eng C, Ellis LM, et al. Management of bevacizumab-associated bowel perforation: a case series and review of the literature. Ann Oncol 2008;19(3):577—82.
[20] Wolf I, Urban D, Pfeffer R, Catane R, Aderka D. High incidence of fistula formation during bevacizumab treatment in rectal cancer patients. Acta Oncol 2007;46(4):550—3.
[21] August DA, Serrano D, Poplin E. ''Spontaneous'' delayed colon and rectal anastomotic complications associated with bevacizumab therapy. J Surg Oncol 2008;97(2):180—5.
[22] Abbrederis K, Kremer M, Schuhmacher C. Ischemic anastomotic bowel perforation during treatment with bevacizumab 10 months after surgery. Der Chirurg 2008;79(4):351—5.
[23] Bege T, Lelong B, Viret F, Turrini O, Guiramand J, Topart D, et al. Bevacizumab-related surgical site complication despite primary tumor resection in colorectal cancer patients. Ann Surg Oncol 2009;16(4):856—60.
[24] Deshaies I, Malka D, Soria JC, Massard C, Bahleda R, Elias D. Antiangiogenic agents and late anastomotic complications. J Surg Oncol 2010;101:180-183.

Please cite this article in press as: Eveno C, et al. Late anastomotic colonic dehiscence due to antiangiogenic treatment, a specific drug-class complication requiring specific treatment: An example of pazopanib complication. Clin Res Hepatol Gastroenterol (2011), doi:10.1016/j.clinre.2010.10.003

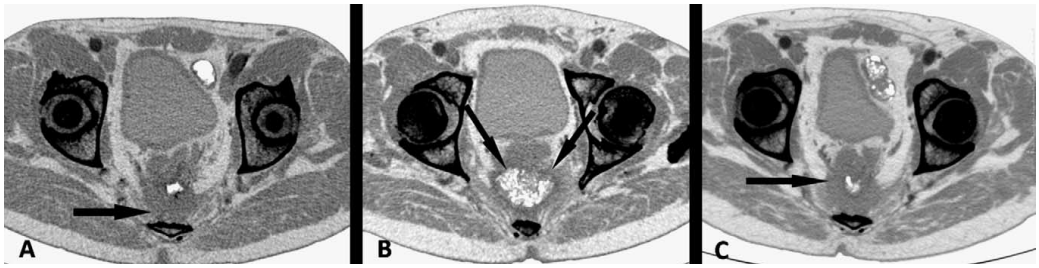

Figure 1 Computed tomography in the axial plane. A: shows marked thickening of the presacral space (arrow) with circumferential thickening of the anastomosis; B: shows fully open posterior dehiscence with obvious fecal fistula (arrows) after two cycles of bevacizumab at a dose of 7.5 mg/kg; C: shows marked circumferential thickening the anastomosis (arrow) 5 months after bevacizumab stop.

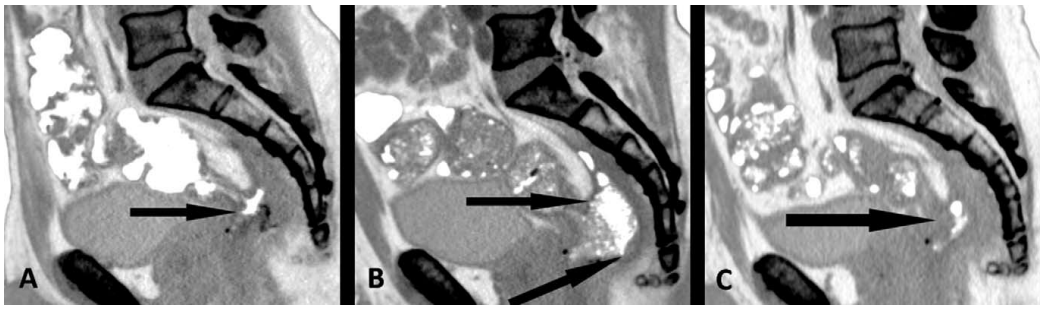

Figure 2 Computed tomography in the sagittal plane. A: shows marked thickening of the presacral space (arrow) with circumferential thickening of the anastomosis; B: shows fully open posterior dehiscence with obvious fecal fistula (arrows) after two cycles of bevacizumab at a dose of 7.5 mg/kg; C: shows marked circumferential thickening the anastomosis (arrow) 5 months after bevacizumab stop.

The rapid onset of reopening of the anastomotic dehiscence has important implications. Previous cases were described in patients treated for gastrointestinal cancers who received a lower dose of bevacizumab by comparison with that given to our patient. In the literature, time of occurrence of this complication was 3 months of treatment [2]. In the current case, anastomotic dehiscence came out only after two cycles of bevacizumab. It may be reasonably hypothesized that the higher dose given to our patient might have resulted in an earlier complication.

The second interest is that of therapeutic management. We initially offset the subsequent course of chemotherapy schedule for biopsies. Bevacizumab has been suspended immediately, but chemotherapy has been continued. In this regard, our case suggests that CT may have a major role in the management of anastomotic leakage in patients receiving bevacizumab. In our case, CT showed a well-delineated, presacral fistula tract that was circumscribed by fibrous tissue. Those pelvic sinus has for consequence that a communication with the intraperitoneal space could be excluded, thus virtually eliminating a risk for peritoneal infection. This was confirmed by excellent tolerance to the reintroduction of conventional chemotherapy. These two characteristics should be known by oncologists and surgeons on the occurrence of such complications related to anti-angiogenic agents: making a diagnosis and not interrupting the chemotherapy if it is not needed.

Disclosure of interest

The authors declare that they have no conflicts of interest concerning this article.

References

[1] Konishi T, Watanabe T, Kishimoto J, Nagawa H. Risk factors for anastomotic leakage after surgery for colorectal cancer: results of prospective surveillance. J Am Coll Surg 2006;202:439—44.
[2] August DA, Serrano D, Poplin E. Spontaneous, delayed colon and rectal anastomotic complications associated with bevacizumab therapy. J Surg Oncol 2008;97:180—5.
[3] Deshaies I, Malka D, Soria JC, Massard C, Bahleda R, Elias D. Anti-angiogenic agents and late anastomotic complications. J Surg Oncol 2010;101:180—3.
[4] Sandler A, Gray R, Perry MC, Brahmer J, Schiller JH, Dowlati A, et al. Paclitaxel-carboplatin alone or with bevacizumab for non-small-cell lung cancer. N Engl J Med 2006;355:2542—50.

C. Eveno[a,b]
P. Soyer[c]
L. Teixeira[d]
L. Staudacher[d]
M. Pocard[a,b,*]
[a] *Département médico-chirurgical de pathologie digestive, hôpital Lariboisière, AP—HP, université Diderot Paris 7, 2, rue Ambroise-Paré, 75010 Paris, France*
[b] *UMR Inserm 965 Paris 7, angiogenèse et recherche translationnelle, hôpital Lariboisière, AP—HP, 2, rue Ambroise-Paré, 75010 Paris, France*
[c] *Département de radiologie diagnostique et interventionnelle, hôpital Lariboisière, AP—HP, université Diderot Paris 7, 2, rue Amboise-Paré, 75010 Paris, France*
[d] *Unité de cancérologie thoracique, hôpital Saint-Louis, AP—HP, université Diderot Paris 7, 1, avenue Claude-Vellefaux, 75010 Paris, France*

[*] Corresponding author.
E-mail address: marc.pocard@lrb.aphp.fr (M. Pocard)

of ERK1, 2 with the inhibitor of MAPKK PD098059 at a dose 10 times lower than the dl 50, inhibited jejunal and ileal mucosal mass by −13 and −12% ($p < 0009$) and expression of dissacharidases by −41 to −43% ($p < 0.0001$) compared to controls receiving the vehicle [11]. The metabolic pathway of Pi-3 kinase was also enhanced because the phosphorylated form of p85, a critical regulatory unit of the PI-3 kinase pathway, was increased by 2.5 fold in rats treated by the probiotic [11,12].

These findings demonstrate that A-RAF- RAS-GAP-ERK1,2 and likely the PI-3 kinase pathways are both critical for the transduction of mitogenic and metabolic signals from the intestinal lumen to the nucleus by the probiotic *S. boulardii*.

Disclosure of interest

The authors declare that they have no conflicts of interest concerning this article.

Cell Adhesion & Migration 6:6, 1–5; November/December 2012; © 2012 Landes Bioscience

VEGF levels and the angiogenic potential of the microenvironment can affect surgical strategy for colorectal liver metastasis

Clarisse Eveno and Marc Pocard*

INSERM U965 Angiogenesis and Translational Research; Paris-Diderot Paris 7 University; Hôpital Lariboisière; Paris, France

Keywords: colorectal liver metastases, microenvironment, angiogenesis, VEGF, pre-metastatic niche, surgical resection

Abbreviations: AAG, anti angiogenic agent; Ang-2/Ang-1, angiopoietins 1 and 2; CA9, carbonic anhydrase 9; CD31, cluster of differentiation 31; EPCs, endothelial progenitors cells; HIF-1α, hypoxia-inducible factor-1; HPCs, hematopoietic progenitor cells; VEGF, vascular endothelial growth factor; VEGFR-1, vascular endothelial growth factor receptor 1; VEGFR-2, vascular endothelial growth factor receptor 2

The hypotheses emerging from basic research on colorectal liver metastases must be tested in clinical situations for the adaptation of current treatment strategies. Pre-metastatic niches have been shown to exist in human colorectal synchronous metastases, with the liver parenchyma adjacent to the synchronous liver metastases providing a favorable, angiogenic environment for metastatic tumor growth. The role of the VEGF signaling pathway in liver regeneration and tumor growth remains unclear, but the use of antiangiogenic agents in combination with surgical treatment is almost certainly beneficial.

Colorectal cancer is the second leading cause of cancer-related deaths, often due to uncontrolled metastatic disease.[1] The liver is the most common site of metastasis for colorectal cancer. Almost half the patients present liver metastases at diagnosis (synchronous metastasis) or develop liver metastases (metachronous) during the course of the disease. No randomized trial has been performed to assess the benefits of the surgical resection of liver metastases, but 25% to 30% of patients survive for at least five years after the complete resection of metastases, whereas very few unresected patients survived three years in historical series.[2]

The major elements of liver metastasis treatment are listed in **Table 1**. These elements are of importance because they may have major consequences. In particular, patients may die during the postoperative period, if the remnant liver is nonfunctional; death may be late and related to a disease recurrence if the metastases are not completely resected. New strategies have been developed and could be combined:

(1) Surgical methods of liver metastasis ablation, such as cryotherapy, radiofrequency treatment and laser hyperthermia ablation, could facilitate the treatment of central and/or multiple metastases;

(2) Preoperative radiological portal embolization to induce the hypertrophy of a particular segment of the liver, to increase the technical possibilities for liver resection;[3]

(3) Preoperative and postoperative chemotherapy, including VEGF-targeting or other antiangiogenic agents.[4,5]

Unfortunately, recurrences are still observed in two thirds of patients after the resection of liver metastases, and various approaches to reducing this risk are being investigated.[4-6] One such approach involves the use of preoperative treatment to select patients for surgery. Patients with multiple, large metastases diagnosed shortly after the resection of a stage III primary colon cancer are known to have a higher risk of recurrence after liver resection than those with small, solitary metastases occurring several years after the resection of a stage II cancer.[7,8] Long-term survival is possible only with surgical treatment. This has led to a trend to be more aggressive, with an increase in indications for the surgical resection of liver metastases. Long-term survival is now observed in patients undergoing the resection of large or multiple liver metastases, who would have been refused surgery in the past.

The optimal moment for chemotherapy, with or without antiangiogenic treatment, remains unclear and there is still debate about whether pre- or postoperative chemotherapy is preferable.[5]

Several recent studies have reported that the addition of a biological agent, such as cetuximab, panitumumab or bevacizumab, to the chemotherapy regimen increases the response to treatment and renders a larger proportion of tumors suitable for resection (**Box 1**).[9] Despite the proposal of new drugs for treatment, new concepts, such as the tumor microenvironment and metastatic niches, have not yet reached surgical practice. We performed a translational study, using VEGF-based concepts and hypotheses about interactions with the tumor microenvironment to reassess treatment in particular clinical situations.

There is considerable debate about the most appropriate treatment options for patients with colorectal cancer and synchronous

*Correspondence to: Marc Pocard; Email: marc.pocard@inserm.fr
Submitted: 10/06/12; Revised: 12/10/12; Accepted: 12/13/12
http://dx.doi.org/10.4161/cam.23247

Table 1. Available treatment strategies for colorectal liver metastases

Major element	Purpose	If not possible or uncertain	Possible consequences if not obtained
Complete resection or ablation of metastases	Cure	Preoperative chemotherapy with AAG	Liver recurrence
Prior systemic chemotherapy	Control of premetastic niches	Preoperative chemotherapy	Metastatic progression, even outside the liver
Ensuring a large enough volume of liver parenchyma	Avoiding postoperative failure	Portal vein embolization or two surgical interventions on the liver	Postoperative mortality
Ensuring that the remnant liver is biologically functional	Avoid postoperative failure	Stop preoperative chemotherapy	Postoperative mortality
Preoperative chemotherapy	Controlling and decreasing the size of the tumor	VEGF-targeting agent associated with chemotherapy	Liver recurrence
Postoperative chemotherapy	Decreasing the rate of tumor recurrence	VEGF-targeting agent associated with chemotherapy	Liver recurrence or metastatic progression, even outside the liver

AAG, anti-angiogenic agent.

unresectable metastases.[10] The impact of chemotherapy on the survival of such patients is unknown, with various authors presenting different opinions on this matter, but no conclusive evidence is yet obtained. Almost all the studies performed to date have been retrospective single-center or registry-based studies. It should be emphasized that in the series reported by Karoui et al., anti-VEGF therapy was a significant factor associated with overall survival in multivariate analysis.[10] The study populations were often heterogeneous in terms of chemotherapy regimen, the onset of metastatic disease (i.e., synchronous vs. metachronous) and the characteristics of the metastases. There is therefore a need to investigate more theoretical concepts originating from basic research.

Kaplan et al. showed that bone marrow-derived hematopoietic cells (HPCs) expressing VEGFR-1 colonize pre-metastatic sites in a mouse tumor model, thereby preparing the way for the arrival of the metastatic cells.[11] This new concept, the metastatic niche concept, was heralded as a major breakthrough. However, the animal model used, which is far removed from an orthotopic animal model, is of limited relevance, and no clinical demonstration was provided.

Seven years later, an analysis of human tissues led to the description of pre-metastatic niches in human specimens.[12] The study concerned aimed to investigate whether the presence of primary colorectal cancer was associated with changes in the angiogenic status of the adjacent liver parenchyma in patients with liver metastases. The authors compared three groups of patients, undergoing: (1) simultaneous resection of synchronous liver metastases and primary tumors (SS-group), (2) resection of synchronous liver metastases 3 to 12 mo after resection of the primary tumor [late synchronous (LS-group)] and (3) resection of metachronous metastases more than 14 mo after resection of the primary tumor (M-group). Gene expression and the localization of CD31, HIF-1α, components of the vascular endothelial growth factor (VEGF) and angiopoietin (Ang) systems were studied by quantitative RT-PCR and immunohistochemistry, in colorectal liver metastases and non-tumorous liver parenchyma adjacent to the tumors.

In all three groups, the authors reported the levels of angiogenic factors to be higher in the adjacent liver parenchyma than in the metastases. The VEGFR-2 gene was strongly expressed in the adjacent liver parenchyma in all three groups. This highlights the need to focus research not only on the cancer cells themselves, but also on their microenvironment, including angiogenesis-related aspects in particular. VEGF-A and VEGFR-1 levels in the adjacent parenchyma in the SS-group were approximately 2.5 and 10 times higher, respectively, than those in metachronous adjacent liver parenchyma. The VEGFR-2 gene was systematically more strongly expressed in the adjacent liver parenchyma than in the corresponding metastases, with the highest levels of expression for this gene recorded for the liver parenchyma adjacent to SS metastases. In this particular situation, VEGFR-2 mRNA levels were 14 times higher in the adjacent liver parenchyma than in the metastases. The Ang-2/Ang-1 ratio, indicating the net angiogenic effect of angiopoietins, was highest in the SS group, in both the metastases and the adjacent liver, and this high ratio was accompanied by a high turnover of tumor cells. The authors concluded that, in the presence of the primary tumor, the liver parenchyma adjacent to the synchronous liver metastases provided an angiogenic environment favoring metastatic tumor growth.

These results have important implications because one of the treatment options for cases of colon cancer with synchronous liver metastases is prolonged chemotherapy without primary cancer resection. Conversely, several retrospective studies have analyzed survival in patients with unresectable colorectal liver metastases, comparing groups of patients in which the primary section was or was not resected. These studies were not randomized and were performed almost at a single center, and most reported few data concerning the use of systemic therapy. In addition, patients with extensive disease were more likely to be offered chemotherapy rather than surgery, and this introduced an additional bias.

Despite these limitations, median overall survival was found to be higher in patients undergoing resection than in those not undergoing resection, in most studies. A recent meta-analysis of eight retrospective, comparative studies including 1,062 patients showed an improvement in the survival of patients managed by palliative resection of the primary tumor.[13] However, results from an ongoing high quality randomized controlled trial will help to answer this question, because others meta-analysis did not reported improvement of survival with surgical resection.

If the primary cancer creates a pre-metastatic niche, as suggested for ovarian cancer,[14] then primary tumor treatments that do not include resection are unlikely to be effective. The primary tumor should thus be resected, or specific combinations of drugs should be administered together with chemotherapy, to control the formation of pre-metastatic niches.

However, in patients undergoing partial hepatectomy, there is an instantaneous release of endothelial progenitor cells (EPCs) after laparotomy and liver mobilization. Recent studies have shown that bone marrow-derived EPCs play an important role in regulating the metastatic angiogenic switch.[11,15] In a model of lung cancer based on subcutaneous injection and a model of spontaneous breast cancer in transgenic mice, Gao et al. showed that the transition from micro (< 1 mm) to macro metastases in the lung was accompanied by the formation of a vascular network.[15] The EPCs infiltrated the periphery of avascular micro-metastases and were then incorporated into the lumina of macrovascular metastasis vessels. The transcription factor Id1 is known to be involved in tumor angiogenesis, and Id1 knockout mice display impaired tumor growth due to damage to angiogenesis-related bone marrow progenitors.[16,17] Id1 appears to be crucial for the mobilization of EPCs and their recruitment to micro-metastases. Gao et al. showed that EPCs were the only bone marrow-derived cells expressing Id1, and that the inhibition of Id1 expression with shRNA had no effect on initial metastatic colonization of the lung, instead inhibiting de novo angiogenesis and progression to macro-metastasis due to a lack of EPC recruitment. This study highlights the functional importance of EPCs in the metastatic angiogenic switch, because this cell type accounts for only 12% of the total number of endothelial cells in tumor vessels. Kaplan et al. confirmed that EPCs (VEGFR2-positive) arrived with tumor cells, in the pre-metastatic niche formed by the HPCs (VEGFR1-positive). Anti-VEGFR2 treatment did not prevent the formation of HPC clusters, but limited metastatic progression.[11]

Surgery also increases plasma VEGF concentrations.[18] Circulating angiogenic factors in colorectal cancer patients with liver metastases may promote tumor growth and contribute to liver regeneration after partial hepatectomy. New treatments should therefore aim to decrease the risk of liver metastasis, by reducing the population of EPCs and VEGF levels, through immunomodulatory or antiangiogenic treatment.[19]

In conclusion, the VEGF pathway and the pre-metastatic niche may influence oncological results for primary tumors with synchronous metastases, because liver surgery may increase the levels of VEGF and EPCs, thereby promoting cancer growth.

Box 1. Major effect expected for VEGF targeting agent
- Normal liver regeneration and wound healing modification
- Direct tumor control
- Indirect tumor control regarding microenvironment
- Decrease resistance for associated chemotherapy
- Predict clinical evolution as a prognostic marker
- Predict of response as a predictive marker

Based on this theoretical analysis, we can conclude that:

(1) Primary colon cancers should be resected rapidly, to minimize the activation of a pre-metastatic niche;

(2) Surgery should be followed by systemic chemotherapy associated with a combination of anti-angiogenic drugs to control the progression of liver metastasis;

(3) Any liver metastases should be resected;

(4) Immunomodulatory and anti-angiogenic treatments should be administered to minimize the risk of recurrence.

Each step in this clinical strategy will require testing and evaluation, rendering the design of any phase III clinical trial highly complex. Furthermore, particular situations may affect the likelihood of metastasis, modifying treatment requirements. For example, portal embolization may promote angiogenesis. In specific anatomic cases, portal vein embolization is performed to increase the volume of the non-embolized liver.[3] However, this stimulation of liver growth may also favor metastasis in the remnant liver. For this reason, chemotherapy is continued during the interval between embolization and surgery. In patients treated with bevacizumab before embolization, the question is whether or not to continue the anti-angiogenic treatment, as VEGF is thought to favor liver growth. One French study concluded that liver regeneration is affected by bevacizumab,[20] and suggested that treatment with this drug should be stopped during the interval between embolization and surgery. However, an American study came to the opposite conclusion, finding no effect on liver regeneration, and suggested the continuation of bevacizumab treatment.[21] These conflicting results indicate that the VEGR pathway is not the only pathway that should be targeted and that synchronous metastases are probably specific.

Some studies have reported a relationship between preoperative or postoperative VEGF levels and the risk of recurrence,[22] whereas others have found no such relationship.[23,24] In pathology, analyses of the interface between colorectal liver metastases and non-tumor liver parenchyma have generated conflicting results. Vermeulen et al. observed three different growth patterns (replacement, pushing and desmoplastic).[25] In replacement growth, tumor cells replace the hepatocytes in the hepatic plate, preserving the reticulin network of the liver parenchyma. In pushing growth, the hepatic plates are pushed aside and run parallel to the circumference of the metastases. In desmoplastic growth, the metastases are separated from the surrounding liver parenchyma by a rim of desmoplastic stroma. These authors subsequently confirmed the existence of these three growth patterns, in a larger study of 196 patients. Pushing growth is associated with an angiogenic pattern, with high rates of tumor and endothelial cell proliferation and a poor prognosis. This type of de novo angiogenesis is driven at least partially by hypoxia, with

high levels of CA9 expression at the edge of the tumor.[26] Another study, with a smaller number of patients, found no difference in microvascular density or survival between capsulated and non-capsulated colorectal liver metastases.[27]

However, no clinical test (levels of VEGF or other angiogenic factors, microparticles, microvascular density, etc.) is currently accepted as valid for use in routine practice. Most published univariate analyses have identified VEGF as a prognostic factor related to recurrence after primary tumor resection, but multivariate analyses of prognostic factors have revealed that it is actually lymph node metastasis from the primary tumor, R1 liver resection and general status that are significantly associated with worse prognosis, rather than VEGF.[28]

No biological test is yet available for determining the most appropriate treatment strategy, but the involvement of VEGF in pre-metastatic niches and the balance between tumor growth and liver regeneration could be used in clinical practice, to improve the outcome of surgery. Provided that this concept can be validated, treatment with anti-VEGF agents could be proposed and integrated into surgical strategies. Angiogenic factors are required for wound healing[29] and liver regeneration after the surgical resection of liver metastases. VEGF expression is therefore a physiological requirement to minimize postoperative complications. However, circulating angiogenic factors promote tumor growth and, probably, tumor recurrence, and high VEGF levels are therefore undesirable. The most important translational research target in the next years will be determining the exact balance between positive and negative effects on the patient and maintaining the correct balance at various points in the disease. Translational research will need to focus on plasma profiles of combinations of angiogenic factors, determinations of single factors, such as VEGF, and other associated biological findings, such as microparticle levels.

Disclosure of Potential Conflicts of Interest

No potential conflicts of interest were disclosed.

References

1. http://publications.cancerresearchuk.org/
2. Rougier P, Milan C, Lazorthes F, Fourtanier G, Partensky C, Baumel H, et al. Prospective study of prognostic factors in patients with unresected hepatic metastases from colorectal cancer. Fondation Française de Cancérologie Digestive. Br J Surg 1995; 82:1397-400; PMID:7489177; http://dx.doi.org/10.1002/bjs.1800821034.
3. Lim C, Farges O. Portal vein occlusion before major hepatectomy in patients with colorectal liver metastases: rationale, indications, technical aspects, complications and outcome. J Visc Surg 2012; 149:e86-96; PMID:22504072; http://dx.doi.org/10.1016/j.jviscsurg.2012.03.003.
4. Nordlinger B, Sorbye H, Glimelius B, Poston GJ, Schlag PM, Rougier P, et al.; EORTC Gastro-Intestinal Tract Cancer Group; Cancer Research UK; Arbeitsgruppe Lebermetastasen und-tumoren in der Chirurgischen Arbeitsgemeinschaft Onkologie (ALM-CAO); Australasian Gastro-Intestinal Trials Group (AGITG); Fédération Francophone de Cancérologie Digestive (FFCD). Perioperative chemotherapy with FOLFOX4 and surgery versus surgery alone for resectable liver metastases from colorectal cancer (EORTC Intergroup trial 40983): a randomised controlled trial. Lancet 2008; 371:1007-16; PMID:18358928; http://dx.doi.org/10.1016/S0140-6736(08)60455-9.
5. Nathan H, Bridges JF, Cosgrove DP, Diaz LA Jr., Laheru DA, Herman JM, et al. Treating patients with colon cancer liver metastasis: a nationwide analysis of therapeutic decision making. Ann Surg Oncol 2012; 19:3668-76; PMID:22875647; http://dx.doi.org/10.1245/s10434-012-2564-3.
6. Power DG, Kemeny NE. Role of adjuvant therapy after resection of colorectal cancer liver metastases. J Clin Oncol 2010; 28:2300-9; PMID:20368552; http://dx.doi.org/10.1200/JCO.2009.26.9340.
7. Nordlinger B, Guiguet M, Vaillant JC, Balladur P, Boudjema K, Bachellier P, et al.; Association Française de Chirurgie. Surgical resection of colorectal carcinoma metastases to the liver. A prognostic scoring system to improve case selection, based on 1568 patients. Cancer 1996; 77:1254-62; PMID:8608500; http://dx.doi.org/10.1002/(SICI)1097-0142(19960401)77:7<1254::AID-CNCR5>3.0.CO;2-I.
8. Fong Y, Fortner J, Sun RL, Brennan MF, Blumgart LH. Clinical score for predicting recurrence after hepatic resection for metastatic colorectal cancer: analysis of 1001 consecutive cases. Ann Surg 1999; 230:309-18, discussion 318-21; PMID:10493478; http://dx.doi.org/10.1097/00000658-199909000-00004.
9. Larsen AK, Ouaret D, El Ouadrani K, Petitprez A. Targeting EGFR and VEGF(R) pathway cross-talk in tumor survival and angiogenesis. Pharmacol Ther 2011; 131:80-90; PMID:21439312; http://dx.doi.org/10.1016/j.pharmthera.2011.03.012.
10. Karoui M, Roudot-Thoraval F, Mesli F, Mitry E, Aparicio T, Des Guetz G, et al. Primary colectomy in patients with stage IV colon cancer and unresectable distant metastases improves overall survival: results of a multicentric study. Dis Colon Rectum 2011; 54:930-8; PMID:21730780; http://dx.doi.org/10.1097/DCR.0b013e31821cced0.
11. Kaplan RN, Riba RD, Zacharoulis S, Bramley AH, Vincent L, Costa C, et al. VEGFR1-positive haematopoietic bone marrow progenitors initiate the pre-metastatic niche. Nature 2005; 438:820-7; PMID:16341007; http://dx.doi.org/10.1038/nature04186.
12. van der Wal GE, Gouw AS, Kamps JA, Moorlag HE, Bulthuis ML, Molema G, et al. Angiogenesis in synchronous and metachronous colorectal liver metastases: the liver as a permissive soil. Ann Surg Oncol 2012; 255:86-94; PMID:22156924; http://dx.doi.org/10.1097/SLA.0b013e318238346a.
13. Stillwell AP, Buettner PG, Ho YH. Meta-analysis of survival of patients with stage IV colorectal cancer managed with surgical resection versus chemotherapy alone. World J Surg 2010; 34:797-807; PMID:20054541; http://dx.doi.org/10.1007/s00268-009-0366-y.
14. Stone RL, Nick AM, McNeish IA, Balkwill F, Han HD, Bottsford-Miller J, et al. Paraneoplastic thrombocytosis in ovarian cancer. N Engl J Med 2012; 366:610-8; PMID:22335738; http://dx.doi.org/10.1056/NEJMoa1110352.
15. Gao D, Nolan DJ, Mellick AS, Bambino K, McDonnell K, Mittal V. Endothelial progenitor cells control the angiogenic switch in mouse lung metastasis. Science 2008; 319:195-8; PMID:18187653; http://dx.doi.org/10.1126/science.1150224.
16. Lyden D, Young AZ, Zagzag D, Yan W, Gerald W, O'Reilly R, et al. Id1 and Id3 are required for neurogenesis, angiogenesis and vascularization of tumour xenografts. Nature 1999; 401:670-7; PMID:10537105; http://dx.doi.org/10.1038/44334.
17. Ruzinova MB, Schoer RA, Gerald W, Egan JE, Pandolfi PP, Rafii S, et al. Effect of angiogenesis inhibition by Id loss and the contribution of bone-marrow-derived endothelial cells in spontaneous murine tumors. Cancer Cell 2003; 4:277-89; PMID:14585355; http://dx.doi.org/10.1016/S1535-6108(03)00240-X.
18. Langenberg MH, Nijkamp MW, Roodhart JM, Snoeren N, Tang T, Shaked Y, et al. Liver surgery induces an immediate mobilization of progenitor cells in liver cancer patients: A potential role for G-CSF. Cancer Biol Ther 2010; 9:743-8; PMID:20215863; http://dx.doi.org/10.4161/cbt.9.9.11551.
19. Li CX, Shao Y, Ng KT, Liu XB, Ling CC, Ma YY, et al. FTY720 suppresses liver tumor metastasis by reducing the population of circulating endothelial progenitor cells. PLoS One 2012; 7:e32380; PMID:22384233; http://dx.doi.org/10.1371/journal.pone.0032380.
20. Aussilhou B, Dokmak S, Faivre S, Paradis V, Vilgrain V, Belghiti J. Preoperative liver hypertrophy induced by portal flow occlusion before major hepatic resection for colorectal metastases can be impaired by bevacizumab. Ann Surg Oncol 2009; 16:1553-9; PMID:19363584; http://dx.doi.org/10.1245/s10434-009-0447-z.
21. Zorzi D, Chun YS, Madoff DC, Abdalla EK, Vauthey JN. Chemotherapy with bevacizumab does not affect liver regeneration after portal vein embolization in the treatment of colorectal liver metastases. Ann Surg Oncol 2008; 15:2765-72; PMID:18636296; http://dx.doi.org/10.1245/s10434-008-0035-7.
22. Yoon SS, Kim SH, Gonen M, Heffernan NM, Detwiller KY, Jarnagin WR, et al. Profile of plasma angiogenic factors before and after hepatectomy for colorectal cancer liver metastases. Ann Surg Oncol 2006; 13:353-62; PMID:16474912; http://dx.doi.org/10.1245/ASO.2006.03.060.
23. Li Q, Wang D, Li J, Chen P. Clinicopathological and prognostic significance of HER-2/neu and VEGF expression in colon carcinomas. BMC Cancer 2011; 11:277; PMID:21708009; http://dx.doi.org/10.1186/1471-2407-11-277.
24. Yasuda H, Tanaka K, Saigusa S, Toiyama Y, Koike Y, Okugawa Y, et al. Elevated CD133, but not VEGF or EGFR, as a predictive marker of distant recurrence after preoperative chemoradiotherapy in rectal cancer. Oncol Rep 2009; 22:709-17; PMID:19724847.
25. Vermeulen PB, Colpaert C, Salgado R, Royers R, Hellemans H, Van Den Heuvel E, et al. Liver metastases from colorectal adenocarcinomas grow in three patterns with different angiogenesis and desmoplasia. J Pathol 2001; 195:336-42; PMID:11673831; http://dx.doi.org/10.1002/path.966.

26. Van den Eynden GG, Bird NC, Majeed AW, Van Laere S, Dirix LY, Vermeulen PB. The histological growth pattern of colorectal cancer liver metastases has prognostic value. Clin Exp Metastasis 2012; 29:541-9; PMID:22476470; http://dx.doi.org/10.1007/s10585-012-9469-1.
27. Rajaganeshan R, Prasad R, Guillou PJ, Chalmers CR, Scott N, Sarkar R, et al. The influence of invasive growth pattern and microvessel density on prognosis in colorectal cancer and colorectal liver metastases. Br J Cancer 2007; 96:1112-7; PMID:17353920; http://dx.doi.org/10.1038/sj.bjc.6603677.
28. Min BS, Kim NK, Jeong HC, Chung HC. High levels of serum VEGF and TIMP-1 are correlated with colon cancer liver metastasis and intrahepatic recurrence after liver resection. Oncol Lett 2012; 4:123-30; PMID:22807974.
29. Scappaticci FA, Fehrenbacher L, Cartwright T, Hainsworth JD, Heim W, Berlin J, et al. Surgical wound healing complications in metastatic colorectal cancer patients treated with bevacizumab. J Surg Oncol 2005; 91:173-80; PMID:16118771; http://dx.doi.org/10.1002/jso.20301.

Annexe 2 : Fiches Techniques

1) Anesthésie:

L'anesthésie des animaux est réalisée par l'injection intra péritonéale de 100µl/ 25g de poids d'une solution de Xylazine 2mg/ml (solution injectable 2% ROMPUN® BAYER) et Kétamine 20 mg/ml (Kétamine 1000 10g/100 ml VIBRAC France)

2) Type de cellules utilisées:

La lignée LS174 (issue de l'ATCC) provient d'un adénocarcinome colique DUKES B d'une femme de 58 ans.

3) Tumeurs sous cutanées

Type de souris: Nude, femelles, 6-8 semaines

Injection: 2 x 10^6 cellules dans 100µl de milieu de culture (DMEM) sont injectées en sous cutané dans le flanc des souris

Monitorage: mesure de la tumeur deux fois par semaine selon la formule

Volume (mm^3)= [Longueur (mm) x [Largeur (mm)] ^{2} x ∏]/6

Sacrifice:

- Lorsque la tumeur mesure entre 1 et 2 cm^3 ou en cas d'ulcération cutanée.

- Exérèse de la tumeur dissociée dans du DMEM pour obtenir des fragments de 1mm^3 (Fig.1 A, B)

- Greffés soit en intra cæcale (pour greffe orthotopique de CCR, cf) ou en sous cutané (constitution du réservoir tumoral) ; après incision cutanée sur la nuque et dissection de l'espace rétro nucale, le fragment tumoral est implanté. La fermeture cutanée est assurée par une agrafe de Michel.

4) Modèle orthotopique de cancer colorectal :

A) Greffe Intra-Caecale:

Type de souris: Nude, femelles, 6-8 semaines

Chirurgie: Après désinfection locale, une incision médiane est effectuée. Le caecum est extériorisé. (Fig.1 C). Greffe par suture et enfouissement intra caecale du fragment tumoral avec du vicryl 4.0 (Fig.1 D). L'étanchéité est assurée par l'application de colle biologique (Tissucol® Baxter Fig.1 E; puis le caecum est réintroduit dans la cavité péritonéale et la fermeture pariétale est assurée par du Vicryl 4.0 et cutanée par des agrafes de Michel.

Monitorage: quotidiennement et pesée deux fois par semaine

Figure 1

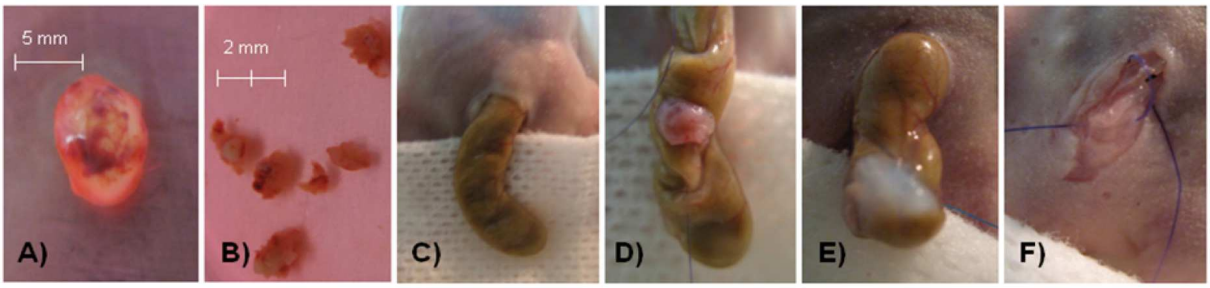

B) Résection de la tumeur caecale: 8 jours après la greffe caecale:

Chirurgie: reprise de l'incision médiane, extériorisation du caecum (Fig.2 A), résection de la tumeur est réséquée après application d'un clip chirurgical pour assurer l'hémostase et l'étanchéité digestive (Fig.2 B, C). Puis le colon restant est réintroduit dans la cavité péritonéale et la fermeture pariétale est assurée par du Vicryl 4.0 et cutanée par des agrafes de Michel. La tumeur est mesurée (Fig.2 D) et le volume tumoral calculé selon la formule précédente.

Monitorage: quotidiennement et pesée deux fois par semaine

Figure 2

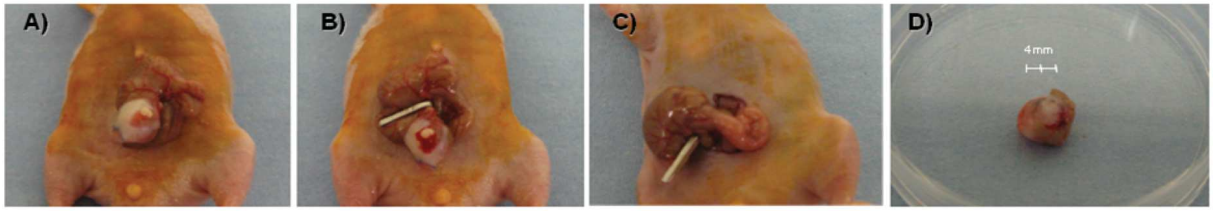

5) Modèle orthotopique de métastases hépatiques de cancer colorectal: injection intra splénique

Type de souris: Nod Scid, femelles, 6-8 semaines

Chirurgie: Après désinfection et dépilation locale, réalisation d'une incision sous costale gauche. Après luxation et extériorisation de la rate une injection intra-splénique de 2 x 10^6 cellules dans 100µl de milieu de culture (DMEM) avec une Aiguille de 26 G est effectuée.

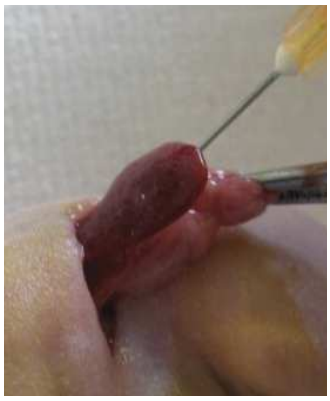

L'hémostase est assurée par compression douce de la rate pendant 2 minutes à l'aide d'un coton tige préalablement désinfecté. La fermeture péritonéale se fait au vicryl 4.0 et la fermeture cutanée à l'aide d'agrafes de Michel.

Monitorage: quotidiennement et pesée deux fois par semaine

Sacrifice à différents temps, J14, J28, J42:

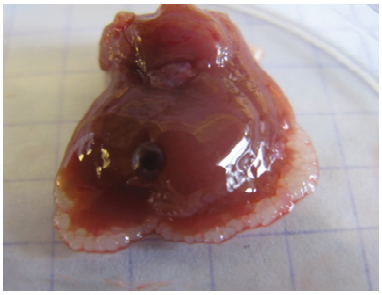

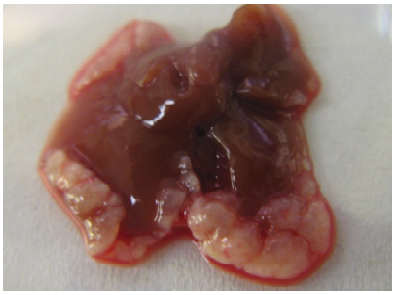

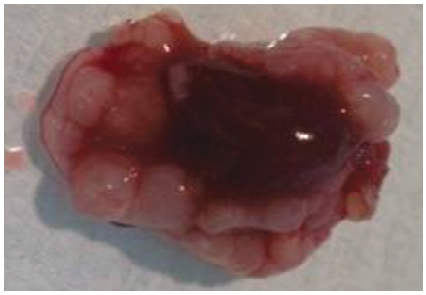

6) Modèle de régénération hépatique par hépatectomie partielle à 50%

Type de souris: BalbC (ou Nudes en cas de métastases hépatiques associées), femelles, 6-8 semaines

Chirurgie: Après désinfection cutanée et dépilation locale, une incision médiane est effectuée avec exérèse du processus xiphoïdien. Un écarteur auto statique est mis en place. La préhension du lobe inférieur gauche (Left Lower Lobe, LLL) permet l'application d'un clip hémostatique au niveau de son pédicule. La section du lobe ainsi dévascularisé est alors effectuée. La même procédure est réalisée pour le lobe supérieur gauche (Left Upper Lobe, LL) permettant ainsi une hépatectomie à 50%. Les pièces d'exérèse sont systématiquement pesées pour s'assurer de la reproductibilité de la chirurgie. Pour compenser les modifications de la volémie, 500 µL de PBS sont ensuite injectés dans la cavité péritonéale. La fermeture péritonéale se fait au PDS 5.0 et la fermeture cutanée à l'aide d'agrafes de Michel.

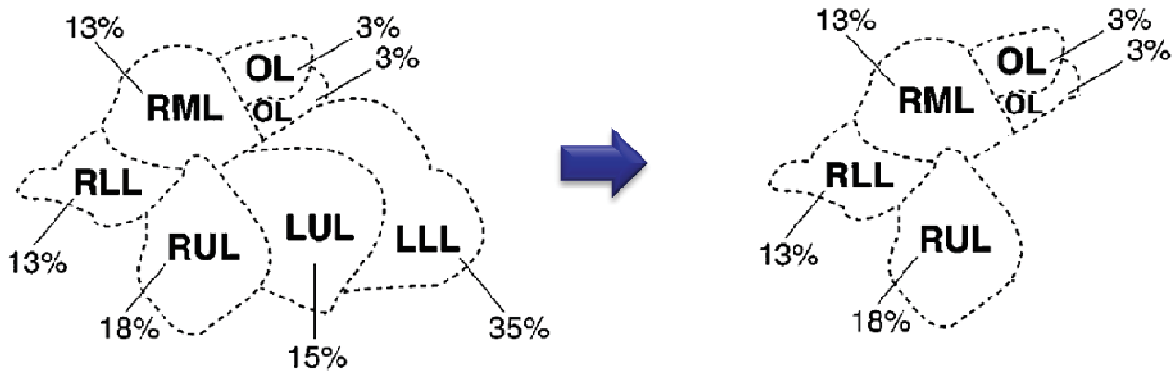

Monitorage: quotidiennement et pesée deux fois par semaine

7) Modèle orthotopique de carcinose péritonéale

Type de souris: Nude, femelles, 6-8 semaines

Injection: Chez des animaux éveillés, 2 x 10^6 cellules dans 500µl de milieu de culture (DMEM) sont injectées intra péritonéale. Les animaux sont surveillés quotidiennement et pesés deux fois par semaine.

Monitorage: quotidiennement et pesée deux fois par semaine

Sacrifice: Lorsque des souris montrent des signes précoces de souffrance, d'amaigrissement.

- pesée

- collecte de l'ascite par une petite incision médiane et mesure du volume à l'aide d'une seringue à tuberculine (1ml).

- prolongement de l'incision pour permettre la prise de photo et la quantification de la carcinose à l'aide d'un score (Peritoneal Cancer Index) modifié pour la souris. Score allouant a chacun des 13 cadrant de l'abdomen un score de 0 a 3 (0= absence lésion visible; 1= tumeur < 2mm; 2= 2.1mm < tumeur < 5 mm; 3= tumeur > 5 mm) pour un score maximum de 39.

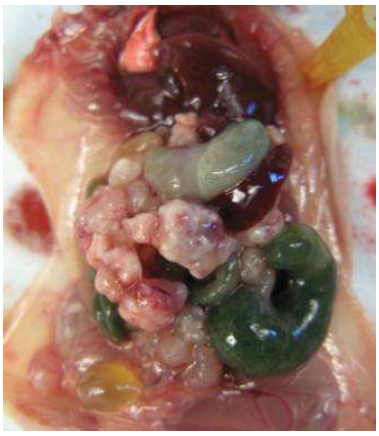

BIBLIOGRAPHIE

1. Gupta GP, Massague J. Cancer metastasis: building a framework. *Cell* 2006; **127**(4): 679-95.
2. Chambers AF, Groom AC, MacDonald IC. Dissemination and growth of cancer cells in metastatic sites. *Nature reviews Cancer* 2002; **2**(8): 563-72.
3. Luzzi KJ, MacDonald IC, Schmidt EE, et al. Multistep nature of metastatic inefficiency: dormancy of solitary cells after successful extravasation and limited survival of early micrometastases. *The American journal of pathology* 1998; **153**(3): 865-73.
4. Weigelt B, Bissell MJ. Unraveling the microenvironmental influences on the normal mammary gland and breast cancer. *Seminars in cancer biology* 2008; **18**(5): 311-21.
5. Folkman J. Role of angiogenesis in tumor growth and metastasis. *Seminars in oncology* 2002; **29**(6 Suppl 16): 15-8.
6. Mantovani A, Allavena P, Sica A, Balkwill F. Cancer-related inflammation. *Nature* 2008; **454**(7203): 436-44.
7. Paget S. The distribution of secondary growths in cancer of the breast. 1889. *Cancer metastasis reviews* 1989; **8**(2): 98-101.
8. Paget S. The distribution of secondary growths in cancer of the breast. . *Lancet* 1889; **1**: 571–3.
9. Collaborative Ocular Melanoma Study G. Assessment of metastatic disease status at death in 435 patients with large choroidal melanoma in the Collaborative Ocular Melanoma Study (COMS): COMS report no. 15. *Archives of ophthalmology* 2001; **119**(5): 670-6.
10. Ewing J. Neoplastic diseases 6th edn. *W B Saunders Co, Philadelphia* 1928.
11. Fidler IJ, Kripke ML. Metastasis results from preexisting variant cells within a malignant tumor. *Science* 1977; **197**(4306): 893-5.
12. Hart IR, Fidler IJ. Role of organ selectivity in the determination of metastatic patterns of B16 melanoma. *Cancer research* 1980; **40**(7): 2281-7.
13. Kaplan RN, Riba RD, Zacharoulis S, et al. VEGFR1-positive haematopoietic bone marrow progenitors initiate the pre-metastatic niche. *Nature* 2005; **438**(7069): 820-7.
14. Weiss L, Mayhew E, Rapp DG, Holmes JC. Metastatic inefficiency in mice bearing B16 melanomas. *British journal of cancer* 1982; **45**(1): 44-53.
15. Hiratsuka S, Watanabe A, Aburatani H, Maru Y. Tumour-mediated upregulation of chemoattractants and recruitment of myeloid cells predetermines lung metastasis. *Nature cell biology* 2006; **8**(12): 1369-75.
16. Hiratsuka S, Nakamura K, Iwai S, et al. MMP9 induction by vascular endothelial growth factor receptor-1 is involved in lung-specific metastasis. *Cancer cell* 2002; **2**(4): 289-300.
17. Kalluri R, Zeisberg M. Fibroblasts in cancer. *Nature reviews Cancer* 2006; **6**(5): 392-401.
18. Friedman SL. Mechanisms of hepatic fibrogenesis. *Gastroenterology* 2008; **134**(6): 1655-69.
19. Olaso E, Santisteban A, Bidaurrazaga J, Gressner AM, Rosenbaum J, Vidal-Vanaclocha F. Tumor-dependent activation of rodent hepatic stellate cells during experimental melanoma metastasis. *Hepatology* 1997; **26**(3): 634-42.
20. Mendoza L, Carrascal T, De Luca M, et al. Hydrogen peroxide mediates vascular cell adhesion molecule-1 expression from interleukin-18-activated hepatic sinusoidal endothelium: implications for circulating cancer cell arrest in the murine liver. *Hepatology* 2001; **34**(2): 298-310.
21. Monvoisin A, Bisson C, Si-Tayeb K, Balabaud C, Desmouliere A, Rosenbaum J. Involvement of matrix metalloproteinase type-3 in hepatocyte growth factor-induced invasion of human hepatocellular carcinoma cells. *International journal of cancer Journal international du cancer* 2002; **97**(2): 157-62.
22. Theret N, Musso O, Turlin B, et al. Increased extracellular matrix remodeling is associated with tumor progression in human hepatocellular carcinomas. *Hepatology* 2001; **34**(1): 82-8.
23. Kang N, Gores GJ, Shah VH. Hepatic stellate cells: partners in crime for liver metastases? *Hepatology* 2011; **54**(2): 707-13.
24. Olaso E, Salado C, Egilegor E, et al. Proangiogenic role of tumor-activated hepatic stellate cells in experimental melanoma metastasis. *Hepatology* 2003; **37**(3): 674-85.

25. Taura K, De Minicis S, Seki E, et al. Hepatic stellate cells secrete angiopoietin 1 that induces angiogenesis in liver fibrosis. *Gastroenterology* 2008; **135**(5): 1729-38.
26. Torimura T, Ueno T, Kin M, et al. Overexpression of angiopoietin-1 and angiopoietin-2 in hepatocellular carcinoma. *Journal of hepatology* 2004; **40**(5): 799-807.
27. Zhao W, Zhang L, Yin Z, et al. Activated hepatic stellate cells promote hepatocellular carcinoma development in immunocompetent mice. *International journal of cancer Journal international du cancer* 2011; **129**(11): 2651-61.
28. Du R, Lu KV, Petritsch C, et al. HIF1alpha induces the recruitment of bone marrow-derived vascular modulatory cells to regulate tumor angiogenesis and invasion. *Cancer cell* 2008; **13**(3): 206-20.
29. Erler JT, Bennewith KL, Cox TR, et al. Hypoxia-induced lysyl oxidase is a critical mediator of bone marrow cell recruitment to form the premetastatic niche. *Cancer cell* 2009; **15**(1): 35-44.
30. Holmgren L, O'Reilly MS, Folkman J. Dormancy of micrometastases: balanced proliferation and apoptosis in the presence of angiogenesis suppression. *Nature medicine* 1995; **1**(2): 149-53.
31. Naumov GN, Akslen LA, Folkman J. Role of angiogenesis in human tumor dormancy: animal models of the angiogenic switch. *Cell cycle* 2006; **5**(16): 1779-87.
32. Gao D, Nolan DJ, Mellick AS, Bambino K, McDonnell K, Mittal V. Endothelial progenitor cells control the angiogenic switch in mouse lung metastasis. *Science* 2008; **319**(5860): 195-8.
33. Lyden D, Young AZ, Zagzag D, et al. Id1 and Id3 are required for neurogenesis, angiogenesis and vascularization of tumour xenografts. *Nature* 1999; **401**(6754): 670-7.
34. Ruzinova MB, Schoer RA, Gerald W, et al. Effect of angiogenesis inhibition by Id loss and the contribution of bone-marrow-derived endothelial cells in spontaneous murine tumors. *Cancer cell* 2003; **4**(4): 277-89.
35. Baluk P, Hashizume H, McDonald DM. Cellular abnormalities of blood vessels as targets in cancer. *Current opinion in genetics & development* 2005; **15**(1): 102-11.
36. Folkman J. Tumor angiogenesis: therapeutic implications. *The New England journal of medicine* 1971; **285**(21): 1182-6.
37. Benjamin LE, Golijanin D, Itin A, Pode D, Keshet E. Selective ablation of immature blood vessels in established human tumors follows vascular endothelial growth factor withdrawal. *The Journal of clinical investigation* 1999; **103**(2): 159-65.
38. Chang YS, di Tomaso E, McDonald DM, Jones R, Jain RK, Munn LL. Mosaic blood vessels in tumors: frequency of cancer cells in contact with flowing blood. *Proceedings of the National Academy of Sciences of the United States of America* 2000; **97**(26): 14608-13.
39. Carmeliet P, Jain RK. Angiogenesis in cancer and other diseases. *Nature* 2000; **407**(6801): 249-57.
40. Dome B, Hendrix MJ, Paku S, Tovari J, Timar J. Alternative vascularization mechanisms in cancer: Pathology and therapeutic implications. *The American journal of pathology* 2007; **170**(1): 1-15.
41. Carmeliet P. Angiogenesis in life, disease and medicine. *Nature* 2005; **438**(7070): 932-6.
42. Holash J, Maisonpierre PC, Compton D, et al. Vessel cooption, regression, and growth in tumors mediated by angiopoietins and VEGF. *Science* 1999; **284**(5422): 1994-8.
43. Folberg R, Hendrix MJ, Maniotis AJ. Vasculogenic mimicry and tumor angiogenesis. *The American journal of pathology* 2000; **156**(2): 361-81.
44. Maniotis AJ, Folberg R, Hess A, et al. Vascular channel formation by human melanoma cells in vivo and in vitro: vasculogenic mimicry. *The American journal of pathology* 1999; **155**(3): 739-52.
45. Vermeulen PB, Colpaert C, Salgado R, et al. Liver metastases from colorectal adenocarcinomas grow in three patterns with different angiogenesis and desmoplasia. *The Journal of pathology* 2001; **195**(3): 336-42.
46. Van den Eynden GG, Bird NC, Majeed AW, Van Laere S, Dirix LY, Vermeulen PB. The histological growth pattern of colorectal cancer liver metastases has prognostic value. *Clinical & experimental metastasis* 2012; **29**(6): 541-9.

47. Rajaganeshan R, Prasad R, Guillou PJ, et al. The influence of invasive growth pattern and microvessel density on prognosis in colorectal cancer and colorectal liver metastases. *British journal of cancer* 2007; **96**(7): 1112-7.
48. Yamaguchi J, Komuta K, Matsuzaki S, Okudaira S, Fujioka H, Kanematsu T. Mode of infiltrative growth of colorectal liver metastases is a useful predictor of recurrence after hepatic resection. *World journal of surgery* 2002; **26**(9): 1122-5.
49. Eefsen RL, Van den Eynden GG, Hoyer-Hansen G, et al. Histopathological growth pattern, proteolysis and angiogenesis in chemonaive patients resected for multiple colorectal liver metastases. *Journal of oncology* 2012; **2012**: 907971.
50. Van den Eynden GG, Majeed AW, Illemann M, et al. The multifaceted role of the microenvironment in liver metastasis: biology and clinical implications. *Cancer research* 2013; **73**(7): 2031-43.
51. Okano K, Yamamoto J, Kosuge T, et al. Fibrous pseudocapsule of metastatic liver tumors from colorectal carcinoma. Clinicopathologic study of 152 first resection cases. *Cancer* 2000; **89**(2): 267-75.
52. Lunevicius R, Nakanishi H, Ito S, et al. Clinicopathological significance of fibrotic capsule formation around liver metastasis from colorectal cancer. *Journal of cancer research and clinical oncology* 2001; **127**(3): 193-9.
53. Stessels F, Van den Eynden G, Van der Auwera I, et al. Breast adenocarcinoma liver metastases, in contrast to colorectal cancer liver metastases, display a non-angiogenic growth pattern that preserves the stroma and lacks hypoxia. *British journal of cancer* 2004; **90**(7): 1429-36.
54. Paku S, Lapis K. Morphological aspects of angiogenesis in experimental liver metastases. *The American journal of pathology* 1993; **143**(3): 926-36.
55. Terayama N, Terada T, Nakanuma Y. A morphometric and immunohistochemical study on angiogenesis of human metastatic carcinomas of the liver. *Hepatology* 1996; **24**(4): 816-9.
56. Paku S, Kopper L, Nagy P. Development of the vasculature in "pushing-type" liver metastases of an experimental colorectal cancer. *International journal of cancer Journal international du cancer* 2005; **115**(6): 893-902.
57. Baeten CI, Hillen F, Pauwels P, de Bruine AP, Baeten CG. Prognostic role of vasculogenic mimicry in colorectal cancer. *Diseases of the colon and rectum* 2009; **52**(12): 2028-35.
58. Friedman SL. Hepatic stellate cells: protean, multifunctional, and enigmatic cells of the liver. *Physiological reviews* 2008; **88**(1): 125-72.
59. Amann T, Bataille F, Spruss T, et al. Activated hepatic stellate cells promote tumorigenicity of hepatocellular carcinoma. *Cancer science* 2009; **100**(4): 646-53.
60. Neaud V, Faouzi S, Guirouilh J, et al. Human hepatic myofibroblasts increase invasiveness of hepatocellular carcinoma cells: evidence for a role of hepatocyte growth factor. *Hepatology* 1997; **26**(6): 1458-66.
61. Mazzocca A, Coppari R, De Franco R, et al. A secreted form of ADAM9 promotes carcinoma invasion through tumor-stromal interactions. *Cancer research* 2005; **65**(11): 4728-38.
62. Okabe H, Beppu T, Hayashi H, et al. Hepatic stellate cells may relate to progression of intrahepatic cholangiocarcinoma. *Annals of surgical oncology* 2009; **16**(9): 2555-64.
63. Musso O, Theret N, Campion JP, et al. In situ detection of matrix metalloproteinase-2 (MMP2) and the metalloproteinase inhibitor TIMP2 transcripts in human primary hepatocellular carcinoma and in liver metastasis. *Journal of hepatology* 1997; **26**(3): 593-605.
64. Theret N, Musso O, Campion JP, et al. Overexpression of matrix metalloproteinase-2 and tissue inhibitor of matrix metalloproteinase-2 in liver from patients with gastrointestinal adenocarcinoma and no detectable metastasis. *International journal of cancer Journal international du cancer* 1997; **74**(4): 426-32.
65. Okabe H, Beppu T, Hayashi H, et al. Hepatic stellate cells accelerate the malignant behavior of cholangiocarcinoma cells. *Annals of surgical oncology* 2011; **18**(4): 1175-84.

66. Matsusue R, Kubo H, Hisamori S, et al. Hepatic stellate cells promote liver metastasis of colon cancer cells by the action of SDF-1/CXCR4 axis. *Annals of surgical oncology* 2009; **16**(9): 2645-53.
67. Badiola I, Olaso E, Crende O, Friedman SL, Vidal-Vanaclocha F. Discoidin domain receptor 2 deficiency predisposes hepatic tissue to colon carcinoma metastasis. *Gut* 2012; **61**(10): 1465-72.
68. Wirz W, Antoine M, Tag CG, et al. Hepatic stellate cells display a functional vascular smooth muscle cell phenotype in a three-dimensional co-culture model with endothelial cells. *Differentiation; research in biological diversity* 2008; **76**(7): 784-94.
69. Ferrara N, Kerbel RS. Angiogenesis as a therapeutic target. *Nature* 2005; **438**(7070): 967-74.
70. Macchiarini P, Fontanini G, Hardin MJ, Squartini F, Angeletti CA. Relation of neovascularisation to metastasis of non-small-cell lung cancer. *Lancet* 1992; **340**(8812): 145-6.
71. Weidner N, Carroll PR, Flax J, Blumenfeld W, Folkman J. Tumor angiogenesis correlates with metastasis in invasive prostate carcinoma. *The American journal of pathology* 1993; **143**(2): 401-9.
72. Weidner N, Folkman J, Pozza F, et al. Tumor angiogenesis: a new significant and independent prognostic indicator in early-stage breast carcinoma. *Journal of the National Cancer Institute* 1992; **84**(24): 1875-87.
73. Weidner N, Semple JP, Welch WR, Folkman J. Tumor angiogenesis and metastasis--correlation in invasive breast carcinoma. *The New England journal of medicine* 1991; **324**(1): 1-8.
74. Choi HJ, Hyun MS, Jung GJ, Kim SS, Hong SH. Tumor angiogenesis as a prognostic predictor in colorectal carcinoma with special reference to mode of metastasis and recurrence. *Oncology* 1998; **55**(6): 575-81.
75. Frank RE, Saclarides TJ, Leurgans S, Speziale NJ, Drab EA, Rubin DB. Tumor angiogenesis as a predictor of recurrence and survival in patients with node-negative colon cancer. *Annals of surgery* 1995; **222**(6): 695-9.
76. Giatromanolaki A, Sivridis E, Minopoulos G, et al. Differential assessment of vascular survival ability and tumor angiogenic activity in colorectal cancer. *Clinical cancer research : an official journal of the American Association for Cancer Research* 2002; **8**(5): 1185-91.
77. Liang JT, Huang KC, Jeng YM, Lee PH, Lai HS, Hsu HC. Microvessel density, cyclo-oxygenase 2 expression, K-ras mutation and p53 overexpression in colonic cancer. *The British journal of surgery* 2004; **91**(3): 355-61.
78. Sternfeld T, Foss HD, Kruschewski M, Runkel N. The prognostic significance of tumor vascularization in patients with localized colorectal cancer. *International journal of colorectal disease* 1999; **14**(6): 272-6.
79. Takebayashi Y, Aklyama S, Yamada K, Akiba S, Aikou T. Angiogenesis as an unfavorable prognostic factor in human colorectal carcinoma. *Cancer* 1996; **78**(2): 226-31.
80. Tanigawa N, Amaya H, Matsumura M, et al. Tumor angiogenesis and mode of metastasis in patients with colorectal cancer. *Cancer research* 1997; **57**(6): 1043-6.
81. Vermeulen PB, Van den Eynden GG, Huget P, et al. Prospective study of intratumoral microvessel density, p53 expression and survival in colorectal cancer. *British journal of cancer* 1999; **79**(2): 316-22.
82. Lindmark G, Gerdin B, Sundberg C, Pahlman L, Bergstrom R, Glimelius B. Prognostic significance of the microvascular count in colorectal cancer. *Journal of clinical oncology : official journal of the American Society of Clinical Oncology* 1996; **14**(2): 461-6.
83. Prall F, Gringmuth U, Nizze H, Barten M. Microvessel densities and microvascular architecture in colorectal carcinomas and their liver metastases: significant correlation of high microvessel densities with better survival. *Histopathology* 2003; **42**(5): 482-91.
84. Shan YS, Lee JC, Chow NH, Yang HB, Wang ST. Immunohistochemical microvessel count is not a reliable prognostic predictor in colorectal carcinoma. *Hepato-gastroenterology* 2003; **50**(53): 1316-20.
85. Bossi P, Viale G, Lee AK, Alfano R, Coggi G, Bosari S. Angiogenesis in colorectal tumors: microvessel quantitation in adenomas and carcinomas with clinicopathological correlations. *Cancer research* 1995; **55**(21): 5049-53.

86. Galizia G, Lieto E, Ferraraccio F, et al. Determination of molecular marker expression can predict clinical outcome in colon carcinomas. *Clinical cancer research : an official journal of the American Association for Cancer Research* 2004; **10**(10): 3490-9.
87. Kaio E, Tanaka S, Kitadai Y, et al. Clinical significance of angiogenic factor expression at the deepest invasive site of advanced colorectal carcinoma. *Oncology* 2003; **64**(1): 61-73.
88. Nanni O, Volpi A, Frassineti GL, et al. Role of biological markers in the clinical outcome of colon cancer. *British journal of cancer* 2002; **87**(8): 868-75.
89. Pavlopoulos PM, Konstantinidou AE, Agapitos E, Kavantzas N, Nikolopoulou P, Davaris P. A morphometric study of neovascularization in colorectal carcinoma. *Cancer* 1998; **83**(10): 2067-75.
90. Pietra N, Sarli L, Caruana P, et al. Is tumour angiogenesis a prognostic factor in patients with colorectal cancer and no involved nodes? *The European journal of surgery = Acta chirurgica* 2000; **166**(7): 552-6.
91. Tomisaki S, Ohno S, Ichiyoshi Y, Kuwano H, Maehara Y, Sugimachi K. Microvessel quantification and its possible relation with liver metastasis in colorectal cancer. *Cancer* 1996; **77**(8 Suppl): 1722-8.
92. Des Guetz G, Uzzan B, Nicolas P, et al. Microvessel density and VEGF expression are prognostic factors in colorectal cancer. Meta-analysis of the literature. *British journal of cancer* 2006; **94**(12): 1823-32.
93. De Bruyne S, Van Damme N, Smeets P, et al. Value of DCE-MRI and FDG-PET/CT in the prediction of response to preoperative chemotherapy with bevacizumab for colorectal liver metastases. *British journal of cancer* 2012; **106**(12): 1926-33.
94. Miyagawa S, Miwa S, Soeda J, Kobayashi A, Kawasaki S. Morphometric analysis of liver macrophages in patients with colorectal liver metastasis. *Clinical & experimental metastasis* 2002; **19**(2): 119-25.
95. Nanashima A, Shibata K, Nakayama T, et al. Clinical significance of microvessel count in patients with metastatic liver cancer originating from colorectal carcinoma. *Annals of surgical oncology* 2009; **16**(8): 2130-7.
96. de Jong KP, Gouw AS, Peeters PM, et al. P53 mutation analysis of colorectal liver metastases: relation to actual survival, angiogenic status, and p53 overexpression. *Clinical cancer research : an official journal of the American Association for Cancer Research* 2005; **11**(11): 4067-73.
97. Amaya H, Tanigawa N, Lu C, et al. Association of vascular endothelial growth factor expression with tumor angiogenesis, survival and thymidine phosphorylase/platelet-derived endothelial cell growth factor expression in human colorectal cancer. *Cancer letters* 1997; **119**(2): 227-35.
98. Cascinu S, Staccioli MP, Gasparini G, et al. Expression of vascular endothelial growth factor can predict event-free survival in stage II colon cancer. *Clinical cancer research : an official journal of the American Association for Cancer Research* 2000; **6**(7): 2803-7.
99. Harada Y, Ogata Y, Shirouzu K. Expression of vascular endothelial growth factor and its receptor KDR (kinase domain-containing receptor)/Flk-1 (fetal liver kinase-1) as prognostic factors in human colorectal cancer. *International journal of clinical oncology* 2001; **6**(5): 221-8.
100. Maeda K, Nishiguchi Y, Yashiro M, et al. Expression of vascular endothelial growth factor and thrombospondin-1 in colorectal carcinoma. *International journal of molecular medicine* 2000; **5**(4): 373-8.
101. Lee JC, Chow NH, Wang ST, Huang SM. Prognostic value of vascular endothelial growth factor expression in colorectal cancer patients. *European journal of cancer* 2000; **36**(6): 748-53.
102. Khorana AA, Ryan CK, Cox C, Eberly S, Sahasrabudhe DM. Vascular endothelial growth factor, CD68, and epidermal growth factor receptor expression and survival in patients with Stage II and Stage III colon carcinoma: a role for the host response in prognosis. *Cancer* 2003; **97**(4): 960-8.
103. Nanashima A, Ito M, Sekine I, et al. Significance of angiogenic factors in liver metastatic tumors originating from colorectal cancers. *Digestive diseases and sciences* 1998; **43**(12): 2634-40.
104. Noike T, Miwa S, Soeda J, Kobayashi A, Miyagawa S. Increased expression of thioredoxin-1, vascular endothelial growth factor, and redox factor-1 is associated with poor prognosis in patients with liver metastasis from colorectal cancer. *Human pathology* 2008; **39**(2): 201-8.

105. Poon RT, Fan ST, Wong J. Clinical implications of circulating angiogenic factors in cancer patients. *Journal of clinical oncology : official journal of the American Society of Clinical Oncology* 2001; **19**(4): 1207-25.
106. Alabi AA, Suppiah A, Madden LA, Monson JR, Greenman J. Preoperative serum vascular endothelial growth factor-a is a marker for subsequent recurrence in colorectal cancer patients. *Diseases of the colon and rectum* 2009; **52**(5): 993-9.
107. Chin KF, Greenman J, Gardiner E, Kumar H, Topping K, Monson J. Pre-operative serum vascular endothelial growth factor can select patients for adjuvant treatment after curative resection in colorectal cancer. *British journal of cancer* 2000; **83**(11): 1425-31.
108. De Vita F, Orditura M, Lieto E, et al. Elevated perioperative serum vascular endothelial growth factor levels in patients with colon carcinoma. *Cancer* 2004; **100**(2): 270-8.
109. Karayiannakis AJ, Syrigos KN, Zbar A, et al. Clinical significance of preoperative serum vascular endothelial growth factor levels in patients with colorectal cancer and the effect of tumor surgery. *Surgery* 2002; **131**(5): 548-55.
110. Kumar H, Heer K, Lee PW, et al. Preoperative serum vascular endothelial growth factor can predict stage in colorectal cancer. *Clinical cancer research : an official journal of the American Association for Cancer Research* 1998; **4**(5): 1279-85.
111. Kwon KA, Kim SH, Oh SY, et al. Clinical significance of preoperative serum vascular endothelial growth factor, interleukin-6, and C-reactive protein level in colorectal cancer. *BMC cancer* 2010; **10**: 203.
112. Min BS, Kim NK, Jeong HC, Chung HC. High levels of serum VEGF and TIMP-1 are correlated with colon cancer liver metastasis and intrahepatic recurrence after liver resection. *Oncology letters* 2012; **4**(1): 123-30.
113. Roumen RM, Slooter GD, Croiset van Uchelen FA, Huib LV. Preoperative serum vascular endothelial growth factor is not a marker for subsequent recurrence during long-term follow-up of colorectal cancer patients. *Diseases of the colon and rectum* 2005; **48**(5): 1070-5.
114. Wei SC, Liang JT, Tsao PN, Hsieh FJ, Yu SC, Wong JM. Preoperative serum placenta growth factor level is a prognostic biomarker in colorectal cancer. *Diseases of the colon and rectum* 2009; **52**(9): 1630-6.
115. Werther K, Christensen IJ, Brunner N, Nielsen HJ. Soluble vascular endothelial growth factor levels in patients with primary colorectal carcinoma. The Danish RANX05 Colorectal Cancer Study Group. *European journal of surgical oncology : the journal of the European Society of Surgical Oncology and the British Association of Surgical Oncology* 2000; **26**(7): 657-62.
116. Yoon SS, Kim SH, Gonen M, et al. Profile of plasma angiogenic factors before and after hepatectomy for colorectal cancer liver metastases. *Annals of surgical oncology* 2006; **13**(3): 353-62.
117. Rahbari NN, Reissfelder C, Muhlbayer M, et al. Correlation of circulating angiogenic factors with circulating tumor cells and disease recurrence in patients undergoing curative resection for colorectal liver metastases. *Annals of surgical oncology* 2011; **18**(8): 2182-91.
118. Kopetz S, Chang GJ, Overman MJ, et al. Improved survival in metastatic colorectal cancer is associated with adoption of hepatic resection and improved chemotherapy. *Journal of clinical oncology : official journal of the American Society of Clinical Oncology* 2009; **27**(22): 3677-83.
119. Siegel R, Naishadham D, Jemal A. Cancer statistics, 2013. *CA: a cancer journal for clinicians* 2013; **63**(1): 11-30.
120. Abdalla EK, Adam R, Bilchik AJ, Jaeck D, Vauthey JN, Mahvi D. Improving resectability of hepatic colorectal metastases: expert consensus statement. *Annals of surgical oncology* 2006; **13**(10): 1271-80.
121. Choti MA, Sitzmann JV, Tiburi MF, et al. Trends in long-term survival following liver resection for hepatic colorectal metastases. *Annals of surgery* 2002; **235**(6): 759-66.
122. Gallagher DJ, Zheng J, Capanu M, et al. Response to neoadjuvant chemotherapy does not predict overall survival for patients with synchronous colorectal hepatic metastases. *Annals of surgical oncology* 2009; **16**(7): 1844-51.

123. Adam R, Delvart V, Pascal G, et al. Rescue surgery for unresectable colorectal liver metastases downstaged by chemotherapy: a model to predict long-term survival. *Annals of surgery* 2004; **240**(4): 644-57; discussion 57-8.
124. Adam R, Pascal G, Castaing D, et al. Tumor progression while on chemotherapy: a contraindication to liver resection for multiple colorectal metastases? *Annals of surgery* 2004; **240**(6): 1052-61; discussion 61-4.
125. Sorbye H, Mauer M, Gruenberger T, et al. Predictive factors for the benefit of perioperative FOLFOX for resectable liver metastasis in colorectal cancer patients (EORTC Intergroup Trial 40983). *Annals of surgery* 2012; **255**(3): 534-9.
126. Nordlinger B, Sorbye H, Glimelius B, et al. Perioperative chemotherapy with FOLFOX4 and surgery versus surgery alone for resectable liver metastases from colorectal cancer (EORTC Intergroup trial 40983): a randomised controlled trial. *Lancet* 2008; **371**(9617): 1007-16.
127. Gallagher DJ, Kemeny N. Metastatic colorectal cancer: from improved survival to potential cure. *Oncology* 2010; **78**(3-4): 237-48.
128. Ferrara N, Gerber HP, LeCouter J. The biology of VEGF and its receptors. *Nature medicine* 2003; **9**(6): 669-76.
129. Folkman J, Shing Y. Angiogenesis. *The Journal of biological chemistry* 1992; **267**(16): 10931-4.
130. Nissen NN, Polverini PJ, Koch AE, Volin MV, Gamelli RL, DiPietro LA. Vascular endothelial growth factor mediates angiogenic activity during the proliferative phase of wound healing. *The American journal of pathology* 1998; **152**(6): 1445-52.
131. Reynaert H, Chavez M, Geerts A. Vascular endothelial growth factor and liver regeneration. *Journal of hepatology* 2001; **34**(5): 759-61.
132. Jain RK. Barriers to drug delivery in solid tumors. *Scientific American* 1994; **271**(1): 58-65.
133. Giantonio BJ, Catalano PJ, Meropol NJ, et al. Bevacizumab in combination with oxaliplatin, fluorouracil, and leucovorin (FOLFOX4) for previously treated metastatic colorectal cancer: results from the Eastern Cooperative Oncology Group Study E3200. *Journal of clinical oncology : official journal of the American Society of Clinical Oncology* 2007; **25**(12): 1539-44.
134. Hochster HS, Hart LL, Ramanathan RK, et al. Safety and efficacy of oxaliplatin and fluoropyrimidine regimens with or without bevacizumab as first-line treatment of metastatic colorectal cancer: results of the TREE Study. *Journal of clinical oncology : official journal of the American Society of Clinical Oncology* 2008; **26**(21): 3523-9.
135. Hurwitz H, Fehrenbacher L, Novotny W, et al. Bevacizumab plus irinotecan, fluorouracil, and leucovorin for metastatic colorectal cancer. *The New England journal of medicine* 2004; **350**(23): 2335-42.
136. Kabbinavar FF, Hambleton J, Mass RD, Hurwitz HI, Bergsland E, Sarkar S. Combined analysis of efficacy: the addition of bevacizumab to fluorouracil/leucovorin improves survival for patients with metastatic colorectal cancer. *Journal of clinical oncology : official journal of the American Society of Clinical Oncology* 2005; **23**(16): 3706-12.
137. Allegra CJ, Yothers G, O'Connell MJ, et al. Phase III trial assessing bevacizumab in stages II and III carcinoma of the colon: results of NSABP protocol C-08. *Journal of clinical oncology : official journal of the American Society of Clinical Oncology* 2011; **29**(1): 11-6.
138. Allegra CJ, Yothers G, O'Connell MJ, et al. Bevacizumab in stage II-III colon cancer: 5-year update of the National Surgical Adjuvant Breast and Bowel Project C-08 trial. *Journal of clinical oncology : official journal of the American Society of Clinical Oncology* 2013; **31**(3): 359-64.
139. de Gramont A, Van Cutsem E, Schmoll HJ, et al. Bevacizumab plus oxaliplatin-based chemotherapy as adjuvant treatment for colon cancer (AVANT): a phase 3 randomised controlled trial. *The lancet oncology* 2012; **13**(12): 1225-33.
140. Andre T, Boni C, Mounedji-Boudiaf L, et al. Oxaliplatin, fluorouracil, and leucovorin as adjuvant treatment for colon cancer. *The New England journal of medicine* 2004; **350**(23): 2343-51.

141. Kuebler JP, Wieand HS, O'Connell MJ, et al. Oxaliplatin combined with weekly bolus fluorouracil and leucovorin as surgical adjuvant chemotherapy for stage II and III colon cancer: results from NSABP C-07. *Journal of clinical oncology : official journal of the American Society of Clinical Oncology* 2007; **25**(16): 2198-204.
142. Bergers G, Hanahan D. Modes of resistance to anti-angiogenic therapy. *Nature reviews Cancer* 2008; **8**(8): 592-603.
143. Mancuso MR, Davis R, Norberg SM, et al. Rapid vascular regrowth in tumors after reversal of VEGF inhibition. *The Journal of clinical investigation* 2006; **116**(10): 2610-21.
144. Ebos JM, Lee CR, Cruz-Munoz W, Bjarnason GA, Christensen JG, Kerbel RS. Accelerated metastasis after short-term treatment with a potent inhibitor of tumor angiogenesis. *Cancer cell* 2009; **15**(3): 232-9.
145. Paez-Ribes M, Allen E, Hudock J, et al. Antiangiogenic therapy elicits malignant progression of tumors to increased local invasion and distant metastasis. *Cancer cell* 2009; **15**(3): 220-31.
146. Miles D, Harbeck N, Escudier B, et al. Disease course patterns after discontinuation of bevacizumab: pooled analysis of randomized phase III trials. *Journal of clinical oncology : official journal of the American Society of Clinical Oncology* 2011; **29**(1): 83-8.
147. Almog N. Molecular mechanisms underlying tumor dormancy. *Cancer letters* 2010; **294**(2): 139-46.
148. Grothey A, Sugrue MM, Purdie DM, et al. Bevacizumab beyond first progression is associated with prolonged overall survival in metastatic colorectal cancer: results from a large observational cohort study (BRiTE). *Journal of clinical oncology : official journal of the American Society of Clinical Oncology* 2008; **26**(33): 5326-34.
149. Kabbinavar F, Hurwitz HI, Fehrenbacher L, et al. Phase II, randomized trial comparing bevacizumab plus fluorouracil (FU)/leucovorin (LV) with FU/LV alone in patients with metastatic colorectal cancer. *Journal of clinical oncology : official journal of the American Society of Clinical Oncology* 2003; **21**(1): 60-5.
150. Van Cutsem E, Rivera F, Berry S, et al. Safety and efficacy of first-line bevacizumab with FOLFOX, XELOX, FOLFIRI and fluoropyrimidines in metastatic colorectal cancer: the BEAT study. *Annals of oncology : official journal of the European Society for Medical Oncology / ESMO* 2009; **20**(11): 1842-7.
151. Stillwell AP, Buettner PG, Ho YH. Meta-analysis of survival of patients with stage IV colorectal cancer managed with surgical resection versus chemotherapy alone. *World journal of surgery* 2010; **34**(4): 797-807.
152. Venderbosch S, de Wilt JH, Teerenstra S, et al. Prognostic value of resection of primary tumor in patients with stage IV colorectal cancer: retrospective analysis of two randomized studies and a review of the literature. *Annals of surgical oncology* 2011; **18**(12): 3252-60.
153. Karoui M, Roudot-Thoraval F, Mesli F, et al. Primary colectomy in patients with stage IV colon cancer and unresectable distant metastases improves overall survival: results of a multicentric study. *Diseases of the colon and rectum* 2011; **54**(8): 930-8.
154. van der Wal GE, Gouw AS, Kamps JA, et al. Angiogenesis in synchronous and metachronous colorectal liver metastases: the liver as a permissive soil. *Annals of surgery* 2012; **255**(1): 86-94.
155. Azoulay D, Castaing D, Krissat J, et al. Percutaneous portal vein embolization increases the feasibility and safety of major liver resection for hepatocellular carcinoma in injured liver. *Annals of surgery* 2000; **232**(5): 665-72.
156. Chun YS, Vauthey JN, Ribero D, et al. Systemic chemotherapy and two-stage hepatectomy for extensive bilateral colorectal liver metastases: perioperative safety and survival. *Journal of gastrointestinal surgery : official journal of the Society for Surgery of the Alimentary Tract* 2007; **11**(11): 1498-504; discussion 504-5.
157. Jaeck D, Oussoultzoglou E, Rosso E, Greget M, Weber JC, Bachellier P. A two-stage hepatectomy procedure combined with portal vein embolization to achieve curative resection for initially unresectable multiple and bilobar colorectal liver metastases. *Annals of surgery* 2004; **240**(6): 1037-49; discussion 49-51.

158. Folprecht G, Gruenberger T, Bechstein WO, et al. Tumour response and secondary resectability of colorectal liver metastases following neoadjuvant chemotherapy with cetuximab: the CELIM randomised phase 2 trial. *The lancet oncology* 2010; **11**(1): 38-47.
159. Gruenberger B, Tamandl D, Schueller J, et al. Bevacizumab, capecitabine, and oxaliplatin as neoadjuvant therapy for patients with potentially curable metastatic colorectal cancer. *Journal of clinical oncology : official journal of the American Society of Clinical Oncology* 2008; **26**(11): 1830-5.
160. Wong R SC, Barbachano Y, Chau I, Valle J, Hickish T, et al. BOXER: a multicentre phase II trial of capecitabine and oxaliplatin plus bevacizumab as neoadjuvant treatment for patients with liver-only metastases from colo- rectal cancer unsuitable for upfront resection. *Eur J Cancer Suppl* 2009; **7**(2): 344-5.
161. Blazer DG, 3rd, Kishi Y, Maru DM, et al. Pathologic response to preoperative chemotherapy: a new outcome end point after resection of hepatic colorectal metastases. *Journal of clinical oncology : official journal of the American Society of Clinical Oncology* 2008; **26**(33): 5344-51.
162. Klinger M, Tamandl D, Eipeldauer S, et al. Bevacizumab improves pathological response of colorectal cancer liver metastases treated with XELOX/FOLFOX. *Annals of surgical oncology* 2010; **17**(8): 2059-65.
163. Rubbia-Brandt L, Giostra E, Brezault C, et al. Importance of histological tumor response assessment in predicting the outcome in patients with colorectal liver metastases treated with neo-adjuvant chemotherapy followed by liver surgery. *Annals of oncology : official journal of the European Society for Medical Oncology / ESMO* 2007; **18**(2): 299-304.
164. Andreou A, Aloia TA, Brouquet A, et al. Margin status remains an important determinant of survival after surgical resection of colorectal liver metastases in the era of modern chemotherapy. *Annals of surgery* 2013; **257**(6): 1079-88.
165. Kishi Y, Zorzi D, Contreras CM, et al. Extended preoperative chemotherapy does not improve pathologic response and increases postoperative liver insufficiency after hepatic resection for colorectal liver metastases. *Annals of surgical oncology* 2010; **17**(11): 2870-6.
166. Ribero D, Wang H, Donadon M, et al. Bevacizumab improves pathologic response and protects against hepatic injury in patients treated with oxaliplatin-based chemotherapy for colorectal liver metastases. *Cancer* 2007; **110**(12): 2761-7.
167. Tamandl D, Klinger M, Eipeldauer S, et al. Sinusoidal obstruction syndrome impairs long-term outcome of colorectal liver metastases treated with resection after neoadjuvant chemotherapy. *Annals of surgical oncology* 2011; **18**(2): 421-30.
168. Drixler TA, Vogten MJ, Ritchie ED, et al. Liver regeneration is an angiogenesis- associated phenomenon. *Annals of surgery* 2002; **236**(6): 703-11; discussion 11-2.
169. Nadalin S, Testa G, Malago M, et al. Volumetric and functional recovery of the liver after right hepatectomy for living donation. *Liver transplantation : official publication of the American Association for the Study of Liver Diseases and the International Liver Transplantation Society* 2004; **10**(8): 1024-9.
170. Shimizu H, Miyazaki M, Wakabayashi Y, et al. Vascular endothelial growth factor secreted by replicating hepatocytes induces sinusoidal endothelial cell proliferation during regeneration after partial hepatectomy in rats. *Journal of hepatology* 2001; **34**(5): 683-9.
171. Taniguchi E, Sakisaka S, Matsuo K, Tanikawa K, Sata M. Expression and role of vascular endothelial growth factor in liver regeneration after partial hepatectomy in rats. *The journal of histochemistry and cytochemistry : official journal of the Histochemistry Society* 2001; **49**(1): 121-30.
172. Ding BS, Nolan DJ, Butler JM, et al. Inductive angiocrine signals from sinusoidal endothelium are required for liver regeneration. *Nature* 2010; **468**(7321): 310-5.
173. Van Buren G, 2nd, Yang AD, Dallas NA, et al. Effect of molecular therapeutics on liver regeneration in a murine model. *Journal of clinical oncology : official journal of the American Society of Clinical Oncology* 2008; **26**(11): 1836-42.
174. Starlinger P, Alidzanovic L, Schauer D, et al. Neoadjuvant bevacizumab persistently inactivates VEGF at the time of surgery despite preoperative cessation. *British journal of cancer* 2012; **107**(6): 961-6.

175. Aussilhou B, Dokmak S, Faivre S, Paradis V, Vilgrain V, Belghiti J. Preoperative liver hypertrophy induced by portal flow occlusion before major hepatic resection for colorectal metastases can be impaired by bevacizumab. *Annals of surgical oncology* 2009; **16**(6): 1553-9.
176. Zorzi D, Chun YS, Madoff DC, Abdalla EK, Vauthey JN. Chemotherapy with bevacizumab does not affect liver regeneration after portal vein embolization in the treatment of colorectal liver metastases. *Annals of surgical oncology* 2008; **15**(10): 2765-72.
177. Millet G, Truant S, Leteurtre E, et al. Volumetric analysis of remnant liver regeneration after major hepatectomy in bevacizumab-treated patients: a case-matched study in 82 patients. *Annals of surgery* 2012; **256**(5): 755-61; discussion 61-2.
178. Kemeny NE, Jarnagin WR, Capanu M, et al. Randomized phase II trial of adjuvant hepatic arterial infusion and systemic chemotherapy with or without bevacizumab in patients with resected hepatic metastases from colorectal cancer. *Journal of clinical oncology : official journal of the American Society of Clinical Oncology* 2011; **29**(7): 884-9.
179. Turan N, Benekli M, Koca D, et al. Adjuvant systemic chemotherapy with or without bevacizumab in patients with resected liver metastases from colorectal cancer. *Oncology* 2013; **84**(1): 14-21.
180. Gryfe R, Kim H, Hsieh ET, et al. Tumor microsatellite instability and clinical outcome in young patients with colorectal cancer. *The New England journal of medicine* 2000; **342**(2): 69-77.
181. Gunderson LL, Jessup JM, Sargent DJ, Greene FL, Stewart AK. Revised TN categorization for colon cancer based on national survival outcomes data. *Journal of clinical oncology : official journal of the American Society of Clinical Oncology* 2010; **28**(2): 264-71.
182. Psaila B, Lyden D. The metastatic niche: adapting the foreign soil. *Nature reviews Cancer* 2009; **9**(4): 285-93.
183. Shinagawa K, Kitadai Y, Tanaka M, et al. Mesenchymal stem cells enhance growth and metastasis of colon cancer. *International journal of cancer Journal international du cancer* 2010; **127**(10): 2323-33.
184. Liang WC, Wu X, Peale FV, et al. Cross-species vascular endothelial growth factor (VEGF)-blocking antibodies completely inhibit the growth of human tumor xenografts and measure the contribution of stromal VEGF. *The Journal of biological chemistry* 2006; **281**(2): 951-61.
185. Yu L, Wu X, Cheng Z, et al. Interaction between bevacizumab and murine VEGF-A: a reassessment. *Investigative ophthalmology & visual science* 2008; **49**(2): 522-7.
186. Kerbel RS. Tumor angiogenesis. *The New England journal of medicine* 2008; **358**(19): 2039-49.
187. Eichmann A, Makinen T, Alitalo K. Neural guidance molecules regulate vascular remodeling and vessel navigation. *Genes & development* 2005; **19**(9): 1013-21.
188. Larrivee B, Freitas C, Trombe M, et al. Activation of the UNC5B receptor by Netrin-1 inhibits sprouting angiogenesis. *Genes & development* 2007; **21**(19): 2433-47.
189. Lu X, Le Noble F, Yuan L, et al. The netrin receptor UNC5B mediates guidance events controlling morphogenesis of the vascular system. *Nature* 2004; **432**(7014): 179-86.
190. Wilson BD, Ii M, Park KW, et al. Netrins promote developmental and therapeutic angiogenesis. *Science* 2006; **313**(5787): 640-4.
191. Lejmi E, Leconte L, Pedron-Mazoyer S, et al. Netrin-4 inhibits angiogenesis via binding to neogenin and recruitment of Unc5B. *Proceedings of the National Academy of Sciences of the United States of America* 2008; **105**(34): 12491-6.
192. Nacht M, St Martin TB, Byrne A, et al. Netrin-4 regulates angiogenic responses and tumor cell growth. *Experimental cell research* 2009; **315**(5): 784-94.
193. Cuenod C, Leconte I, Siauve N, et al. Early changes in liver perfusion caused by occult metastases in rats: detection with quantitative CT. *Radiology* 2001; **218**(2): 556-61.
194. Kruskal JB, Thomas P, Kane RA, Goldberg SN. Hepatic perfusion changes in mice livers with developing colorectal cancer metastases. *Radiology* 2004; **231**(2): 482-90.

195. Kruskal JB, Thomas P, Nasser I, Cay O, Kane RA. Hepatic colon cancer metastases in mice: dynamic in vivo correlation with hypoechoic rims visible at US. *Radiology* 2000; **215**(3): 852-7.
196. Yarmenitis SD, Kalogeropoulou CP, Hatjikondi O, et al. An experimental approach of the Doppler perfusion index of the liver in detecting occult hepatic metastases: histological findings related to the hemodynamic measurements in Wistar rats. *European radiology* 2000; **10**(3): 417-24.
197. Liu Y, Matsui O. Changes of intratumoral microvessels and blood perfusion during establishment of hepatic metastases in mice. *Radiology* 2007; **243**(2): 386-95.
198. Leggett DA, Kelley BB, Bunce IH, Miles KA. Colorectal cancer: diagnostic potential of CT measurements of hepatic perfusion and implications for contrast enhancement protocols. *Radiology* 1997; **205**(3): 716-20.
199. Platt JF, Francis IR, Ellis JH, Reige KA. Liver metastases: early detection based on abnormal contrast material enhancement at dual-phase helical CT. *Radiology* 1997; **205**(1): 49-53.
200. Leen E, Goldberg JA, Angerson WJ, McArdle CS. Potential role of doppler perfusion index in selection of patients with colorectal cancer for adjuvant chemotherapy. *Lancet* 2000; **355**(9197): 34-7.

201. Bonnin P, Coelho J, Pocard M, Levy BI, Marteau P. Anti-TNFα therapy early improves hemodynamics in local intestinal and extraintestinal circulations in active Crohn's disease. *J Crohns Colitis* 2013; **7**(6):451-9.